Early stages in the biogenesis of mitochondrial β-barrel proteins

Dissertation
der Mathematisch-Naturwissenschaftlichen Fakultät
der Eberhard Karls Universität Tübingen
zur Erlangung des Grades eines
Doktors der Naturwissenschaften
(Dr. rer. nat.)

vorgelegt von
Tobias Ulrich Jores
aus Reutlingen

Tübingen
2018

Gedruckt mit Genehmigung der Mathematisch-Naturwissenschaftlichen Fakultät der Eberhard Karls Universität Tübingen.

Tag der mündlichen Qualifikation:	02.05.2018
Dekan:	Prof. Dr. Wolfgang Rosenstiel
1. Berichterstatter:	Prof. Dr. Doron Rapaport
2. Berichterstatter:	Prof. Dr. Andrei Lupas
3. Berichterstatter:	Prof. Dr. Jan Riemer

Contents

1 List of Abbreviations

BAM	β-barrel assembly machinery
BiFC	bimolecular fluorescence complementation
Bpa	*p*-benzoyl-L-phenylalanine
CL	cardiolipin
DHFR	dihydrofolate reductase
Dox	doxycycline
FL	full-length
GFP	green fluorescent protein
Hsp	heat shock protein
IMM	inner mitochondrial membrane
IMP	inner membrane peptidase
IMS	intermembrane space
MIA	mitochondrial intermembrane space import and assembly
MIM	mitochondrial import
MPP	mitochondrial processing peptidase
MTS	mitochondrial targeting sequence
NMR	nuclear magnetic resonance
OEP	outer envelope protein
OMM	outer mitochondrial membrane
PA	phosphatidic acid
PAM	presequence translocase-associated motor
SAM	sorting and assembly machinery
TIM	translocase of the inner mitochondrial membrane
TMS	transmembrane segment
TOB	topogenesis of outer membrane β-barrel proteins
TOM	translocase of the outer mitochondrial membrane
UV	ultraviolet
VDAC	voltage-dependent anion channel
WT	wild type
YadA	*Yersinia* adhesin A
YFP	yellow fluorescent protein

2 Summary

Mitochondria are eukaryotic organelles involved in many essential cellular processes. Their functions include the production of energy and the biosynthesis of iron-sulfur clusters and heme. Furthermore, they engage in lipid and amino acid metabolism, signaling pathways, and apoptosis. Considering this functional diversity, it is not surprising that mitochondrial dysfunctions are implicated in neurodegenerative disorders like Parkinson's and Alzheimer's disease, in the development of cancer and in aging. To properly fulfill their roles, mitochondria harbor a diverse set of proteins. However, most of these are encoded in the nucleus, translated on cytosolic ribosomes, and are then imported into the organelle. To date, we have a detailed understanding of the intra-organellar stages of the mitochondrial import process. In contrast, little is known about the early, pre-mitochondrial events in the biogenesis of mitochondrial precursor proteins. To better understand the processes in the cytosol that precede the mitochondrial import, I analyzed such early events as part of the biogenesis of β-barrel proteins. These proteins are imported and assembled into the mitochondrial outer membrane by a well-defined pathway. However, so far, it is not clear how they reach this membrane in the first place.

In my study, I examined the nature of the targeting signal that directs β-barrel proteins to mitochondria. The results demonstrate that a dedicated β-hairpin motif is necessary and sufficient for the mitochondrial targeting of these proteins. Such a β-hairpin motif is composed of two β-strands connected by a short loop and it can form a β-sheet with one very hydrophobic face. Moreover, in this study, I could identify Tom20 as the major import receptor that recognizes this signal.

Next, I analyzed the interactions of newly synthesized β-barrel proteins with cytosolic chaperones. I identified a set of chaperones and co-chaperones that bind to β-barrel proteins in the cytosol. Furthermore, I could demonstrate that these chaperone/β-barrel protein interactions are required for optimal mitochondrial import of the latter. Of note, a β-hairpin element that can serve as a β-barrel protein targeting signal is sufficient for the recognition by the cytosolic (co-)chaperones.

Collectively, my findings allow us to outline the early, cytosolic events in the biogenesis of mitochondrial β-barrel proteins. Upon their synthesis on cytosolic ribosomes, these proteins associate with molecular chaperones that keep them in an import-competent conformation. The β-barrel proteins are then targeted to mitochondria via the docking of bound chaperones on the import receptor Tom70 as well as through the interaction of Tom20 with their targeting signal in the form of a dedicated β-hairpin motif.

3 Zusammenfassung

Mitochondrien sind eukaryotische Zellorganellen, die an vielen grundlegenden zellulären Prozessen beteiligt sind. Sie werden benötigt für die Energieproduktion, die Biosynthese von Eisen-Schwefel-Clustern und von Häm sowie für den Stoffwechsel von Aminosäuren und Fetten. Des Weiteren sind sie an einigen zellulären Signalwegen und an der Apoptose beteiligt. Angesichts dieser Vielfalt an Funktionen ist es nicht verwunderlich, dass mitochondriale Fehlfunktionen zum Altern sowie zur Entwicklung von Krebs oder von neurodegenerativen Störungen wie der Alzheimer- und der Parkinson-Krankheit beitragen können. Um alle ihre Funktionen korrekt erfüllen zu können, enthalten Mitochondrien einen spezialisierten Satz an Proteinen, die aber größtenteils im Zellkern kodiert sind, von zytosolischen Ribosomen synthetisiert werden und dann in die Mitochondrien importiert werden müssen. Heutzutage haben wir ein gutes Verständnis von den intramitochondrialen Vorgängen die zum Proteinimport in Mitochondrien beitragen. Im Gegensatz dazu wissen wir noch wenig über die Prozesse in der Biogenese von mitochondrialen Proteinen die ablaufen, bevor diese Proteine die Mitochondrien erreicht haben. Um diese Prozesse besser zu verstehen, habe ich sie am Beispiel der Biogenese von β-barrel Proteinen untersucht. Der Import und Einbau dieser Proteine in die mitochondriale Außenmembran ist gut erforscht. Es ist bislang aber nicht klar, wie β-barrel Proteine diese Membran erreichen.

In meiner Arbeit habe ich die Beschaffenheit des Signals untersucht, das β-barrel Proteine zu den Mitochondrien dirigiert. Die Ergebnisse zeigen, dass ein spezialisiertes β-hairpin Element notwendig und ausreichend für die mitochondriale Lokalisierung von β-barrel Proteinen ist. Ein solches β-hairpin Element besteht aus zwei miteinander verknüpften β-Strängen die ein β-Faltblatt mit einer sehr hydrophoben Seite bilden können. In dieser Arbeit konnte ich außerdem zeigen, dass der Importrezeptor Tom20 dieses β-hairpin Signal spezifisch erkennt.

Darüber hinaus, habe ich Interaktionen zwischen neu synthetisierten β-barrel Proteinen und zytosolichen Chaperonen untersucht. Ich habe einen Satz von Chaperonen und Co-Chaperonen identifiziert, die im Zytosol an β-barrel Proteine binden und für den optimalen mitochondrialen Import dieser Proteine notwendig sind. Interessanterweise ist ein β-hairpin Element wie oben beschrieben ausreichend für eine spezifische Interaktion mit Chaperonen.

Zusammengenommen ermöglichen uns diese Forschungsergebnisse ein Modell für die frühen, zytosolischen Vorgänge in der Biogenese von mitochondrialen β-barrel Proteinen zu erstellen. Nach der Synthese durch zytosolische Ribosomen werden die β-barrel Proteine von molekularen Chaperonen in einer importfähigen Konformation gehalten. Die β-barrel Proteine werden dann zu den Mitochondrien dirigiert indem die gebundenen Chaperone an den Importrezeptor Tom70 andocken und das β-hairpin Element mit dem Rezeptor Tom20 interagiert.

4 List of publications contained in this thesis

a) Accepted articles

1. Sauerwald, J.[*], **T. Jores**[*], M. Eisenberg-Bord, S. G. Chuartzman, M. Schuldiner, and D. Rapaport (2015). Genome-wide screens in *Saccharomyces cerevisiae* highlight a role for cardiolipin in biogenesis of mitochondrial outer membrane multispan proteins. *Molecular and Cellular Biology* 35 (18), 3200–3211.
   [*] equal contributors.

2. **Jores**, **T.**, A. Klinger, L. E. Groß, S. Kawano, N. Flinner, E. Duchardt-Ferner, J. Wöhnert, H. Kalbacher, T. Endo, E. Schleiff, and D. Rapaport (2016). Characterization of the targeting signal in mitochondrial β-barrel proteins. *Nature Communications* 7, 12036.

3. Hoseini, H., S. Pandey, **T. Jores**, A. Schmitt, M. Franz-Wachtel, B. Macek, J. Buchner, K. S. Dimmer, and D. Rapaport (2016). The cytosolic cochaperone Sti1 is relevant for mitochondrial biogenesis and morphology. *FEBS Journal* 283 (18), 3338–3352.

4. **Jores**, **T.** and D. Rapaport (2017). Early stages in the biogenesis of eukaryotic β-barrel proteins. *FEBS Letters* 591 (17), 2671–2681.

b) Manuscripts in revision

5. **Jores**, **T.**, J. Lawatscheck, V. Beke, M. Franz-Wachtel, K. Yunoki, B. Macek, T. Endo, H. Kalbacher, J. Buchner, and D. Rapaport (2017). Cytosolic Hsp70 and Hsp40 chaperones enable the biogenesis of mitochondrial β-barrel proteins. *in revision*.

5 Personal contribution to the publications contained in this thesis

1. Sauerwald, J.*, **T. Jores***, M. Eisenberg-Bord, S. G. Chuartzman, M. Schuldiner, and D. Rapaport (2015). Genome-wide screens in *Saccharomyces cerevisiae* highlight a role for cardiolipin in biogenesis of mitochondrial outer membrane multispan proteins. *Molecular and Cellular Biology* 35 (18), 3200–3211.
   * equal contributors.

I isolated mitochondria from *crd1Δ* cells and analyzed the steady state levels of their proteins (Fig. 4B and C). Moreover, I performed *in vitro* import experiments with these mitochondria using Scm4 and pSu9-DHFR as substrate proteins (Fig. 5B and C). To generalize the findings, I performed similar experiments with mitochondria isolated from *gep4Δ* cells (Fig. 6). Furthermore, I performed some of the biological repeats for the experiments described in Fig. 1B and C, in Fig. 3C and D, in Fig. 4A and in Supplemental Fig. 1B. I participated in writing the manuscript and prepared the figures.

2. **Jores**, **T.**, A. Klinger, L. E. Groß, S. Kawano, N. Flinner, E. Duchardt-Ferner, J. Wöhnert, H. Kalbacher, T. Endo, E. Schleiff, and D. Rapaport (2016). Characterization of the targeting signal in mitochondrial β-barrel proteins. *Nature Communications* 7, 12036.

To test if a β-hairpin peptide can inhibit the biogenesis of β-barrel proteins, I performed *in vitro* import experiments in the presence of β-hairpin peptides (Fig. 1). I tested the capacity of β-hairpin peptide to target fused passenger proteins to mitochondria *in vitro* an *in vivo* (Fig. 2 and Supplementary Fig. 2) and I analyzed the correlation between the hydrophobicity of the β-hairpin peptide and its mitochondrial targeting capacity (Fig. 6). Using β-hairpin peptides, I identified interaction partners by photo-crosslinking (Fig. 7). Moreover, I used a split-YFP approach to show the interaction of a β-hairpin peptide with the mitochondrial import receptor Tom20 (Fig. 8 and Supplementary Fig. 8). Furthermore, I tested the dependency of the biogenesis of human VDAC1 on the presence of its C-terminal β-hairpin (Supplementary Fig. 6). I participated in writing the manuscript and prepared the figures for the experiments described above.

Part of the experiments included in Fig. 1b, d, e, and f and in Fig. 2c and d were performed during my diploma studies and are already included in my diploma thesis “The β-hairpin motif functions as a targeting signal in mitochondrial β-barrel proteins.” (Jores 2013).

3. Hoseini, H., S. Pandey, **T. Jores**, A. Schmitt, M. Franz-Wachtel, B. Macek, J. Buchner, K. S. Dimmer, and D. Rapaport (2016). The cytosolic cochaperone Sti1 is relevant for mitochondrial biogenesis and morphology. *FEBS Journal* 283 (18), 3338–3352.

I analyzed the mitochondrial morphology in wildtype and *sti1Δ* cells by fluorescence microscopy (Fig. 7C and D) and helped in preparing the relevant figures.

4. **Jores**, **T.** and D. Rapaport (2017). Early stages in the biogenesis of eukaryotic β-barrel proteins. *FEBS Letters* 591 (17), 2671–2681.

I wrote this review and created all figures.

5. **Jores**, **T.**, J. Lawatscheck, V. Beke, M. Franz-Wachtel, K. Yunoki, B. Macek, T. Endo, H. Kalbacher, J. Buchner, and D. Rapaport (2017). Cytosolic Hsp70 and Hsp40 chaperones enable the biogenesis of mitochondrial β-barrel proteins. *in revision*.

I performed pull-down experiments with β-barrel proteins translated *in vitro* in a yeast extract to identify cytosolic interaction partners and analyzed how the observed interactions are influenced by various conditions (Fig. 1a–c and Supplementary Fig. 1). I used photo-crosslinking to show that a β-hairpin motif is sufficient for interactions with chaperones and that these interactions also occur *in vivo* (Fig. 1d and Fig. 4). Next, I analyzed the physiological relevance of the chaperone/β-barrel protein interactions (Fig. 3 and Supplementary Fig. 2). To investigate the role of co-chaperones in the import of β-barrel proteins, I created strains that can be depleted of certain co-chaperones and studied how the depletion of the co-chaperones affects the biogenesis of β-barrel proteins (Fig. 5). Finally, I performed pull-down and import experiments to test if the chaperone/β-barrel protein interactions and their physiological relevance are conserved also in mammals (Fig. 6). I wrote the manuscript and prepared all figures.

6 Introduction

6.1 Origin, structure, and function of mitochondria

Mitochondria are organelles found in almost all eukaryotic cells. They evolved from an α-proteobacterium that was endosymbiotically incorporated into an anaerobic host cell concomitant with or shortly after the origin of the eukaryotic lineage (Gray 2012). During evolution, most of the mitochondrial genes were transferred to the host cell's nucleus.

Like their prokaryotic progenitors, mitochondria are enclosed by two membranes that divide the organelle into four subcompartments. The outer mitochondrial membrane (OMM) separates the organelle from the cytosol and, together with the inner mitochondrial membrane (IMM), encloses the intermembrane space (IMS). The innermost subcompartment of the mitochondrium is called matrix. Mitochondria form a branched, tubular network that can dynamically change shape by fusion and fission events (Hoffmann and Avers 1973; Pellegrini 1980; Okamoto and Shaw 2005).

The IMM harbors the complexes of the respiratory chain, making mitochondria a key player in the cellular energy production. Apart from this, mitochondria are also involved in several essential cellular processes. Iron-sulfur clusters and heme are synthesized in mitochondria and mitochondrial enzymes participate in the metabolism of lipids and amino acids. Furthermore, mitochondria play active roles in cellular signaling and apoptosis (Seth *et al.* 2005; Pizzo and Pozzan 2007; Pradelli *et al.* 2010). Considering this multitude of functions, it is not surprising that mitochondrial dysfunctions can lead to severe phenotypes. Mitochondria have been implicated in the development of cancer and of several neurodegenerative disorders including Alzheimer's and Parkinson's disease (Beal 2005; Chatterjee *et al.* 2011). Additionally, mitochondrial dysfunctions often contribute to aging (Bratic and Larsson 2013).

6.2 Protein import into mitochondria

To properly fulfill its functions, mitochondria harbor a large set of specialized enzymes and other proteins. The vast majority of these proteins is encoded in the nuclear genome. Therefore, they are translated by cytosolic ribosomes and have to be imported into mitochondria. The OMM and IMM harbor several protein complexes that are dedicated to the import and intra-mitochondrial sorting of cytosolically synthesized proteins (Fig. 1).

The translocase of the outer mitochondrial membrane (TOM) complex forms the general entry gate into mitochondria. It is composed of the pore-forming subunit Tom40, accompanied

by three small subunits, namely Tom5, Tom6, and Tom7, that requlate its assembly and stability. Furthermore the three import receptors Tom20, Tom22 and Tom70/Tom71 are part of the TOM complex. These receptor proteins make first contact with the mitochondrial precursor proteins coming from the cytosol.

Tom20 and Tom22 mainly recognize mitochodrial preproteins that carry a mitochondrial targeting sequence (MTS) (Söllner *et al.* 1989; Moczko *et al.* 1993; Yamano *et al.* 2008). Such an MTS is an N-terminal, cleavable presequence of 20–50 amino acids that can form an amphiphillic α-helix with one hydrophobic and one positively charged face (Heijne 1986; Hammen and Weiner 1998; Vögtle *et al.* 2009). The MTS can bind to a hydrophobic groove on the surface of Tom20 and interact with the negatively charged, cytosolic domain of Tom22 (Hönlinger *et al.* 1995; Mayer *et al.* 1995; Brix *et al.* 1997; Abe *et al.* 2000; Pfanner 2000; Saitoh *et al.* 2007).

While most mitochondrial preproteins contain an MTS, there are also proteins that are directed to mitochondria by internal targeting signals present in the mature protein. These proteins are recognized by the receptor Tom70 prior to their import into mitochondria (Hines *et al.* 1990; Söllner *et al.* 1990).

Despite these different substrate preferences, the two receptors Tom20 and Tom70 posses partially overlapping recognition patterns and can complement the absence of each other (Steger *et al.* 1990; Ramage *et al.* 1993). In line with this, Tom70 was shown to also contain a presequence binding groove and to be involved in the import of aggregation-prone, MTS-containing preproteins (Yamamoto *et al.* 2009; Melin *et al.* 2015).

With the exception of some α-helical OMM proteins (Fig. 1, pathway 1 and 2; see also section 6.3.1), all mitochondrial precursor proteins are translocated across the OMM by the TOM complex. After crossing the OMM, the pathways of precursors destined for different pathways diverge.

Mitochondrial IMS proteins often contain twin cysteine motifs composed of two cysteine residues spaced three or nine amino acids apart (Gabriel *et al.* 2007). Upon reaching the IMS, the mitochondrial intermembrane space import and assembly (MIA) system, composed of Mia40 and Erv1, catalyzes disulfide bridge formations within these precursor proteins. This locks the precusor proteins in a tightly-folded state that prevents them from leaving the mitochondria (Chacinska *et al.* 2004; Fig. 1, pathway 3). Similarly, some IMS proteins adopt a tight folding upon acquisition of a metal cofactor or a prosthetic group such as heme (Hewitt *et al.* 2014). Finally, proteins can also reach the IMS by first following an import pathway into the IMM followed by a proteolytic cleavage that releases the mature part of the protein from its transmembrane segment (TMS) (Schneider *et al.* 1991; Glick *et al.* 1992).

Proteins destined for the IMM reach their destination via one of four different pathways. The mitochondrial genome codes for a small number (8 in yeast and 13 in humans) of proteins. These are translated on mitochondrial ribosomes and inserted into the IMM co-translationally with the help of Oxa1 (Hell *et al.* 2001; Keil *et al.* 2012; Pfeffer *et al.* 2015).

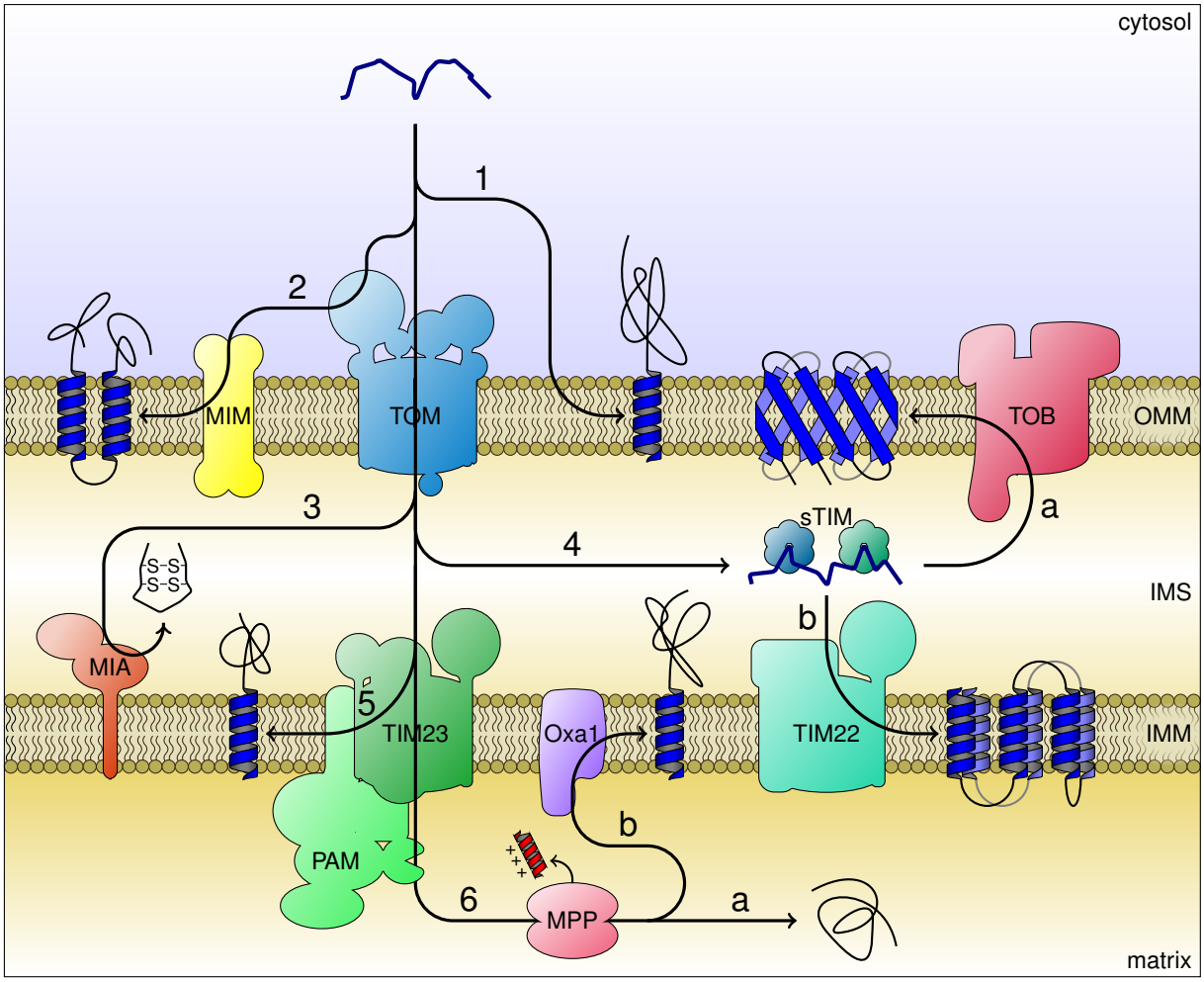

Figure 1: Mitochondrial import machineries and pathways. Some α-helical proteins of the OMM can insert into the membrane spontaneously (1), while the import of all other proteins requires dedicated import complexes. Multispan proteins of the OMM are recognized by the import receptor Tom70, transferred to the MIM complex and inserted into the membrane (2). Cysteine-rich proteins cross the OMM via the TOM complex and are trapped in the IMS after disulfid bond formation catalyzed by the MIA system (3). The TOM complex transports β-barrel and carrier proteins into the IMS where they interact with the small TIM (sTIM) chaperone complexes (4). The β-barrel proteins are then inserted into the OMM by the TOB complex (4a), while the TIM22 complex facilitates integration of carrier proteins into the IMM (4b). Proteins with an MTS are imported by the TIM23 complex that either inserts them into the IMM (5) or translocates them into the matrix (6). The MPP cleaves off the MTS and the proteins either stay in the matrix (6a) or are inserted into the IMM by Oxa1 (6b).

Most IMM proteins, however, are encoded in the nucleus, imported into mitochondria via the TOM complex and inserted into the membrane by one of the two translocase of the inner mitochondrial membrane (TIM) complexes. After emerging from the TOM complex, the polytopic proteins of the IMM carrier family interact with chaperone complexes formed by the small TIM proteins Tim9 and Tim10 or Tim8 and Tim13. These chaperones help in sorting the precursor proteins to the TIM22 complex that facilitates their membrane insertion (Davis *et al.* 2007; Ferramosca and Zara 2013; Fig. 1, pathway 4b).

The TIM23 complex mediates IMM insertion of MTS-containing proteins by a stop-transfer mechanism. When the precursor protein's TMS reaches the TIM23 complex, translocation is

halted and the protein is laterally released into the IMM (Glick *et al.* 1992; Fig. 1, pathway 5).

Finally, some IMM proteins reach their destination by a process termed conservative sorting. For this, they are first imported into the mitochondrial matrix and then inserted into the IMM by Oxa1 (Hell *et al.* 1998; Fig. 1, pathway 6b).

Precursor proteins destined for the mitochondrial matrix usually contain an N-terminal MTS. These proteins are imported via the TOM complex that hands them over to the TIM23 complex. The latter, in combination with the presequence translocase-associated motor (PAM) complex, facilitates translocation of the precursor protein through the IMM (Mokranjac and Neupert 2010). The membrane potential across the IMM and ATP hydrolysis by the PAM complex drive the import of proteins into the matrix (Pfanner and Neupert 1986). In the matrix, the mitochondrial processing peptidase (MPP) cleaves off the MTS thereby releasing the mature protein (Yang *et al.* 1988; Fig. 1, pathway 6a).

6.3 Biogenesis of mitochondrial outer membrane proteins

Proteins of the OMM account for only a small portion of the total mitochondrial proteins (Schnaitman and Greenawalt 1968), yet they often mediate crucial functions for biogenesis, maintenance and morphology of the organelle. Additionally, due to their location at the boundary of mitochondria and the cytosol, the OMM proteins can make contact with the other cell organelles (Elbaz-Alon 2017; Szymański *et al.* 2017).

The proteins residing in the OMM can be grouped according to their topology. Tail-anchored proteins are embedded within the membrane by a single TMS at their C-terminus (Fig. 2A, type 1), while the TMS of signal-anchored proteins is located near their N-terminus (Fig. 2A, type 2). Most signal-anchored proteins expose their soluble, C-terminal domain to the cytosol (Fig. 2A, type 2a), but there is at least one protein, OM45, that adopts an inverted topology with the C-terminus in the IMS (Fig. 2A, type 2b). The OMM also harbors a third class of singlespan proteins that contain an internal TMS as well as soluble domains at both termini (Fig. 2A, type 3). Finally, there are two distinct groups of proteins that span the membrane with at least two TMSs, namely α-helical multispan proteins and β-barrel proteins (Fig. 2A, type 4 or 5, respectively). OMM proteins that share the same topology are usually also imported via the same pathway.

6.3.1 Biogenesis of α-helical proteins

In contrast to all other mitochondrial proteins, some tail-anchored OMM proteins can insert spontaneously into their target membrane without requiring any of the known import machineries (Fig. 2B, pathway 1). While the membrane integration of tail-anchored proteins does not depend on proteinaceous factors, the correct sterol content of the membrane is important (Setoguchi *et al.* 2006; Kemper *et al.* 2008; Krumpe *et al.* 2012).

Signal-anchored OMM proteins are inserted into the membrane by the mitochondrial import (MIM) complex composed of Mim1 and Mim2 (Becker *et al.* 2008; Dimmer *et al.* 2012; Fig. 2B,

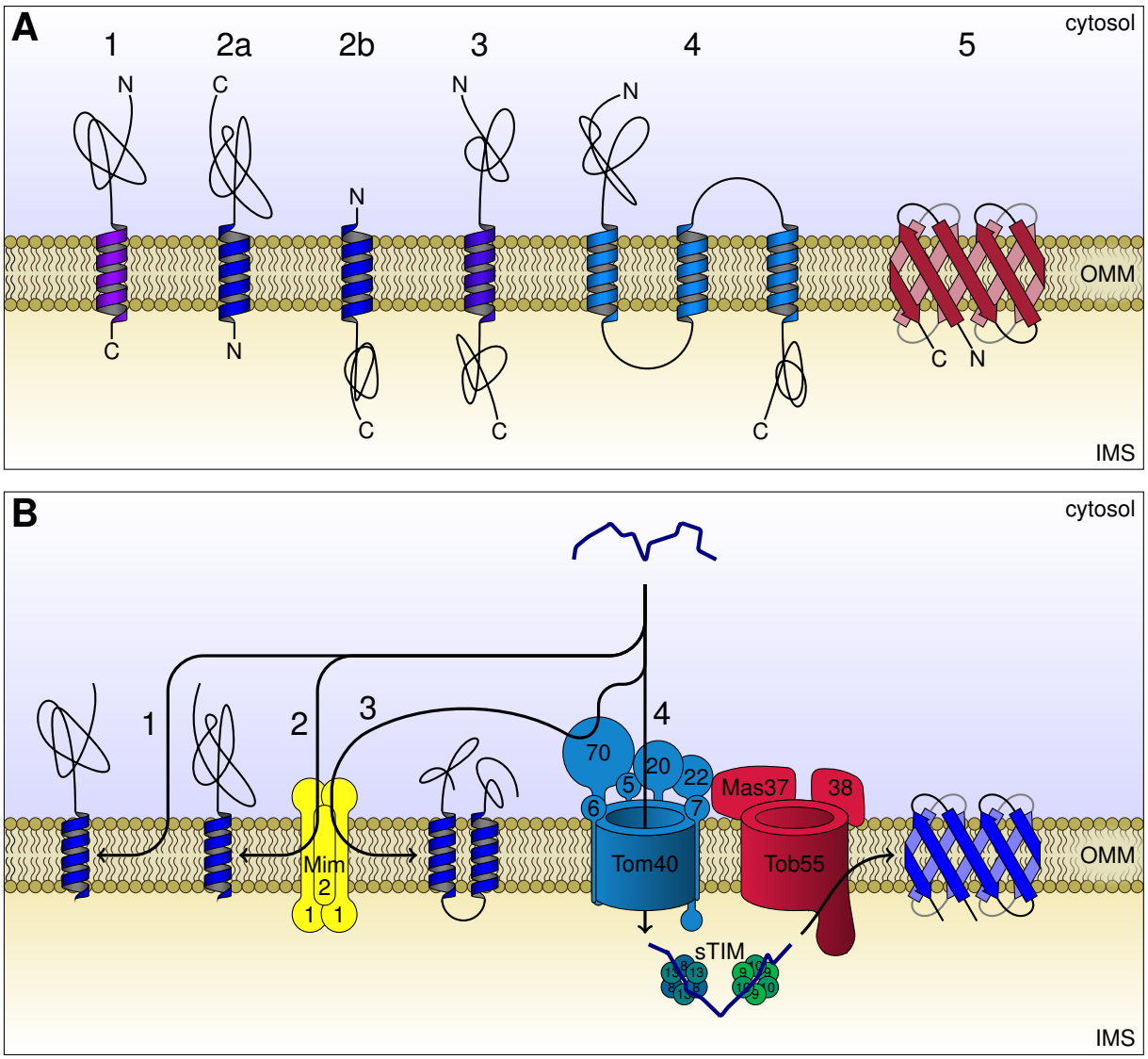

Figure 2: Topologies and biogenesis of mitochondrial outer membrane proteins. (**A**) Mitochondrial OMM proteins adopt different topologies and span the membrane once (1–3) or multiple times (4 and 5) with either α-helices (1–4) or β-strands (5). (**B**) Some mitochondrial tail-anchored proteins can insert into the OMM spontaneously (1), while signal-anchored (2) and multispan proteins (3) require the MIM complex for their membrane integration. Mitochondrial β-barrel proteins are imported into the OMM by a supercomplex formed between the TOM and TOB complexes (4). In the IMS, the β-barrel precursor proteins interact with the small TIM (sTIM) chaperones.

pathway 2). Most signal-anchored proteins expose their C-terminus to the cytosol and are imported directly by the MIM complex. Interestingly, the signal-anchored OMM protein Om45 has a soluble, C-terminal domain in the IMS and takes a different import pathway. It is first translocated across the OMM by the action of the TOM and TIM23 complexes. Then, Om45 is inserted into the OMM from the IMS by the MIM complex (Song *et al.* 2014; Wenz *et al.* 2014).

Apart from signal-anchored proteins, the MIM complex is also involved in the biogenesis of α-helical multispan proteins of the OMM. These proteins additionally require an interaction with the mitochondrial import receptor Tom70 prior to their membrane integration (Otera *et al.* 2007; Becker *et al.* 2011; Papić *et al.* 2011; Fig. 2B, pathway 3).

Recently, a new biogenesis pathway for a multispan OMM protein was discovered. The protein Mcp3 is first imported into the IMM by the TOM and TIM23 complex. It is then cleaved by the inner membrane peptidase (IMP) and the released mature part of the protein is inserted into the OMM probably with help from the MIM complex (Sinzel *et al.* 2016). This pathway resembles in some aspects the one that Om45 utilizes. Both proteins are first translocated across the OMM and then inserted into the OMM from the IMS side of the membrane.

6.3.2 Biogenesis of β-barrel proteins

The OMM harbors not only α-helical proteins, but also β-barrel ones. These proteins are embedded in the membrane via multiple antiparallel β-strands that together form a cylindrical structure. Interestingly, membrane-embedded β-barrel proteins can only be found in the outer membrane of Gram-negative bacteria, chloroplasts and mitochondria. Since the latter two are both organelles of endosymbiotic origin, the existence of β-barrel proteins in their outer membranes supports the endosymbiotic theory.

While almost all bacterial outer membrane proteins are β-barrel proteins, mitochondria harbor only five β-barrel proteins. They were probably conserved due to their important function for the organelle. Two β-barrel proteins, Tom40 and Tob55, are central subunits of OMM import complexes and both are essential for viability. In addition, mitochondria of yeast contain two isoforms of the general solute channel-forming β-barrel protein Porin. The mammalian homologue of Porin is called voltage-dependent anion channel (VDAC) and is present with three isoforms in human mitochondria. Finally, Mdm10 is a β-barrel protein that is conserved only in fungi and has important functions in the biogenesis of the TOM complex and in the maintenance of the mitochondrial lipid homeostasis and morphology (Sogo and Yaffe 1994; Kornmann *et al.* 2009; Yamano *et al.* 2010; Ellenrieder *et al.* 2016). While neither Porin nor Mdm10 are essential, their absence leads to a severe growth defect (Sogo and Yaffe 1994; Blachly-Dyson *et al.* 1997).

The import of mitochondrial β-barrel proteins depends on two complexes in the OMM, namely the TOM complex and the topogenesis of outer membrane β-barrel proteins (TOB) complex (also known as sorting and assembly machinery, SAM), as well as on the small TIM chaperone complexes in the IMS (Fig. 2B, pathway 4).

After translation in the cytosol and approaching the mitochondrial surface, the β-barrel precursor proteins are recognized by the receptors of the TOM complex. Most studies favor Tom20 as the main import receptor for β-barrel proteins (Rapaport and Neupert 1999; Krimmer *et al.* 2001; Yamano *et al.* 2008), although there are also some indications that Tom70 might be involved in the recognition of these proteins (Keil *et al.* 1993).

After initial interactions with the receptors of the TOM complex, the β-barrel precursor proteins are imported via the Tom40 pore into the IMS. Here the small TIM chaperone complexes Tim8/13 and Tim9/10 prevent the aggregation of the *in transit* β-barrel proteins. Finally, the TOB complex composed of the central subunit Tob55 and two peripheral OMM proteins, Tob38 and Mas37, facilitates the membrane insertion of the β-barrel proteins (Paschen *et al.* 2003;

Wiedemann *et al.* 2003; Milenkovic *et al.* 2004; Habib *et al.* 2005; Chan and Lithgow 2008). Of note, Tob55 is a homologue of BamA, the central subunit of the bacterial β-barrel assembly machinery (BAM) complex (Gentle *et al.* 2004).

The atomic structure of BamA revealed weak interactions between its first and last β-strands, suggesting that they might form a lateral gate that can open to release β-barrel precursor proteins into the membrane (Noinaj *et al.* 2013; Albrecht *et al.* 2014; Iadanza *et al.* 2016). Along the same line, a recent study could show that in yeast, β-barrel precusor proteins are translocated through the interior of Tob55 and its lateral gate into the OMM (Höhr *et al.* 2018). For this, they insert β-hairpins into the opening formed by the lateral gate. Once the full precursor is inserted, it is released into the membrane.

To ensure the correct intra-mitochondrial sorting, eukaryotic β-barrel proteins contain a conserved amino acid sequence termed β-signal in their most C-terminal β-strand. Recognition of this signal by Tob38 leads to the membrane insertion of the β-barrel proteins (Kutik *et al.* 2008b). Yet, while this signal seems to be important for the membrane integration of eukaryotic β-barrel proteins, their bacterial counterparts are devoid of such a signal but can still be assembled into the OMM by the TOB complex (see below).

Recently, it was discovered that the TOM and TOB complexes cooperate tightly for the import of β-barrel proteins by forming a supercomplex. The association of the two complexes ensures an efficient transfer of the precursor protein from the TOM to the TOB complex (Qiu *et al.* 2013). The supercomplex formation is mediated by an interaction between Tom22 and Mas37 (Qiu *et al.* 2013; Wenz *et al.* 2015).

As mentioned above, the existence of β-barrel proteins in the OMM was conserved during the evolution of mitochondria. This raised the question whether the organelles can import and assemble also β-barrel proteins of prokaryotic origin. Several studies could show that mitochondria can indeed import bacterial β-barrel proteins (Müller *et al.* 2002; Walther *et al.* 2009a; Kozjak-Pavlovic *et al.* 2011; Müller *et al.* 2011; Ulrich *et al.* 2014). Interestingly, bacteria are also able to assemble eukaryotic β-barrel proteins into their outer membrane (Walther *et al.* 2010). Furthermore, yeast mitochondria posses the ability to import and insert chloroplast β-barrel proteins (Ulrich *et al.* 2012).

6.4 Early stages in the biogenesis of mitochondrial proteins

As described above, we have a detailed understanding of the intra-mitochondrial stages that precursor proteins go through to reach their destination within the organelle. In contrast to this, our knowledge about the early, cytosolic events that are required for the biogenesis of mitochondrial proteins is scarce. In order to be imported into mitochondria, the preproteins have to fulfill two prerequisites: the preproteins must contain a signal that ensures their targeting to mitochondria and they must be in an import-competent conformation.

6.4.1 Targeting signals of mitochondrial proteins

The majority of the mitochondrial precursor proteins is targeted to the organelle via their MTS. Yet, several mitochondrial proteins do not contain an MTS and, therefore, need to be targeted to the mitochondria by different signals. To date, these signals are often not well defined. The group of proteins without an MTS includes the carrier proteins of the IMM, several small proteins in the IMS and almost all proteins of the OMM.

The IMM carrier proteins are anchored in the membrane with six α-helical TMSs and several studies could show that different truncated versions of these proteins contain sufficient information for mitochondrial targeting (Adrian *et al.* 1986; Pfanner *et al.* 1987; Smagula and Douglas 1988). This indicates that the carrier proteins contain several internal sequences that can serve as targeting signals. These signals promote an interaction with the mitochondrial import receptor Tom70 and cooperate in the biogenesis of the carrier proteins (Wiedemann *et al.* 2001). The exact nature of these signals has remained elusive. However, IMM carrier proteins contain three copies of a conserved amino acid sequence, termed carrier signature, that might function as a targeting signal (Ferramosca and Zara 2013).

Proteins that are imported into the mitochondrial IMS via the MIA pathway contain characteristic twin cysteine motifs. In the IMS, these motifs can form disulfide bridges that prevent the proteins from escaping the IMS (Gabriel *et al.* 2007). Interestingly, the sequences just up- or downstream of these cysteine motifs serve as targeting signals and can even direct fused passenger proteins to mitochondria (Milenkovic *et al.* 2007; Milenkovic *et al.* 2009; Sideris *et al.* 2009). Additionally, a specific internal targeting signal was identified for heme lyases of the IMS (Diekert *et al.* 1999).

With the exception of Mcp3, none of the OMM proteins contain an MTS (Sinzel *et al.* 2016). The targeting information for signal- and tail-anchored proteins of the OMM was shown to be encoded in their TMS and its flanking regions. The length and hydrophobicity of the TMS, as well as the number of positively charged residues close to it seems to be crucial for correct targeting (Kanaji *et al.* 2000; Borgese *et al.* 2001; Horie *et al.* 2002; Waizenegger *et al.* 2003). In contrast to this, the targeting information of almost all OMM proteins with an internal TMS or with multiple TMSs has not been identified yet. The only exception, Tom22, a protein with an internal TMS, harbors a targeting signal in its N-terminal, cytosolic domain (Rodriguez-Cousiño *et al.* 1998; Nakamura *et al.* 2004).

Similarly, the signal that targets β-barrel proteins to mitochondria has remained elusive. Biochemical and bioinformatic analyses could not detect a conserved, linear amino acid sequence that might function as a targeting signal. Therefore, it was suggested that the mitochondrial targeting information of β-barrel proteins is contained in a structural element (Rapaport and Neupert 1999; Walther *et al.* 2009b). This hypothesis is supported by the observation that bacterial β-barrel proteins can be imported into mitochondria (see above). While the sequence homology between bacterial and mitochondrial β-barrel proteins is usually rather low, they form

similar structures in the membrane. Experiments with *Yersinia* adhesin A (YadA) demonstrated that even a partial β-barrel structure can be sufficient for mitochondrial targeting. YadA is a bacterial, trimeric autotransporter protein that assembles into a 12-stranded β-barrel in the membrane. Each monomer of YadA contributes four β-strands to the β-barrel (Hoiczyk *et al.* 2000; Linke *et al.* 2006). These four β-strands are sufficient for the import into the OMM when the protein is expressed in yeast cells (Müller *et al.* 2011; Ulrich *et al.* 2014). However, which element within this fragment is responsible for the mitochondrial targeting was not defined.

6.4.2 Cytosolic factors involved in the biogenesis of mitochondrial proteins

While the targeting information is crucial to deliver the mitochondrial precursor proteins to the surface of mitochondria, the import into the organelle can only proceed when the precursor proteins are in an import-competent conformation. A tight folding, as well as an aggregation of the proteins would inhibit the import process.

The cell contains a multitude of molecular chaperones. These chaperone proteins can help their substrate proteins to fold into their native structure. Additionally, molecular chaperones are often involved in preventing the mis-folding or aggregation of their substrates (Kim *et al.* 2013). It is, thus, tempting to assume that molecular chaperones in the cytosol help in keeping mitochondrial precursor proteins in an import-competent conformation. Indeed, such an involvement of cytosolic chaperones in the biogenesis of mitochondrial proteins could be demonstrated in some cases (see below).

Many of the molecular chaperones are upregulated under stress conditions that can destabilize proteins like temperature or oxidative stress. Therefore, many chaperones are termed heat shock proteins (Hsps). Proteins of the Hsp70 and the Hsp90 families form the two major chaperone systems in the cytosol. Hsp70 and Hsp90 chaperones are ATPases and use cycles of ATP binding and hydrolysis to regulate the binding and release of their substrate proteins. Both proteins have a very broad substrate range and their activity and specificity is often fine-tuned by co-chaperones (Young *et al.* 2001; Walsh *et al.* 2004; Terasawa *et al.* 2005; Kampinga and Craig 2010; Clerico *et al.* 2015).

In yeast, the MTS-containing IMM protein $F_1\beta$ was shown to depend on the cytosolic Hsp70 chaperone Ssa1 for an efficient mitochondrial import (Deshaies *et al.* 1988). Ssa1 can also interact with other mitochondrial presequences indicating that it could be involved in the biogenesis of many, or even all, MTS-containing proteins (Endo *et al.* 1996).

Studies analyzing the import of IMM carrier proteins demonstrated that cytosolic Hsp70 chaperones are involved in their biogenesis in mammalian and yeast cells. Furthermore, Hsp90 chaperones were shown to be required for the mitochondrial import of carrier proteins in mammals (Young *et al.* 2003; Bhangoo *et al.* 2007).

These studies also identified several Hsp40 co-chaperones that interact with IMM carrier proteins (Bhangoo *et al.* 2007). Hsp40 proteins (also known as J proteins) are co-chaperones of Hsp70 and regulate its substrate specificity and ATPase activity (Kampinga and Craig 2010). In

yeast, the Hsp40 co-chaperone Ydj1 is involved in the biogenesis of $F_1\beta$ (Caplan *et al.* 1992). Additionally, the Hsp40 protein Djp1 was shown to be required for the optimal biogenesis of the OMM protein Mim1 (Papić *et al.* 2013).

The Hsp70 and Hsp90 chaperones do not only prevent the folding or aggregation of their mitochondrial substrate but can actively help in targeting these proteins to the TOM complex by interacting with its receptor Tom70 (Young *et al.* 2003; Li *et al.* 2009; Zanphorlin *et al.* 2016).

While it was shown that cytosolic chaperones and co-chaperones are involved in the biogenesis of some mitochondrial proteins, it is still unclear whether this is specific only to the tested proteins or also true for the other types of mitochondrial precursor proteins.

7 Research objectives

Despite considerable progress in our understanding of the mitochondrial import process, several questions still remain to be answered. While many import complexes involved in the biogenesis of mitochondrial proteins where identified, there might be additional factors that still await identification. Furthermore, in contrast to our knowledge of the intra-mitochondrial stages of the mitochondrial protein import, information about the early, cytosolic stages of this process is scarce. While the targeting information in many mitochondrial proteins could be decoded, there are some classes of proteins for which the targeting signal remains to be identified. Additionally, it has become clear that cytosolic proteins, especially chaperones, are required for an efficient mitochondrial import of some proteins. Their exact nature and function, however, is not always known and it is also still unclear whether their involvement is required only for a subset of the mitochondrial proteome or whether this is a general priciple.

To better understand the processes that are required for the biogenesis of OMM proteins, I investigated the import of α-helical multispan proteins and of β-barrel proteins. I focused on three main questions:

1. Are there additional factors that play a role in the biogenesis of α-helical multispan proteins of the OMM? In the article "Genome-wide screens in *Saccharomyces cerevisiae* highlight a role for cardiolipin in biogenesis of mitochondrial outer membrane multispan proteins." (Sauerwald *et al.* 2015), we used high-throughput screens and biochemical analyses to identify such factors.

2. What is the nature of the targeting signal that delivers β-barrel proteins to mitochondria and how is this signal decoded by the mitochondrial import machinery? This question was addressed in the article "Characterization of the targeting signal in mitochondrial β-barrel proteins." (Jores *et al.* 2016).

3. Which cytosolic proteins are involved in the biogenesis of mitochondrial β-barrel proteins? In the article "Cytosolic Hsp70 and Hsp40 chaperones enable the biogenesis of mitochondrial β-barrel proteins." (Jores *et al.* 2017), I searched for cytosolic proteins that interact with newly-synthesized β-barrel proteins and analyzed the relevance of these interactions in the context of the β-barrel biogenesis pathway.

8 Summary of the results

8.1 Genome-wide screens in *Saccharomyces cerevisiae* highlight a role for cardiolipin in biogenesis of mitochondrial outer membrane multispan proteins. (Sauerwald *et al.* 2015)

Previous studies could show that the import of α-helical multispan proteins of the OMM depends on the mitochondrial import receptor Tom70 as well as on the MIM complex (Otera *et al.* 2007; Becker *et al.* 2011; Papić *et al.* 2011; Dimmer *et al.* 2012). Interestingly, Tom70 is the only subunit of the TOM complex required for the biogenesis of this family of proteins (Becker *et al.* 2011; Papić *et al.* 2011). However, we were wondering if there are still other proteins that are involved in the biogenesis of α-helical multispan proteins.

To address this question, we applied a high-throughput visual screen utilizing the α-helical multispan protein Om14 fused to green fluorescent protein (GFP) in a yeast gene deletion library. In a complementary approach we used a growth screen based on the hybrid protein Ura3-HA-Om14-degron. This protein will enable the cell to synthesize uracil when inserted correctly into the OMM. Yet, if the membrane integration fails, Ura3-HA-Om14-degron will be degraded rapidly and the cells will not grow on media lacking uracil (Fig. 3A).

We verified that by subcellular fractionation experiments the query proteins GFP-Om14 and Ura3-HA-Om14-degron are localized to mitochondria (Fig. 1B and Fig. 3C) and that they adopt a topology similar to the one of native Om14 by carbonate extraction and proteinase K protection assays (Fig. 1C and Fig. 3D).

Both, the high-throughput visual and growth screens identified the cardiolipin (CL) synthase Crd1 as a candidate protein that could be involved in the biogenesis of α-helical multispan proteins. To verify the involvement of Crd1 in this process, we analyzed mitochondria isolated from cells deleted for *CRD1*. The steady state levels of the multispan OMM proteins GFP-Om14, Ugo1, and Scm4 were reduced when compared to mitochondria from wild type (WT) cells (Fig. 4). Next, we tested the *in vitro* import of α-helical multispan proteins into mitochondria isolated from WT or *crd1Δ* cells. The import of the multispan proteins Ugo1 and Scm4 was reduced in the absence of Crd1 while the import of the control protein pSu9-DHFR was not affected (Fig. 5).

Crd1 catalyzes the last step in the biosynthesis of the mitochondria-specific phospholipid CL (Chang *et al.* 1998; Osman *et al.* 2011). Mitochondria from *crd1Δ* cells do not contain CL. To verify that this absence of CL, rather than an accumulation of an intermediate, causes the observed defects in the biogenesis of α-helical multispan proteins, we performed experiments

with mitochondria from cells deleted for *GEP4* which codes for another enzyme in the CL biosynthesis pathway (Osman *et al.* 2010).

Similar to the situation in *crd1Δ* cells, the steady state levels of the OMM multispan proteins Ugo1, Scm4, and Om14 are reduced in mitochondria from *gep4Δ* cells (Fig. 6A). Furthermore, also the *in vitro* import of the multispan proteins into isolated mitochondria lacking Gep4 is impaired (Fig. 6B and C). In summary, we could show that the import of α-helical multispan proteins into the OMM depends on the presence of the phospholipid CL.

8.2 Characterization of the targeting signal in mitochondrial β-barrel proteins. (Jores *et al.* 2016)

Mitochondrial β-barrel proteins perform many important functions required for the biogenesis, maintenance and morphology of mitochondria. While we have obtained a detailed understanding of the intra-mitochondrial import pathway that these proteins take after their synthesis on cytosolic ribosomes, it is not clear how they are targeted to and recognized by the organelle. Mitochondrial β-barrel proteins contain neither a canonical mitochondrial targeting signal nor a conserved, linear amino acid sequence that could serve as a targeting signal. Instead, it was suggested that the targeting information is encoded by a unique structural motif within the β-barrel proteins (Rapaport and Neupert 1999; Walther *et al.* 2009b). This hypothesis is also supported by the observation that bacterial and chloroplast β-barrel proteins can be targeted to mitochondria (Müller *et al.* 2002; Walther *et al.* 2009a; Kozjak-Pavlovic *et al.* 2011; Ulrich *et al.* 2012).

Interestingly, mitochondria are also able to recognize, import and assemble the trimeric autotransporter YadA (Müller *et al.* 2011; Ulrich *et al.* 2014). Since the β-barrel of YadA is built by three independent subunits, this finding demonstrates that a fragment of a β-barrel structure containing only four β-strands contains sufficient information for mitochondrial targeting. Therefore, we asked whether even a β-hairpin motif composed of two β-strands and a short connecting loop could serve as a targeting signal. Such a β-hairpin motif can be considered as the minimal building block of all β-barrel proteins (Arnold *et al.* 2007; Remmert *et al.* 2010).

To test this hypothesis, I used different chemically synthesized peptides derived from the C-terminal β-hairpin of human VDAC1. This protein was chosen, as it is the only mitochondrial β-barrel protein for which the atomic structure was determined (Bayrhuber *et al.* 2008; Hiller *et al.* 2008; Ujwal *et al.* 2008). The peptides utilized in this study were composed of either the last β-strand (peptide SL) or the last two β-strands (peptide LL). Additionally, a third peptide was synthesized with the same sequence as the peptide LL but the N- and C-termini were covalently linked yielding a cyclic peptide (peptide CYC; Fig. 1a). As cyclization restricts the possible conformations that the CYC peptide can adopt, this peptide is more likely to form a β-hairpin structure.

If such a β-hairpin peptide indeed resembles the targeting signal of mitochondrial β-barrel

proteins, it should be able to bind to elements that recognize β-barrel proteins and, thereby, competitively inhibit their import. Using *in vitro* import assays, I could show that the CYC peptide specifically inhibits the mitochondrial import of β-barrel proteins (Fig. 1b–f). This inhibition was not or only to a lesser extent observed for non-β-barrel proteins. Furthermore, the SL and LL peptides did not show an inhibitory effect. This indicates that the secondary structure of the peptide is important as the CYC peptide, as mentioned above, is more likely to adopt a β-hairpin conformation.

Next, I tested whether a similar β-hairpin peptide (hp18) can actively target fused passenger proteins like dihydrofolate reductase (DHFR) or GFP to mitochondria. In *in vitro* import experiments, fusion of a β-hairpin peptide to a destabilized version of DHFR ($DHFR^{mut}$) lead to its mitochondrial import while an α-helical control peptide (cp) did not mediate import (Fig. 2a and b). Moreover, in *in vivo* experiments, DHFR and GFP were enriched in a crude mitochondrial fraction when fused to a β-hairpin peptide but not when attached to the α-helical control peptide (Fig. 2c–f).

The above-mentioned experiments demonstrate that the last β-hairpin of VDAC1 is sufficient for mitochondrial targeting. To test if it is also necessary, I constructed truncated version of VDAC1 that lack either the first (VDAC1Δhp1) or last β-hairpin (VDAC1Δhp18). When these constructs were expressed in yeast cells only the full-length (FL) version and VDAC1Δhp1 were able to rescue the growth defect of cells deleted for *POR1*, the yeast homolog of VDAC1. In contrast, VDAC1Δhp18 had only a very limited complementation capacity and was detected at lower levels than the other variants (Supplementary Fig. 6). Collectively, these results show that the last β-hairpin of VDAC1 is necessary and sufficient for mitochondrial targeting of β-barrel proteins.

Since β-hairpin motifs are common also in non-β-barrel proteins, I next searched for additional properties of such a motif that enable it to serve as such a targeting signal. To that end, I fused the passenger protein DHFR to various β-hairpin peptides derived from either human VDAC1 or yeast Porin and analyzed the mitochondrial enrichment of the resulting fusion proteins. I found a strong correlation between the mitochondrial targeting capacity of the β-hairpin peptides and the hydrophobicity of the hydrophobic face of the β-sheet they form (Fig. 6a and b). Furthermore, I could demonstrate that reducing the hydrophobicity of the last β-hairpin of VDAC1 reduces its mitochondrial targeting capacity (Fig. 6c). Along the same line, increasing the hydrophobicity of the β-hairpin 17 of VDAC1, also lead to an elevated mitochondrial enrichment of the corresponding fusion protein (Fig. 6d). Taken together, I could show that a β-hairpin motif with one very hydrophobic face can serve as the targeting signal of mitochondrial β-barrel proteins.

Next, to investigate how this signal is recognized within the cell, I used a photo-crosslinking approach to identify mitochondrial proteins that can specifically interact with such a β-hairpin element. To this end, we synthesized a modified version of the β-hairpin peptides that contains the photo-reactive, unnatural amino acid *p*-benzoyl-L-phenylalanine (Bpa). When I mixed the

Bpa-containing peptides with isolated mitochondria and illuminated the samples with ultraviolet (UV)-light, I could detect specific photo-adducts between the cyclic β-hairpin peptide and several subunits of the TOM and TOB complexes (Fig. 7). Of note, no crosslinking adducts were observed for control proteins of the OMM and matrix or with the linear β-hairpin peptide.

Since Tom20 was among the proteins that could be crosslinked to the cyclic β-hairpin peptide and several studies suggested that it is the major import receptor for mitochondrial β-barrel proteins (Söllner *et al.* 1989; Rapaport and Neupert 1999; Schleiff *et al.* 1999; Krimmer *et al.* 2001; Yamano *et al.* 2008), I wanted to test if the interaction of Tom20 with a β-hairpin peptide also takes place *in vivo*. To this end, I performed bimolecular fluorescence complementation (BiFC) experiments using a fusion protein of Tom20 and the C-terminal part of yellow fluorescent protein (YFP) (Fig. 8a). This fusion protein is assembled into the OMM in a topology similar to native Tom20 (Supplementary Fig. 8) and is functional as it can rescue the growth defect of *tom20Δ* yeast cells (Fig. 8b). When Tom20-YFP(C) was coexpressed with a fusion protein composed of a β-hairpin peptide and the N-terminal part of YFP, a yellow fluorescence staining of mitochondria was observed (Fig. 8c). This signal is specific for the interaction of Tom20 with the β-hairpin peptide, as it was not detected when the N-terminal part of YFP was fused to an α-helical control peptide or when the C-terminal part of YFP was fused to the OMM protein Mcr1 (Fig. 8c and d).

Collectively, in this study, I could elucidate how mitochondrial β-barrel proteins are targeted to the correct organelle. This targeting relies on a dedicated β-hairpin motif containing a very hydrophobic face that is recognized by an interaction with the mitochondrial import receptor Tom20.

8.3 Cytosolic Hsp70 and Hsp40 chaperones enable the biogenesis of mitochondrial β-barrel proteins. (Jores *et al.* 2017)

Currently, little is known about the processes that ensure the safe passage of newly synthesized β-barrel proteins through the cytosol. This is especially critical as β-barrel proteins are prone to aggregation due to their hydrophobic nature and tendency to form β-sheets (Hecht 1994).

The cell possesses a multitude of different molecular chaperones that can prevent the aggregation of mis- or unfolded proteins. To test if newly synthesized β-barrel proteins interact with molecular chaperones in the cytosol, I performed pull-down experiments with various β-barrel proteins translated *in vitro* with yeast extract. I found that the Hsp70 chaperones Ssa1 and Ssa2, as well as the Hsp90 chaperones Hsp82 and Hsc82 co-eluted with β-barrel proteins, but not with the control protein DHFR. Additionally, several co-chaperones including Sti1, Aha1 and the Hsp40 proteins Ydj1, Sis1, and Djp1 were present in the eluates obtained after pulling-down β-barrel proteins (Fig. 1a and Table 1).

Next, I analyzed if the chaperone/β-barrel protein interactions can dynamically adapt to changing conditions. To this end, I performed pull-down experiments in the presence or absence

of ATP. The association of Ssa1 and Hsp82 with the *in vitro* translated β-barrel protein Porin was affected by the change in the energy level of the system. This is not surprising as both, Ssa1 and Hsp82, are ATPases. Interestingly, adding an excess of ATP strongly altered the levels of the co-eluted Hsp40 proteins Ydj1, Sis1 and Djp1 (Fig. 1b).

To test if the interactions between chaperones and newly synthesized β-barrel proteins are stable over long time periods, I increased the translation time and analyzed the co-eluted proteins. While the levels of most (co-)chaperones were reduced over time, the disaggregase proteins Hsp104 and Hsp42 increased slightly (Fig. 1c). This indicates that the Hsp70 and Hsp90 chaperones can keep the β-barrel proteins in solution only for a limited time. When this system fails, the β-barrel proteins aggregate and disaggregase proteins are recruited.

Finally, I investigated whether the chaperone/β-barrel protein interactions depend on single co-chaperones. I observed that the absence of Sti1, Ydj1, and Sis1 affects the levels of some of the interacting (co-)chaperones (Supplementary Fig. 1). However, the association of β-barrel proteins with chaperones was not completely abolished. This demonstrated that the absence of one of the co-chaperones can be complemented by the remaining ones.

Next, I asked whether a complete β-barrel protein is required or whether even a β-hairpin motif is sufficient for binding to chaperones. To this end, I performed photo-crosslinking experiments using the Bpa-containing β-hairpin peptides described above. When the peptides were mixed with a yeast extract, I observed the formation of specific photo-adducts with Ssa1, Ydj1, Djp1, and Hsp104. Of note, the photo-adducts were obtained with the cyclic, but not with the linear, β-hairpin peptide (Fig. 1d).

To further characterize the interactions between chaperones and the β-hairpin peptide, we performed, in a collaboration with the Buchner's group in Munich, fluorescence anisotropy measurements using recombinant Ssa1 and Ydj1 and measured their binding to a rhodamine-labeled version of the cyclic β-hairpin peptide (Fig. 2). These experiments revealed that both proteins can bind the cyclic β-hairpin peptide with affinities similar to the ones previously observed for interactions between Hsp70 or Hsp40 chaperones and other substrate peptides (Schmid *et al.* 1994; Endo *et al.* 1996; Pierpaoli *et al.* 1997; Li and Sha 2004; Ricci and Williams 2008; Schneider *et al.* 2016).

To analyze if chaperones interact also *in vivo* with newly synthesized β-barrel proteins, I used a fusion protein composed of a β-hairpin peptide fused to DHFR (Jores *et al.* 2016). Since the chaperone/β-barrel protein interactions are probably transient, I employed a photo-crosslinking approach to take a snapshot of the interactions of the β-hairpin peptide. For this, the photo-reactive amino acid Bpa was inserted into the β-hairpin peptide by an amber suppression system (Chen *et al.* 2007). When the resulting fusion protein was expressed in yeast cells it formed, upon UV irradiation, specific photo-adducts with Ssa1, Hsp82, Ydj1, and Sis1 (Fig. 4). These findings confirm that newly translated β-barrel proteins interact also *in vivo* with cytosolic chaperones.

Collectively, I was able to identify a set of cytosolic chaperones that can bind to and prevent the aggregation of newly synthesized β-barrel proteins. This chaperone system can dynami-

cally adapt to changing conditions and does not strictly depend on any single co-chaperone. Furthermore, we could show that a β-hairpin motif is sufficient for the interaction with cytosolic chaperones.

Since I could demonstrate that β-barrel proteins interact *in vitro* and *in vivo* with cytosolic chaperones, I next asked whether these interactions are also of physiological relevance for the biogenesis of mitochondrial β-barrel proteins. To address this question, I performed *in vitro* import experiments with radiolabeled precursor proteins in the presence of chaperone inhibitors.

First, I analyzed the effect of the inhibitor C90 on the mitochondrial import of β-barrel proteins. C90 is composed of the C-terminus of human Hsp90 and was previously reported to block the binding site for Hsp70 and Hsp90 chaperones on the mitochondrial import receptor Tom70 (Young *et al.* 2003; Bhangoo *et al.* 2007). This inhibitor reduced the mitochondrial import of the β-barrel proteins Porin, *Neurospora crassa* Tom40 (NcTom40), and *Saccharomyces cerevisiae* Tom40 (ScTom40) but not of the MTS-containing control protein pSu9-DHFR (Fig. 3a–c and Supplementary Fig. 2a).

Since C90 cannot distinguish between Hsp70 and Hsp90 family chaperones, I additionally used the Hsp70-specific inhibitor cBag, which is derived from the C-terminal Bag domain of human Bag-1M (Young *et al.* 2003; Bhangoo *et al.* 2007), to test if it affects the biogenesis of mitochondrial β-barrel proteins. Indeed, I observed a specific cBag-mediated import inhibition of β-barrel proteins (Fig. 3d–e and Supplementary Fig. 2b). Taken together, these findings demonstrate that cytosolic Hsp70 chaperones are required for an efficient import of mitochondrial β-barrel proteins.

Next, I examined the role of the Hsp40 co-chaperones Ydj1 and Sis1 in the biogenesis of mitochondrial β-barrel proteins. To this end, I created yeast strains where either one or both of the genes coding for these co-chaperones are under control of a tetracycline-repressible promoter. Cells from these strains can be depleted of the corresponding co-chaperone by the addition of the tetracycline analogue doxycycline (Dox) to the growth medium. I then performed metabolic labeling experiments that enabled me to follow *in vivo* the biogenesis of the β-barrel protein Porin in these strains. Of note, Dox itself does not affect the import of Porin (Fig. 5a). When I analyzed cells that were depleted of either Ydj1 or Sis1, I observed only a marginal reduction in the biogenesis of Porin (Fig. 5b and c). Interestingly, a simultaneous depletion of Ydj1 and Sis1 lead to a strongly reduced import of the β-barrel protein (Fig. 5d). Collectively, these results show that both the Hsp40 co-chaperones Ydj1 and Sis1 are involved in the biogenesis of β-barrel proteins. Apparently, the two proteins perform partially redundant functions and can complement the absence of each other.

Finally, I asked whether the involvement of cytosolic chaperones in the biogenesis of mitochondrial β-barrrel proteins is conserved also in higher eukaryotes. To this end, I performed pull-down and import experiments where the β-barrel precursor proteins were translated in a rabbit reticulocyte lysate system. Here, I observed that the Hsp70 family chaperone Hsc70 specifically binds to the β-barrel proteins Porin and VDAC1 but not to the control protein

DHFR (Fig. 6a). Furthermore, when the Hsp70 inhibitor cBag was added to Porin-containing rabbit reticulocyte lysate, the mitochondrial import of the β-barrel protein was strongly reduced (Fig. 6b). These results indicate that cytosolic Hsp70 chaperones mediate the biogenesis of mitochondrial β-barrel proteins also in higher eukaryotes.

9 Discussion

9.1 Genome-wide screens in *Saccharomyces cerevisiae* highlight a role for cardiolipin in biogenesis of mitochondrial outer membrane multispan proteins.

Many studies have contributed to our understanding of the processes underlying protein import into the OMM (reviewed in Ellenrieder *et al.* 2015). To date, we know three complexes in the OMM, namely, the TOM, TOB, and MIM complexes, that are involved in mitochondrial protein import. However, there might be additional, so far unidentified, proteins that are involved in this process.

We aimed to find such novel import components by screening for gene deletions in yeast that hamper the biogenesis of α-helical multispan OMM proteins. While we did not identify any additional proteins that are directly involved in the import of such proteins, our findings highlight a role of the mitochondria-specific phospholipid CL in their biogenesis.

We observed that a deletion of either *CRD1* or *GEP4* led to reduced steady state levels and an impaired mitochondrial import of several α-helical OMM proteins. Since both, *CRD1* and *GEP4*, code for enzymes involved in the biosynthesis of CL (Chang *et al.* 1998; Osman *et al.* 2010; Osman *et al.* 2011), we suggest that their involvement in the biogenesis of multispan OMM proteins is not a direct one. Instead, the absence of CL in strains deleted for *CRD1* or *GEP4* is probably causing the observed phenotype.

Such an involvement of phospholipids in the biogenesis of mitochondrial proteins has been reported before (reviewed in Böttinger *et al.* 2015). Several studies showed that the stability of the TIM23 complex is reduced in the absence of CL leading to a decreased import of IMM and matrix proteins (Kutik *et al.* 2008a; Tamura *et al.* 2009; Malhotra *et al.* 2017). Additionally, it was reported that the absence of CL destabilizes the TOM and TOB complexes and, therefore, leads to a hampered biogenesis of OMM β-barrel proteins (Gebert *et al.* 2009).

The import of α-helical multispan proteins into the OMM, however, does not depend on the whole TOM complex but only on its import receptor Tom70 and on the MIM complex, which is not affected by the absence of CL (our findings and Gebert *et al.* 2009). Therefore, it is unlikely that the observed import deficiency of α-helical multispan proteins into mitochondria from *crd1Δ* and *gep4Δ* cells is the result of destabilized import complexes. Instead, CL could directly be required for the membrane insertion of α-helical multispan proteins. Of note, a direct involvement of lipids in the biogenesis of these proteins has been reported before when Vögtle *et al.* showed that phosphatidic acid (PA) promotes the membrane insertion of Ugo1 (Vögtle

et al. 2015). How PA and CL mediate the integration of multispan proteins into the OMM is not clear. One possibility is that they can form microdomains within the membrane that then serve as the insertion point for these proteins. Currently, experimental proof for this hypothesis is still lacking.

9.2 Characterization of the targeting signal in mitochondrial β-barrel proteins.

The main focus of my study was to investigate the early, pre-mitochondrial stages in the biogenesis of β-barrel proteins. While we have a detailed understanding of the import process that takes place after the β-barrel proteins reach the mitochondria, it was not clear how they get there in the first place. Two questions had remained elusive, namely how are β-barrel proteins targeted to mitochondria and how does the cell ensure that they reach their target in an import-competent conformation.

While most mitochondrial proteins are targeted to their organelle by means of an MTS at their N-terminus, β-barrel proteins are devoid of this feature. Additionally, they do not contain a conserved amino acid sequence that could serve as a targeting signal. Therefore, it was suggested that the targeting signal of these proteins is encoded by a structural element (Rapaport and Neupert 1999; Walther *et al.* 2009b). In this study, I could show that a dedicated β-hairpin motif can fulfill this role.

This finding can explain the observation that bacterial and chloroplast β-barrel proteins are targeted to mitochondria when expressed in non-plant eukaryotic cells (Müller *et al.* 2002; Walther *et al.* 2009a; Kozjak-Pavlovic *et al.* 2011; Müller *et al.* 2011; Ulrich *et al.* 2012; Ulrich *et al.* 2014). These proteins often share only little sequence homology with mitochondrial β-barrels but they are all composed of multiple β-hairpin elements which are the minimal building block of all β-barrel proteins (Arnold *et al.* 2007; Remmert *et al.* 2010).

However, β-hairpin motifs also frequently occur in non-mitochondrial proteins. Therefore, to serve as a mitochondrial targeting signal, the β-hairpin targeting element must fulfill additional requirements. Since the mitochondrial β-barrel proteins are embedded in the lipid bilayer, the amino acid residues facing the lipid core are mostly hydrophobic. Indeed, I could show that this hydrophobicity is a key element in determining whether a β-hairpin motif can serve as a mitochondrial targeting signal. Only β-hairpins that form a β-sheet with one face that is very hydrophobic can target proteins to mitochondria.

Targeting signals are often recognized by dedicated receptors. In the case of the β-barrel protein targeting signal, I could show by cross-linking and BiFC assays that Tom20 functions as such a receptor. Furthermore, nuclear magnetic resonance (NMR) experiments performed by my collaboration partners could identify the binding site of the β-hairpin signal on Tom20. Interestingly, the β-hairpin element binds to the same hydrophobic groove that serves also as the binding site for the MTS. This can be explained by the common amphiphilic structure of the

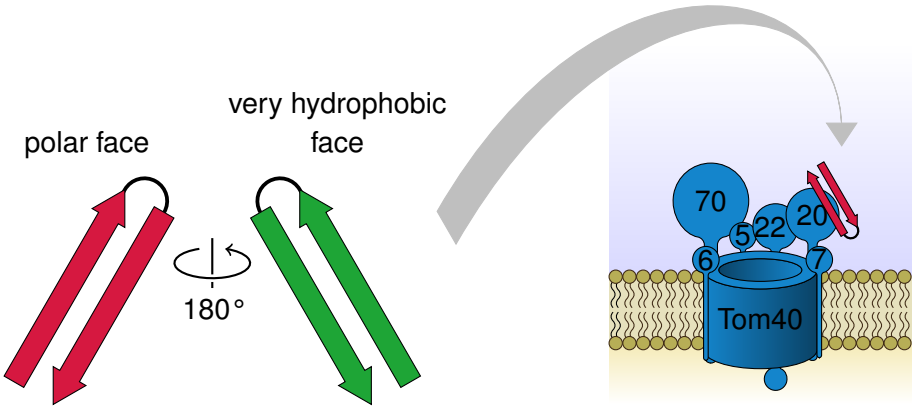

Figure 3: The targeting signal of mitochondrial β-barrel proteins. Mitochondrial β-barrel proteins are targeted to their organelle by a β-hairpin motif with one highly hydrophobic and one polar face. This signal is recognized by the import receptor Tom20.

β-hairpin motif and the MTS as both elements fold into structures with one hydrophobic and one polar face. This finding can also explain the reduced mitochondrial import of MTS-containing proteins in the presence of a β-hairpin peptide and the previous observation that an MTS peptide could compete for the import of Porin (Millar and Shore 1996).

Previous studies showed that MTSs can also be bound by Tom22 and Tom70, the other two import receptors of the TOM complex (Hönlinger *et al.* 1995; Mayer *et al.* 1995; Brix *et al.* 1997; Melin *et al.* 2015). In this study, both receptors formed photo-adducts with a Bpa-containing cyclic β-hairpin peptide. Therefore, Tom22 and/or Tom70 could also be involved in the recognition of the targeting signal of mitochondrial β-barrel proteins. In line with this, it was shown that the mitochondrial import of β-barrel proteins is inhibited by a proteolytic removal of the cytosolic domain of Tom22 or by an antibody against Tom70 (Keil *et al.* 1993; Yamano *et al.* 2008). The ability of the β-hairpin element to bind to the receptors Tom20, Tom22 and Tom70 might help to increase the avidity of the interaction between the TOM complex and β-barrel precursor proteins. One can envisage a situation where different β-hairpins of the precursor protein could be bound simultaneously by the different receptors of the TOM complex.

Often, targeting signals have to occur at a specific position within the protein to be recognized properly. This is, however, not the case for the targeting signal of mitochondrial β-barrel proteins. While the most hydrophobic β-hairpin of human VDAC1 is located at the C-terminus of the protein, Porin of yeast harbors its most hydrophobic β-hairpin close to the N-terminus. Despite their different location, both β-hairpins are efficient targeting signals. Furthermore, the β-hairpins could target passenger proteins to mitochondria when they were fused to the N-terminus of these proteins. Taken together, the targeting signal of β-barrel proteins is not restricted to a certain location within the full-length protein.

In summary, I could decipher how mitochondrial β-barrel proteins are targeted to mitochondria. They contain a dedicated β-hairpin motif that has one highly hydrophobic and one polar face. This β-hairpin serves as a targeting signal and is recognized by the mitochondrial import receptor Tom20 (Fig. 3).

The targeting of β-barrel proteins in non-plant eukaryotic cells is rather straightforward as there is only one organelle as a putative destination. The situation gets more complicated in plant cells as these harbor two organelles, mitochondria and chloroplast, that contain β-barrel proteins in their outer membranes. To better understand how plant cells ensure the correct targeting of mitochondrial or chloroplast β-barrel proteins, my collaboration partners analyzed the subcellular localization of plant mitochondrial VDAC1, of chloroplast outer envelope protein (OEP)24, and of hydbrids between these proteins. They could show that the C-terminal β-hairpin of VDAC1 is necessary for the correct targeting of the protein to mitochondria. Moreover, when the C-terminal β-hairpin of OEP24 was replaced with the one from VDAC1, the resulting hybrid protein was also targeted to mitochondria (Jores *et al.* 2016). These findings show that, also in plant cells, a β-hairpin motif serves as a mitochondrial targeting signal.

To date, it is not clear how chloroplast β-barrel proteins prevent that their β-hairpins are recognized as a targeting signal for mitochondria. Furthermore, we also do not know how they are targeted to the chloroplasts. One possibility is, that plant cells contain specific guidance factors in the cytosol that recognize and target chloroplast β-barrel proteins to their organelle. Such a cytosolic factor would also be in line with the observation that chloroplast β-barrel proteins can be imported into mitochondria *in vitro* and are specifically located to chloroplasts only *in vivo* (Ulrich *et al.* 2012). However, so far, no cytosolic proteins interacting with newly synthesized chloroplast β-barrel proteins have been reported.

9.3 Cytosolic Hsp70 and Hsp40 chaperones enable the biogenesis of mitochondrial β-barrel proteins.

To better understand the early stages of the biogenesis of β-barrel proteins, I searched for cytosolic proteins that interact with such precursor proteins and help them reach the mitochondria. Using pull-down and crosslinking assays, I could identify a set of cytosolic chaperones that specifically bind to β-barrel proteins upon their synthesis on cytosolic ribosomes.

Newly synthesized β-barrel proteins interact with the cytosolic Hsp70 chaperones Ssa1 and Ssa2, and with the Hsp90 chaperones Hsp82 and Hsc82. The Hsp70 and Hsp90 families comprise the most abundant molecular chaperones. Members of these chaperone families have been implicated with mitochondrial import before. Hsp70 chaperones were reported to mediate the import of MTS-containing preproteins (Deshaies *et al.* 1988; Endo *et al.* 1996). Furthermore, in mammalian cells, Hsp70 and Hsp90 chaperones are required for the import of carrier proteins destined for the IMM. Interestingly, in yeast cells, carrier proteins are efficiently imported into mitochondria without the help of Hsp90 chaperones (Young *et al.* 2003). Similarly, while I could detect binding of newly translated β-barrel proteins to the yeast Hsp90 proteins Hsp82 and Hsc82, inhibitors of these proteins did not lead to a reduced import of β-barrel proteins in *in vitro* import experiments (data not shown). Therefore, under the tested conditions, I could not demonstrate a physiological role for the Hsp90/β-barrel interactions.

In contrast, the interactions between Hsp70 family chaperones and newly synthesized β-barrel proteins are required for an efficient biogenesis of the latter. Import of β-barrel proteins into mitochondria is severely affected by inhibitors that disrupt the binding of Hsp70 chaperones to the import receptor Tom70 or to their substrates. Since Hsp70 proteins are ATPases, their involvement in the biogenesis of β-barrel proteins is also supported by the previously unexplained observation that a pool of ATP outside of mitochondria is required for this process (Pfanner *et al.* 1988; Hwang and Schatz 1989; Rapaport and Neupert 1999).

Chaperones of the Hsp70 family are present in all kingdoms of life and are amongst the most conserved proteins (Gupta and Golding 1993; Daugaard *et al.* 2007). Accordingly, I could show that the Hsp70/β-barrel protein interactions and their physiological relevance are conserved from yeast to mammals.

Hsp70 chaperones possess a very broad substrate range and their specificity is often fine-tuned by co-chaperones of the Hsp40 family (Walsh *et al.* 2004; Kampinga and Craig 2010; Cyr and Ramos 2014; Craig and Marszalek 2017). Accordingly, I could detect the specific binding of the Hsp40 chaperones Ydj1, Sis1 and Djp1 to newly synthesized β-barrel proteins. However, most of the observed cytosolic interaction partners of β-barrel proteins were still able to bind to these proteins even in the absence of individual co-chaperones. This indicates that the chaperone system that keeps β-barrel proteins in an import-competent conformation can dynamically adapt to and compensate for the loss of individual members. This adaptiveness could also be demonstrated in experiments with altered ATP levels. Whereas the same (co-)chaperones were bound to β-barrel proteins under all conditions, their relative amounts responded to the change in the energy status.

When I analyzed the physiological relevance of the Hsp40/β-barrel protein interactions, I found that a depletion of either Ydj1 or Sis1 has only a mild effect on the biogenesis of β-barrel proteins. In contrast, when cells were simultaneously depleted of both co-chaperones, the biogenesis of β-barrel proteins was strongly reduced. Taken together, Ydj1 and Sis1 are required for the biogenesis of mitochondrial β-barrel proteins. Yet, their functions in this context overlap and they can complement for the absence of each other. Similarly, a previous study reported that Sis1 can rescue the growth defect of a strain harboring a temperature-sensitive allele of Ydj1. The same study also showed that Ydj1 is involved in the biogenesis of the MTS-containing IMM protein $F_1\beta$ (Caplan *et al.* 1992). Sis1, on the other hand, was so far not implicated in the import of mitochondrial precursor proteins.

To better understand how the cytosolic (co-)chaperones recognize mitochondrial β-barrel proteins as substrates, I tested if a partial β-barrel structure is sufficient for chaperone binding. Indeed, even a β-hairpin peptide interacted with various (co-)chaperones *in vitro* and *in vivo*. Therefore, it is possible that cytosolic chaperones associate with β-barrel proteins already while they are still being translated. Such a co-translational interaction could prevent aggregation of hydrophobic elements within the β-barrel proteins immediately upon their exit from the ribosomes.

In collaboration with the group of Johannes Buchner (Munich), we could determine the binding affinities between the β-hairpin peptide and the Hsp70 chaperone Ssa1 or the Hsp40 co-chaperone Ydj1. The affinity of Ssa1 for the β-hairpin peptide is higher than the one of Ydj1. This raises the possibility that the newly synthesized β-barrel proteins are first recognized by the more specific Hsp40 co-chaperones which then transfer them to the general Hsp70 chaperone system. However, experimental proof for such a sequential binding is still lacking.

Irrespective of the binding order, once the chaperones are bound to mitochondrial β-barrel proteins they perform two important functions. They keep the newly synthesized proteins in an import-competent conformation by preventing both tight folding as well as aggregation and they can actively help in targeting the β-barrel proteins to the mitochondria by docking to the import receptor Tom70. Interactions of Hsp70 and Hsp90 chaperones with IMM carrier proteins and their relevance for the import of these proteins by binding to Tom70 have previously been reported (Young *et al.* 2003).

To date, most studies reached the conclusion that Tom20 is the main import receptor for mitochondrial β-barrel proteins (Söllner *et al.* 1989; Rapaport and Neupert 1999; Schleiff *et al.* 1999; Krimmer *et al.* 2001; Yamano *et al.* 2008). Indeed, we could show that a β-hairpin motif that serves as a targeting signal for β-barrel proteins binds to the import receptor Tom20 in the MTS binding groove. The results contained in this thesis argue also for an involvement of Tom70 in the biogenesis of β-barrel proteins. This involvement could even be twofold. First, Tom70 can serve as a primary docking site for cytosolic Hsp70 chaperones that are associated with newly synthesized β-barrel proteins. I could show that blocking this Tom70/Hsp70 interaction hampers the import of β-barrel proteins. Secondly, Tom70 can probably recognize the targeting signal of β-barrel proteins directly. This idea is supported by the observation of photo-adducts between Tom70 and a cyclic β-hairpin peptide. Moreover, a binding groove for MTSs was also identified on the surface of Tom70 (Melin *et al.* 2015). Therefore, it is possible that a β-hairpin motif will also bind to this area on Tom70.

Taken together, the findings presented in this thesis give rise to a new working model for the early stages of the biogenesis of mitochondrial β-barrel proteins (Fig. 4): Mitochondrial β-barrel proteins are encoded and transcribed in the nucleus (1). Concomitant with, or shortly after, their synthesis on cytosolic ribosomes (2), the β-barrel proteins associate with cytosolic (co-)chaperones including the Hsp70 proteins Ssa1 and Ssa2, as well as the Hsp40 co-chaperones Ydj1 and Sis1. The (co-)chaperones keep the newly synthesized β-barrel proteins in an import-competent conformation on their way to the mitochondria (3). Upon reaching the mitochondrial surface, the Hsp70 chaperones can dock on the import receptor Tom70, while a dedicated β-hairpin element, that serves as a targeting signal for β-barrel proteins, is recognized by the receptor Tom20. Following recognition by the import receptors, the β-barrel proteins are translocated across the OMM by the TOM complex (4).

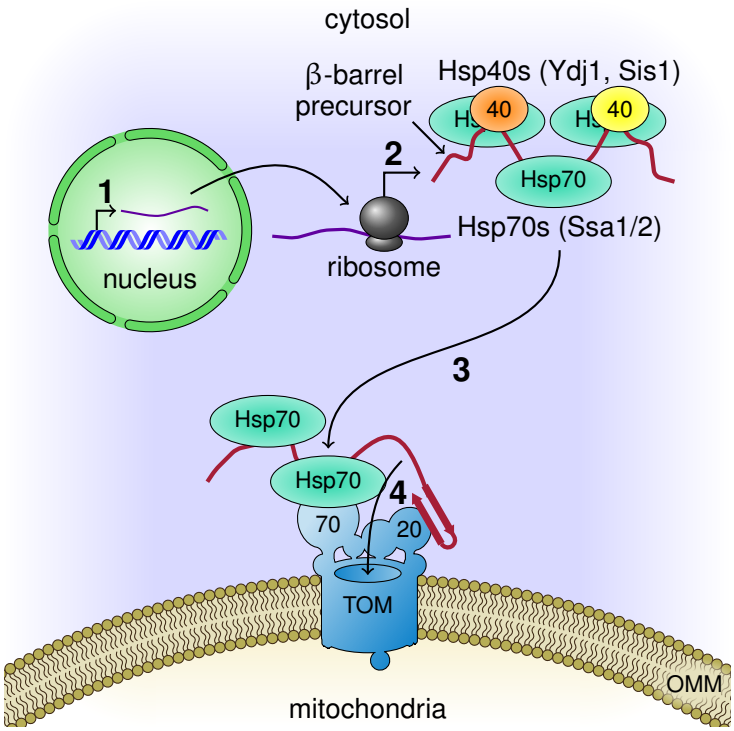

Figure 4: Working model for the early events in the biogenesis of mitochondrial β-barrel proteins. See text for details.

10 References

Abe, Y., T. Shodai, T. Muto, K. Mihara, H. Torii, S. Nishikawa, T. Endo, and D. Kohda (2000). Structural basis of presequence recognition by the mitochondrial protein import receptor Tom20. *Cell* 100 (5), 551–560.

Adrian, G. S., M. T. McCammon, D. L. Montgomery, and M. G. Douglas (1986). Sequences required for delivery and localization of the ADP/ATP translocator to the mitochondrial inner membrane. *Molecular and Cellular Biology* 6 (2), 626–634.

Albrecht, R., M. Schütz, P. Oberhettinger, M. Faulstich, I. Bermejo, T. Rudel, K. Diederichs, and K. Zeth (2014). Structure of BamA, an essential factor in outer membrane protein biogenesis. *Acta Crystallographica. Section D, Biological Crystallography* 70 (Pt 6), 1779–1789.

Arnold, T., M. Poynor, S. Nussberger, A. N. Lupas, and D. Linke (2007). Gene duplication of the eight-stranded beta-barrel OmpX produces a functional pore: a scenario for the evolution of transmembrane beta-barrels. *Journal of Molecular Biology* 366 (4), 1174–1184.

Bayrhuber, M., T. Meins, M. Habeck, S. Becker, K. Giller, S. Villinger, C. Vonrhein, C. Griesinger, M. Zweckstetter, and K. Zeth (2008). Structure of the human voltage-dependent anion channel. *Proceedings of the National academy of Sciences of the United States of America* 105 (40), 15370–15375.

Beal, M. F. (2005). Mitochondria take center stage in aging and neurodegeneration. *Annals of Neurology* 58 (4), 495–505.

Becker, T., S. Pfannschmidt, B. Guiard, D. Stojanovski, D. Milenkovic, S. Kutik, N. Pfanner, C. Meisinger, and N. Wiedemann (2008). Biogenesis of the mitochondrial TOM complex: Mim1 promotes insertion and assembly of signal-anchored receptors. *Journal of Biological Chemistry* 283 (1), 120–127.

Becker, T., L.-S. Wenz, V. Krüger, W. Lehmann, J. M. Müller, L. Goroncy, N. Zufall, T. Lithgow, B. Guiard, A. Chacinska, R. Wagner, C. Meisinger, and N. Pfanner (2011). The mitochondrial import protein Mim1 promotes biogenesis of multispanning outer membrane proteins. *Journal of Cell Biology* 194 (3), 387–395.

Bhangoo, M. K., S. Tzankov, A. C. Y. Fan, K. Dejgaard, D. Y. Thomas, and J. C. Young (2007). Multiple 40-kDa heat-shock protein chaperones function in Tom70-dependent mitochondrial import. *Molecular Biology of the Cell* 18 (9), 3414–3428.

Blachly-Dyson, E., J. Song, W. J. Wolfgang, M. Colombini, and M. Forte (1997). Multicopy suppressors of phenotypes resulting from the absence of yeast VDAC encode a VDAC-like protein. *Molecular and Cellular Biology* 17 (10), 5727–5738.

Borgese, N., I. Gazzoni, M. Barberi, S. Colombo, and E. Pedrazzini (2001). Targeting of a tail-anchored protein to endoplasmic reticulum and mitochondrial outer membrane by independent but competing pathways. *Molecular Biology of the Cell* 12 (8), 2482–2496.

Böttinger, L., L. Ellenrieder, and T. Becker (2015). How lipids modulate mitochondrial protein import. *Journal of Bioenergetics and Biomembranes* 48(2), 125–135.

Bratic, A. and N.-G. Larsson (2013). The role of mitochondria in aging. *Journal of Clinical Investigation* 123 (3), 951–957.

Brix, J., K. Dietmeier, and N. Pfanner (1997). Differential recognition of preproteins by the purified cytosolic domains of the mitochondrial import receptors Tom20, Tom22, and Tom70. *Journal of Biological Chemistry* 272 (33), 20730–20735.

Caplan, A. J., D. M. Cyr, and M. G. Douglas (1992). YDJ1p facilitates polypeptide translocation across different intracellular membranes by a conserved mechanism. *Cell* 71 (7), 1143–1155.

Chacinska, A., S. Pfannschmidt, N. Wiedemann, V. Kozjak, L. K. Sanjuán Szklarz, A. Schulze-Specking, K. N. Truscott, B. Guiard, C. Meisinger, and N. Pfanner (2004). Essential role of Mia40 in import and assembly of mitochondrial intermembrane space proteins. *EMBO Journal* 23 (19), 3735–3746.

Chan, N. C. and T. Lithgow (2008). The peripheral membrane subunits of the SAM complex function codependently in mitochondrial outer membrane biogenesis. *Molecular Biology of the Cell* 19 (1), 126–136.

Chang, S. C., P. N. Heacock, E. Mileykovskaya, D. R. Voelker, and W. Dowhan (1998). Isolation and characterization of the gene (CLS1) encoding cardiolipin synthase in Saccharomyces cerevisiae. *Journal of Biological Chemistry* 273 (24), 14933–14941.

Chatterjee, A., S. Dasgupta, and D. Sidransky (2011). Mitochondrial subversion in cancer. *Cancer Prevention Research* 4 (5), 638–654.

Chen, S., P. G. Schultz, and A. Brock (2007). An improved system for the generation and analysis of mutant proteins containing unnatural amino acids in Saccharomyces cerevisiae. *Journal of Molecular Biology* 371 (1), 112–122.

Clerico, E. M., J. M. Tilitsky, W. Meng, and L. M. Gierasch (2015). How Hsp70 molecular machines interact with their substrates to mediate diverse physiological functions. *Journal of Molecular Biology* 427 (7), 1575–1588.

Craig, E. A. and J. Marszalek (2017). How Do J-Proteins Get Hsp70 to Do So Many Different Things? *Trends in Biochemical Sciences* 42(5), 355–368.

Cyr, D. M. and C. H. Ramos (2014). Specification of Hsp70 Function by Type I and Type II Hsp40. In: *Subcellular Biochemistry*. Springer International Publishing, 91–102.

Daugaard, M., M. Rohde, and M. Jäättelä (2007). The heat shock protein 70 family: Highly homologous proteins with overlapping and distinct functions. *FEBS Letters* 581(19), 3702–3710.

Davis, A. J., N. N. Alder, R. E. Jensen, and A. E. Johnson (2007). The Tim9p/10p and Tim8p/13p complexes bind to specific sites on Tim23p during mitochondrial protein import. *Molecular Biology of the Cell* 18 (2), 475–486.

Deshaies, R. J., B. D. Koch, M. Werner-Washburne, E. A. Craig, and R. Schekman (1988). A subfamily of stress proteins facilitates translocation of secretory and mitochondrial precursor polypeptides. *Nature* 332 (6167), 800–805.

Diekert, K., G. Kispal, B. Guiard, and R. Lill (1999). An internal targeting signal directing proteins into the mitochondrial intermembrane space. *Proceedings of the National Academy of Sciences of the United States of America* 96 (21), 11752–11757.

Dimmer, K. S., D. Papić, B. Schumann, D. Sperl, K. Krumpe, D. M. Walther, and D. Rapaport (2012). A crucial role for Mim2 in the biogenesis of mitochondrial outer membrane proteins. *Journal of Cell Science* 125 (14), 3464–3473.

Elbaz-Alon, Y. (2017). Mitochondria-organelle contact sites: the plot thickens. *Biochemical Society Transactions* 45 (2), 477–488.

Ellenrieder, L., C. U. Mårtensson, and T. Becker (2015). Biogenesis of mitochondrial outer membrane proteins, problems and diseases. *Biological Chemistry* 396(11).

Ellenrieder, L., Ł. Opaliński, L. Becker, V. Krüger, O. Mirus, S. P. Straub, K. Ebell, N. Flinner, S. B. Stiller, B. Guiard, C. Meisinger, N. Wiedemann, E. Schleiff, R. Wagner, N. Pfanner, and T. Becker (2016). Separating mitochondrial protein assembly and endoplasmic reticulum tethering by selective coupling of Mdm10. *Nature Communications* 7, 13021.

Endo, T., S. Mitsui, M. Nakai, and D. Roise (1996). Binding of mitochondrial presequences to yeast cytosolic heat shock protein 70 depends on the amphiphilicity of the presequence. *Journal of Biological Chemistry* 271 (8), 4161–4167.

Ferramosca, A. and V. Zara (2013). Biogenesis of mitochondrial carrier proteins: molecular mechanisms of import into mitochondria. *Biochimica et Biophysica Acta* 1833 (3), 494–502.

Gabriel, K., D. Milenkovic, A. Chacinska, J. Müller, B. Guiard, N. Pfanner, and C. Meisinger (2007). Novel mitochondrial intermembrane space proteins as substrates of the MIA import pathway. *Journal of Molecular Biology* 365 (3), 612–620.

Gebert, N., A. S. Joshi, S. Kutik, T. Becker, M. McKenzie, X. L. Guan, V. P. Mooga, D. A. Stroud, G. Kulkarni, M. R. Wenk, P. Rehling, C. Meisinger, M. T. Ryan, N. Wiedemann, M. L. Greenberg, and N. Pfanner (2009). Mitochondrial Cardiolipin Involved in Outer-Membrane Protein Biogenesis: Implications for Barth Syndrome. *Current Biology* 19(24), 2133–2139.

Gentle, I., K. Gabriel, P. Beech, R. Waller, and T. Lithgow (2004). The Omp85 family of proteins is essential for outer membrane biogenesis in mitochondria and bacteria. *Journal of Cell Biology* 164 (1), 19–24.

Glick, B. S., A. Brandt, K. Cunningham, S. Müller, R. L. Hallberg, and G. Schatz (1992). Cytochromes c1 and b2 are sorted to the intermembrane space of yeast mitochondria by a stop-transfer mechanism. *Cell* 69 (5), 809–822.

Gray, M. W. (2012). Mitochondrial evolution. *Cold Spring Harbor Perspectives in Biology* 4 (9), a011403.

Gupta, R. S. and G. B. Golding (1993). Evolution of HSP70 gene and its implications regarding relationships between archaebacteria, eubacteria, and eukaryotes. *Journal of Molecular Evolution* 37(6).

Habib, S. J., T. Waizenegger, M. Lech, W. Neupert, and D. Rapaport (2005). Assembly of the TOB complex of mitochondria. *Journal of Biological Chemistry* 280 (8), 6434–6440.

Hammen, P. K. and H. Weiner (1998). Mitochondrial leader sequences: structural similarities and sequence differences. *Journal of Experimental Zoology* 282 (1-2), 280–283.

Hecht, M. H. (1994). De novo design of beta-sheet proteins. *Proceedings of the National academy of Sciences of the United States of America* 91 (19), 8729–8730.

Heijne, G. von (1986). Mitochondrial targeting sequences may form amphiphilic helices. *EMBO Journal* 5 (6), 1335–1342.

Hell, K., J. M. Herrmann, E. Pratje, W. Neupert, and R. A. Stuart (1998). Oxa1p, an essential component of the N-tail protein export machinery in mitochondria. *Proceedings of the National academy of Sciences of the United States of America* 95 (5), 2250–2255.

Hell, K., W. Neupert, and R. A. Stuart (2001). Oxa1p acts as a general membrane insertion machinery for proteins encoded by mitochondrial DNA. *EMBO Journal* 20 (6), 1281–1288.

Hewitt, V. L., K. Gabriel, and A. Traven (2014). The ins and outs of the intermembrane space: diverse mechanisms and evolutionary rewiring of mitochondrial protein import routes. *Biochimica et Biophysica Acta* 1840 (4), 1246–1253.

Hiller, S., R. G. Garces, T. J. Malia, V. Y. Orekhov, M. Colombini, and G. Wagner (2008). Solution structure of the integral human membrane protein VDAC-1 in detergent micelles. *Science* 321 (5893), 1206–1210.

Hines, V., A. Brandt, G. Griffiths, H. Horstmann, H. Brütsch, and G. Schatz (1990). Protein import into yeast mitochondria is accelerated by the outer membrane protein MAS70. *EMBO Journal* 9 (10), 3191–3200.

Hoffmann, H. P. and C. J. Avers (1973). Mitochondrion of yeast: ultrastructural evidence for one giant, branched organelle per cell. *Science* 181 (4101), 749–751.

Höhr, A. I. C., C. Lindau, C. Wirth, J. Qiu, D. A. Stroud, S. Kutik, B. Guiard, C. Hunte, T. Becker, N. Pfanner, and N. Wiedemann (2018). Membrane protein insertion through a mitochondrial β-barrel gate. *Science* 359(6373).

Hoiczyk, E., A. Roggenkamp, M. Reichenbecher, A. Lupas, and J. Heesemann (2000). Structure and sequence analysis of *Yersinia* YadA and *Moraxella* UspAs reveal a novel class of adhesins. *EMBO journal* 19 (22), 5989–5999.

Hönlinger, A., M. Kübrich, M. Moczko, F. Gärtner, L. Mallet, F. Bussereau, C. Eckerskorn, F. Lottspeich, K. Dietmeier, and M. Jacquet (1995). The mitochondrial receptor complex: Mom22 is essential for cell viability and directly interacts with preproteins. *Molecular and Cellular Biology* 15(6), 3382–3389.

Horie, C., H. Suzuki, M. Sakaguchi, and K. Mihara (2002). Characterization of signal that directs C-tail-anchored proteins to mammalian mitochondrial outer membrane. *Molecular Biology of the Cell* 13 (5), 1615–1625.

Hwang, S. T. and G. Schatz (1989). Translocation of proteins across the mitochondrial inner membrane, but not into the outer membrane, requires nucleoside triphosphates in the matrix. *Proceedings of the National academy of Sciences of the United States of America* 86(21), 8432–8436.

Iadanza, M. G., A. J. Higgins, B. Schiffrin, A. N. Calabrese, D. J. Brockwell, A. E. Ashcroft, S. E. Radford, and N. A. Ranson (2016). Lateral opening in the intact β-barrel assembly machinery captured by cryo-EM. *Nature Communications* 7, 12865.

Jores, T. (2013). The β-hairpin motif functions as a targeting signal in mitochondrial β-barrel proteins. *Diploma thesis*. University of Tübingen.

Jores, T., A. Klinger, L. E. Groß, S. Kawano, N. Flinner, E. Duchardt-Ferner, J. Wöhnert, H. Kalbacher, T. Endo, E. Schleiff, and D. Rapaport (2016). Characterization of the targeting signal in mitochondrial β-barrel proteins. *Nature Communications* 7, 12036.

Jores, T., J. Lawatscheck, V. Beke, M. Franz-Wachtel, K. Yunoki, B. Macek, T. Endo, H. Kalbacher, J. Buchner, and D. Rapaport (2017). Cytosolic Hsp70 and Hsp40 chaperones enable the biogenesis of mitochondrial β-barrel proteins. *in revision*.

Kampinga, H. H. and E. A. Craig (2010). The HSP70 chaperone machinery: J proteins as drivers of functional specificity. *Nature Reviews. Molecular Cell Biology* 11 (8), 579–592.

Kanaji, S., J. Iwahashi, Y. Kida, M. Sakaguchi, and K. Mihara (2000). Characterization of the signal that directs Tom20 to the mitochondrial outer membrane. *Journal of Cell Biology* 151 (2), 277–288.

Keil, M., B. Bareth, M. W. Woellhaf, V. Peleh, M. Prestele, P. Rehling, and J. M. Herrmann (2012). Oxa1-ribosome complexes coordinate the assembly of cytochrome C oxidase in mitochondria. *Journal of Biological Chemistry* 287 (41), 34484–34493.

Keil, P., A. Weinzierl, M. Kiebler, K. Dietmeier, T. Söllner, and N. Pfanner (1993). Biogenesis of the mitochondrial receptor complex. Two receptors are required for binding of MOM38 to the outer membrane surface. *Journal of Biological Chemistry* 268 (26), 19177–19180.

Kemper, C., S. J. Habib, G. Engl, P. Heckmeyer, K. S. Dimmer, and D. Rapaport (2008). Integration of tail-anchored proteins into the mitochondrial outer membrane does not require any known import components. *Journal of Cell Science* 121 (12), 1990–1998.

Kim, Y. E., M. S. Hipp, A. Bracher, M. Hayer-Hartl, and F. U. Hartl (2013). Molecular chaperone functions in protein folding and proteostasis. *Annual Review of Biochemistry* 82, 323–355.

Kornmann, B., E. Currie, S. R. Collins, M. Schuldiner, J. Nunnari, J. S. Weissman, and P. Walter (2009). An ER-mitochondria tethering complex revealed by a synthetic biology screen. *Science* 325 (5939), 477–481.

Kozjak-Pavlovic, V., C. Ott, M. Götz, and T. Rudel (2011). Neisserial Omp85 protein is selectively recognized and assembled into functional complexes in the outer membrane of human mitochondria. *Journal of Biological Chemistry* 286 (30), 27019–27026.

Krimmer, T., D. Rapaport, M. T. Ryan, C. Meisinger, C. K. Kassenbrock, E. Blachly-Dyson, M. Forte, M. G. Douglas, W. Neupert, F. E. Nargang, and N. Pfanner (2001). Biogenesis of porin of the outer mitochondrial membrane involves an import pathway via receptors and the general import pore of the TOM complex. *Journal of Cell Biology* 152 (2), 289–300.

Krumpe, K., I. Frumkin, Y. Herzig, N. Rimon, C. Özbalci, B. Brügger, D. Rapaport, and M. Schuldiner (2012). Ergosterol content specifies targeting of tail-anchored proteins to mitochondrial outer membranes. *Molecular Biology of the Cell* 23 (20), 3927–3935.

Kutik, S., M. Rissler, X. L. Guan, B. Guiard, G. Shui, N. Gebert, P. N. Heacock, P. Rehling, W. Dowhan, M. R. Wenk, N. Pfanner, and N. Wiedemann (2008a). The translocator maintenance protein Tam41 is required for mitochondrial cardiolipin biosynthesis. *Journal of Cell Biology* 183(7), 1213–1221.

Kutik, S., D. Stojanovski, L. Becker, T. Becker, M. Meinecke, V. Krüger, C. Prinz, C. Meisinger, B. Guiard, R. Wagner, N. Pfanner, and N. Wiedemann (2008b). Dissecting membrane insertion of mitochondrial beta-barrel proteins. *Cell* 132 (6), 1011–1024.

Li, J., X. Qian, J. Hu, and B. Sha (2009). Molecular chaperone Hsp70/Hsp90 prepares the mitochondrial outer membrane translocon receptor Tom71 for preprotein loading. *Journal of Biological Chemistry* 284 (35), 23852–23859.

Li, J. and B. Sha (2004). Peptide substrate identification for yeast Hsp40 Ydj1 by screening the phage display library. *Biological Procedures Online* 6, 204–208.

Linke, D., T. Riess, I. B. Autenrieth, A. Lupas, and V. A. J. Kempf (2006). Trimeric autotransporter adhesins: variable structure, common function. *Trends in Microbiology* 14 (6), 264–270.

Malhotra, K., A. Modak, S. Nangia, T. H. Daman, U. Gunsel, V. L. Robinson, D. Mokranjac, E. R. May, and N. N. Alder (2017). Cardiolipin mediates membrane and channel interactions of the mitochondrial TIM23 protein import complex receptor Tim50. *Science Advances* 3(9), e1700532.

Mayer, A., F. Nargang, W. Neupert, and R. Lill (1995). MOM22 is a receptor for mitochondrial targeting sequences and cooperates with MOM19. *EMBO Journal* 14(17), 4204–4211.

Melin, J., M. Kilisch, P. Neumann, O. Lytovchenko, R. Gomkale, A. Schendzielorz, B. Schmidt, T. Liepold, R. Ficner, O. Jahn, P. Rehling, and C. Schulz (2015). A presequence-binding groove in Tom70 supports import of Mdl1 into mitochondria. *Biochimica et Biophysica Acta* 1853 (8), 1850–1859.

Milenkovic, D., K. Gabriel, B. Guiard, A. Schulze-Specking, N. Pfanner, and A. Chacinska (2007). Biogenesis of the essential Tim9-Tim10 chaperone complex of mitochondria: site-specific recognition of cysteine residues by the intermembrane space receptor Mia40. *Journal of Biological Chemistry* 282 (31), 22472–22480.

Milenkovic, D., V. Kozjak, N. Wiedemann, C. Lohaus, H. E. Meyer, B. Guiard, N. Pfanner, and C. Meisinger (2004). Sam35 of the mitochondrial protein sorting and assembly machinery is a peripheral outer membrane protein essential for cell viability. *Journal of Biological Chemistry* 279 (21), 22781–22785.

Milenkovic, D., T. Ramming, J. M. Müller, L.-S. Wenz, N. Gebert, A. Schulze-Specking, D. Stojanovski, S. Rospert, and A. Chacinska (2009). Identification of the signal directing Tim9 and Tim10 into the intermembrane space of mitochondria. *Molecular Biology of the Cell* 20 (10), 2530–2539.

Millar, D. G. and G. C. Shore (1996). Signal anchor sequence insertion into the outer mitochondrial membrane: comparison with Porin and the matrix protein targeting pathway. *Journal of Biological Chemistry* 271(42), 25823–25829.

Moczko, M., F. Gärtner, and N. Pfanner (1993). The protein import receptor MOM19 of yeast mitochondria. *FEBS Letters* 326 (1-3), 251–254.

Mokranjac, D. and W. Neupert (2010). The many faces of the mitochondrial TIM23 complex. *Biochimica et Biophysica Acta* 1797 (6-7), 1045–1054.

Müller, A., J. Rassow, J. Grimm, N. Machuy, T. F. Meyer, and T. Rudel (2002). VDAC and the bacterial porin PorB of *Neisseria gonorrhoeae* share mitochondrial import pathways. *EMBO Journal* 21 (8), 1916–1929.

Müller, J. E. N., D. Papic, T. Ulrich, I. Grin, M. Schütz, P. Oberhettinger, J. Tommassen, D. Linke, K. S. Dimmer, I. B. Autenrieth, and D. Rapaport (2011). Mitochondria can recognize and assemble fragments of a beta-barrel structure. *Molecular Biology of the Cell* 22 (10), 1638–1647.

Nakamura, Y., H. Suzuki, M. Sakaguchi, and K. Mihara (2004). Targeting and assembly of rat mitochondrial translocase of outer membrane 22 (TOM22) into the TOM complex. *Journal of Biological Chemistry* 279 (20), 21223–21232.

Noinaj, N., A. J. Kuszak, J. C. Gumbart, P. Lukacik, H. Chang, N. C. Easley, T. Lithgow, and S. K. Buchanan (2013). Structural insight into the biogenesis of β-barrel membrane proteins. *Nature* 501 (7467), 385–390.

Okamoto, K. and J. M. Shaw (2005). Mitochondrial morphology and dynamics in yeast and multicellular eukaryotes. *Annual Review of Genetics* 39, 503–536.

Osman, C., M. Haag, F. T. Wieland, B. Brügger, and T. Langer (2010). A mitochondrial phosphatase required for cardiolipin biosynthesis: the PGP phosphatase Gep4. *EMBO Journal* 29(12), 1976–1987.

Osman, C., D. R. Voelker, and T. Langer (2011). Making heads or tails of phospholipids in mitochondria. *Journal of Cell Biology* 192 (1), 7–16.

Otera, H., Y. Taira, C. Horie, Y. Suzuki, H. Suzuki, K. Setoguchi, H. Kato, T. Oka, and K. Mihara (2007). A novel insertion pathway of mitochondrial outer membrane proteins with multiple transmembrane segments. *Journal of Cell Biology* 179 (7), 1355–1363.

Papić, D., Y. Elbaz-Alon, S. N. Koerdt, K. Leopold, D. Worm, M. Jung, M. Schuldiner, and D. Rapaport (2013). The role of Djp1 in import of the mitochondrial protein Mim1 demonstrates specificity between a cochaperone and its substrate protein. *Molecular and Cellular Biology* 33 (20), 4083–4094.

Papić, D., K. Krumpe, J. Dukanovic, K. S. Dimmer, and D. Rapaport (2011). Multispan mitochondrial outer membrane protein Ugo1 follows a unique Mim1-dependent import pathway. *Journal of Cell Biology* 194 (3), 397–405.

Paschen, S. A., T. Waizenegger, T. Stan, M. Preuss, M. Cyrklaff, K. Hell, D. Rapaport, and W. Neupert (2003). Evolutionary conservation of biogenesis of beta-barrel membrane proteins. *Nature* 426 (6968), 862–866.

Pellegrini, M. (1980). Three-dimensional reconstruction of organelles in *Euglena gracilis Z.* I. Qualitative and quantitative changes of chloroplasts and mitochondrial reticulum in synchronous photoautotrophic culture. *Journal of Cell Science* 43, 137–166.

Pfanner, N. (2000). Protein sorting: recognizing mitochondrial presequences. *Current Biology* 10 (11), R412–R415.

Pfanner, N., P. Hoeben, M. Tropschug, and W. Neupert (1987). The carboxyl-terminal two-thirds of the ADP/ATP carrier polypeptide contains sufficient information to direct translocation into mitochondria. *Journal of Biological Chemistry* 262 (31), 14851–14854.

Pfanner, N. and W. Neupert (1986). Transport of F1-ATPase subunit β into mitochondria depends on both a membrane potential and nucleoside triphosphates. *FEBS Letters* 209 (2), 152–156.

Pfanner, N., R. Pfaller, R. Kleene, M. Ito, M. Tropschug, and W. Neupert (1988). Role of ATP in mitochondrial protein import. Conformational alteration of a precursor protein can substitute for ATP requirement. *Journal of Biological Chemistry* 263(9), 4049–4051.

Pfeffer, S., M. W. Woellhaf, J. M. Herrmann, and F. Förster (2015). Organization of the mitochondrial translation machinery studied in situ by cryoelectron tomography. *Nature Communications* 6, 6019.

Pierpaoli, E. V., E. Sandmeier, A. Baici, H. J. Schönfeld, S. Gisler, and P. Christen (1997). The power stroke of the DnaK/DnaJ/GrpE molecular chaperone system. *Journal of Molecular Biology* 269 (5), 757–768.

Pizzo, P. and T. Pozzan (2007). Mitochondria-endoplasmic reticulum choreography: structure and signaling dynamics. *Trends in Cell Biology* 17 (10), 511–517.

Pradelli, L. A., M. Bénéteau, and J.-E. Ricci (2010). Mitochondrial control of caspase-dependent and -independent cell death. *Cellular and Molecular Life Sciences* 67(10), 1589–1597.

Qiu, J., L.-S. Wenz, R. M. Zerbes, S. Oeljeklaus, M. Bohnert, D. A. Stroud, C. Wirth, L. Ellenrieder, N. Thornton, S. Kutik, S. Wiese, A. Schulze-Specking, N. Zufall, A. Chacinska, B. Guiard, C. Hunte, B. Warscheid, M. van der Laan, N. Pfanner, N. Wiedemann, and T. Becker (2013). Coupling of mitochondrial import and export translocases by receptor-mediated supercomplex formation. *Cell* 154 (3), 596–608.

Ramage, L., T. Junne, K. Hahne, T. Lithgow, and G. Schatz (1993). Functional cooperation of mitochondrial protein import receptors in yeast. *EMBO Journal* 12 (11), 4115–4123.

Rapaport, D. and W. Neupert (1999). Biogenesis of Tom40, core component of the TOM complex of mitochondria. *Journal of Cell Biology* 146 (2), 321–331.

Remmert, M., A. Biegert, D. Linke, A. N. Lupas, and J. Söding (2010). Evolution of outer membrane β-barrels from an ancestral ββ hairpin. *Molecular Biology and Evolution* 27(6), 1348–1358.

Ricci, L. and K. P. Williams (2008). Development of fluorescence polarization assays for the molecular chaperone Hsp70 family members: Hsp72 and DnaK. *Current Chemical Genomics* 2, 90–95.

Rodriguez-Cousiño, N., F. E. Nargang, R. Baardman, W. Neupert, R. Lill, and D. A. Court (1998). An import signal in the cytosolic domain of the Neurospora mitochondrial outer membrane protein TOM22. *Journal of Biological Chemistry* 273 (19), 11527–11532.

Saitoh, T., M. Igura, T. Obita, T. Ose, R. Kojima, K. Maenaka, T. Endo, and D. Kohda (2007). Tom20 recognizes mitochondrial presequences through dynamic equilibrium among multiple bound states. *EMBO Journal* 26 (22), 4777–4787.

Sauerwald, J., T. Jores, M. Eisenberg-Bord, S. G. Chuartzman, M. Schuldiner, and D. Rapaport (2015). Genome-wide screens in *Saccharomyces cerevisiae* highlight a role for cardiolipin in biogenesis of mitochondrial outer membrane multispan proteins. *Molecular and Cellular Biology* 35 (18), 3200–3211.

Schleiff, E., J. R. Silvius, and G. C. Shore (1999). Direct membrane insertion of voltage-dependent anion-selective channel protein catalyzed by mitochondrial Tom20. *Journal of Cell Biology* 145 (5), 973–978.

Schmid, D., A. Baici, H. Gehring, and P. Christen (1994). Kinetics of molecular chaperone action. *Science* 263 (5149), 971–973.

Schnaitman, C. and J. W. Greenawalt (1968). Enzymatic properties of the inner and outer membranes of rat liver mitochondria. *Journal of Cell Biology* 38 (1), 158–175.

Schneider, A., M. Behrens, P. Scherer, E. Pratje, G. Michaelis, and G. Schatz (1991). Inner membrane protease I, an enzyme mediating intramitochondrial protein sorting in yeast. *EMBO Journal* 10 (2), 247–254.

Schneider, M., M. Rosam, M. Glaser, A. Patronov, H. Shah, K. C. Back, M. A. Daake, J. Buchner, and I. Antes (2016). BiPPred: Combined sequence- and structure-based prediction of peptide binding to the Hsp70 chaperone BiP. *Proteins* 84 (10), 1390–1407.

Seth, R. B., L. Sun, C.-K. Ea, and Z. J. Chen (2005). Identification and characterization of MAVS, a mitochondrial antiviral signaling protein that activates NF-kappaB and IRF 3. *Cell* 122 (5), 669–682.

Setoguchi, K., H. Otera, and K. Mihara (2006). Cytosolic factor- and TOM-independent import of C-tail-anchored mitochondrial outer membrane proteins. *EMBO Journal* 25 (24), 5635–5647.

Sideris, D. P., N. Petrakis, N. Katrakili, D. Mikropoulou, A. Gallo, S. Ciofi-Baffoni, L. Banci, I. Bertini, and K. Tokatlidis (2009). A novel intermembrane space-targeting signal docks cysteines onto Mia40 during mitochondrial oxidative folding. *Journal of Cell Biology* 187 (7), 1007–1022.

Sinzel, M., T. Tan, P. Wendling, H. Kalbacher, C. Özbalci, X. Chelius, B. Westermann, B. Brügger, D. Rapaport, and K. S. Dimmer (2016). Mcp3 is a novel mitochondrial outer membrane protein that follows a unique IMP-dependent biogenesis pathway. *EMBO Reports* 17 (7), 965–981.

Smagula, C. and M. G. Douglas (1988). Mitochondrial import of the ADP/ATP carrier protein in *Saccharomyces cerevisiae*. Sequences required for receptor binding and membrane translocation. *Journal of Biological Chemistry* 263 (14), 6783–6790.

Sogo, L. F. and M. P. Yaffe (1994). Regulation of mitochondrial morphology and inheritance by Mdm10p, a protein of the mitochondrial outer membrane. *Journal of Cell Biology* 126 (6), 1361–1373.

Söllner, T., G. Griffiths, R. Pfaller, N. Pfanner, and W. Neupert (1989). MOM19, an import receptor for mitochondrial precursor proteins. *Cell* 59 (6), 1061–1070.

Söllner, T., R. Pfaller, G. Griffiths, N. Pfanner, and W. Neupert (1990). A mitochondrial import receptor for the ADP/ATP carrier. *Cell* 62 (1), 107–115.

Song, J., Y. Tamura, T. Yoshihisa, and T. Endo (2014). A novel import route for an N-anchor mitochondrial outer membrane protein aided by the TIM23 complex. *EMBO Reports* 15 (6), 670–677.

Steger, H. F., T. Söllner, M. Kiebler, K. A. Dietmeier, R. Pfaller, K. S. Trülzsch, M. Tropschug, W. Neupert, and N. Pfanner (1990). Import of ADP/ATP carrier into mitochondria: two receptors act in parallel. *Journal of Cell Biology* 111 (6), 2353–2363.

Szymański, J., J. Janikiewicz, B. Michalska, P. Patalas-Krawczyk, M. Perrone, W. Ziółkowski, J. Duszyński, P. Pinton, A. Dobrzyń, and M. R. Więckowski (2017). Interaction of Mitochondria with the Endoplasmic Reticulum and Plasma Membrane in Calcium Homeostasis, Lipid Trafficking and Mitochondrial Structure. *International Journal of Molecular Sciences* 18 (7).

Tamura, Y., T. Endo, M. Iijima, and H. Sesaki (2009). Ups1p and Ups2p antagonistically regulate cardiolipin metabolism in mitochondria. *Journal of Cell Biology* 185(6), 1029–1045.

Terasawa, K., M. Minami, and Y. Minami (2005). Constantly updated knowledge of Hsp90. *Journal of Biochemistry* 137 (4), 443–447.

Ujwal, R., D. Cascio, J.-P. Colletier, S. Faham, J. Zhang, L. Toro, P. Ping, and J. Abramson (2008). The crystal structure of mouse VDAC1 at 2.3 A resolution reveals mechanistic insights into metabolite gating. *Proceedings of the National academy of Sciences of the United States of America* 105 (46), 17742–17747.

Ulrich, T., L. E. Gross, M. S. Sommer, E. Schleiff, and D. Rapaport (2012). Chloroplast β-barrel proteins are assembled into the mitochondrial outer membrane in a process that depends on the TOM and TOB complexes. *Journal of Biological Chemistry* 287 (33), 27467–27479.

Ulrich, T., P. Oberhettinger, M. Schütz, K. Holzer, A. S. Ramms, D. Linke, I. B. Autenrieth, and D. Rapaport (2014). Evolutionary conservation in biogenesis of β-barrel proteins allows mitochondria to assemble a functional bacterial trimeric autotransporter protein. *Journal of Biological Chemistry* 289 (43), 29457–29470.

Vögtle, F.-N., M. Keller, A. A. Taskin, S. E. Horvath, X. L. Guan, C. Prinz, M. Opalińska, C. Zorzin, M. van der Laan, M. R. Wenk, R. Schubert, N. Wiedemann, M. Holzer, and C. Meisinger (2015). The fusogenic lipid phosphatidic acid promotes the biogenesis of mitochondrial outer membrane protein Ugo1. *Journal of Cell Biology* 210 (6), 951–960.

Vögtle, F.-N., S. Wortelkamp, R. P. Zahedi, D. Becker, C. Leidhold, K. Gevaert, J. Kellermann, W. Voos, A. Sickmann, N. Pfanner, and C. Meisinger (2009). Global analysis of the mitochondrial N-proteome identifies a processing peptidase critical for protein stability. *Cell* 139 (2), 428–439.

Waizenegger, T., T. Stan, W. Neupert, and D. Rapaport (2003). Signal-anchor domains of proteins of the outer membrane of mitochondria: structural and functional characteristics. *Journal of Biological Chemistry* 278 (43), 42064–42071.

Walsh, P., D. Bursać, Y. C. Law, D. Cyr, and T. Lithgow (2004). The J-protein family: modulating protein assembly, disassembly and translocation. *EMBO Reports* 5 (6), 567–571.

Walther, D. M., M. P. Bos, D. Rapaport, and J. Tommassen (2010). The mitochondrial porin, VDAC, has retained the ability to be assembled in the bacterial outer membrane. *Molecular Biology and Evolution* 27 (4), 887–895.

Walther, D. M., D. Papić, M. P. Bos, J. Tommassen, and D. Rapaport (2009a). Signals in bacterial beta-barrel proteins are functional in eukaryotic cells for targeting to and assembly in mitochondria. *Proceedings of the National academy of Sciences of the United States of America* 106 (8), 2531–2536.

Walther, D. M., D. Rapaport, and J. Tommassen (2009b). Biogenesis of beta-barrel membrane proteins in bacteria and eukaryotes: evolutionary conservation and divergence. *Cellular and Molecular Life Sciences* 66 (17), 2789–2804.

Wenz, L.-S., L. Ellenrieder, J. Qiu, M. Bohnert, N. Zufall, M. van der Laan, N. Pfanner, N. Wiedemann, and T. Becker (2015). Sam37 is crucial for formation of the mitochondrial TOM-SAM supercomplex, thereby promoting β-barrel biogenesis. *Journal of Cell Biology* 210 (7), 1047–1054.

Wenz, L.-S., L. Opaliński, M.-H. Schuler, L. Ellenrieder, R. Ieva, L. Böttinger, J. Qiu, M. van der Laan, N. Wiedemann, B. Guiard, N. Pfanner, and T. Becker (2014). The presequence pathway is involved in protein sorting to the mitochondrial outer membrane. *EMBO Reports* 15 (6), 678–685.

Wiedemann, N., N. Pfanner, and M. T. Ryan (2001). The three modules of ADP/ATP carrier cooperate in receptor recruitment and translocation into mitochondria. *EMBO Journal* 20 (5), 951–960.

Wiedemann, N., V. Kozjak, A. Chacinska, B. Schönfisch, S. Rospert, M. T. Ryan, N. Pfanner, and C. Meisinger (2003). Machinery for protein sorting and assembly in the mitochondrial outer membrane. *Nature* 424 (6948), 565–571.

Yamamoto, H., K. Fukui, H. Takahashi, S. Kitamura, T. Shiota, K. Terao, M. Uchida, M. Esaki, S.-i. Nishikawa, T. Yoshihisa, K. Yamano, and T. Endo (2009). Roles of Tom70 in import of presequence-containing mitochondrial proteins. *Journal of Biological Chemistry* 284 (46), 31635–31646.

Yamano, K., S. Tanaka-Yamano, and T. Endo (2010). Mdm10 as a dynamic constituent of the TOB/SAM complex directs coordinated assembly of Tom40. *EMBO Reports* 11 (3), 187–193.

Yamano, K., Y.-I. Yatsukawa, M. Esaki, A. E. A. Hobbs, R. E. Jensen, and T. Endo (2008). Tom20 and Tom22 share the common signal recognition pathway in mitochondrial protein import. *Journal of Biological Chemistry* 283 (7), 3799–3807.

Yang, M., R. E. Jensen, M. P. Yaffe, W. Oppliger, and G. Schatz (1988). Import of proteins into yeast mitochondria: the purified matrix processing protease contains two subunits which are encoded by the nuclear MAS1 and MAS2 genes. *EMBO Journal* 7 (12), 3857–3862.

Young, J. C., I. Moarefi, and F. U. Hartl (2001). Hsp90: a specialized but essential protein-folding tool. *Journal of Cell Biology* 154 (2), 267–273.

Young, J. C., N. J. Hoogenraad, and F. U. Hartl (2003). Molecular chaperones Hsp90 and Hsp70 deliver preproteins to the mitochondrial import receptor Tom70. *Cell* 112 (1), 41–50.

Zanphorlin, L. M., T. B. Lima, M. J. Wong, T. S. Balbuena, C. A. S. A. Minetti, D. P. Remeta, J. C. Young, L. R. S. Barbosa, F. C. Gozzo, and C. H. I. Ramos (2016). Heat shock protein 90 kDa (Hsp90) has a second functional interaction site with the mitochondrial import receptor Tom70. *Journal of Biological Chemistry* 291 (36), 18620–18631.

11 Acknowledgements

First of all, I would like to thank Prof. Dr. Doron Rapaport for hosting me in his lab and for the interesting projects he entrusted to me. I am especially grateful for his extensive support and guidance as well as for his optimism when things did not go as planned.

I am happy to work in a lab with so many wonderful colleagues that created a nice working atmosphere. I am grateful for all the scientific and nonsensical discussions, for the activities in and outside of the lab and for all the help and support they offered. Additionally, I would like to thank them for the bravery to try and eat all my cake concoctions even in the face of imminent diabetes.

Special thanks go to Julia Sauerwald for trusting me with her project, for her support in scientific and personal matters, for always cheering me up and for her unwaivering belief in me. To Dr. Kai Stefan Dimmer and Monika Sinzel for critically reading this manuscript and for the help, materials and methods they shared with me. Again to Moni for sharing breakfast cakes and afternoon cokes. To Thomas Ulrich and Dražen Papić for introducing me to the work in the lab and for their patience during this time. To Elena Kracker for her excellent technical assistance and for preventing the lab from drifting into absolute chaos. To Janani Natarajan for all the silly jokes and for extending lunch time. To Daniela Vitali for not laughing at my attempts to speak italian and for always being entertaining. To Diana Antunes for sharing a bench and a pipette and for pushing me to visit the gym more often. To Ravi Singhal for his food and drinks. To Bogdan Cichocki for his curses and his pierogi. To Hoda for her many timer cakes. To Fenja Odendall, Layla Drwesh and Jialin Zhou for taking over when we leave and for being eager students. To my bachelor and master students Dominik Brücher, Vanessa Hertlein, Carina Bergmann, Saroj Pandey and Viktor Beke for their help with my projects.

Furthermore, I would like to thank Hubert Kalbacher for supplying me with peptides, encouragement and praise. Thanks go to my collaboration partners in Tübingen, Frankfurt, Munich, Tokyo, Grenoble and Prague for their contributions to my work and for entrusting me with part of theirs.

I would also like to thank all my friends for the fun times we had and for being there when needed. Further thanks go to the acrobats of Tübingen for taking me in and giving me lots of good reasons to leave the lab for.

Last but not least I am especially grateful towards my parents for the unconditional support and love and for always having faith in me!

12 Appendix

a) Accepted articles

1. Sauerwald, J.[*], **T. Jores**[*], M. Eisenberg-Bord, S. G. Chuartzman, M. Schuldiner, and D. Rapaport (2015). Genome-wide screens in *Saccharomyces cerevisiae* highlight a role for cardiolipin in biogenesis of mitochondrial outer membrane multispan proteins. *Molecular and Cellular Biology* 35 (18), 3200–3211.
   [*] equal contributors.

    doi:10.1128/MCB.00107-15.

2. **Jores**, **T.**, A. Klinger, L. E. Groß, S. Kawano, N. Flinner, E. Duchardt-Ferner, J. Wöhnert, H. Kalbacher, T. Endo, E. Schleiff, and D. Rapaport (2016). Characterization of the targeting signal in mitochondrial β-barrel proteins. *Nature Communications* 7, 12036.

    doi:10.1038/ncomms12036.

3. Hoseini, H., S. Pandey, **T. Jores**, A. Schmitt, M. Franz-Wachtel, B. Macek, J. Buchner, K. S. Dimmer, and D. Rapaport (2016). The cytosolic cochaperone Sti1 is relevant for mitochondrial biogenesis and morphology. *FEBS Journal* 283 (18), 3338–3352.

 doi:10.1111/febs.13813. Reprint license number 4223720262672.

4. **Jores**, **T.** and D. Rapaport (2017). Early stages in the biogenesis of eukaryotic β-barrel proteins. *FEBS Letters* 591 (17), 2671–2681.

 doi:10.1002/1873-3468.12726. Reprint license number 4223720067895.

MCB
Journals.ASM.org

Genome-Wide Screens in *Saccharomyces cerevisiae* Highlight a Role for Cardiolipin in Biogenesis of Mitochondrial Outer Membrane Multispan Proteins

Julia Sauerwald,[a]* Tobias Jores,[a] Michal Eisenberg-Bord,[b] Silvia Gabriela Chuartzman,[b] Maya Schuldiner,[b] Doron Rapaport[a]

Interfaculty Institute of Biochemistry, University of Tuebingen, Tuebingen, Germany[a]; Department of Molecular Genetics, Weizmann Institute of Science, Rehovot, Israel[b]

A special group of mitochondrial outer membrane (MOM) proteins spans the membrane several times via multiple helical segments. Such multispan proteins are synthesized on cytosolic ribosomes before their targeting to mitochondria and insertion into the MOM. Previous work recognized the import receptor Tom70 and the mitochondrial import (MIM) complex, both residents of the MOM, as required for optimal biogenesis of these proteins. However, their involvement is not sufficient to explain either the entire import pathway or its regulation. To identify additional factors that are involved in the biogenesis of MOM multispan proteins, we performed complementary high-throughput visual and growth screens in *Saccharomyces cerevisiae*. Cardiolipin (CL) synthase (Crd1) appeared as a candidate in both screens. Our results indeed demonstrate lower steady-state levels of the multispan proteins Ugo1, Scm4, and Om14 in mitochondria from *crd1*Δ cells. Importantly, MOM single-span proteins were not affected by this mutation. Furthermore, organelles lacking Crd1 had a lower *in vitro* capacity to import newly synthesized Ugo1 and Scm4 molecules. Crd1, which is located in the mitochondrial inner membrane, condenses phosphatidylglycerol together with CDP-diacylglycerol to obtain *de novo* synthesized CL molecules. Hence, our findings suggest that CL is an important component in the biogenesis of MOM multispan proteins.

All mitochondrial outer membrane (MOM) proteins are nuclearly encoded and synthesized on cytosolic ribosomes. Therefore, they have to bear proper signals that ensure both their correct import into the organelle and their ability to acquire different topologies in the lipid bilayer. None of the known MOM proteins contain a canonical cleavable N-terminal presequence; rather, they carry internal noncleavable targeting and sorting signals that are difficult to identify (1). Multispan proteins comprise a distinct class of such proteins embedded into the lipid bilayer via multiple α-helical transmembrane segments (TMS) that are interconnected by loops. Some of them, like Fzo1 in yeast (Mfn1/2 in mammals), cross the membrane twice, exposing N- and C-terminal domains toward the cytosol. Additional multispan MOM proteins with three or more TMSs are, for example, Ugo1, Scm4, and Om14 in *Saccharomyces cerevisiae* and the human peripheral benzodiazepine receptor (PBR). Members of this group fulfil various functions such as serving as a mitochondrial receptor for cytosolic ribosomes (Om14) or mediating mitochondrial fusion and dynamics (Fzo1 and Ugo1).

Studies on the import pathway of multispan proteins suggested that import receptors appear to play a role in the membrane integration of these proteins. For example, Fzo1 was reported to require a protease-sensitive import receptor(s) for its integration into the MOM (2). Furthermore, import of PBR and Mfn2 into mammalian organelles involves interactions with Tom70 and an unknown intermembrane space (IMS) component but is independent of other components of the translocase of the outer membrane (TOM) (3). Recently, we and others reported on a unique import pathway in yeast for MOM multispan proteins (4, 5). This pathway involves the import receptor Tom70 but not its partner, Tom20, in the initial recognition of the multispan precursor proteins. Other TOM subunits and components residing in the mitochondrial IMS were not required for this process. On the other hand, the MOM protein Mim1 was found to play a crucial role in the membrane integration of these proteins (4, 5). In a subsequent study, the novel protein Mim2 was demonstrated to interact with Mim1 and to form with the latter the functional MIM insertase complex (6).

Despite the recent progress, the full mechanism by which multispan proteins are recognized and inserted into the MOM remains poorly defined. To shed new light on this process, we performed two high-throughput screens covering all yeast mutants' backgrounds using the model multispan protein Om14. The first screen was based on the ability to visually monitor the correct intracellular distribution of the green fluorescent protein-Om14 (GFP-Om14) fusion protein on all yeast mutant backgrounds. The second screen included the ability of strains expressing the chimeric protein Ura3-Om14-Degron to grow on medium lacking uracil as a probe for the correct membrane topology of the

Received 28 January 2015 **Returned for modification** 18 February 2015
Accepted 26 June 2015

Accepted manuscript posted online 6 July 2015

Citation Sauerwald J, Jores T, Eisenberg-Bord M, Chuartzman SG, Schuldiner M, Rapaport D. 2015. Genome-wide screens in *Saccharomyces cerevisiae* highlight a role for cardiolipin in biogenesis of mitochondrial outer membrane multispan proteins. Mol Cell Biol 35:3200–3211. doi:10.1128/MCB.00107-15.

Address correspondence to Maya Schuldiner, maya.schuldiner@weizmann.ac.il, or Dororn Rapaport, doron.rapaport@uni-tuebingen.de.

* Present address: Julia Sauerwald, Institute of Molecular Life Sciences, University of Zurich, Zurich, Switzerland.

J.S. and T.J. contributed equally to this article.

Supplemental material for this article may be found at http://dx.doi.org/10.1128/MCB.00107-15.

doi:10.1128/MCB.00107-15

TABLE 1 Yeast strains used in this study

Strain	Mating type	Genotype	Source or reference
BY4741	*MAT***a**	S288C *his3Δ1 leu2Δ0 met15Δ0 ura3Δ0*	Euroscarf
YMS116	*MAT***a**	S288C *his3Δ1 leu2Δ0 met15Δ0 ura3Δ0::KAN*^{R}	ATCC
YMS135	*MAT*α	S288C *his3Δ1 leu2Δ0 lys2*$^+$ *met15Δ0 ura3Δ0 can1Δ::STE2pr-spHIS5 lyp1Δ*	25
YMS721	*MAT*α	S288C *his3Δ1 leu2Δ0 met15Δ0ura3Δ0 can1Δ::STE2pr-spHIS5 lyp1Δ::STE3pr-LEU2*	23
YMS1169	*MAT*α	S288C *his3Δ1::TEF2pr-Cherry::URA3 leu2Δ0 lys2*$^+$ *lys*$^+$ *met15Δ0 ura3Δ0 can1Δ::STE2pr-spHIS5 lyp1Δ::STE3pr-LEU2*	23
YMS1641	*MAT*α	YMS1169 *om14Δ::Nat*^{R}*::ADHpr-GFP-OM14*	Dalia Elinger
YJS01	*MAT*α	YMS721 *ugo1Δ::Nat*^{R}*::TEF2pr-GFP-UGO1*	This study
YJS02	*MAT*α	S288C *his3Δ1 leu2Δ0 lys2*$^+$ *met15Δ0 ura3Δ0::TPIpr-URA3-HA-OM14-SL17::LEU2 can1Δ::STE2pr-spHIS5 lyp1Δ*	This study
*ugo1*Δ strain	*MAT***a**	BY4741 *ugo1Δ::KAN*^{R}	24
*crd1*Δ strain	*MAT***a**	BY4741 *crd1Δ::KAN*^{R}	24
*fmp32*Δ strain	*MAT***a**	BY4741 *fmp32Δ::KAN*^{R}	24
*fmp33*Δ strain	*MAT***a**	BY4741 *fmp33Δ::KAN*^{R}	24
*hit1*Δ strain	*MAT***a**	BY4741 *hit1Δ::KAN*^{R}	24
*jlp2*Δ strain	*MAT***a**	BY4741 *jlp2Δ::KAN*^{R}	24
*ngr1*Δ strain	*MAT***a**	BY4741 *ngr1Δ::KAN*^{R}	24
*yfl034w*Δ strain	*MAT***a**	BY4741 *yfl034w2Δ::KAN*^{R}	24
*ypl067c*Δ strain	*MAT***a**	BY4741 *ypl067cΔ::KAN*^{R}	24
*SGA crd1*Δ *GFP-OM14* strain	*MAT***a**	S288C *crd1Δ::KAN*^{R} *om14Δ::Nat*^{R}*::ADHpr GFP-OM14 his3Δ1::TEF2pr-Cherry::URA3 can1Δ::STE2pr-spHIS5 lyp1Δ::STE3pr-LEU2*	This study
*SGA fmp32*Δ *GFP-OM14* strain	*MAT***a**	S288C *fmp32Δ::KAN*^{R} *om14Δ::Nat*^{R}*::ADHpr GFP-OM14 his3Δ1::TEF2pr-Cherry::URA3 can1Δ::STE2pr-spHIS5 lyp1Δ::STE3pr-LEU*	This study
*SGA fmp33*Δ *GFP-OM14* strain	*MAT***a**	S288C *fmp33Δ::KAN*^{R} *om14Δ::Nat*^{R}*::ADHpr GFP-OM14 his3Δ1::TEF2pr-Cherry::URA3 can1Δ::STE2pr-spHIS5 lyp1Δ::STE3pr-LEU*	This study
*SGA hit1*Δ *GFP-OM14* strain	*MAT***a**	S288C *hit1Δ::KAN*^{R} *om14Δ::Nat*^{R}*::ADHpr GFP-OM14 his3Δ1::TEF2pr-Cherry::URA3 can1Δ::STE2pr-spHIS5 lyp1Δ::STE3pr-LEU*	This study
*SGA jlp2*Δ *GFP-OM14* strain	*MAT***a**	S288C *jlp2Δ::KAN*^{R} *om14Δ::Nat*^{R}*::ADHpr GFP-OM14 his3Δ1::TEF2pr-Cherry::URA3 can1Δ::STE2pr-spHIS5 lyp1Δ::STE3pr-LEU*	This study
*SGA ngr1*Δ *GFP-OM14* strain	*MAT***a**	S288C *ngr1Δ::KAN*^{R} *om14Δ::Nat*^{R}*::ADHpr GFP-OM14 his3Δ1::TEF2pr-Cherry::URA3 can1Δ::STE2pr-spHIS5 lyp1Δ::STE3pr-LEU*	This study
*SGA yfl034w*Δ *GFP-OM14* strain	*MAT***a**	S288C *yfl034wΔ::KAN*^{R} *om14Δ::Nat*^{R}*::ADHpr GFP-OM14 his3Δ1::TEF2pr-Cherry::URA3 can1Δ::STE2pr-spHIS5 lyp1Δ::STE3pr-LEU*	This study
*SGA ypl067c*Δ *GFP-OM14* strain	*MAT***a**	S288C *ypl067cΔ::KAN*^{R} *om14Δ::Nat*^{R}*::ADHpr GFP-OM14 his3Δ1::TEF2pr-Cherry::URA3 can1Δ::STE2pr-spHIS5 lyp1Δ::STE3pr-LEU*	This study

protein. One mutated gene that was identified by both screens as an effector of integration was the cardiolipin (CL) synthase Crd1.

CL is considered to be the signature lipid of mitochondria as it is rarely found in any other cellular membrane whereas in mitochondria it compromises a large fraction, about 10% to 15%, of total phospholipids (7–9). *De novo* synthesis of CL occurs within mitochondria, and the CL synthase, Crd1, is essential for the last reaction in this multistep pathway (10, 11). Although CL was traditionally believed to exist only in the mitochondrial inner membrane, several studies demonstrated that it is also a component of the MOM as well as of contact sites between the two membranes (7, 9, 12). CL is essential for the function of many proteins residing in mitochondrial membranes. It interacts with proteins in the mitochondrial inner membrane such as the ADP/ATP carrier and respiratory chain complexes facilitating formation of respiratory supercomplexes that are essential for energy production by respiration (13–16). However, the importance of CL extends beyond respiration, as it also modulates the function of the general translocase of the MOM, the TOM complex (12). Deficiency in CL therefore leads to many alterations in cellular functions such as mitochondrial dynamics, mitochondrial protein import, apoptosis, cell cycle, aging, mitophagy, cell wall biogenesis, and lysosome function (17–21). The importance of this phospholipid is further reflected by the fact that alterations in CL underlie diseases such as Barth syndrome (22).

The results of our current study suggest yet another function for this special phospholipid and substantiate the importance of CL for the proper biogenesis of MOM multispan proteins.

MATERIALS AND METHODS

Construction of Om14 variants and yeast strains. Unless stated otherwise, the yeast strains used here were based on the BY4741 background. Strains included in this study are listed in Table 1. For cloning of *URA3*-hemagglutinin (HA)-*OM14*-SL17 into the pYX142 plasmid, *URA3* without a stop codon was amplified from pYX142-*URA3*-SL17 and cloned into the vector pGEM4 using EcoRI and BamHI restriction sites. Subsequently, *OM14* without a stop codon was cloned into the same vector via BamHI and SalI restriction sites. Additionally, an HA tag was added at the N terminus during amplification from pGEM4-*OM14* with an appropriately designed forward primer. SL17, in contrast, was amplified from pYX142-*URA3*-SL17 and cloned into pYX142 with flanking SalI and XhoI restriction sites. Finally, *URA3* and HA-*OM14* were subcloned sequentially from pGEM4-*URA3*-HA-*OM14*-"nostop" into pYX142 containing SL17. The *URA3*-HA-*OM14*-SL17 query strain (YJS02) was created by homologous recombination using an insertion cassette amplified from the pYX142-*URA3*-HA-*OM14*-SL17 plasmid with homology arms for the *URA3* locus.

To create the query strain harboring GFP-Om14, an insertion cassette for homologous recombination was amplified from the vector pYM-N9 natNT2-ADHpr-yEGFP (yeast-enhanced green fluorescent protein) with homology arms for the 5′ untranslated region (UTR) of *OM14* and the beginning of its coding sequence. The insertion cassette itself consisted of a nourseothricin resistance (Nat^r) gene upstream of an ADHpr-yEGFP construct. The cassette was introduced into the genome of strain YMS1169, resulting in the generation of the GFP-Om14 query strain (YMS1641). Hence, the endogenous *OM14* gene in this strain was replaced by GFP-*OM14* under the control of the constitutive ADH promoter. The GFP-Ugo1 query strain (YJS01) was generated in a similar way. The insertion cassette for homologous recombination was amplified from the vector pFA6a-NatMX4-TEF2pr-EGFP-ADH1term with homology arms for the 5′ UTR of *UGO1* and the onset of its coding sequence. The insertion cassette, comprising a Nat^r gene upstream of a TEF2pr-eGFP construct, was integrated into the genome of strain YMS721. Consequently, the generated query strain revealed overexpression of GFP-Ugo1 under the control of the TEF2 promoter instead of endogenously expressed Ugo1.

Synthetic genetic array. The synthetic genetic array (SGA) procedure was used to systematically insert GFP-*OM14* and *URA3*-HA-*OM14*-SL17 into entire yeast libraries (25, 26).

Fluorescence microscopy. High-throughput screens were performed with a system previously described (26, 27). The microscopy for follow-up analysis was performed using an Olympus IX71 microscope controlled by Delta Vision SoftWoRx 3.5.1 software with either 60× or 100× oil lenses. Images were captured by a Photometrics Coolsnap HQ camera with excitation at 490/20 nm and emission at 528/38 nm (GFP) or excitation at 555/28 nm and emission at 617/73 nm (mCherry). Images were transferred to Adobe Photoshop CS2 or ImageJ for slight contrast and brightness adjustments.

Biochemical procedures. Mitochondria were isolated from yeast cells by differential centrifugation as previously described (28). Subcellular fractionation was performed according to published procedures (29). In the carbonate extraction reaction, mitochondria were dissolved in 0.1 M Na_2CO_3. After 30 min on ice, the samples were centrifuged (100,000 × *g*, 30 min, 2°C) and pellets as well as supernatant were analyzed. Protein samples were analyzed by SDS-PAGE and blotting to nitrocellulose membranes followed by incubation with antibodies and visualization by the enhanced-chemoluminescence (ECL) method. The intensity of the observed bands was quantified using AIDA software. Unless stated otherwise, the data from each presented experiment represent results of at least three independent repetitions.

***In vitro* protein import.** Import experiments were performed with radiolabeled precursor proteins and isolated mitochondria in an import buffer containing 250 mM sucrose, 2.5 mg/ml bovine serum albumin (BSA), 80 mM KCl, 5 mM $MgCl_2$, 10 mM MOPS (morpholinepropanesulfonic acid)-KOH, 2 mM NADH, and 2 mM ATP [pH 7.2]. Radiolabeled precursor proteins were synthesized in rabbit reticulocyte lysate in the presence of [^{35}S]methionine. Protease treatment of mitochondria was performed by adding trypsin or proteinase K (50 μg/ml) for 30 min on ice. The protease was then inhibited by adding for 10 min on ice either soybean trypsin inhibitor (1.5 mg/ml) or phenylmethanesulfonyl fluoride (PMSF) (4 mM), respectively.

Blue native PAGE. Mitochondria were lysed in 50 μl digitonin buffer (1% digitonin, 20 mM Tris-HCl, 0.1 mM EDTA, 50 mM NaCl, 10% glycerol, 1 mM PMSF, pH 7.4). After incubation for 30 min at 4°C and a clarifying spin procedure (30,000 × *g*, 15 min, 2°C), 5 μl sample buffer (5% [wt/vol] Coomassie brilliant blue G-250, 100 mM Bis-Tris, 500 mM 6-aminocaproic acid, pH 7.0) was added, and the mixture was analyzed by electrophoresis in a blue native gel containing a 6%-to-13% gradient of acrylamide (30). Gels were blotted onto polyvinylidene fluoride membranes, and proteins were further analyzed by immunodecoration or autoradiography.

RESULTS

GFP-Om14 serves as a model protein for correct membrane insertion of mitochondrial outer membrane multispan proteins. To identify novel effectors of the biogenesis of MOM multispan proteins, we set out to look for a suitable MOM multispan model protein for a high-content screen. We hypothesized that MOM multispan polypeptides that are not properly integrated into the MOM are likely to be degraded or mistargeted to other organelles. For example, we anticipated that a green fluorescent protein (GFP)-tagged model protein on the background of mutations in required genes would display altered localization of the fusion proteins (altered GFP signal pattern) and/or a reduction in its detected levels (altered GFP intensity). Accordingly, our aim was to monitor the localization of a model protein and its levels on the background of all deletion yeast strains (of nonessential genes) or of strains harboring downregulation alleles (of essential genes). Such screens would allow us to spot those proteins that support the biogenesis of these multispan proteins.

To that end, we added a GFP tag at the N terminus of Om14 (GFP-Om14) in a query strain suitable for automated mating approaches like the use of a Synthetic Genetic Array (SGA) (see strain YMS1641 data in Table 1 and references 25 and 26). To validate the correct mitochondrial targeting of GFP-Om14, we used fluorescence microscopy and observed that the GFP signal indeed colocalizes with the mitochondrial marker protein Aco2-Cherry (Fig. 1A). To substantiate this finding, we also monitored the location of the protein by subcellular fractionation. Similar to native Om14 (as observed in the wild-type [WT] strain), GFP-Om14 was highly enriched in purified mitochondria and cofractionated with the Tom70 mitochondrial marker protein (Fig. 1B). Next, we were interested to test whether the tagged protein is properly embedded within the MOM or only associates with the organelle. For this, isolated mitochondria harboring the protein were subjected to carbonate extraction. GFP-Om14, like native Om14, was found mainly in the pellet fraction that also contained other MOM proteins such as Tom20 and porin. Of note, as was previously reported (31), a small portion of GFP-Om14 and of native Om14 is found in the supernatant fraction that harbors peripheral and soluble proteins such as aconitase (Fig. 1C, lanes 3 and 7).

To verify that membrane integration occurred in the correct and functional topology, we used a protease protection assay. Since the N terminus of Om14 is known to be located in the cytosol (31), the fusion protein GFP-Om14 should expose the GFP moiety on the mitochondrial surface. To verify this assumption, we added proteinase K to isolated mitochondria harboring the fusion protein. As expected, this treatment resulted in a cleavage of both the native and the GFP-tagged proteins and disappearance of the signal (Fig. 1C, lanes 4 and 8). The matrix protein aconitase was barely affected under these conditions, demonstrating that the organelles were intact. Taken together, these findings indicate that GFP-Om14 is targeted to mitochondria and can be integrated into the MOM with a native-like conformation.

OM14 was recently demonstrated to serve as a mitochondrial receptor for cytosolic ribosomes (32). However, since *om14*Δ cells display neither a mitochondrial morphology phenotype nor a growth phenotype (31, 32), the functionality of the fusion protein was difficult to test. However, the normal behavior of GFP-Om14

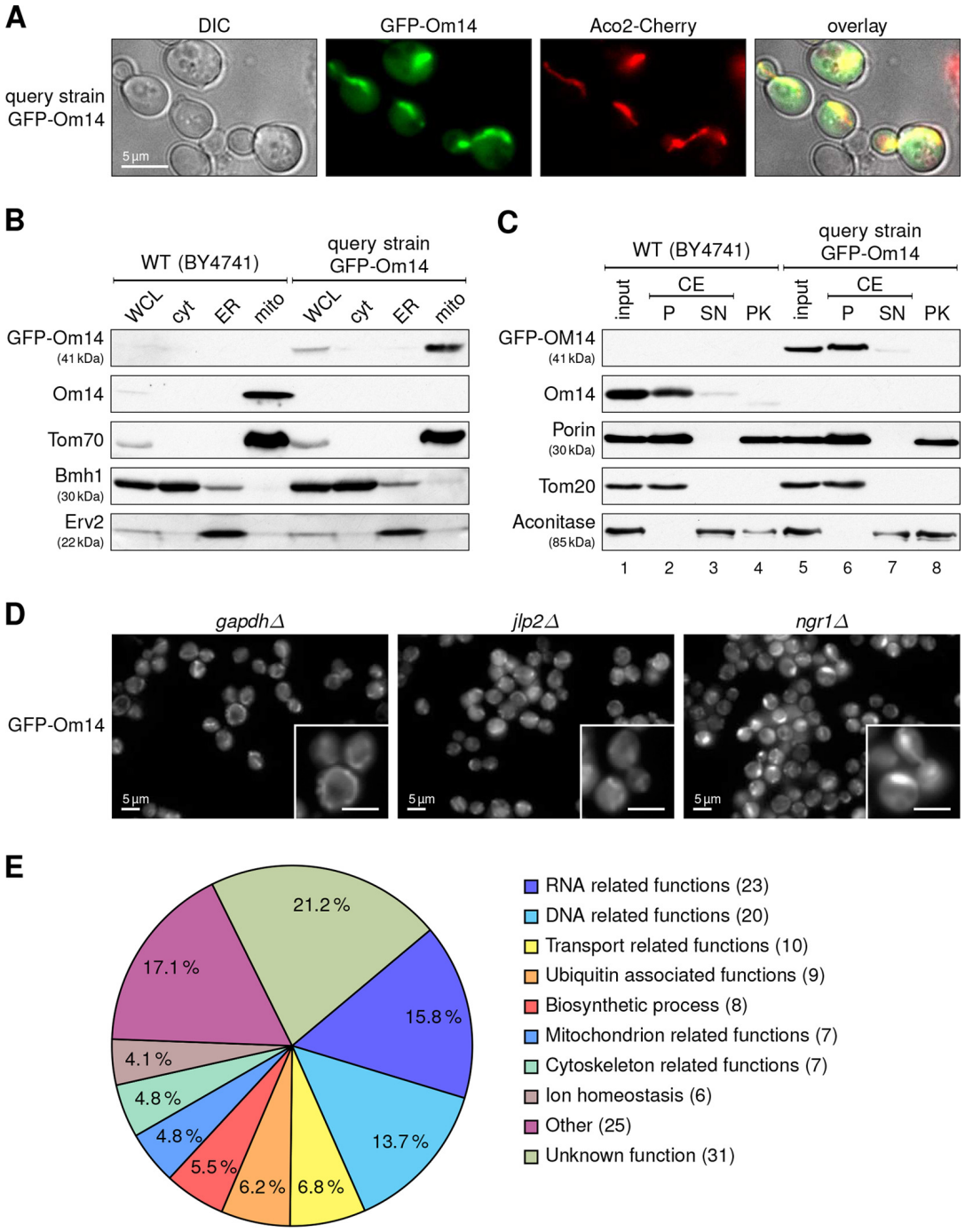

FIG 1 Establishment of an *in vivo* visual assay to monitor the biogenesis of Om14. (A) The GFP-Om14 query strain expressing mitochondrial Aco2-Cherry was subjected to fluorescence microscopy. DIC, differential inference contrast. (B) Subcellular fractionation of the GFP-Om14 query strain. Equal amounts of whole-cell lysate (WCL) and of fractions corresponding to cytosol (cyt), ER, and mitochondria (mito) were analyzed by SDS-PAGE and immunodecoration. The indicated antibodies against marker proteins for mitochondria (Om14 and Tom70), cytosol/nucleus (Bmh1), and ER (Erv2) were used. (C) Carbonate extraction (CE) of mitochondria isolated from either the wild-type strain or the GFP-Om14 query strain was performed, and samples were separated to membrane-embedded proteins in the pellet fraction (P) and soluble proteins in the supernatant (SN). Where indicated (lanes 4 and 8), additional mitochondrial samples were treated with 20 μg/ml proteinase K (PK). All samples were analyzed by SDS-PAGE and immunodecoration. Porin, MOM protein resistant to PK; Tom20, MOM protein sensitive to PK; aconitase, matrix protein resistant to PK. (D) Fluorescence microscopy of representative deletion strains expressing GFP-Om14. (E) Cellular functions of proteins identified as hits by the visual screen. Functions have been assigned according to the *Saccharomyces* Genome Database.

in all available assays prompted us to continue using it as a probe for MOM protein integration in a high-throughput visual screen.

A high-content screen identifies factors involved in the biogenesis of multispan MOM proteins. To integrate the GFP-Om14 into a library of deletions in all nonessential genes (24) and a library of hypomorphic alleles of all essential genes (23), we used SGA to attain nearly 6,000 haploid strains, with each expressing GFP-*OM14* on the background of one mutation. The strains were

TABLE 2 The most promising hits of the visual screen performed with GFP-Om14

Systematic name	Standard name	Size (kDa)	Description (according to the *Saccharomyces* Genome Database)	Hit in GFP-Ugo1 screen
YFL046W	Fmp32	24	Putative protein of unknown function	No
YJL161W	Fmp33	20.2	Putative protein of unknown function	No
YMR132C	Jlp2	24.6	Protein of unknown function that contains sequence closely resembling a J domain	No
YDL142C	Crd1	32	Cardiolipin synthase produces cardiolipin	Yes
YFL034W		119	Putative integral membrane protein that interacts with a component of the ribosomal stalk	No
YJR055W	Hit1	18	Protein of unknown function that is required for growth at high temp	No
YGR078C	Gim2	23	Part of the heteromeric cochaperone GimC/prefoldin complex that promotes efficient protein folding	Yes
YBR212W	Ngr1	75	RNA binding protein that negatively regulates growth rate	No
YPL067C		23	Putative protein of unknown function	No

then visualized using a previously described high-content microscopy setup (27). Normal mitochondrial staining was observed in the vast majority (97.8%) of the inspected mutated strains (see, for example, Fig. 1D, *gapdh*Δ). In contrast, in some strains (1.5%), we observed strong cytosolic mislocalization of GFP-Om14 (see, for example, Fig. 1D, *jlp2*Δ), whereas the mitochondrial staining by GFP seemed to be altered for other strains (0.7%) (see, for example, Fig. 1D, *ngr1*Δ). In the latter cases, mitochondria were usually aggregated, probably due to the elevated levels of GFP-Om14 in the MOM. However, in contrast to mutants that affect targeting of MOM single-span proteins (33, 34), none of the inspected strains displayed mistargeting to other organelles. Manually annotating the resulting images for changes in localization or automatically extracting intensity data, we could find 146 strain backgrounds with altered intensity and/or altered localization of the GFP construct (see Table S1 in the supplemental material). Analyzing the functions of these hits, it appears that the two largest groups were of genes involved in DNA and RNA homeostasis, transcription, and translation (Fig. 1E). In addition, genes that are involved in protein turnover, the cytoskeleton, and ion homeostasis were also represented.

Of note, factors with known function in the biogenesis of MOM multispan proteins (such as Tom70, Tom71, Mim1, and Mim2) did not appear as hits in this screen (see Table S1 in the supplemental material). We assume that the single deletion of either Tom70 or Tom71 did not result in a clear phenotype, since the two receptor proteins have redundant functions and in the absence of one of them the paralogue protein can take over its function. In addition, both can be partially replaced by the other import receptor, Tom20. The Mim1 gene was initially annotated as an essential gene and therefore is not included in the deletion collection but rather in the Decreased Abundance by mRNA Perturbation (DAmP) library, where the levels of depletion are not clear. Finally, the Mim2 gene open reading frame (ORF) was first annotated as a dubious ORF and hence is not included in any library.

We assumed that many of the effects of the genes belonging to the groups mentioned above (such as general effects on transcription and/or translation of the GFP-Om14 marker) might be indirect. Hence, based on their potential relevance for mitochondrial protein biogenesis and the extent of the fluorescence alterations, these initial 146 hits were narrowed down to 9 strains with which we were interested in continuing to work (Table 2).

To further characterize this limited group of hits, we created another query strain in which a GFP tag was added at the N terminus of another MOM multispan protein, Ugo1 (GFP-Ugo1; strain YJS01 in Table 1). This fusion protein was correctly localized to mitochondria and inserted into the outer membrane but was not functional, as it could not support regular mitochondrial morphology (see Fig. S1 in the supplemental material). Crossing this query strain with the nine deletion strains revealed an altered biogenesis of GFP-Ugo1 in only two of those strains, the *crd1*Δ and *gim1*Δ strains (Fig. 2 and Table 2). As Crd1 is a mitochondrial protein, while a clear relevance of Gim1 to mitochondrial function is not obvious, *CRD1* was the most promising hit from the visual assays.

Ura3-Om14-degron can be used to probe membrane integration of Om14 *in vivo*. The visual screen was aimed to uncover proteins that are essential for targeting Om14 to the mitochondria. However, fluorescence staining of mitochondria could not monitor whether the model protein obtained its correct topology at the MOM. Thus, as a complementary method to identify factors that are required for the correct membrane integration of multispan outer membrane proteins, we also employed a growth screen. As a probe, we used a fusion protein that is based on Om14. This hybrid protein contains the Ura3 enzyme, a cytosolic enzyme that catalyzes one of the steps in UTP synthesis, fused to the cytosol-facing N terminus of Om14. In addition, our hybrid protein contained the 50-amino-acid "degron" SL17 sequence, which targets proteins for degradation by the ubiquitin-proteasome system (35), attached to the C terminus of the protein that should face the IMS (Fig. 3A). We have previously used a similar method to successfully monitor the membrane insertion of the MOM single-span protein Mim1 (34). When the Om14 fusion protein is integrated into the MOM with its native topology (31), Ura3 is exposed to the cytosol (where it is functional), whereas SL17 is hidden in the IMS and is not exposed to the ubiquitin-proteasome system (Fig. 3A). Thus, the native topology is expected to abolish the uracil auxotrophy of the yeast strains in the collection of the mutants. However, if Om14 membrane integration is compromised, then the degron region is exposed to the cytosol where it causes degradation of the entire hybrid protein. Accordingly, the cells become auxotrophic for uracil.

To perform such a screen, we first constructed the Ura3-HA-Om14-SL17 fusion protein and cloned it into a yeast expression vector. Next, to validate its compatibility with the growth screen,

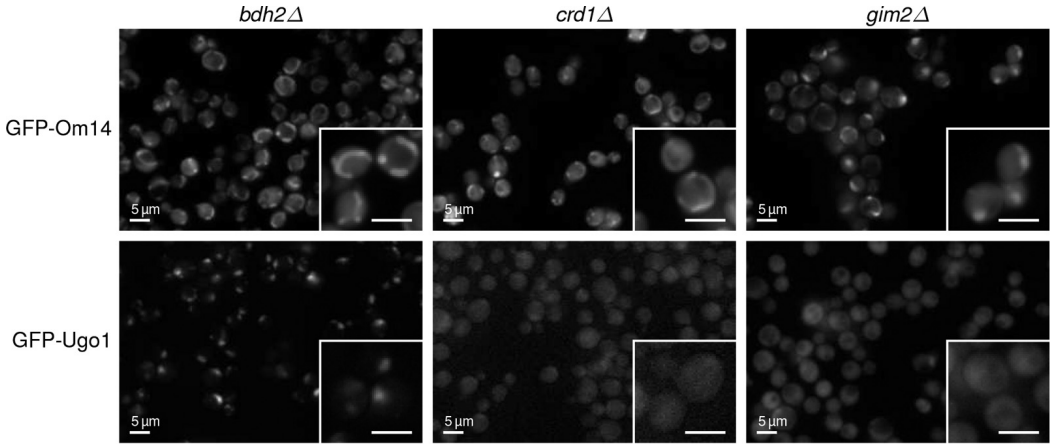

FIG 2 GFP-Om14 and GFP-Ugo1 have an altered appearance in *crd1*Δ and *gim2*Δ deletion strains. Strains with *BDH2* (as a control), *CRD1*, or *GIM2* deleted, expressing either GFP-Om14 (upper panels) or GFP-Ugo1 (lower panels), were observed by fluorescence microscopy. Selected regions from each image were enlarged and are shown separately.

wild-type cells were transformed with an expression vector encoding Ura3, Ura3-SL17, or Ura3-HA-Om14-SL17. Of note, the yeast expression plasmid used in this study contains *LEU2* as a selection marker, and, as expected, all transformed cells grew equally well on synthetic dextrose (SD)-Leu plates (Fig. 3B). In contrast, as hypothesized, Ura3 and Ura3-HA-Om14-SL17, but not Ura3-SL17, which is constantly degraded, also supported growth in the absence of uracil (SD-Leu-Ura plates, Fig. 3B). These findings demonstrate that Ura3 is functional even when localized to the mitochondrial surface by Om14. Next, this construct was introduced into the *URA3* locus of a query strain, resulting in construction of the Ura3-HA-Om14-SL17 query strain (YJS02, Table 1). This strain also contains the native endogenous Om14 protein. To test the suitability of the generated query strain for the desired growth screen, both the mitochondrial targeting and membrane insertion of the hybrid protein were analyzed in more detail. The Ura3-HA-Om14-SL17 query strain was subjected to subcellular fractionation, and, as expected, the hybrid protein was detected solely in the mitochondrial fraction (Fig. 3C). Next, we verified by carbonate extraction and protease treatment that the fusion protein behaves like native Om14 and is indeed embedded correctly within the outer membrane (Fig. 3D).

A growth screen uncovers Crd1 as an important factor for correct membrane topology of Om14. To perform the growth screen, we used SGA to integrate Ura3-HA-Om14-SL17 on the background of the same mutant arrays as used for the visual screens. We performed the growth screen by comparing the colony sizes of the resulting haploids on synthetic galactose-containing medium (SGal) to the colony sizes seen on the same medium lacking uracil (SGal-Ura). Galactose was used to allow robust growth while avoiding the repression of mitochondrial biogenesis that is caused by glucose. This screen uncovered many mutants in whose absence strains grew more poorly on SGal-Ura (see Table S2 in the supplemental material). However, among those potential candidates, only the *crd1*Δ strain also produced a hit in the visual screen. We further verified on the single-gene level that the *crd1*Δ strain expressing the Ura3-HA-Om14-SL17 hybrid protein grew slower when uracil was omitted from a galactose-containing liquid medium (Fig. 3E). In a control experiment, the deletion of an unrelated gene, *CMK2*, did not show this phenotype (Fig. 3E). We anticipated that an important protein for biogenesis of MOM multispan proteins should affect both the association of the protein with the membrane and its correct membrane topology. As both (visual and growth) screens identified Crd1 as a protein that is required for optimal biogenesis of the Om14 variants, we decided to focus on this protein in subsequent biochemical assays.

Mitochondria from *crd1*Δ cells display reduced insertion efficiency of multispan proteins. To confirm the outcome of the high-throughput screens, we isolated crude mitochondria from either control or *crd1*Δ cells overexpressing the GFP-Om14 fusion protein and found that the fusion protein was indeed detected at reduced levels (Fig. 4A). When we next analyzed pure organelles, we observed that the steady-state levels of native Om14 were not affected whereas those of two other MOM multispan proteins, Ugo1 and Scm4, were reduced to about half of normal (Fig. 4B). These observations suggest that Crd1 functionality is especially required when the system is challenged with elevated amounts of multispan proteins. Of note, neither single-span proteins such as Mim1, Tom70, and Tom20 nor the Yah1 matrix protein was affected in the mutant cells (Fig. 4A and B).

It is well-established that Mim1 and Tom70 are required for the biogenesis of multispan proteins (4, 5). Therefore, we asked whether the observed effect on GFP-Om14, Scm4, and Ugo1 is secondary to reduced amounts of Tom70 and/or Mim1. However, both proteins were detected in the mutated organelles at levels that were not significantly altered compared to their amounts in control organelles (Fig. 4A and B). As a further control, we analyzed both the TOM and MIM complexes by blue native PAGE. Although, as previously reported (12), the TOM complex from the mutated cells migrated at an apparently lower molecular mass, the two complexes displayed similar levels in mutated and control mitochondria (Fig. 4C). Hence, it appears that the absence of Crd1 can directly influence the biogenesis of multispan proteins.

To determine whether the reduced amounts of Ugo1, Scm4, and GFP-OM14 were really a result of reduced targeting and not of reduced production or stability, we next used established *in vitro* insertion assays based on purified mitochondria and cell-free synthesized radiolabeled Ugo1 or Scm4 molecules (4, 5). Supporting the aforementioned observations, we found that mitochondria isolated from *crd1*Δ cells had a reduced capacity to import

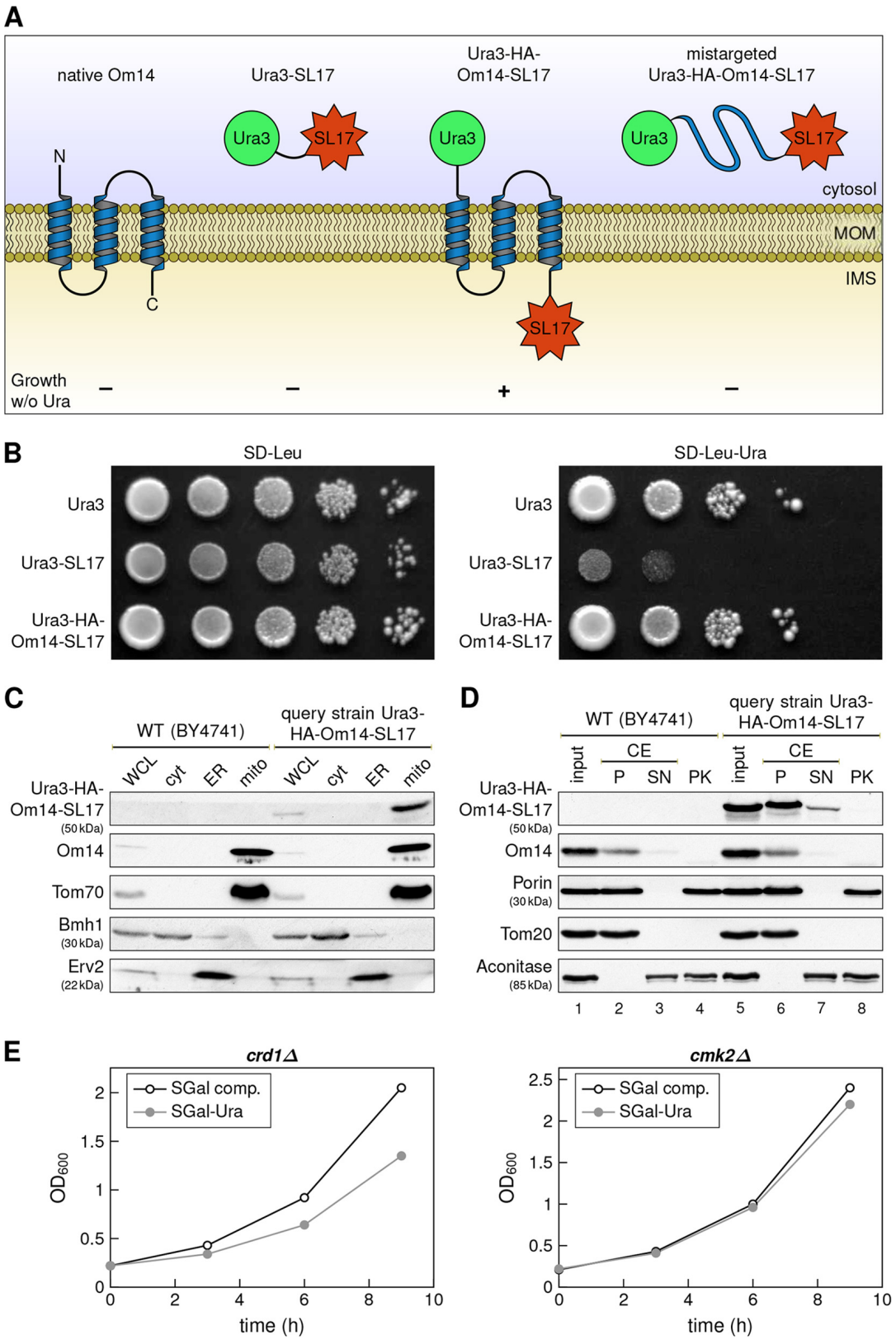

FIG 3 Growth assay to monitor the biogenesis of Om14. (A) Schematic representation of the various fusion proteins used. The expected potential of these proteins to support growth on synthetic medium without uracil is indicated at the bottom. (B) Yeast cells expressing the indicated constructs were analyzed at 30°C by drop-dilution assay on synthetic medium lacking either leucine only (SD-Leu) or leucine and uracil (SD-Leu-Ura). (C) Subcellular fractionation of the Ura3-HA-Om14-SL17 query strain. Equal amounts of whole-cell lysate (WCL) and of fractions corresponding to cytosol (cyt), ER, and mitochondria (mito) were analyzed as described in the Fig. 1B legend. (D) Mitochondria isolated from either the WT strain or the Ura3-HA-Om14-SL17 query strain were treated and analyzed as described in the Fig. 1C legend. (E) *crd1*Δ and *cmk2*Δ (as a control) cells expressing Ura3-HA-Om14-SL17 were grown on galactose-containing liquid medium in the presence (SGal comp.) or absence (SGal-Ura) of uracil. The optical density at 600 nm (OD_{600}) of the cultures was measured and is depicted as a function of incubation time.

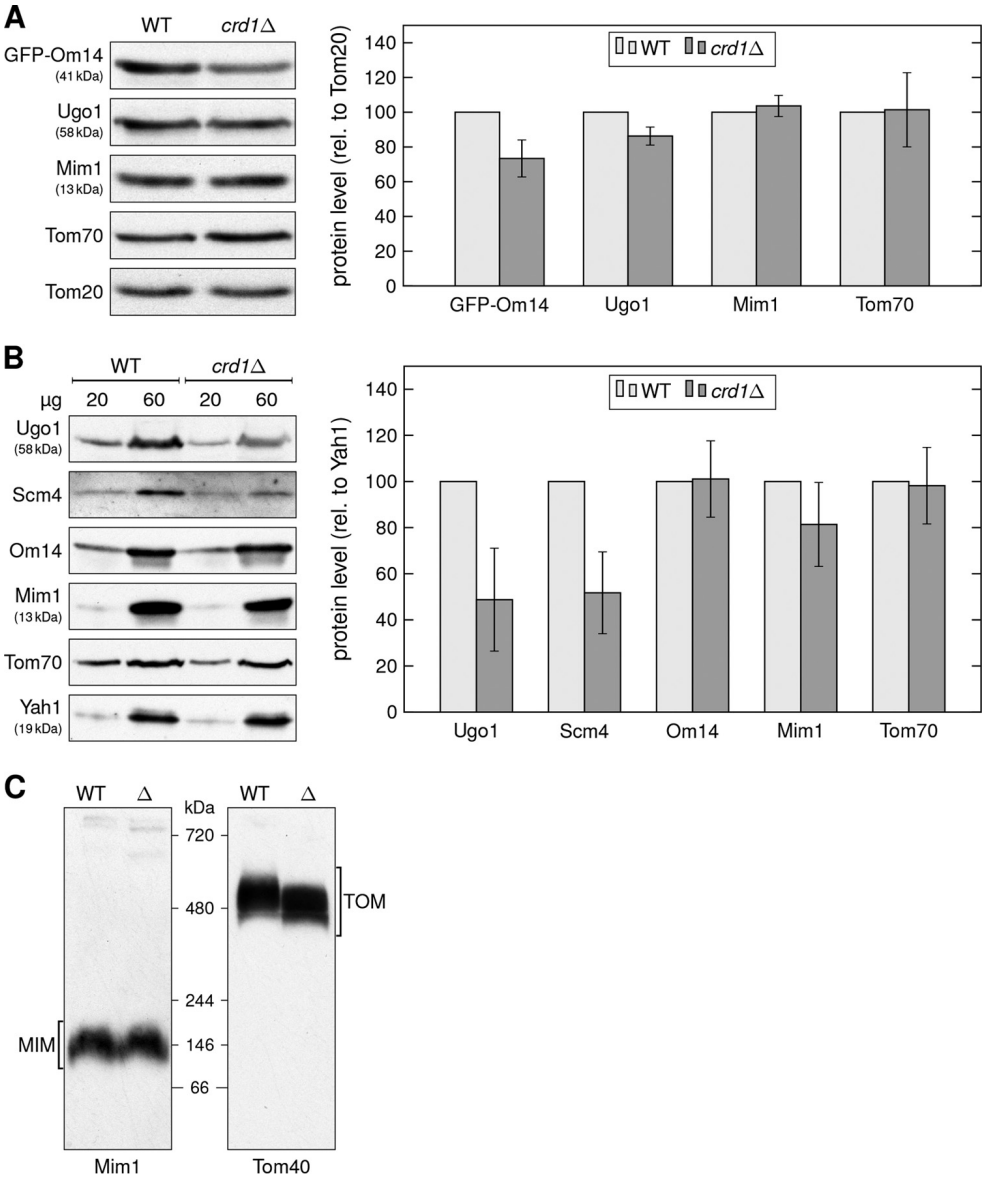

FIG 4 The absence of cardiolipin affects the steady-state levels of multispan proteins. (A) Steady-state levels of GFP-Om14 are decreased in *crd1*Δ mitochondria. (Left panel) Crude mitochondria from wild-type (WT) and *crd1*Δ yeast strains were isolated and analyzed by SDS-PAGE and immunodecoration with the indicated antibodies. (Right panel) The bands resulting from three independent experiments were quantified and normalized to the level of Tom20, and the protein levels in the WT strain were set to 100%. Error bars represent standard deviations ($n = 3$). rel., relative. (B) Steady-state levels of Ugo1 and Scm4 are decreased in *crd1*Δ organelles. Mitochondria were isolated from either WT or *crd1*Δ cells, and the indicated amounts were analyzed as described for panel A. The resulting bands were quantified and normalized to the level of Yah1, and the protein levels in the WT strain were set to 100% (right panel). Error bars represent standard deviations ($n = 6$ [3 biological experiments with 2 technical repeats each]). (C) Mitochondria isolated as described for panel B were subjected to blue native PAGE and immunodecoration with antibodies against Mim1 or Tom40. The MIM and the TOM complexes are indicated.

Ugo1 and Scm4 compared to organelles isolated from control cells (Fig. 5A and B). In contrast, the import of the model matrix protein, pSu9-dihydrofolate reductase (pSu9-DHFR), was not hampered by the deletion of Crd1 (Fig. 5C). Taking the results together, it appears that the absence of Crd1 does not affect the general import capacity of mitochondria but instead specifically reduces the ability of the organelle to integrate multispan proteins.

Crd1 catalyzes the last step in the biosynthesis pathway of CL. Hence, depletion of Crd1 could affect integration of multispan proteins due to either depletion of CL or accumulation of its precursor, phosphatidylglycerol (PG). To test this, we looked at the effect of mutating one enzyme, Gep4, upstream in the pathway that creates PG. First, we monitored the steady-state levels of proteins in mitochondria isolated from cells lacking Gep4. Our analysis demonstrates that all three MOM multispan proteins, Ugo1, Scm4, and Om14, are found in reduced levels in the altered organelles (Fig. 6A). Importantly, the levels of Tom70 and Mim1 were hardly affected in the mitochondria from *gep4*Δ cells. Next, we tested the capacity of such isolated mitochondria to import *in vitro* radiolabeled mitochondrial proteins. Whereas the absence of Gep4 resulted in a slight reduction in the import of Ugo1, a significant effect on the import of Scm4 was observed (Fig. 6B and

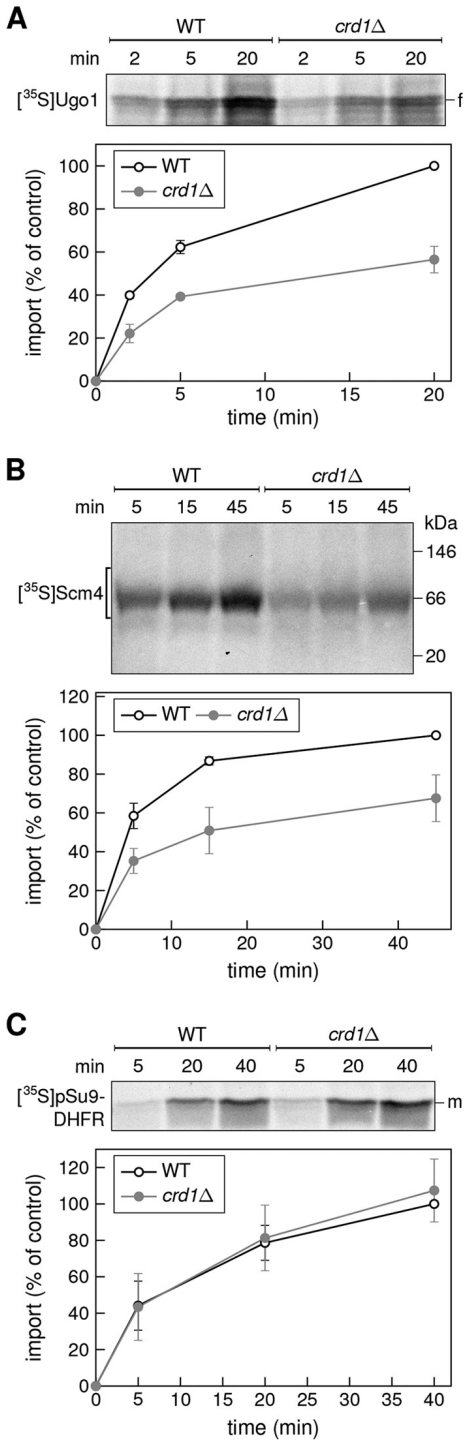

FIG 5 Mitochondria lacking Crd1 have a lower *in vitro* capacity to import multispan proteins. (A) Radiolabeled molecules of Ugo1-2HA were incubated with mitochondria isolated from either WT or *crd1*Δ cells for the indicated time periods. After import, mitochondria were treated with trypsin and subjected to SDS-PAGE and autoradiography. The trypsin-protected fragment is indicated (f). (Lower panel) Bands representing this fragment were quantified, and the intensity of the band upon import into control mitochondria for 20 min was set as 100%. Data represent averages of the results of three independent experiments. (B) Radiolabeled molecules of Scm4 were incubated with isolated mitochondria as described for panel A. After import, mitochondria were solubilized by the use of digitonin and subjected to blue native PAGE and autoradiography. The Scm4-containing band is indicated. (Lower panel) Bands were quantified, and the intensity of the band upon import into control mitochondria for 45 min was set as 100%. Data represent averages of the results of three independent experiments. (C) Radiolabeled molecules of pSu9-DHFR were incubated with isolated mitochondria as described for panel A. After import, mitochondria were treated with proteinase K (PK) and subjected to SDS-PAGE and autoradiography. The PK-protected mature form is indicated (m). (Lower panel) Bands representing the mature form were quantified, and the intensity of the band upon import into control mitochondria for 40 min was set as 100%. Data represent averages of the results of three independent experiments.

C). Of note, the import of the matrix-destined protein pSu9-DHFR was highly reduced in the mutant mitochondria, suggesting a general import defect in this strain (Fig. 6D). Such a general biogenesis defect is in line with the severe growth phenotypes of cells lacking Gep4 and its requirement for the stability of respiratory chain supercomplexes (36). Collectively, these findings demonstrate that Crd1 and Gep4 are required for optimal biogenesis of MOM multispan proteins, strongly suggesting that the lack of CL itself is the cause for the compromised membrane integration.

DISCUSSION

In the current study, we performed visual and growth screens to identify proteins that are required for the biogenesis of multispan proteins residing in the MOM. We concentrated in these screens on the model protein Om14 and its variants. In this context, we confirmed that GFP-Om14 is targeted to mitochondria and integrated into the MOM with a native-like topology. Interestingly, our visual screen could not identify mutants that result in mistargeting of Om14 to the endoplasmic reticulum (ER). This is in contrast to previous studies with MOM single-span proteins such as Mim1 or Gem1 where deletions of *DJP1* (34) or *SPF1* (33), respectively, resulted in mislocalization of the mitochondrial protein to the ER. Hence, it seems that, whereas the single-span proteins can, in principle, under certain conditions, also get integrated into the ER membrane, the multispan proteins lack this capacity or else might get efficiently and rapidly degraded in the event that they do. A speculative explanation for this difference is the divergence in the integration pathways of single- or multispan proteins into the ER membrane. While the membrane insertion of single-span proteins is mediated by the guided entry of TA protein (GET) machinery and is probably more flexible regarding substrate specificity, the targeting pathways for proteins that must use the Sec translocon for their membrane integration might be more restrictive regarding their substrates.

The most prominent hit in our screens was Crd1, and subsequent biochemical assays verified its important role for optimal biogenesis of MOM multispan proteins. The performed screens provided, in addition to Crd1, various potential hits for proteins that might be involved in the biogenesis of multispan proteins. However, since Crd1 was the only gene that appeared as a hit in both screens, we decided in the current study to concentrate on the characterization of its contribution. Future studies can address the relevance of the other potential hits.

Crd1 catalyzes the final step in the *de novo* synthesis of the CL diphosphatidylglycerol. Due to its importance for various processes, deficiency of and/or variations in CL result in a wide variety of alterations in cellular functions such as the cell cycle, aging, mitophagy, cell wall biogenesis, mitochondrial dynamics, mitochondrial protein import, and apoptosis (21). Our report adds another important process in which CL is playing a central role,

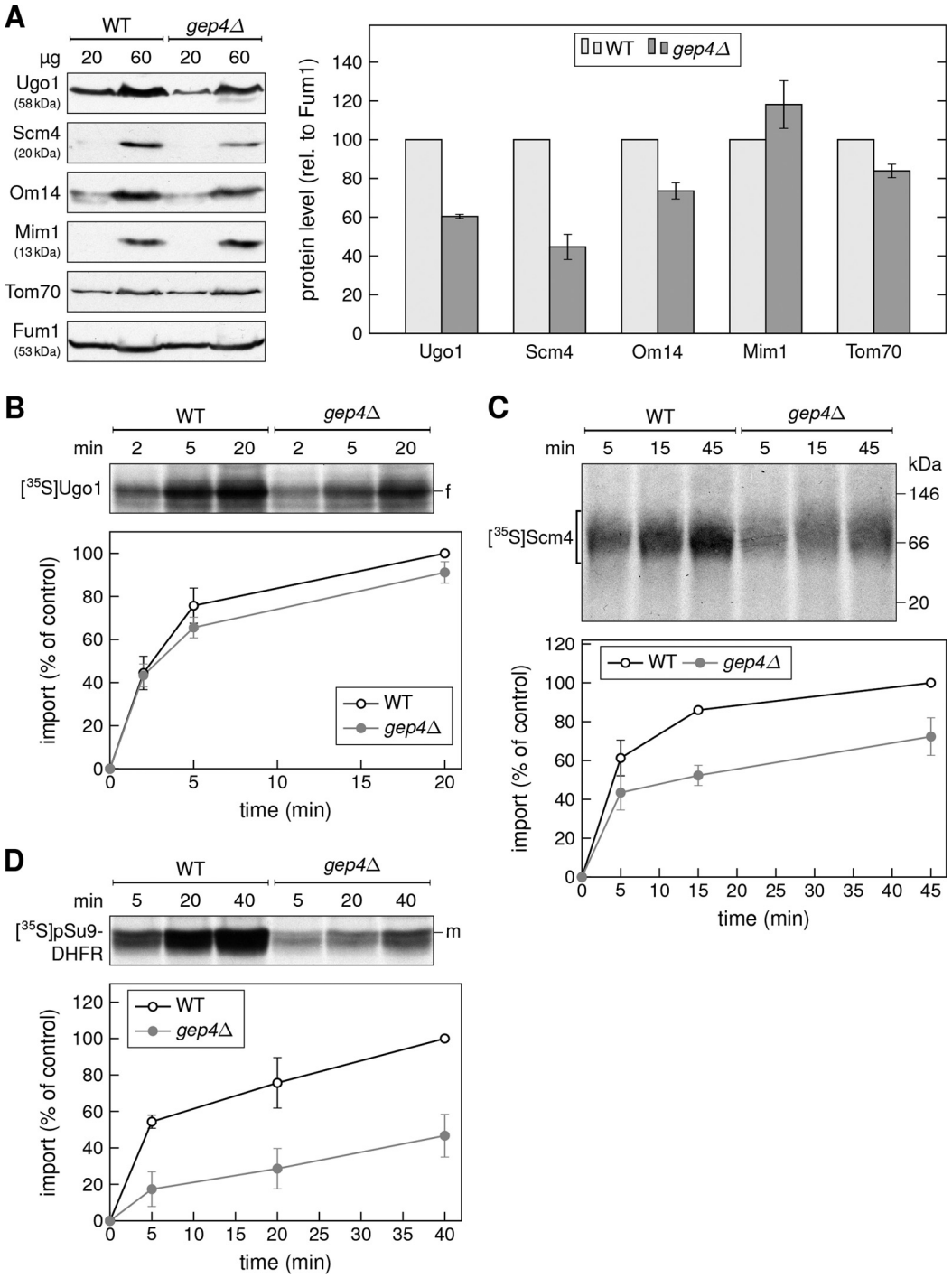

FIG 6 Deletion of Gep4 causes a reduction in the biogenesis of multispan proteins. (A) Mitochondria were isolated from either WT or *gep4*Δ cells, and the indicated amounts were analyzed as described in the Fig. 4B legend. The resulting bands were quantified and normalized to the level of fumarase (Fum1), and the protein levels in the WT strain were set to 100% (right panel). (B to D) The indicated radiolabeled proteins were incubated with isolated organelles and further analyzed as described in the Fig. 5 legend.

namely, in the membrane integration of MOM multispan proteins. We observed very specific alterations in the biogenesis of Ugo1, Scm4, and Om14 upon deletion of *CRD1* but not of other MOM or matrix proteins. Our observations are also in line with a previous report of a study in which the absence of Crd1 caused a reduction in the steady-state levels of the two multispan proteins Ugo1 and Fzo1 (20). The requirement for CL in the biogenesis of MOM multispan proteins also supports, by providing functional relevance, the idea of the presence of CL in the MOM, as its occurrence in this membrane is rather controversial (12). The idea of the importance of CL for the biogenesis process is further supported by the similar effects of deletion of Gep4, the upstream enzyme in this pathway (36).

It is currently unclear how CL modulates all the aforemen-

tioned processes, specifically, the biogenesis of multispan protein. As it has a dimeric structure and harbors a net negative charge, one can speculate that its negative charges may contribute to this effect. However, CL forms only ca. 1% to 3% of the MOM phospholipids whereas phosphatidylinositol (PI), which is also negatively charged, is far more abundant (12% [9]). Thus, it is unlikely that the contribution of CL is limited to electrostatic interactions with membrane proteins, as those interactions probably could also be facilitated by other lipid molecules in the membrane. The reported observation that CL stabilizes the TOM complex (12) could have provided another explanation of the requirement for CL in this process. However, we disfavor this possibility, because we and others reported that it is not the core TOM complex that is involved in the biogenesis of multispan proteins but rather the import receptor Tom70 and the MIM complex (4, 5), both of which do not seem destabilized in this background. Therefore, we favor the idea of a direct contribution of CL to unique structures within the membrane that facilitate integration and stabilization of multispan proteins. Such structures might be CL-rich microdomains that provide a convenient insertion site for the newly synthesized multispan proteins. Regardless of the actual mechanism, the data from the current study indicate that a defined phospholipid composition of the MOM modulates the capacity of this membrane to integrate multispan proteins. As the importance of CL is emphasized by the fact that alterations in its composition underlie diseases such as Barth syndrome, our findings may help also to shed light on disease progression.

ACKNOWLEDGMENTS

We thank E. Kracker, L. Gal, and D. Elinger for excellent technical support and T. Becker and N. Pfanner for the kind gift of antibodies against Om14 and Scm4.

This work was supported by the Deutsche Forschungsgemeinschaft (RA 1048/5-1 and RA 1048/7-1 to D.R.), the PROMOS program of the DAAD (J.S.), and a Minerva grant and a European Research Council (ERC) starting grant (StG) (260395) to the laboratory of M.S.

REFERENCES

1. **Dukanovic J, Rapaport D.** 2011. Multiple pathways in the integration of proteins into the mitochondrial outer membrane. Biochim Biophys Acta **1808:**971–980. http://dx.doi.org/10.1016/j.bbamem.2010.06.021.
2. **Fritz S, Rapaport D, Klanner E, Neupert W, Westermann B.** 2001. Connection of the mitochondrial outer and inner membranes by Fzo1 is critical for organellar fusion. J Cell Biol **152:**683–692. http://dx.doi.org/10.1083/jcb.152.4.683.
3. **Otera H, Taira Y, Horie C, Suzuki Y, Suzuki H, Setoguchi K, Kato H, Oka T, Mihara K.** 2007. A novel insertion pathway of mitochondrial outer membrane proteins with multiple transmembrane segments. J Cell Biol **179:**1355–1363. http://dx.doi.org/10.1083/jcb.200702143.
4. **Becker T, Wenz LS, Kruger V, Lehmann W, Muller JM, Goroncy L, Zufall N, Lithgow T, Guiard B, Chacinska A, Wagner R, Meisinger C, Pfanner N.** 2011. The mitochondrial import protein Mim1 promotes biogenesis of multispanning outer membrane proteins. J Cell Biol **194:**387–395. http://dx.doi.org/10.1083/jcb.201102044.
5. **Papic D, Krumpe K, Dukanovic J, Dimmer KS, Rapaport D.** 2011. Multispan mitochondrial outer membrane protein Ugo1 follows a unique Mim1-dependent import pathway. J Cell Biol **194:**397–405. http://dx.doi.org/10.1083/jcb.201102041.
6. **Dimmer KS, Papic D, Schumann B, Sperl D, Krumpe K, Walther DM, Rapaport D.** 2012. A crucial role for Mim2 in the biogenesis of mitochondrial outer membrane proteins. J Cell Sci **125:**3464–3473. http://dx.doi.org/10.1242/jcs.103804.
7. **Sperka-Gottlieb CD, Hermetter A, Paltauf F, Daum G.** 1988. Lipid topology and physical properties of the outer mitochondrial membrane of the yeast, Saccharomyces cerevisiae. Biochim Biophys Acta **946:**227–234. http://dx.doi.org/10.1016/0005-2736(88)90397-5.
8. **Gaigg B, Simbeni R, Hrastnik C, Paltauf F, Daum G.** 1995. Characterization of a microsomal subfraction associated with mitochondria of the yeast, Saccharomyces cerevisiae. Involvement in synthesis and import of phospholipids into mitochondria. Biochim Biophys Acta **1234:**214–220.
9. **de Kroon AIPM, Koorengevel MC, Goerdayal SS, Mulders PC, Janssen MJ, de Kruijff B.** 1999. Isolation and characterization of highly purified mitochondrial outer membranes of the yeast Saccharomyces cerevisiae. Mol Membr Biol **16:**205–211. http://dx.doi.org/10.1080/096876899294670.
10. **Osman C, Voelker DR, Langer T.** 2011. Making heads or tails of phospholipids in mitochondria. J Cell Biol **192:**7–16. http://dx.doi.org/10.1083/jcb.201006159.
11. **Tamura Y, Sesaki H, Endo T.** 2014. Phospholipid transport via mitochondria. Traffic **15:**933–945. http://dx.doi.org/10.1111/tra.12188.
12. **Gebert N, Joshi AS, Kutik S, Becker T, McKenzie M, Guan XL, Mooga VP, Stroud DA, Kulkarni G, Wenk MR, Rehling P, Meisinger C, Ryan MT, Wiedemann N, Greenberg ML, Pfanner N.** 2009. Mitochondrial cardiolipin involved in outer-membrane protein biogenesis: implications for Barth syndrome. Curr Biol **19:**2133–2139. http://dx.doi.org/10.1016/j.cub.2009.10.074.
13. **Brandner K, Mick DU, Frazier AE, Taylor RD, Meisinger C, Rehling P.** 2005. Taz1, an outer mitochondrial membrane protein, affects stability and assembly of inner membrane protein complexes: implications for Barth syndrome. Mol Biol Cell **16:**5202–5214. http://dx.doi.org/10.1091/mbc.E05-03-0256.
14. **Claypool SM, Oktay Y, Boontheung P, Loo JA, Koehler CM.** 2008. Cardiolipin defines the interactome of the major ADP/ATP carrier protein of the mitochondrial inner membrane. J Cell Biol **182:**937–950. http://dx.doi.org/10.1083/jcb.200801152.
15. **Böttinger L, Horvath SE, Kleinschroth T, Hunte C, Daum G, Pfanner N, Becker T.** 2012. Phosphatidylethanolamine and cardiolipin differentially affect the stability of mitochondrial respiratory chain supercomplexes. J Mol Biol **423:**677–686. http://dx.doi.org/10.1016/j.jmb.2012.09.001.
16. **Bazán S, Mileykovskaya E, Mallampalli VK, Heacock P, Sparagna GC, Dowhan W.** 2013. Cardiolipin-dependent reconstitution of respiratory supercomplexes from purified Saccharomyces cerevisiae complexes III and IV. J Biol Chem **288:**401–411. http://dx.doi.org/10.1074/jbc.M112.425876.
17. **Ohtsuka T, Nishijima M, Suzuki K, Akamatsu Y.** 1993. Mitochondrial dysfunction of a cultured Chinese hamster ovary cell mutant deficient in cardiolipin. J Biol Chem **268:**22914–22919.
18. **Chen S, Tarsio M, Kane PM, Greenberg ML.** 2008. Cardiolipin mediates cross-talk between mitochondria and the vacuole. Mol Biol Cell **19:**5047–5058. http://dx.doi.org/10.1091/mbc.E08-05-0486.
19. **Chu CT, Ji J, Dagda RK, Jiang JF, Tyurina YY, Kapralov AA, Tyurin VA, Yanamala N, Shrivastava IH, Mohammadyani D, Qiang Wang KZ, Zhu J, Klein-Seetharaman J, Balasubramanian K, Amoscato AA, Borisenko G, Huang Z, Gusdon AM, Cheikhi A, Steer EK, Wang R, Baty C, Watkins S, Bahar I, Bayir H, Kagan VE.** 2013. Cardiolipin externalization to the outer mitochondrial membrane acts as an elimination signal for mitophagy in neuronal cells. Nat Cell Biol **15:**1197–1205. http://dx.doi.org/10.1038/ncb2837.
20. **Joshi AS, Thompson MN, Fei N, Huttemann M, Greenberg ML.** 2012. Cardiolipin and mitochondrial phosphatidylethanolamine have overlapping functions in mitochondrial fusion in Saccharomyces cerevisiae. J Biol Chem **287:**17589–17597. http://dx.doi.org/10.1074/jbc.M111.330167.
21. **Ren M, Phoon CK, Schlame M.** 2014. Metabolism and function of mitochondrial cardiolipin. Prog Lipid Res **55:**1–16. http://dx.doi.org/10.1016/j.plipres.2014.04.001.
22. **Schlame M, Kelley RI, Feigenbaum A, Towbin JA, Heerdt PM, Schieble T, Wanders RJ, DiMauro S, Blanck TJ.** 2003. Phospholipid abnormalities in children with Barth syndrome. J Am Coll Cardiol **42:**1994–1999. http://dx.doi.org/10.1016/j.jacc.2003.06.015.
23. **Breslow DK, Cameron DM, Collins SR, Schuldiner M, Stewart-Ornstein J, Newman HW, Braun S, Madhani HD, Krogan NJ, Weissman JS.** 2008. A comprehensive strategy enabling high-resolution functional analysis of the yeast genome. Nat Methods **5:**711–718. http://dx.doi.org/10.1038/nmeth.1234.
24. **Giaever G, Chu AM, Ni L, Connelly C, Riles L, Veronneau S, Dow S, Lucau-Danila A, Anderson K, Andre B, Arkin AP, Astromoff A, El-Bakkoury M, Bangham R, Benito R, Brachat S, Campanaro S, Curtiss M, Davis K, Deutschbauer A, Entian KD, Flaherty P, Foury F, Garfinkel DJ, Gerstein M, Gotte D, Guldener U, Hegemann JH, Hempel S, Herman Z, Jaramillo DF, Kelly DE, Kelly SL, Kotter P,**

LaBonte D, Lamb DC, Lan N, Liang H, Liao H, Liu L, Luo C, Lussier M, Mao R, Menard P, Ooi SL, Revuelta JL, Roberts CJ, Rose M, Ross-Macdonald P, Scherens B, et al. 2002. Functional profiling of the Saccharomyces cerevisiae genome. Nature **418:**387–391. http://dx.doi.org/10.1038/nature00935.

25. **Tong AH, Boone C.** 2006. Synthetic genetic array analysis in Saccharomyces cerevisiae. Methods Mol Biol **313:**171–192.
26. **Cohen Y, Schuldiner M.** 2011. Advanced methods for high-throughput microscopy screening of genetically modified yeast libraries. Methods Mol Biol **781:**127–159. http://dx.doi.org/10.1007/978-1-61779-276-2_8.
27. **Breker M, Gymrek M, Schuldiner M.** 2013. A novel single-cell screening platform reveals proteome plasticity during yeast stress responses. J Cell Biol **200:**839–850. http://dx.doi.org/10.1083/jcb.201301120.
28. **Daum G, Böhni PC, Schatz G.** 1982. Import of proteins into mitochondria: cytochrome b2 and cytochrome c peroxidase are located in the intermembrane space of yeast mitochondria. J Biol Chem **257:**13028–13033.
29. **Walther DM, Papic D, Bos MP, Tommassen J, Rapaport D.** 2009. Signals in bacterial β-barrel proteins are functional in eukaryotic cells for targeting to and assembly in mitochondria. Proc Natl Acad Sci U S A **106:**2531–2536. http://dx.doi.org/10.1073/pnas.0807830106.
30. **Schägger H, Cramer WA, von Jagow G.** 1994. Analysis of molecular masses and oligomeric states of protein complexes by blue native electrophoresis and isolation of membrane protein complexes by two-dimensional native electrophoresis. Anal Biochem **217:**220–230. http://dx.doi.org/10.1006/abio.1994.1112.
31. **Burri L, Vascotto K, Gentle IE, Chan NC, Beilharz T, Stapleton DI, Ramage L, Lithgow T.** 2006. Integral membrane proteins in the mitochondrial outer membrane of Saccharomyces cerevisiae. FEBS J **273:**1507–1515. http://dx.doi.org/10.1111/j.1742-4658.2006.05171.x.
32. **Lesnik C, Cohen Y, Atir-Lande A, Schuldiner M, Arava Y.** 2014. OM14 is a mitochondrial receptor for cytosolic ribosomes that supports co-translational import into mitochondria. Nat Commun **5:**5711. http://dx.doi.org/10.1038/ncomms6711.
33. **Krumpe K, Frumkin I, Herzig Y, Rimon N, Ozbalci C, Brugger B, Rapaport D, Schuldiner M.** 2012. Ergosterol content specifies targeting of tail-anchored proteins to mitochondrial outer membranes. Mol Biol Cell **23:**3927–3935. http://dx.doi.org/10.1091/mbc.E11-12-0994.
34. **Papić D, Elbaz-Alon Y, Koerdt SN, Leopold K, Worm D, Jung M, Schuldiner M, Rapaport D.** 2013. The role of Djp1 in import of the mitochondrial protein Mim1 demonstrates specificity between a cochaperone and its substrate protein. Mol Cell Biol **33:**4083–4094. http://dx.doi.org/10.1128/MCB.00227-13.
35. **Gilon T, Chomsky O, Kulka RG.** 1998. Degradation signals for ubiquitin system proteolysis in Saccharomyces cerevisiae. EMBO J **17:**2759–2766. http://dx.doi.org/10.1093/emboj/17.10.2759.
36. **Osman C, Haag M, Wieland FT, Brugger B, Langer T.** 2010. A mitochondrial phosphatase required for cardiolipin biosynthesis: the PGP phosphatase Gep4. EMBO J **29:**1976–1987. http://dx.doi.org/10.1038/emboj.2010.98.

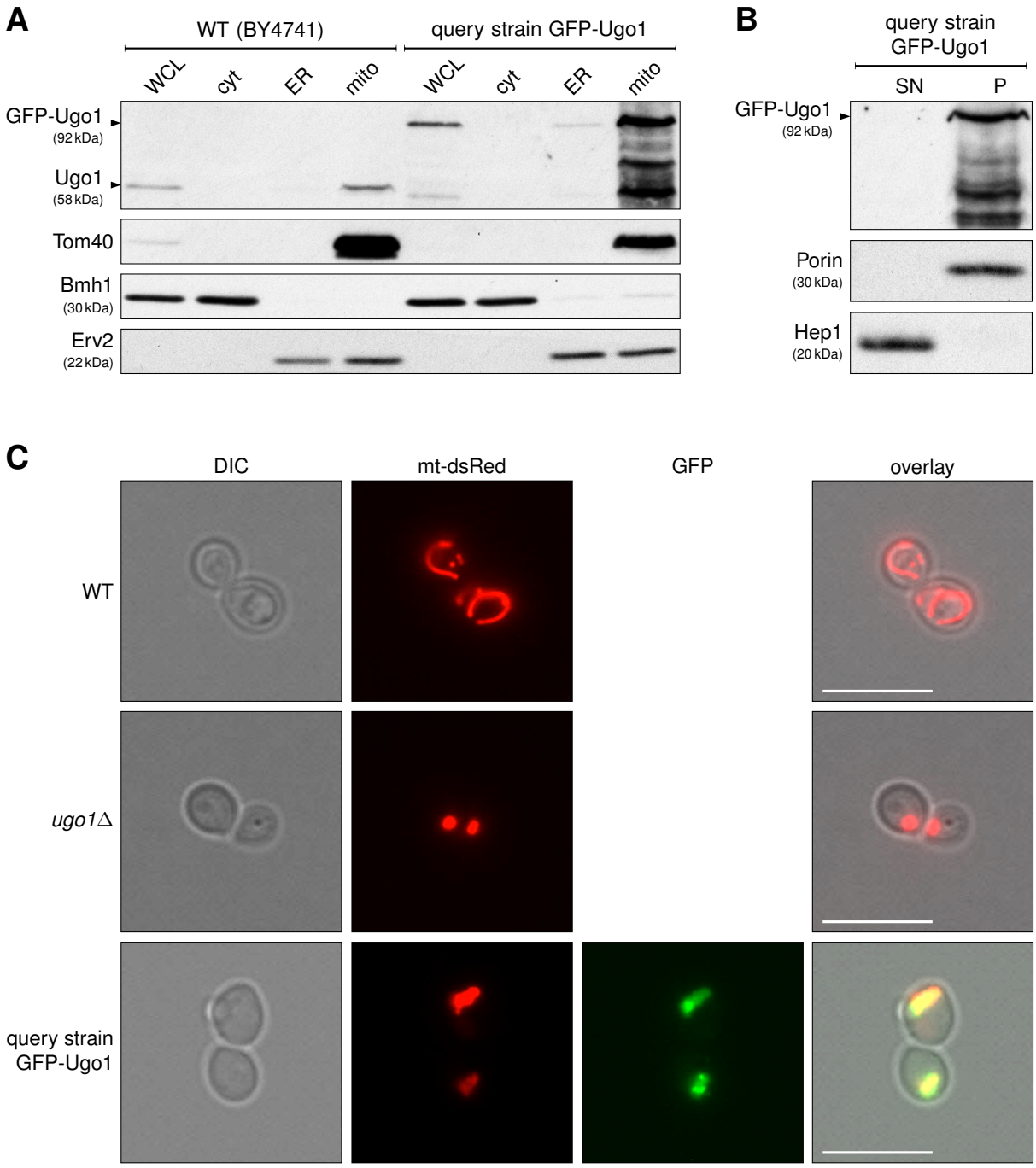

Supplemental Figure 1: Characterization of the GFP-Ugo1 construct.
(A) Subcellular fractionation of the control and query (GFP-Ugo1) strains. Equal amounts of whole cell lysate (WCL) and of fractions corresponding to cytosol (cyt), ER and mitochondria (mito) were analyzed by SDS-PAGE and immunodecoration. The indicated antibodies against marker proteins for mitochondria (Tom40), cytosol/nucleus (Bmh1) and ER (Erv2) were used. **(B)** Carbonate extraction of mitochondria isolated from the query strain GFP-Ugo1 was performed and samples were separated to soluble proteins in the supernatant (SN) fraction and membrane-embedded proteins in the pellet fraction (P). The MOM protein Porin and the matrix protein Hep1 were used as markers for membrane and soluble proteins, respectively. Ugo1 and GFP-Ugo1 were detected with anti-Ugo1 antibody in (A) and (B). **(C)** GFP-Ugo1 is not functional. The BY4741 (WT), *ugo1Δ*, and the query GFP-Ugo1 strains all expressing mitochondrial targeted dsRed (mt-dsRed) were analysed by fluorescence microscopy. Typical images of the three different strains are shown (scale bar: 10 µm).

nature COMMUNICATIONS

ARTICLE

Received 18 Dec 2015 | Accepted 24 May 2016 | Published 27 Jun 2016

DOI: 10.1038/ncomms12036 OPEN

Characterization of the targeting signal in mitochondrial β-barrel proteins

Tobias Jores[1], Anna Klinger[2], Lucia E. Groß[2], Shin Kawano[3], Nadine Flinner[2], Elke Duchardt-Ferner[4], Jens Wöhnert[4], Hubert Kalbacher[1], Toshiya Endo[3], Enrico Schleiff[2,5,6] & Doron Rapaport[1]

Mitochondrial β-barrel proteins are synthesized on cytosolic ribosomes and must be specifically targeted to the organelle before their integration into the mitochondrial outer membrane. The signal that assures such precise targeting and its recognition by the organelle remained obscure. In the present study we show that a specialized β-hairpin motif is this long searched for signal. We demonstrate that a synthetic β-hairpin peptide competes with the import of mitochondrial β-barrel proteins and that proteins harbouring a β-hairpin peptide fused to passenger domains are targeted to mitochondria. Furthermore, a β-hairpin motif from mitochondrial proteins targets chloroplast β-barrel proteins to mitochondria. The mitochondrial targeting depends on the hydrophobicity of the β-hairpin motif. Finally, this motif interacts with the mitochondrial import receptor Tom20. Collectively, we reveal that β-barrel proteins are targeted to mitochondria by a dedicated β-hairpin element, and this motif is recognized at the organelle surface by the outer membrane translocase.

[1] Interfaculty Institute of Biochemistry, University of Tuebingen, Hoppe-Seyler-Str. 4, 72076 Tuebingen, Germany. [2] Molecular Cell Biology of Plants, Goethe University, Max-von-Laue-Str. 9, 60438 Frankfurt, Germany. [3] Faculty of Life Sciences, Kyoto Sangyo University, Kyoto 603-8555, Japan. [4] Institute for Molecular Biosciences, Center for Biomolecular Magnetic Resonance, Goethe University, Max-von-Laue Str. 9, 60438 Frankfurt, Germany. [5] Cluster of Excellence Frankfurt, Goethe University, Max-von-Laue Str. 9, 60438 Frankfurt, Germany. [6] Buchmann Institute for Molecular Life Sciences, Goethe University, Max-von-Laue Str. 9, 60438 Frankfurt, Germany. Correspondence and requests for materials should be addressed to E.S. (email: schleiff@bio.uni-frankfurt.de) or to D.R. (email: doron.rapaport@uni-tuebingen.de).

Membrane-embedded β-barrel proteins are found in both prokaryotic and eukaryotic organisms. In prokaryotes such proteins are found in the outer membrane (OM) of Gram-negative bacteria, whereas in eukaryotes they reside exclusively in the OM of mitochondria and chloroplasts. Bacterial β-barrel proteins are synthesized in the cytoplasm with an N-terminal signal sequence for transport across the inner membrane into the periplasm via the SEC system[1]. Their integration into the OM is facilitated by the β-barrel assembly machinery (Bam), the central component of which is the essential protein BamA (Omp85/YaeT)[2,3].

In mitochondria, precursors of β-barrel proteins are synthesized in the cytosol without a cleavable signal sequence. Upon their synthesis, these precursors are translocated from the cytosol into the intermembrane space (IMS) via the translocase of the outer membrane (TOM complex)[4,5]. Their subsequent assembly into the OM depends on a dedicated translocase, the topogenesis of OM β-barrel proteins (TOB, also known as sorting and assembly machinery, SAM) complex. The central member of this latter complex is the essential protein Tob55/Sam50 that bears sequence and functional homology to BamA[6–8]. The other two subunits of the TOB complex, Mas37/Sam37 and Tob38/Sam35/Tom38, are peripheral membrane proteins exposed to the cytosol that share no obvious sequence similarity with the accessory lipoproteins of the bacterial Bam complex[9–12].

Despite the aforementioned progress in our understanding of the membrane assembly of mitochondrial β-barrel proteins, the mitochondrial targeting signal in such proteins is ill-defined. A conserved linear sequence could not be identified yet and hence it was proposed that the signal is composed by a structural element[13]. However, although cytosolic targeting is a crucial stage in protein biogenesis, neither the character nor the size of such a putative structural signal was identified so far.

In fact, mitochondrial β-barrel proteins in yeast possess a signature (β-signal) that facilitates their intra-mitochondrial sorting[14]. The positioning of this signal in the last strand of the barrel is consistent with the location of a sorting signal in prokaryotic β-barrel proteins[15]. However, this eukaryotic β-signal enhances productive interactions with the TOB complex but does not provide the information required for the initial targeting from the cytosol to the organelle[14,16–18].

In previous efforts to better understand the specific requirements for a mitochondrial targeting signal, bacterial β-barrel proteins were expressed in eukaryotic cells. Such expression resulted in efficient targeting of some of these proteins to mitochondria and their integration into the mitochondrial OM[16–19]. These studies demonstrate that the bacterial β-barrel proteins possess signals that can target the proteins to mitochondria and can be recognized and processed by the mitochondrial import machinery. Especially informative are our previous observations that mitochondria can recognize and assemble a bacterial trimeric autotransporter β-barrel protein[18,19]. The β-barrel anchor of these proteins is formed by a single 12-stranded β-barrel structure to which each monomer contributes four β-strands[20,21]. Thus, these findings demonstrate that four β-strands are sufficient for the mitochondria to recognize and assemble a β-barrel protein. However, the precise identity of the signal and its mode of recognition by the organelle import machinery remained unknown.

In the current study we identify a special form of a β-hairpin element as this long searched for targeting signal. A β-hairpin is a characteristic folding motif formed by two β-strands connected by a short loop, and this motif is the smallest building block of all β-barrel proteins[22]. Our *in vitro*, *in organello* and *in vivo* findings demonstrate that a β-hairpin element with one face composed of highly hydrophobic residues is a mitochondrial targeting signal for β-barrel proteins. This signal is recognized at the surface of the organelle by the TOM complex with its import receptor Tom20.

Results

Design and structural characterization of β-hairpin peptides. In the present study we investigated whether a β-hairpin fold can serve as a targeting signal to direct β-barrel proteins from the cytosol to the mitochondrial surface. To that goal, peptides derived from the human voltage-dependent anion channel 1 (hVDAC1) were chemically synthesized. hVDAC1 was chosen since its atomic structure was solved[23,24], allowing realistic design of peptides corresponding to a β-hairpin motif or its fragment. Three peptides, which differ in their length and potential to form a β-hairpin motif, were used (Fig. 1a). The short linear peptide comprises only the last β-strand of hVDAC1 (a.a. N269 to L279) and is therefore not able to form a β-hairpin. The long linear peptide on the other hand corresponds to the last two β-strands and the loop between them (a.a. L257 to L279) and should be able to adopt a β-hairpin fold. We created a third peptide by extending the C terminus of the long linear peptide by two Pro residues and then this new C terminus was covalently linked to the N terminus, thus cyclizing the peptide (CYC). This cyclization increases the likelihood that the peptide will form a β-hairpin motif. To allow direct comparison, also the two linear peptides were extended by two Pro residues.

To analyze whether the cyclic peptide has indeed a more stable conformation, the long linear and the cyclic peptides were investigated by solution NMR spectroscopy. Although these measurements were not performed in a membrane-mimetic environment like those in which the atomic structure of VDAC was determined, they reflect the cytosolic milieu where the targeting signal should be recognized by the import receptors. Low spectral dispersion of the amide resonances as well as averaged $^{3}J(HN,H\alpha)$ coupling constants point to an averaged, partially structured conformation of both peptides (Supplementary Fig. 1a). As expected, differences in amide proton chemical shifts between the cyclic and the linear peptide are observed for residues at the termini close to the cyclization site (Supplementary Fig. 1b). However, also more distant residues in the C- and in particular in the N-terminal region between residues Leu3 and Gly9 showed marked chemical shift differences suggesting structural variations between the two peptides. In general, the cyclic peptide exhibits larger chemical shift dispersion for resonances in the two termini (Supplementary Fig. 1c). Taken together, the structural analysis shows that, as anticipated, the cyclic peptide is more structured than the linear one.

Cyclic β-hairpin peptide hampers import of β-barrel proteins. We rationalized that a peptide resembling a targeting signal for mitochondrial β-barrel proteins should be able to hinder the *in organello* import of such proteins due to its ability to compete for crucial binding sites. To test this assumption, we added increasing amounts of the three peptides to an *in organello* import reaction containing isolated yeast mitochondria and radiolabelled β-barrel proteins like Tom40, Tob55/Sam50 and Porin. The addition of both linear peptides did not significantly affect the import of the radiolabelled proteins. In contrast, the cyclic peptide demonstrated a dose-dependent capacity to dramatically inhibit the import of all three tested β-barrel proteins (Fig. 1b–d). Since both Tom40 and Porin belong to the VDAC-like branch of mitochondrial β-barrel proteins and Tob55 to the Omp85-like protein family, the observed inhibition capacity suggests that a β-hairpin motif is a general targeting signal.

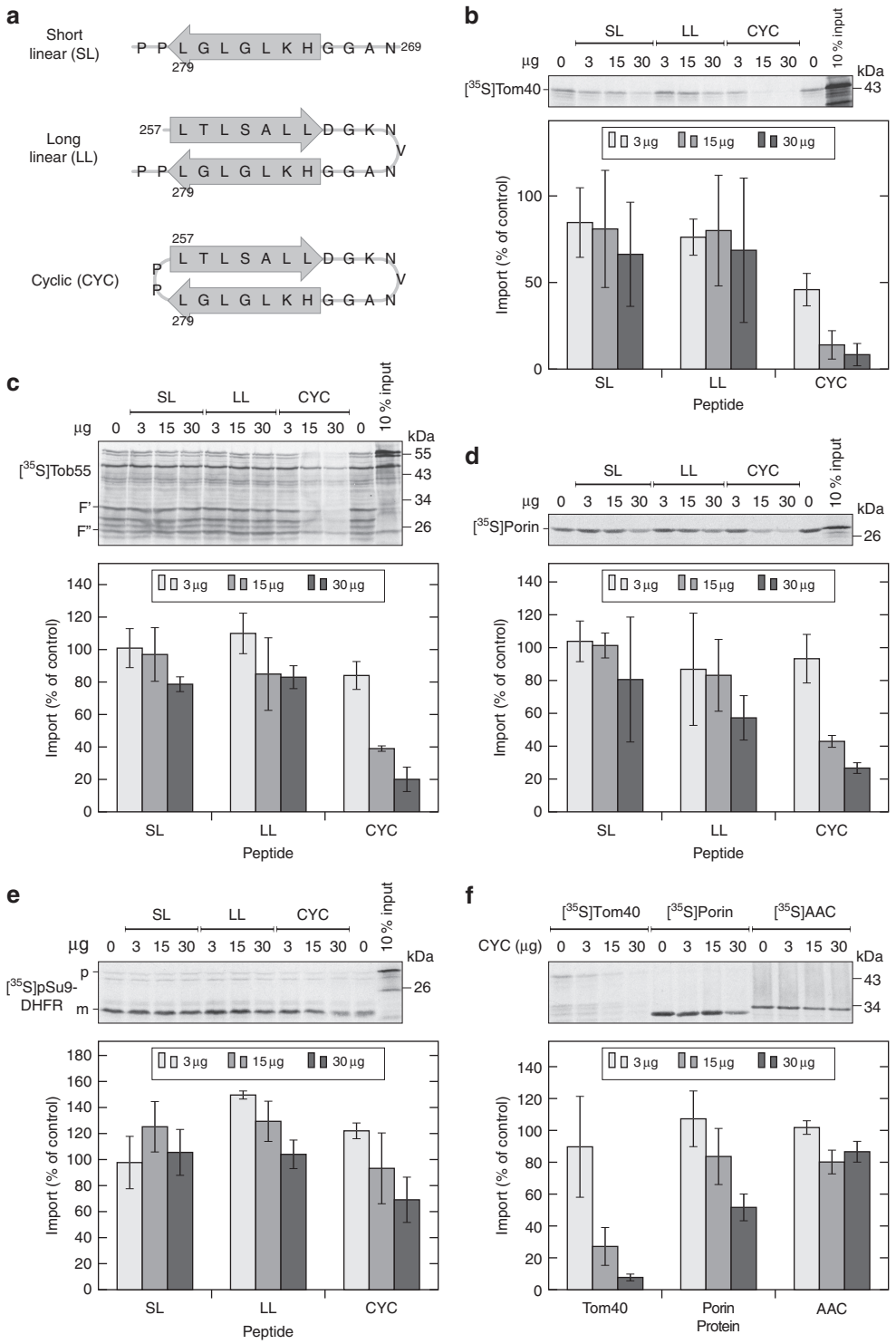

Figure 1 | A cyclic β-hairpin peptide inhibits the *in vitro* import of β-barrel proteins. (**a**) Schemes of the three peptides. Grey arrows indicate the residues that form a β-strand in full-length hVDAC1. Residue numbers correspond to the numbering of full-length hVDAC1. (**b**–**e**) Radiolabelled precursor proteins of Tom40 (**b**), Tob55 (**c**), Porin (**d**) or pSu9-DHFR (**e**) were mixed with isolated mitochondria in the presence of the indicated amounts of the short linear (SL), long linear (LL) or cyclic (CYC) peptide. In the end of the import reactions, samples were treated with proteinase K to degrade non-imported molecules. In the case of Tob55, this treatment led to the generation of two protease-protected fragments (F′ and F″)[27]. Samples were then subjected to SDS–PAGE and autoradiography (top panels). Bottom panels: the intensities of bands corresponding to the full-length form of Tom40 and Porin, the fragment F′ of Tob55 or the mature form of pSu9-DHFR from three independent experiments were quantified and the mean intensity from the import without any peptide was set to 100%. Error bars represent standard deviation. The precursor and mature forms of pSu9-DHFR are indicated by p and m, respectively. (**f**) The indicated radiolabelled proteins were incubated with isolated mitochondria in the presence of various amounts of the cyclic peptide. The import reactions were analyzed as in parts (**b**) and (**d**). AAC, ADP-ATP carrier.

To assure that the peptides do not eliminate the general import capacity of the isolated organelles, we imported the matrix-destined protein pSu9-DHFR in the presence of the peptides and observed only a slight inhibition with the highest amount of the cyclic peptide (Fig. 1e). This minor inhibition is probably due to the interaction of the peptide with the import receptor Tom20 that recognizes also matrix-destined preproteins (see below). β-Barrel proteins and multispan inner membrane proteins are stabilized during their import by small Tim chaperones in the IMS[25–27]. Thus, a possibility that we wanted to exclude was that the import inhibition by the cyclic peptide is due to its ability to rupture the OM and thus to cause release of the small Tim components. However, whereas the import of the β-barrel proteins was strongly affected by the cyclic peptide only a minimal effect on the import of the inner membrane protein ADP–ATP carrier was observed (Fig. 1f). This finding suggests that the small Tims are maintained by the organelles in the presence of the cyclic peptide. Hence, the cyclic peptide specifically inhibits the import of β-barrel proteins.

β-Hairpin motif is sufficient for mitochondrial targeting. The aforementioned results suggest that a β-hairpin peptide can compete the targeting of a β-barrel protein to mitochondria. We next asked whether such a motif can mediate also a translocation across the OM. To that goal, fusion proteins containing the most C-terminal β-hairpin segment (hp18) of hVDAC1 upstream of the soluble dihydrofolate reductase (DHFR) domain were constructed. As a control, the native DHFR domain fused to a control peptide (cp), derived from the hVDAC1 N terminus, which forms a helical structure[23,24], was employed. Next, radiolabelled hp18-DHFR or cp-DHFR were incubated with isolated mitochondria and the samples were then treated with proteinase K (PK) to remove non-imported material. In both cases only marginal amounts of the fusion proteins were protease protected (Fig. 2a,b). We reasoned that the tightly folded DHFR domain prevents full import into the interior of the organelle and thus replaced the native DHFR by a variant that cannot fold properly ($DHFR^{mut}$)[28]. A fusion protein of $DHFR^{mut}$ with a β-hairpin motif could indeed be imported into a protease-protected location whereas the control peptide did not mediate this effect (Fig. 2a,b). Our findings demonstrate that a β-hairpin motif can function *in organello* as a mitochondrial targeting signal.

Next, we asked whether peptides, which represent the last β-hairpin (hp18) of either hVDAC1 or yeast Porin, are able to mediate also *in vivo* mitochondrial targeting of a passenger domain. To that end, the fusion proteins described above and native DHFR moiety without any additive peptide were expressed in yeast cells and the capacity of the fusion proteins to associate with mitochondria was tested by analyzing proteins found with the fraction of crude mitochondria upon subcellular fractionation. As expected, DHFR alone and the cytosolic marker protein Bmh1 were detected in the whole-cell lysate but hardly in the mitochondrial fraction. Similarly, only negligible amounts of the construct with the control peptide associated with the organelles. In contrast, both fusion proteins containing the β-hairpin motif were enriched in the mitochondrial fractions (Fig. 2c,d). Of note, fusion of the β-hairpin peptides C-terminally to DHFR resulted in a lower mitochondrial targeting capacity (Supplementary Fig. 2). It might be that the β-hairpin peptides are not properly exposed in these latter fusion proteins.

To substantiate the *in vivo* targeting capacity, we constructed fusion proteins of hp18(VDAC) or the N-terminal control peptide with green fluorescent protein (GFP). Fluorescence microscopy analysis of cells expressing these proteins demonstrated strong GFP background in the cytosol that prevented observation of clear mitochondrial structures. To overcome this problem we isolated crude mitochondria from lysates of these cells and analyzed the samples by measuring their GFP fluorescence with a fluorimeter or by analyzing the samples with immunodecoration with an anti-GFP antibody. No enrichment of the GFP fluorescence signal on mitochondria was observed for cells with GFP alone or fused to the control peptide. In contrast, about threefold enrichment of the fluorescent signal was measured for mitochondria from cells containing the hp18(VDAC)-GFP construct (Fig. 2e). Accordingly, only the GFP fusion construct containing hp18(VDAC) was detected in the mitochondrial fraction by western blotting (Fig. 2f). Collectively, we conclude that such a β-hairpin motif is sufficient for mitochondrial targeting *in vivo*.

β-Hairpin redirects chloroplast OM proteins to mitochondria. Our aforementioned experiments were performed in yeast cells, and we next wanted to investigate whether the targeting capacity of the β-hairpin motif is conserved in higher eukaryotes. Plant cells provide an optimal experimental system, since in contrast to other eukaryotes, they contain two organelles with membrane-embedded β-barrel proteins, namely, chloroplasts and mitochondria. Thus, mitochondrial β-barrel proteins in such cells must avoid mistargeting to chloroplasts. To study the importance of the C-terminal β-hairpin for mitochondrial targeting, we generated hybrid constructs where the last two or four transmembrane β-strands of the pea chloroplast OM β-barrel protein psOEP24 were replaced by the corresponding C-terminal transmembrane β-strands of the *Arabidopsis* mitochondrial OM β-barrel protein atVDAC1 (Fig. 3). The positions of the β-strands of atVDAC1 were assigned based on an alignment to the mouse VDAC1 sequence. The positions of the β-strands of psOEP24 were predicted as described in the Methods section. To study the location of the hybrid β-barrel proteins *in vivo*, we employed the established self-assembly-GFP assay, where the first 10 β-strands of GFP ($GFP_{S1–10}$) are fused to one protein, whereas the complementing 11th β-strand (GFP_{S11}) is attached to another protein. A GFP signal can be observed only if the two fusion proteins are located in the same cellular compartment[29,30].

We first confirmed that the N terminus of psOEP24 is exposed to the cytosol using a GFP_{S11}-OEP24 construct. GFP fluorescence could be established only when the latter construct was co-expressed with cytosolic $GFP_{S1–10}$. In contrast, no fluorescence signal was obtained upon co-expression with either Mgd1-$GFP_{S1–10}$, which is targeted to the IMS of chloroplasts, or with Tim50-$GFP_{S1–10}$ that is targeted to the mitochondrial IMS (Fig. 3a). These observations confirm the previously observed exclusively plastidic localization of psOEP24 (ref. 31). Next, we analyzed the localization of the mitochondrial atVDAC1. GFP_{S11}-VDAC1 was co-expressed with each of the aforementioned three $GFP_{S1–10}$-containing reporter constructs and GFP fluorescence was observed only upon co-expression with mitochondrial Tim50-$GFP_{S1–10}$. This signal co-localized with MitoTracker-stained mitochondria (Fig. 3b). Hence, the N terminus of atVDAC1 is localized in the mitochondrial IMS.

Next, we analyzed the intracellular location of hybrid proteins composed of the N-terminal portion of psOEP24 and C-terminal β-hairpins of atVDAC1. Interestingly, constructs where the last two or four β-strands of psOEP24 were replaced by β-strands from the mitochondrial atVDAC1 ($OEP24_{1–12}$-$VDAC1_{18–19}$ or $OEP24_{1–10}$-$VDAC1_{16–19}$, respectively, subscript numbers reflect the number of the β-strand in the corresponding protein), assemble fluorescent GFP only upon co-expression with the mitochondrial IMS marker and this staining co-localizes

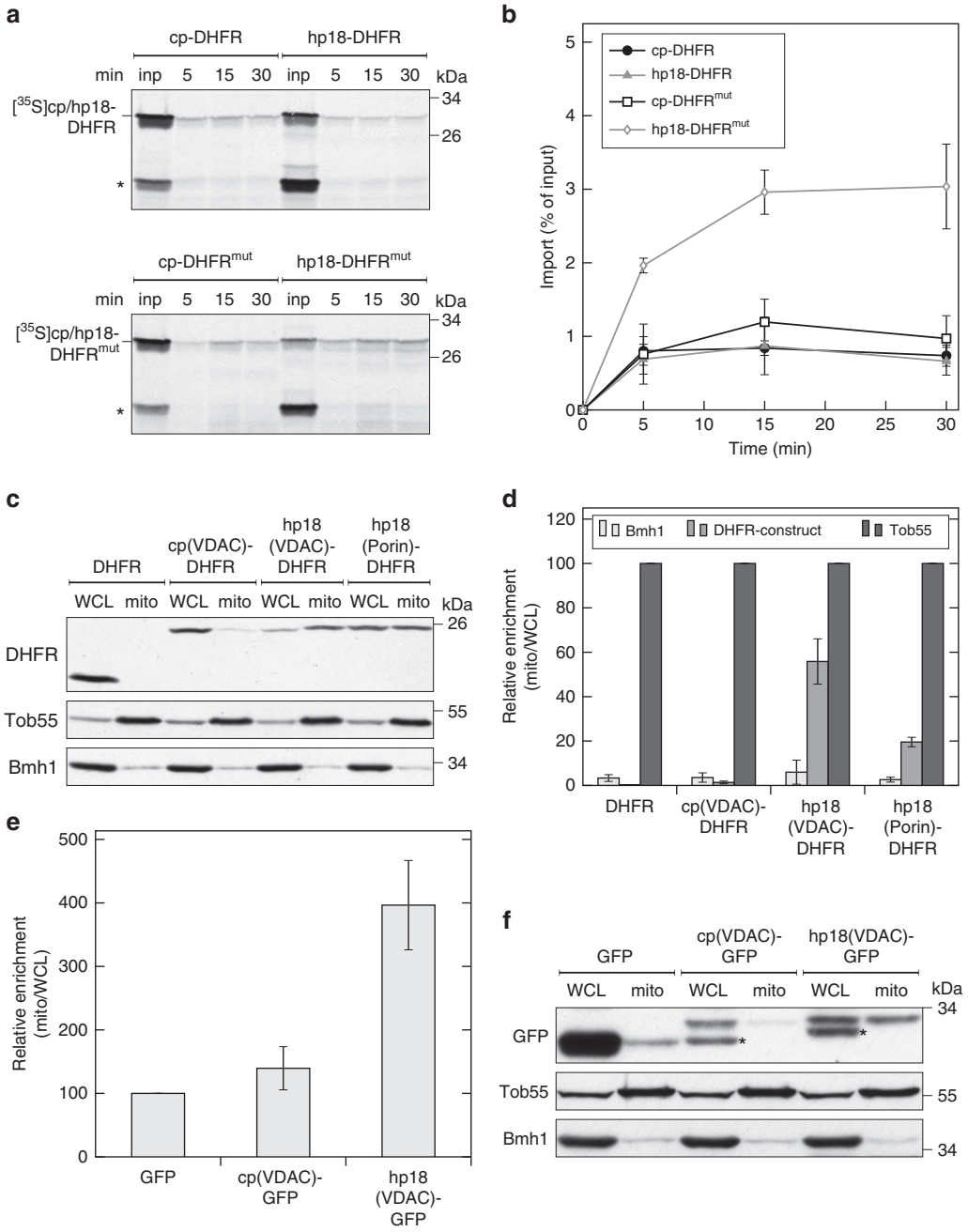

Figure 2 | β-Hairpin peptides can target passenger proteins to mitochondria. (**a**) The specified radiolabelled fusion proteins were imported into isolated mitochondria for the indicated time periods. An asterisk marks a translation product generated from an internal ATG codon corresponding to DHFR or DHFR^{mut}. inp, 5% lysate input. (**b**) The intensity of the bands from three independent experiments as in (**a**) was quantified and plotted against the time of the import reaction. Error bars represent s.d. (**c**) Crude mitochondria were isolated from yeast cells expressing DHFR alone or the indicated fusion proteins. Samples from the whole-cell lysate (WCL) and the crude mitochondria (mito) were analyzed by SDS–PAGE and immunodecoration with antibodies against the indicated proteins. Tob55, mitochondrial β-barrel protein; Bmh1, cytosolic protein. (**d**) The intensity of the bands from three independent experiments as in (**c**) was quantified and the mitochondrial enrichment was calculated by dividing the signal in the mitochondrial fraction by the one in the whole-cell lysate. The mitochondrial enrichment of Tob55 was set to 100. The results represent mean ± s.d. from three independent experiments. (**e**) Samples from the whole-cell lysate and crude mitochondrial fractions of yeast cells expressing the indicated proteins were analyzed for their GFP fluorescence. The mitochondrial enrichment of the GFP signal was calculated and the one of GFP-expressing cells was set to 100. The results represent mean ± s.d. from three independent experiments. (**f**) The samples from the experiments in (**e**) were analyzed by SDS–PAGE and immunodecoration with antibodies against the indicated proteins. An asterisk marks a shorter form of the fusion proteins resulting probably from degradation.

with the MitoTracker signal (Fig. 3c,d). These observations indicate that these hybrid proteins are not targeted to chloroplasts but rather to mitochondria. Of note, the N terminus of these fusion proteins apparently faces the mitochondrial IMS suggesting that although the C terminus of the mitochondrial atVDAC1 can mediate mitochondrial targeting, these fusion proteins are not inserted into the mitochondrial OM in a psOEP24-like topology.

To support our findings with an additional example, we fused GFP$_{S11}$ to a hybrid protein composed of β-strands 1–16 of the

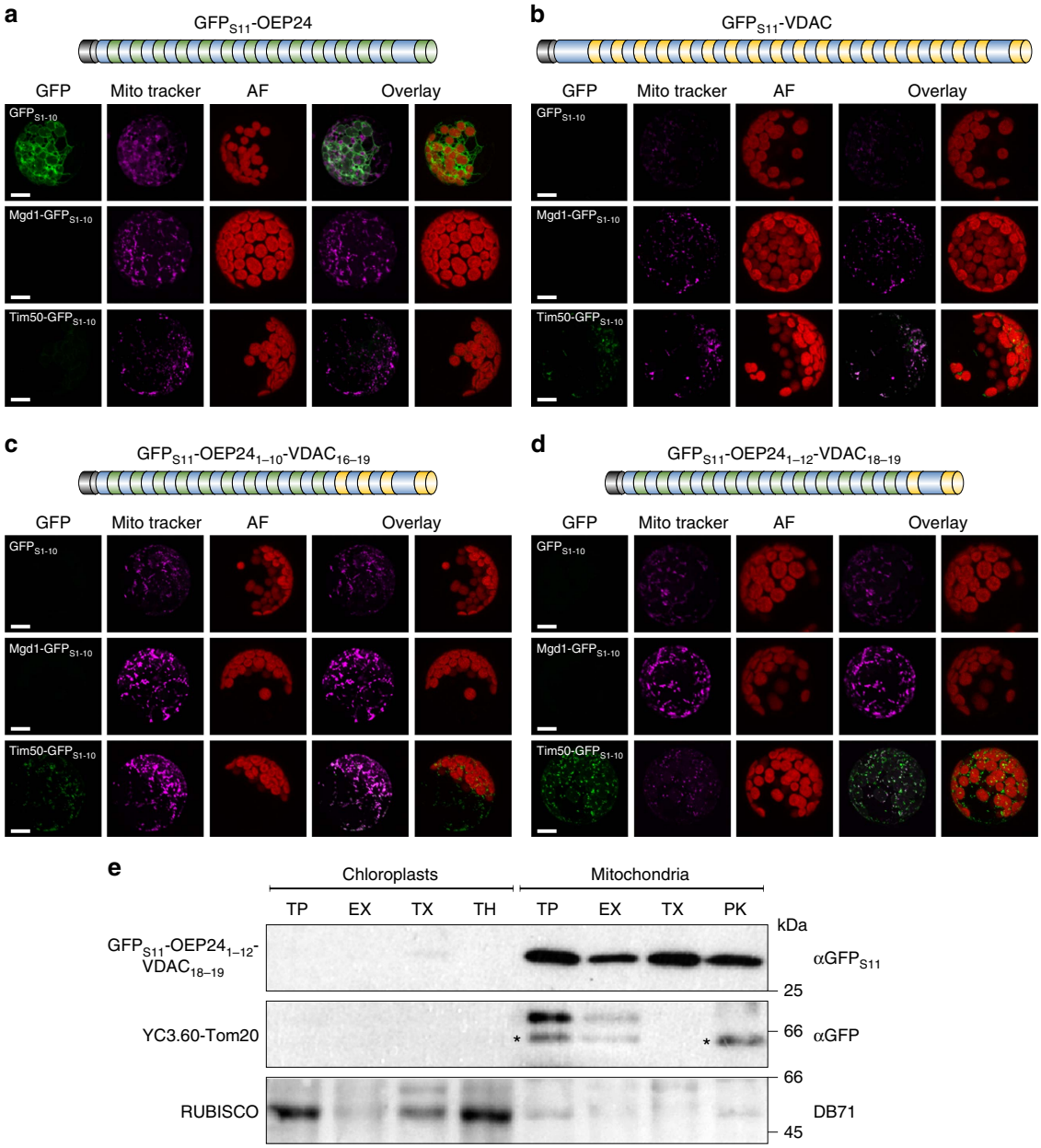

Figure 3 | The last β-hairpin of atVDAC1 directs psOEP24 to mitochondria. (**a**–**d**) The specified fusion proteins and the indicated reporter constructs were co-transformed into *A. thaliana* protoplasts. GFP, MitoTracker and chlorophyll autofluorescence (AF) signal as well as the overlays of GFP with either of the latter two for a representative image from at least three independent experiments is shown. Schemes of psOEP24 and constructs generated are shown. Yellow/green sections indicate transmembrane β-strands of atVDAC1 and psOEP24, respectively, and the black section represents the GFP$_{S11}$ strand. Scale bar, 10 μm. (**e**) Chloroplasts and mitochondria fractions were gained from protoplasts co-transfected with GFP$_{S11}$-OEP24$_{1–12}$-VDAC$_{18–19}$ and YC3.60-Tom20. Samples of the organelles were analyzed directly (total protein, TP) or they were subjected to carbonate extraction and the pellets were loaded (EX). Other samples were solubilized by Triton X-100 (TX), or treated with thermolysin (TH) or PK. Next, the organelles were analyzed by SDS–PAGE and immunodecoration with the indicated antibodies. DB71 stain of RUBISCO is shown as loading control. YC3.60 is fused to the N terminus of Tom20 and the cytosolic domain of Tom20 is removed by PK. Bands resulting from cross-reactivity of the GFP antibody are marked with an asterisk.

chloroplast β-barrel protein psOEP37 and the last β-hairpin of atVDAC1 (GFP$_{S11}$-OEP37$_{1–16}$-VDAC1$_{18–19}$). Similar to our observation with psOEP24, also this hybrid protein was targeted to mitochondria (Supplementary Fig. 3). Thus, it appears that a mitochondrial β-hairpin has a general capacity to target either soluble proteins (DHFR and GFP) or plastidic proteins (OEP24 and OEP37) to mitochondria.

To confirm the mitochondrial localization of the fusion protein GFP$_{S11}$-OEP24$_{1–12}$-VDAC1$_{18–19}$ and to evaluate whether it is indeed inserted into the mitochondrial OM, protoplasts from *Arabidopsis* cells expressing it were fractionated into samples enriched in either chloroplasts or mitochondria. To control for the efficiency of the organelle enrichments, protoplasts co-expressed the mitochondrial OM protein YC3.60-Tom20 (ref. 31). We detected the hybrid β-barrel protein in mitochondria but not in chloroplasts (Fig. 3e). A portion of the hybrid was partially resistant to either carbonate extraction or externally added PK. In contrast, the cytosolic domain of the control protein YC3.60-Tom20 was removed by PK treatment. However, when mitochondria were solubilized by Triton X-100

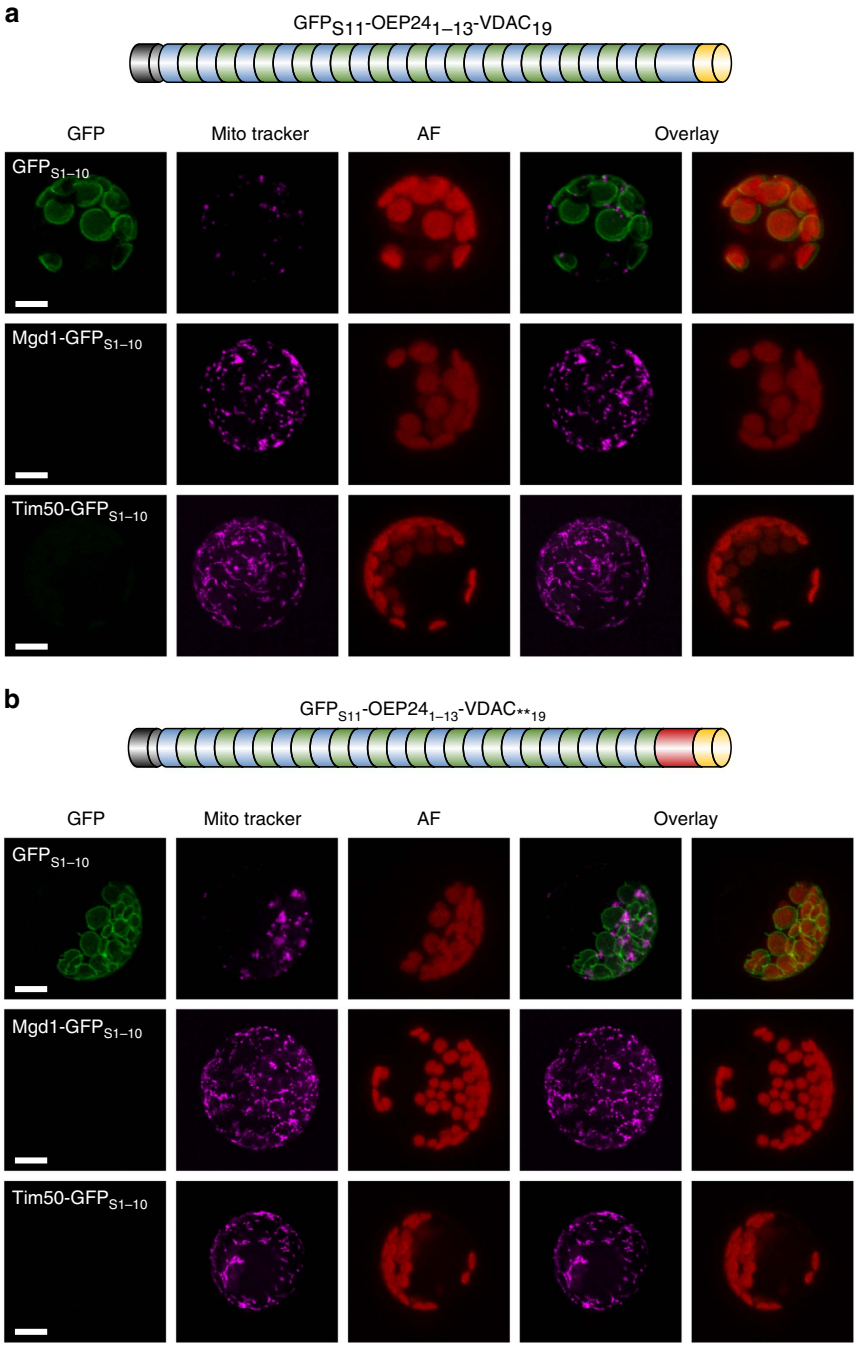

Figure 4 | The ultimate β-strand of atVDAC1 does not direct psOEP24 to mitochondria. (**a**, **b**) The last β-strand (GFP_{S11}-$OEP24_{1–13}$-$VDAC_{19}$) (**a**) or the last β-strand and the last loop (GFP_{S11}-$OEP24_{1–13}$-$VDAC_{**19}$) (**b**) of psOEP24 were replaced by the corresponding regions of atVDAC1 and the resulting fusion proteins were co-transformed with the indicated reporter constructs into *A. thaliana* protoplasts. Signals and schemes are as in Fig. 3a. Scale bar, 10 μm.

(TX), we could detect also a substantial portion of the hybrid protein in the pellet fraction suggesting that these molecules were aggregated (Fig. 3e). Hence, it seems that the hybrid protein can be perfectly targeted to mitochondria but cannot be completely integrated into the membrane and thus remains partially aggregated. Collectively, these findings demonstrate that the last β-hairpin of atVDAC1 is sufficient to target a chloroplast β-barrel protein to mitochondria.

We next wondered whether the capacity to assure mitochondrial targeting is limited to the last β-hairpin from plant atVDAC1 or can be extended to a similar β-hairpin from its yeast homologue scPorin. To that goal we created the hybrid proteins GFP_{S11}-Porin and a construct where the last β-hairpin of psOEP24 is replaced by the last β-hairpin of yeast Porin (GFP_{S11}-$OEP24_{1–12}$-$Porin_{18–19}$) and expressed them in protoplasts. GFP_{S11}-Porin partially aggregates in the cytoplasm, but its majority is localized to mitochondria as judged from the fluorescence signal upon co-expression with Tim50-$GFP_{S1–10}$ and the overlay of the GFP staining with the MitoTracker signal (Supplementary Fig. 4a). As seen for GFP_{S11}-Porin, co-expression of GFP_{S11}-$OEP24_{1–12}$-$Porin_{18–19}$ with $GFP_{S1–10}$ shows that the fusion protein partially aggregates in the cytoplasm. However,

co-expression of this hybrid protein with Tim50-GFP_{S1-10}, but not with Mgd1-GFP_{S1-10} yielded efficient GFP assembly and co-localization of the GFP fluorescence with mitochondria (Supplementary Fig. 4b). These observations suggest that this hybrid protein can be targeted to mitochondria, thereby verifying that the last β-hairpin of yeast Porin is sufficient for mitochondrial targeting. This conclusion is supported by fractionation of the transformed cells and analysis of the mitochondrial and chloroplasts fractions. GFP_{S11}-$OEP24_{1-12}$-$Porin_{18-19}$ was exclusively localized to mitochondria and a major portion of the protein was resistant to carbonate extraction and PK treatment. However, a substantial fraction of the fusion protein is also aggregated as it cannot be solubilized by Triton X-100 treatment (Supplementary Fig. 4c).

To analyze the membrane integration and the location of the N-termini of the various hybrid proteins in additional ways, we first tested the protection of the various constructs to protease treatment of whole protoplast lysate. The N terminus of GFP_{S11}-OEP24, which is targeted to chloroplasts, is exposed to the cytosol and thus was accessible to the protease. In contrast, GFP_{S11}-tagged versions of either atVDAC1 or scPorin and the hybrid proteins of their last β-hairpin with psOEP24 were resistant to such treatment. This resistance was dramatically reduced upon solubilization of organelles with detergent suggesting that the majority of the protection was not solely caused by aggregation (Supplementary Fig. 5a). Thus, it appears that the hybrid proteins are not only targeted to mitochondria but are also able to reach a protease-protected location.

Next, we wanted to confirm, by using an alternative GFP_{S1-10} mitochondrial reporter protein, that the N terminus of the various hybrid proteins is indeed accessible at the mitochondrial IMS. To that goal we constructed a protein that includes the N-terminal region of Tim21-like1 (Tim21(N)), which harbours the mitochondrial import signal and the first transmembrane domain of the protein, and fused it to GFP_{S1-10}. In line with the aforementioned results, co-expression of this reporter with GFP_{S11}-tagged atVDAC1 or scPorin and with their hybrid proteins, but not with GFP_{S11}-OEP24, gave a mitochondrial staining that co-localizes with the MitoTracker signal (Supplementary Fig. 5b). These observations verify that the last β-hairpin of either atVDAC1 or scPorin is sufficient to target a chloroplast β-barrel protein to mitochondria.

The β-signal is not sufficient for mitochondrial targeting. We next asked whether even a single β-strand from the C terminus of atVDAC1 is sufficient to assure mitochondrial targeting. This last strand contains the β-signal, which was proposed to be important for sorting within mitochondria[14]. To address this question we initially replaced either the last β-strand (GFP_{S11}-$OEP24_{1-13}$-$VDAC_{19}$) or the last β-strand together with the last loop of psOEP24 (GFP_{S11}-$OEP24_{1-13}$-$VDAC_{**19}$) by the corresponding regions of atVDAC1. Co-expression of these proteins in protoplasts with the markers for the organellar IMS did not result in an observable signal. In contrast, co-expression of both hybrid proteins with the cytosolic GFP_{S1-10} yielded GFP fluorescence surrounding chloroplasts (Fig. 4). Thus, the last β-strand is not sufficient to target hybrid proteins to mitochondria.

The last β-hairpin is necessary for mitochondrial targeting. Our aforementioned results clearly demonstrate that the last β-hairpin is sufficient by itself for mitochondrial targeting of non-mitochondrial proteins. We next asked whether this segment is also necessary to target native mitochondrial β-barrel proteins. To that end, we replaced either the last two β-strands of atVDAC1 by the last two β-strands of psOEP24 resulting in the construct GFP_{S11}-$VDAC_{1-17}$-$OEP24_{13-14}$ (subscript numbers reflect the number of the β-strand in the corresponding protein) or we replaced only the penultimate β-strand of atVDAC1 by the corresponding penultimate strand of psOEP24 (GFP_{S11}-$VDAC_{1-17}$-$OEP24_{13}$-$VDAC_{19}$). Co-expression of these fusion proteins with the various reporter constructs revealed GFP fluorescence exclusively with the cytosolic marker GFP_{S1-10}. Moreover, the GFP stain did not co-localize with mitochondria (Fig. 5). Thus, the complete last β-hairpin is required for mitochondrial targeting.

We next wondered if the last β-hairpin is also necessary for the targeting and assembly of mammalian VDAC1. To that goal we used the clear growth phenotype at elevated temperatures of yeast cells deleted for *POR1* (refs 30,32). hVDAC1 or its variants where the first (VDAC1Δhp1, lacking β-strands 1 and 2) or last (VDAC1Δhp18, lacking β-strands 18 and 19) β-hairpin is missing were expressed in wild type or *por1*Δ yeast cells and the growth behaviour of the transformed cells was monitored. None of the three constructs had any effect on wild type cells but only the full-length construct and the one lacking the first β-hairpin complemented the absence of yeast Porin. In contrast, the truncated variant without the last β-hairpin demonstrated only a very partial complementation capacity and could not support any growth on a non-fermentable carbon source (YPG) where fully functional mitochondria are required for viability (Supplementary Fig. 6a). Accordingly, VDAC1Δhp18 was detected in much lower levels than the native protein and VDAC1Δhp1 (Supplementary Fig. 6b), suggesting lower stability and higher turnover rate of the former variant. Our findings thus substantiate the importance of the last β-hairpin in the targeting of human mitochondrial β-barrel proteins.

Hydrophobicity of the β-hairpin is crucial for targeting. Since many proteins, including the widely used GFP and its variants, contain β-hairpin motifs but only *bona fide* mitochondrial β-barrel proteins assemble into the mitochondrial OM, we wondered which requirements a β-hairpin motif should fulfil in order to serve as a mitochondrial targeting signal. The membrane-embedded β-strands of β-barrel proteins have amphipathic structures where those amino acids facing the lumen of the barrel are rather hydrophilic, whereas those that face the lipid core are more hydrophobic. Inspection of the amino acids that build the hydrophobic face of hp18 of yeast Porin and hVDAC1 and of hp2 of yeast Porin (containing β-strands 18/19 or 2/3, respectively) suggests that these residues are on average more hydrophobic than the lipid-facing amino acids in other β-hairpins (Fig. 6a). To study the significance of this difference, we fused the passenger domain DHFR to peptides resembling β-hairpins with various hydrophobicities (hairpins 3, 17 and 18 of hVDAC1 and 2, 3 and 18 of Porin). When we then compared the mitochondrial association capacity of the resulting fusion proteins, we observed a clear correlation between the hydrophobicity of the lipid-facing residues of the peptides and the ability of the corresponding peptide to target the passenger domain to mitochondria (Fig. 6b).

Assuming that hydrophobicity is important for the targeting ability of a β-hairpin motif, mutations at the lipid-facing side that replace amino acids by less hydrophobic ones should decrease the targeting capacity of the corresponding β-hairpin motif. To test this prediction, we created several DHFR-containing hybrids where one, two or three of the hydrophobic residues in hp18 of hVDAC1 were replaced by the polar residue Gln (Fig. 6c). When we monitored the mitochondrial association of these hybrids, we

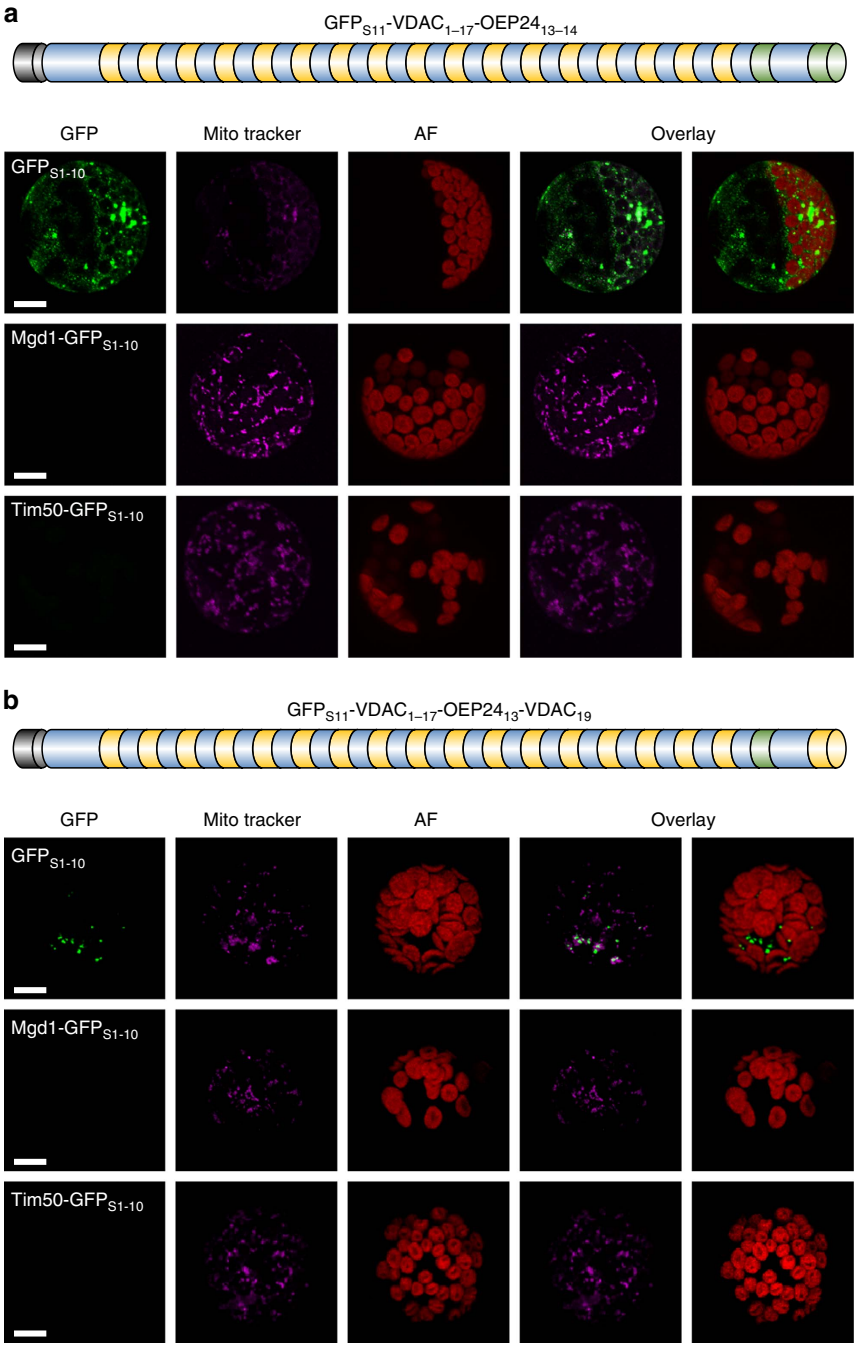

Figure 5 | The last β-hairpin of atVDAC1 is important for mitochondrial targeting. (**a**,**b**) GFP$_{S11}$-VDAC$_{1–17}$-OEP24$_{13–14}$ (**a**) or GFP$_{S11}$-VDAC$_{1–17}$-OEP24$_{13}$-VDAC$_{19}$ (**b**) and the indicated reporter constructs were co-transformed into *A. thaliana* protoplasts. Signals and schemes are as in Fig. 3a. Scale bar, 10 μm.

observed a clear correlation between the number of substituted amino acids and a reduction in the mitochondrial targeting capacity. The targeting capability of constructs with two or three inserted Gln residues was reduced by about 70 or 80%, respectively (Fig. 6c).

Along this line, we anticipated that increasing the hydrophobicity of the lipid-facing side should enhance the mitochondrial targeting capacity of the resulting β-hairpin. Indeed replacing in hp17 of hVDAC1 (containing β-strands 17/18) the polar residue Gln249 by Leu resulted in a clear enhancement in the mitochondrial association of the obtained construct. Moreover, adding to the above mutation also the Tyr247 to Phe replacement resulted in a further considerable augmentation of the mitochondrial binding of the resulting hybrid protein (Fig. 6d).

To substantiate this point also in plant cells, we constructed a hybrid protein where the fifth and sixth β-strands of psOEP24 were replaced by the corresponding β-strands of atVDAC1 (GFP$_{S11}$-OEP24$_{1–4}$-VDAC$_{5–6}$-OEP24$_{7–14}$). The average hydrophobicity of these β-strands of atVDAC1 is lower than that of strands 18 and 19 of the protein (2.1 as compared to 3.4, respectively). When this hybrid protein was co-expressed in protoplasts together with the various marker proteins it aggregated in the cytosol and was not targeted to mitochondria (Supplementary Fig. 7). Collectively, these findings demonstrate that elevated hydrophobicity of the lipid-facing side

a

Hairpin	hVDAC1	scPorin	atVDAC1	psOEP24
hp1	1.57	2.74	1.82	1.58
hp2	0.46	3.00	0.93	2.84
hp3	0.32	1.79	0.56	3.18
hp4	0.98	1.61	1.17	2.29
hp5	1.88	1.64	2.07	2.07
hp6	0.93	1.33	0.66	1.79
hp7	1.20	1.99	1.11	1.04
hp8	2.38	2.01	2.42	1.40
hp9	1.49	2.00	1.03	0.22
hp10	1.06	1.50	0.28	0.35
hp11	1.10	1.40	0.98	0.63
hp12	0.90	1.36	1.42	0.97
hp13	1.29	1.67	1.29	2.87
hp14	1.72	2.17	2.00	
hp15	1.60	2.10	2.30	
hp16	1.01	1.82	1.48	
hp17	2.00	2.12	2.04	
hp18	3.24	2.63	3.37	

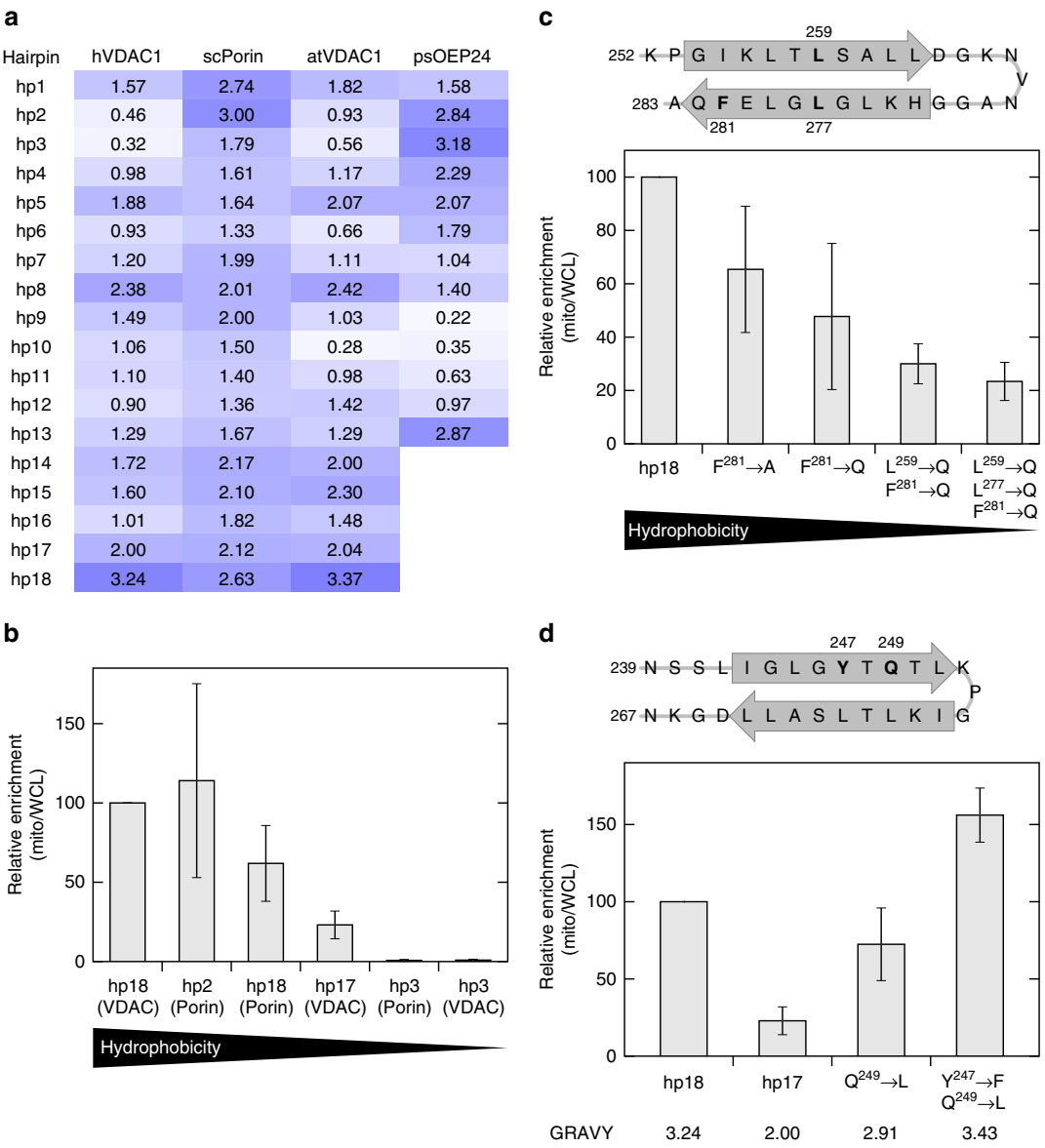

Figure 6 | The hydrophobicity of the β-hairpin motif is important for its mitochondrial targeting efficiency. (**a**) The average hydrophobicity of the hydrophobic face of the β-hairpins of various β-barrel proteins was calculated by summing up the hydropathy values of the residues facing the lipid environment from both β-strands that form each β-hairpin and dividing it by the number of the residues. (**b**) Yeast cells expressing the indicated β-hairpin peptides fused to DHFR were analyzed as in Fig. 2c,d. The mitochondrial enrichment of hp18(VDAC)-DHFR was set to 100. The results represent mean ± s.d. from three independent experiments. (**c**) Top panel: scheme of hp18(VDAC) used in these experiments. Grey arrows indicate the residues that form a β-strand in full-length hVDAC1. Residue numbers correspond to the numbering of full-length hVDAC1. Amino acids that were mutated are shown in bold font. Bottom panel: yeast cells expressing hp18(VDAC) peptide or its variants with the indicated mutations fused to DHFR were analyzed as in Fig. 2c,d. The mitochondrial enrichment of the control hp18-DHFR was set to 100. The results represent mean ± s.d. from three independent experiments. (**d**) Top panel: scheme of hp17(VDAC) depicted as in (c). Bottom panel: yeast cells expressing DHFR fused to hp18(VDAC) peptide, hp17(VDAC) peptide or variants of hp17(VDAC) with the indicated mutations were analyzed as in Fig. 2c,d. The mitochondrial enrichment of the hp18-DHFR protein was set to 100. The results represent mean ± s.d. from three independent experiments. GRAVY, grand average hydrophobicity of the hydrophobic face of the hairpin.

of a β-hairpin is crucial for its function as a mitochondrial targeting signal.

The import receptor Tom20 recognizes the β-hairpin signal. The establishment of a β-hairpin as a mitochondrial targeting signal raised the question, which import elements can recognize it. To address this question, we synthesized the β-hairpin peptide in its linear or cyclic forms and replaced Leu263 by the photo-reactive benzoyl-phenylalanine (Bpa) moiety. Ultraviolet-activation of Bpa results in generation of covalent bonds between the photo-peptide and proteins in its vicinity. Next, we mixed various amounts of the photo-peptides with isolated mitochondria and performed photo-crosslinking. Subsequent western blot analysis demonstrated crosslinking adducts of the cyclic β-hairpin peptide with import components like Tom40, Tom22 and Tom70 (Fig. 7). As anticipated, formation of photo-adducts was also observed with the import receptor Tom20 that was suggested by several studies to be the major mitochondrial import receptor for β-barrel proteins[33–36].

Several cross-linking adducts of the peptide and the various TOM components can be detected. We suppose that this

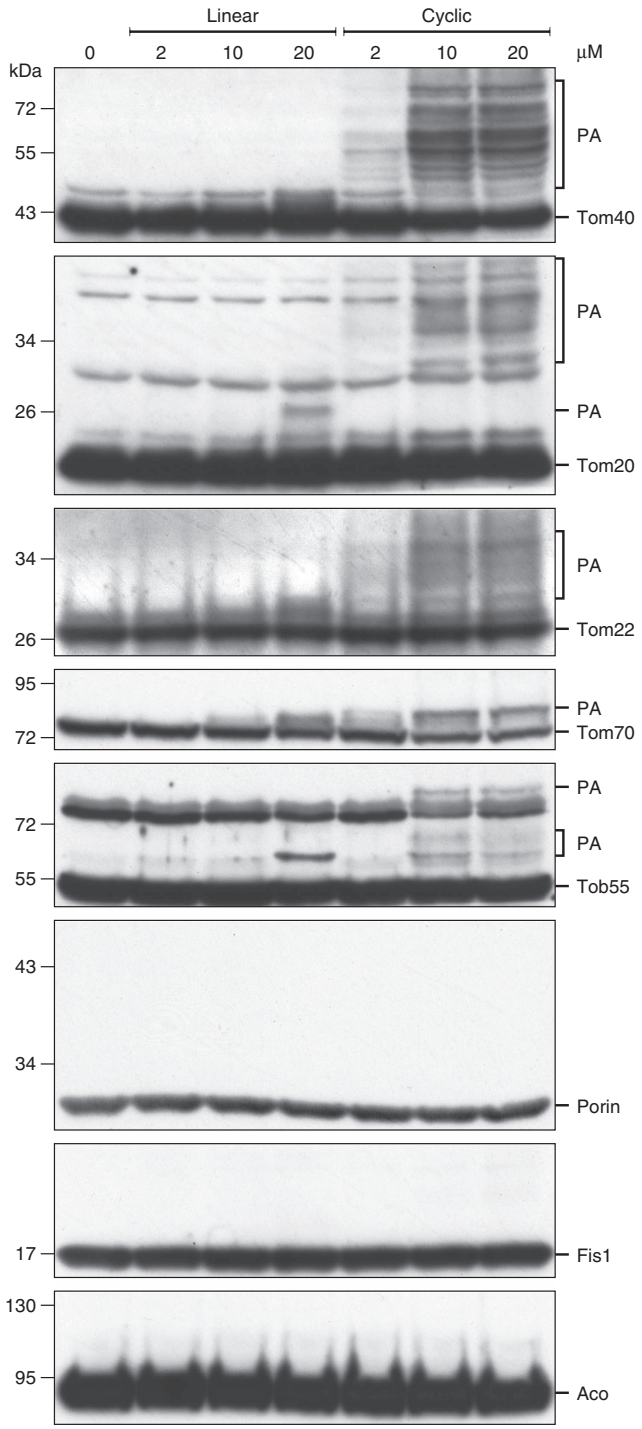

Figure 7 | The cyclic β-hairpin peptide can be cross-linked *in organello* to components of the TOM complex. Isolated mitochondria were incubated with a Bpa-containing linear or cyclic peptide at the indicated concentrations. After ultravoilet-induced cross-linking the samples were analyzed by SDS–PAGE and immunodecoration with antibodies against the indicated proteins. PA, photo-adducts.

variability can result from a variable number of peptides bound to one molecule of protein and from different crosslinking sites on the protein, which in turn can cause different migration behaviour in the SDS–PAGE. Of note, weak cross-linking adducts were also observed with Tob55 suggesting that a small portion of the peptide molecules was translocated across the OM and associated already with the TOB complex. The specificity of the cross-linking adducts is demonstrated by their absence when no peptide or the linear peptide were used and the lack of photo-adducts with unrelated mitochondrial proteins like Fis1, Porin or aconitase. Thus, the crosslinking assay demonstrates that the β-hairpin motif interacts with the TOM complex.

To check *in vivo* the potential interaction of Tom20 with the β-hairpin motif, we employed a bimolecular fluorescence complementation assay (Fig. 8a). Either hp18 or the cp of hVDAC1 were fused to the N-terminal portion of YFP, whereas Tom20 was fused at its C terminus to the C-terminal part of YFP. We verified the functionality of Tom20-YFP(C) by demonstrating its capacity to complement the growth phenotype of cells lacking Tom20 (Fig. 8b). Furthermore, similarly to native Tom20, Tom20-YFP(C) is exposed to the cytosol as suggested by its availability to external protease and it is embedded in the OM as it cannot be extracted by alkaline solution (Supplementary Fig. 8). Thus, Tom20-YFP(C) acquires native-like topology and is fully functional.

Next, various combinations of pairs of fusion proteins were expressed in yeast cells and the cells were analyzed by fluorescence microscopy. As expected, cells harbouring Tom20-YFP(C) alone or in the presence of cytosolically-expressed YFP(N) demonstrated only basal fluorescence signal. Similarly marginal was the signal when Tom20-YFP(C) was co-expressed with the hVDAC1 N-terminal control peptide fused to YFP(N). In sharp contrast, a strong fluorescence staining of mitochondrial structures was observed in cells co-expressing Tom20-YFP(C) and hp18(VDAC)-YFP(N) (Fig. 8c). To control for the specificity of this interaction we fused YFP(C) to another OM protein with a similar topology like Tom20, namely Mcr1. This protein has two isoforms, a longer form that, similar to Tom20, is anchored to the mitochondrial OM via a single N-terminal segment and a shorter, processed one in the IMS[37]. As we previously observed that R4E and R7E mutations in Mcr1 cause an enhanced portion of the molecules in the OM[38], we co-expressed Mcr1(R4E, R7E)-YFP(C) with different YFP(N)-containing fusion proteins. To obtain a reliable quantification of the fluorescence signal, crude mitochondria were isolated from the transformed cells and their fluorescence signal was measured with a fluorimeter. Our results clearly demonstrate that the co-expression of Tom20-YFP(C) and hp18(VDAC)-YFP(N) resulted in several fold stronger fluorescence signal in comparison to all other combinations (Fig. 8d). These findings strongly suggest that the β-hairpin targeting signal is either in close vicinity to Tom20 or physically interacting with the receptor protein.

To directly probe the interactions of the cyclic β-hairpin peptide with the receptor Tom20 and to verify physical contact between the two, we monitored chemical-shift changes in the [^{1}H, ^{15}N]-HSQC NMR spectra of the uniformly [^{15}N]-labelled cytosolic receptor domain of rat Tom20 (dTom20) upon addition of the non-labelled cyclic β-hairpin peptide. The peptide caused chemical-shift perturbations of a subset of the backbone amide signals of dTom20 (Fig. 9a,b). Interestingly, the dTom20 residues affected by the β-hairpin peptide are close to the presequence binding region of dTom20 (Fig. 9c; ref. 39), suggesting that the β-hairpin peptide shares with canonical presequences the same binding site on Tom20. These experiments demonstrate a direct interaction of the β-hairpin element with Tom20.

Discussion

After their synthesis in the cytosol the vast majority of mitochondrial proteins are delivered to the mitochondrial surface

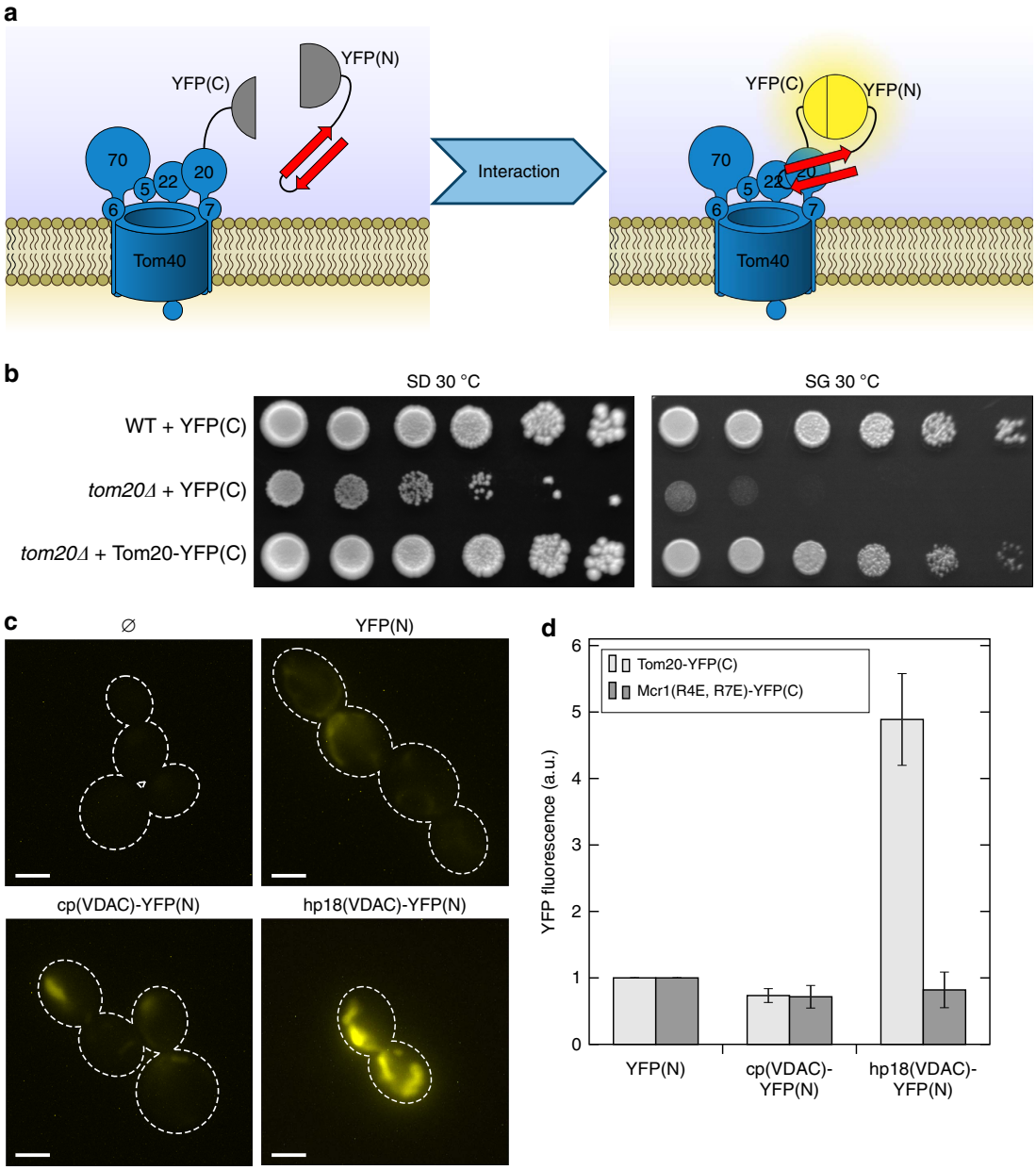

Figure 8 | A β-hairpin peptide interacts with the import receptor Tom20 *in vivo*. (**a**) Schematic representation of the assay. Tom20 was fused with the C-terminal part of YFP (YFP(C)) whereas the N-terminal part of YFP (YFP(N)) was fused to the β-hairpin peptide (red). YFP fluorescence can be observed only upon interaction of the two fusion proteins. (**b**) The growth of WT and *tom20Δ* yeast cells expressing either YFP(C) or the fusion protein Tom20-YFP(C) was analyzed by drop-dilution assay. (**c**) Yeast cells expressing Tom20-YFP(C) alone (Ø), or co-expressing Tom20-YFP(C) with YFP(N), the control peptide (cp(VDAC)) fused to YFP(N) or hp18(VDAC) fused to YFP(N) were subjected to fluorescence microscopy. Representative images are shown. Scale bar, 5 µm. (**d**) Crude mitochondria were isolated from cells co-expressing the indicated YFP(N) fusion proteins and either Tom20-YFP(C) or Mcr1(R4E, R7E)-YFP(C). The YFP fluorescence of the crude mitochondrial fractions was analyzed and the signal of cells expressing YFP(N) without any additive was set to 1. Data represents mean ± s.d. of three independent experiments.

with the help of an N-terminal, cleavable targeting signal, also known as presequence. In contrast, proteins residing in the OM of the organelle do not contain such a signal and their targeting is mediated by elements that are part of the mature protein. Efforts to identify linear sequences within β-barrel proteins that can fulfil this task have failed so far. Thus, it was assumed that the signals are contained in β-barrel-specific structural elements rather than in a conserved linear sequence. In this study we demonstrate that a β-hairpin motif with a highly hydrophobic face is the minimal structural element that can function as a mitochondrial targeting signal.

This motif fulfils all the requirements of a specific intracellular targeting signal. It is necessary for targeting as in its absence the remaining portion of the protein is not targeted properly to mitochondria. The signal is also sufficient by itself and can mediate mitochondrial location of soluble passenger domains. Furthermore, attachment of this signal to chloroplast β-barrel proteins redirects the latter to mitochondria. The β-hairpin motif is also the minimal signal and a single β-strand cannot fulfil this task. Finally, as expected from a targeting signal, the β-hairpin motif is recognized at the cytosolic side of the organelle by an import receptor (Tom20).

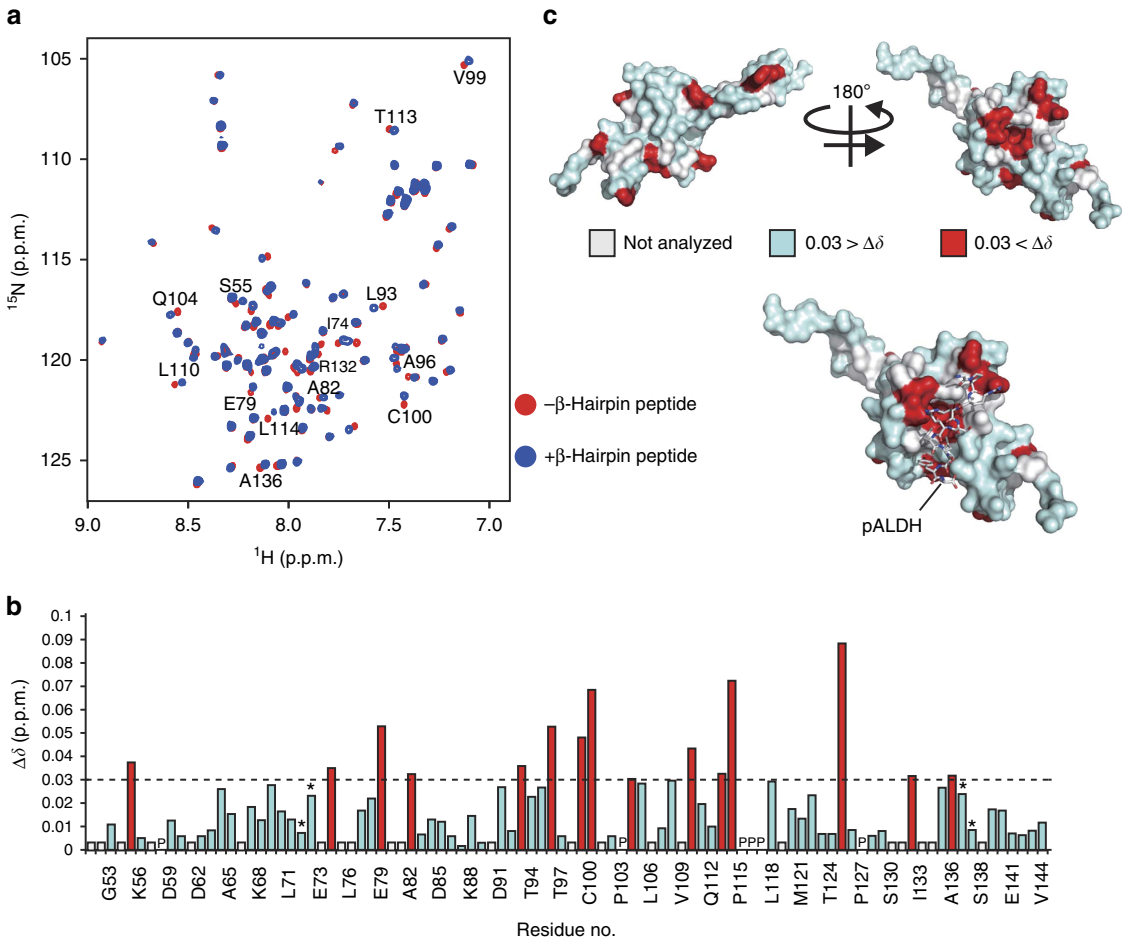

Figure 9 | The β-hairpin peptide binds to the presequence binding region of Tom20. (**a**) [^{1}H, ^{15}N]-HSQC NMR spectra of [^{15}N]-labelled rat dTom20 were recorded before (red spectrum) and after addition of two molar excess cyclic peptide (as in Fig. 1a) in DMSO (blue spectrum) or the same volumes of DMSO as control. (**b**) The chemical shift changes of each backbone amide of dTom20 in (**a**) are presented. Signals from several amino acids were not used for the analysis due to signal overlapping. The signals from some other residues were not assigned. These uncharacterized residues are shown in white. Signals showing chemical shift changes larger than 0.03 p.p.m. are shown in red and the others in pale blue. Asterisks, residues E72 and Q137 gave two signals each. (**c**) The residues whose signals show chemical shift changes larger or lower than 0.03 p.p.m. are shown in red and pale blue, respectively, on the surface model of rat dTom20 in a complex with the presequence peptide derived from rat aldehyde dehydrogenase (pALDH) (PDB ID 1OM2). The residues whose signals were not analyzed are shown in white. The structure of pALDH is shown as a stick model in the lower panel.

In most of the analyzed mitochondrial β-barrel proteins, the last β-hairpin at the C terminus has a high hydrophobicity and can serve as a targeting signal. This function can explain previous observations where mutations in the C-terminal region of the β-barrel proteins Porin and Tom40 hindered mitochondrial targeting of the mutated proteins, whereas mutations in the N-terminal segment did not have this effect[40–42]. The ultimate β-strand contains the previously identified β-signal, which is composed of several amino acids and is recognized by the TOB/SAM complex and serves as an intra-mitochondrial sorting signal[14]. Our finding that the minimal targeting signal is composed of two β-strands with the loop between them explains why the β-signal is neither sufficient nor absolutely required for the targeting from the cytosol to mitochondria. Point mutations in the β-signal affect interactions with the TOB/SAM complex but the mutated β-barrel proteins were still targeted from the cytosol to the organelle[14]. Along this line, our data show that a mutation that disrupts the β-signal (F281A) only moderately affects the targeting capacity of the resulting β-hairpin. Despite the special high targeting capacity of the last β-hairpin, it is probably not the only β-hairpin that can serve as a targeting signal in mitochondrial β-barrel proteins. In addition, in the fusion proteins used in the current study a signal fused N-terminally to a passenger domain could have a mitochondrial targeting capacity. Hence, the location of the signal within the substrate β-barrel protein appears not to be restricted to the most C-terminal β-hairpin. Accordingly, we found that fusion proteins containing the second β-hairpin of Porin are targeted to mitochondria in high efficiency. Furthermore, VDAC1 molecules deleted for the last β-hairpin were still detected on mitochondria (although only in minor amounts) suggesting that other β-hairpins can also fulfil the targeting task although with much lower potential. Hence, an avidity effect of several β-hairpins within the same protein can be anticipated.

The identification of a β-hairpin as a targeting signal can also explain how bacterial proteins that do not share any sequence homology with mitochondrial proteins can be targeted to mitochondria upon their expression in eukaryotic cells[16–19]. The β-hairpin motif is the most basic structural unit of all β-barrel proteins and thus is contained also by the bacterial ones[22]. Whereas in prokaryotes and non-plant eukaryotic cells β-barrel proteins are targeted only to one cellular membrane, the situation is more complicated in plant cells that harbour such proteins in two separate locations namely, mitochondria and

chloroplasts. Hence, a mechanism that assures the specific targeting must have developed in such cells. We previously observed that plant plastidic β-barrel proteins show a clear discrimination between the two organelles only *in vivo*[30]. Our results demonstrate the existence of a specific signal that can target plant β-barrel proteins to mitochondria. However, it is unclear whether this signal and the yet to be discovered chloroplast signal are decoded by dedicated cytosolic guidance factors and/or specific chaperones. Obviously, mitochondrial proteins have to avoid recognition by chloroplasts targeting factors.

Irrespective of the cytosolic events, once the newly synthesized β-barrel protein reaches the surface of the organelle it is recognized by the TOM complex[4,13,43]. In line with these previous reports, the β-hairpin signal can be cross-linked to various components of the TOM complex suggesting that it can be in their vicinity. Previous studies suggested that the major receptor for these proteins is Tom20 that recognizes also presequence-containing mitochondrial proteins[33,35,36,44]. Accordingly, we observed by *in organello* and *in vitro* assays an interaction of the β-hairpin signal with Tom20. Remarkably, our NMR analysis indicated that the canonical presequence and the β-hairpin share the same binding region on Tom20. This similarity can be explained by the common amphiphilic structure of both elements where one face is rather polar and the other is hydrophobic. Our discovery regarding the shared binding site on Tom20 explains also the reduced *in vitro* import of presequence-containing mitochondrial protein upon addition of the cyclic β-hairpin peptide and previous observations where a peptide resembling a presequence could compete for the import of Porin[45]. In addition to Tom20, Tom22 and/or Tom70 were also suggested to be involved in processing of presequence-containing proteins[46,47]. Considering the structural similarity between the two signals and the observed cross-linking adducts of the β-hairpin peptide with the latter two proteins, one can speculate that Tom22 and/or Tom70 might also participate in the recognition of the β-hairpin element.

In summary, a dedicated β-hairpin motif is a newly-discovered genuine targeting signal that is necessary and sufficient for the targeting of mitochondrial β-barrel proteins to the organelle and for their recognition by import receptors.

Methods

Yeast strains and growth methods. Standard genetic techniques were used for growth and manipulation of yeast strains. The wild-type strain W303α was employed. The *tom20Δ* and *por1Δ* strains were described before (refs 18,30, respectively).

Drop-dilution assay. Cells were grown to logarithmic phase in appropriate liquid media, collected by centrifugation, and resuspended in water to an optical density at 600 nm of 2. Cell suspensions were serially diluted fivefold in water, and 5 µl aliquots of the cell suspensions were spotted on appropriate plates, which were then incubated at either 30 or 37 °C.

Recombinant DNA techniques. The plasmids pGEM4-pSu9-DHFR, pGEM4-pSu9-DHFR^{mut} or pYX142-mtGFP were used as templates for the amplification of the DHFR or the green fluorescent protein genes by PCR. The amplification products were inserted into pGEM4 using KpnI and BamHI restriction sites. Fusion proteins containing segments of either hVDAC1 or yeast Porin were generated by PCR using as template the plasmid pGEM4-hVDAC1 or pGEM4-Por1, respectively. The sequences of all PCR primers used in this study are included in Supplementary Table 1. The DNA encoding these peptides was inserted into the previously generated pGEM4-DHFR, pGEM4-DHFR^{mut} or pGEM4-eGFP using EcoRI and KpnI restriction sites. For expression in yeast cells the DHFR or eGFP fusion constructs were sub-cloned into pYX142 using EcoRI and SalI restriction sites. The mutations within hp17(VDAC) and hp18(VDAC) were introduced via site-directed mutagenesis using the QuickChange Site-Directed Mutagenesis Kit (Stratagene) according to the manufacturer's instructions.

The YFP(C) constructs for the BIFC assays were amplified from pRS426-TPI-Tom20 and pGEM4-Mcr1 using standard PCR techniques and subsequently cloned into the plasmid C-YC426ADH[48] using BamHI and HindIII or EcoRI and HindIII restriction sites, respectively. The plasmid C-YN425ADH was used as a template for the PCR amplification of the YFP(N) fragment. The PCR product was inserted into pGEM4 using KpnI and BamHI restriction sites. The DHFR gene in pYX142-DHFR, pYX142-cp(VDAC)-DHFR and pYX142-hp18(DHFR) was then replaced with the YFP(N) fragment by sub-cloning with NcoI and SalI restriction sites.

The plasmid pGEM4-hVDAC1 was used as a template for the PCR amplification of the full-length and the truncated hVDAC1 variants. The amplification products were inserted into pYX142 using BamHI and SalI restriction sites.

All DNA sequences required for the generation of constructs for the self-assembly-GFP assays were amplified from *Arabidopsis thaliana* Col0 or from *Pisum sativum* var. arvika cDNA, by standard PCR techniques. Subsequently the PCR products were cloned into the pAVA plasmid[49] containing the fragments for saGFP11 (GFP_{S11}) (N-terminally) or saGFP1-10 (GFP_{S1-10}). Templates for the $saGFP_{S1-10}$ and $saGFP\text{-}_{S11}$ fragments were obtained from Dr G. S. Waldo (Los Alamos, NM, USA). Chimeric β-barrel proteins were generated using PCR and were cloned into the $saGFP\text{-}_{S11}$ (N-terminally) pAVA vector using KpnI and SpeI as restriction sites. All plasmids used in this study are listed in Supplementary Table 2.

Biochemical procedures. Mitochondria were isolated from yeast cells by differential centrifugation as described[50]. For the isolation of crude mitochondrial fractions, yeast cells were grown in selective media to logarithmic phase and harvested by centrifugation. The cells were resuspended in SEM buffer (250 mM sucrose, 10 mM MOPS, 1 mM EDTA, pH 7.4) supplemented with 2 mM Phenylmethylsulfonyl fluoride (PMSF), mixed with glass beads and lysed by three rounds of 30 s vortexing followed by 30 s on ice. The whole-cell lysate was separated from glass beads and cell debris by centrifugation (1,000*g*, 3 min, 2 °C). Crude mitochondria were isolated from the cell lysate by centrifugation (20,000*g*, 10 min, 2 °C). In addition, a sample from the whole-cell lysate was subjected to chloroform–methanol precipitation. The samples were then subjected to SDS–PAGE.

Radiolabelled proteins were synthesized in rabbit reticulocyte lysate in the presence of ^{35}S-methionine (Perkin-Elmer) after *in vitro* transcription by SP6 polymerase from pGEM4 vectors (Promega). Radiolabelled precursor proteins were incubated at 25 °C with isolated yeast mitochondria in import buffer (250 mM sucrose, 0.25 mg ml^{-1} BSA, 80 mM KCl, 5 mM $MgCl_2$, 10 mM MOPS-KOH, 2 mM NADH, 4 mM ATP, pH 7.2). Non-imported proteins were removed by treatment with PK (50 µg ml^{-1}) for 30 min on ice. After inhibition of PK with 5 mM PMSF, the samples were boiled at 95 °C for few min before their analysis by SDS–PAGE.

Immunoblotting. A list of primary antibodies used in this study is included in Supplementary Table 3. The secondary antibodies were Horseradish peroxidase-coupled goat-anti-rabbit or goat-anti-mouse (Bio-Rad, cat. # 1721019 or cat. # 1721011, respectively) that were diluted 1:10,000 or 1:2,000, respectively. Full uncropped versions of all immunoblot images in all figures are included in Supplementary Fig. 9.

Synthesis and purification of peptides. The linear protected peptide was synthesized using standard Fmoc/tBu chemistry on a multiple peptide synthesizer Syro II (MultiSyntechTech) on an acid labile TCP resin (Intavis) as described[51]. To remove the peptide from the resin after completion of the synthesis, the dried resin was treated for 2 h at room temperature with a mixture of dichloromethane/1,1,1,3,3,3-hexafluoro-2-propanol (8/2 v/v). The mixture was filtered out and the solvent was concentrated with vacuum. The obtained oily product was precipitated from cold diethylether as a white solid. The linear protected peptide was treated with trifluoroacetic acid (TFA) and purified by RP-HPLC as described below. The Matrix-Assisted Laser Desorption Ionization-Time of Flight-Mass Spectrometry (MALDI-TOF-MS) showed the correct mass of $[M+H]^+ = 2{,}454.50$.

A cyclic protected peptide was obtained as follows. Diisopropylethylamine (0.6 mmol) and 1-hydroxybenzotriazol (0.3 mmol) were added to a solution of linear protected peptide (0.1 mmol) in dry 40 ml dimethylformamide. The solution was dropped to a solution of 0.3 mmol *O*-benzotriazol-1-yl-N,N,N′N′-tetramethyluronium tetrafluoroborate in 80 ml dimethylformamide for 2 h, and the solution was stirred overnight. The solvent was removed under reduced pressure affording a light yellow oily residue. The crude cyclic product was then precipitated from ice-cold water and was dried under vacuum for 12 h.

Preparation of free cyclic peptide: The dried residue was treated with a mixture of TFA/thioanisole/water (95:5:5) for 3 h at room temperature and the final cyclic peptide was precipitated as an amorphous solid by the addition of diethylether. Crude peptides were purified further by preparative RP-HPLC on a Reprosil-Pur Basic C8, 5 µm column (250 × 10 mm) (Dr Maisch, Germany) using a linear gradient of 20–70% acetonitrile in water containing 0.05% TFA. Purification was verified by analytical RP-HPLC. The cyclization was confirmed by MALDI-TOF-MS by obtaining the correct mass $[M+H]^+ = 2{,}436.48$.

Modelling and prediction of secondary structures. The secondary structures of atVDAC1 and scPorin were assigned based on an alignment to the crystal structure of mouse VDAC1 (programme: Mafft v6.847b, options: local pair, JTT200 matrix, 2.65 gap open, 0.15 gap extension[52]). For psOEP24 the secondary structure elements were predicted using the consensus prediction of the GeneSilico metaserver[53], the BOCTOPUS server[54] and the PredTMbb server[55]. For each position a score

describing the likelihood of this residue to be part of a β-strand was calculated as follows: the score for each position was increased by 1 if BOCTOPUS and PredTMbb predict the corresponding position as part of a β-strand and by 0.5 if the secondary structure prediction of GeneSilico metaserver predicts β-strand.
The prediction of the GenSilico metaserver had a lower weight because this server predicts β-strands in general whereas the other two predict transmembrane β-strands. Furthermore the score was decreased by 0.5 if the position was assigned as disordered by the GeneSilico metaserver. A residue was assigned to be in a β-strand if its score was higher than 1.5. To avoid missing potential β-strands we additionally checked manually an alignment of OEP24 sequences from several organisms for regions of alternating hydrophobicity[56,57].

Protoplast transfection and fractionation. *A. thaliana* protoplasts were isolated and transfected as described[29]. Two samples of 2.5 million protoplasts each were transfected with 200 µg plasmid DNA of GFP_{S11}-$OEP24_{1-12}$-$VDAC1_{18-19}$ and 150 µg plasmid DNA of YC3.60-TOM20. After 14 h expression under constant light, protoplasts were collected at 100*g* for 5 min and pooled in 5 ml extraction buffer (0.3 M sucrose, 50 mM HEPES-KOH, pH 7.6, 2 mM EDTA, 1% (w/v) polyvinylpyrrolidone (PVP) 40, 1% (w/v) fatty acid-free BSA, 330 mg l^{-1} ascorbate, supplemented immediately before use with 2 mM PMSF). For the total protein extract, 500 µl of protoplast suspension were pelleted at 25,000*g* for 5 min and resuspended in loading buffer (8 M urea, 0.2 M Tris–HCl pH 6.8, 10 mM EDTA pH 8.0, 5% (w/v) SDS, 0.03% bromphenol blue, 10 mM PMSF and 143 mM β-mercaptoethanol). The protoplasts were lysed using an Ultra-Turrax T25 homogenizer for three times of one second each at low intensity (idling speed = 8,000 min^{-1}). The lysate was then aliquoted in 1.5 ml Eppendorf tubes and the crude chloroplasts fraction was harvested at 1,500*g* for 5 min. The pellets were resuspended in a total volume of 2.5 ml washing buffer (0.3 M sucrose, 50 mM HEPES-KOH pH 7.6, 10 mM $MgCl_2$, 10 mM KCl, 2 mM EDTA pH 8.0, 330 mg l^{-1} ascorbate, supplemented immediately before use with 1 mM PMSF). Chloroplasts were purified over a Percoll step gradient (3 ml 85% Percoll and 5.143 ml 45% Percoll both diluted in 0.33 M sorbitol and 50 mM HEPES-KOH, pH 7.6) and washed twice with washing buffer at 1,500*g* for 2 min. The final pellets were pooled in a total volume of 500 µl chloroplast-treatment buffer (0.33 M sorbitol, 50 mM Hepes KOH pH 7.6 and 5 mM $MgCl_2$).

The supernatants of the crude chloroplasts fraction were centrifuged at 1,500*g* for 5 min. The resulting supernatants were centrifuged at 25,000*g* for 15 min to collect the mitochondrial fraction. The pellets were pooled in a total volume of 500 µl mitochondria-treatment buffer (0.3 m sucrose, 50 mM HEPES-KOH pH 7.6, 10 mM $MgCl_2$ and 10 mM KCl). Chloroplast and mitochondrial fractions were portioned into five 100 µl aliquots and the organelles were pelleted again (chloroplasts: 1,500*g*, 5 min; mitochondria: 25,000*g*, 15 min). The purity of the organelles was probed by western blot analysis with an antibody against full-length GFP (Roche) to verify that YC3.60-Tom20 is solely found in the mitochondria enriched fraction. Enrichment of plastidic fraction is shown by DB71 staining of RUBISCO. A fraction of each organelle (100 µl) was subjected to protease treatment (chloroplasts: 120 µg ml^{-1} thermolysin; mitochondria: 5 µg ml^{-1} proteinase K[30]) in the respective treatment buffer. After protease treatments the organelles were pelleted again (chloroplasts: 1,500*g*, 5 min; mitochondria: 25,000*g*, 15 min). Additional two fractions of each organelle (100 µl each) were incubated on ice for 30 min with either 100 mM Na_2CO_3, pH 11.5 or with 1% Triton X-100. All samples including the untreated control samples were centrifuged at 100,000*g* for 30 min at 4 °C and proteins of the pellet were analyzed by SDS–PAGE followed by the western blot analysis with antibodies against GFP_{S11} (Peptide Speciality Laboratories, Antigen: RDHMVLHEYVNAAGIT-C) or full-length GFP to detect the fusion proteins.

Fluorescence microscopy. For analyzing protoplasts by fluorescence microscopy GFP fluorescence, chlorophyll autofluorescence and the MitoTracker signal were monitored by confocal laser scanning microscopy using a TCS SP5 microscope (Leica) with an HCX PL APO Lambda Blue 63 × 1.4 oil objective. Fluorescence was excited and detected as follows: GFP 488/505–525 nm, chlorophyll fluorescence 514/650–750 nm and MitoTracker Orange CNTM Ros 554/576 nm. Images were processed by Leica LAS AF Lite Software.

BIFC assay. Yeast cells co-expressing either Tom20-YFP(C) or Mcr1(R4E, R7E)-YFP(C) and YFP(N) fusion proteins were grown in selective liquid medium to logarithmic phase and were used for fluorescence microscopy with an Axioskop20 fluorescence microscope equipped with an Axiocam MRm camera. For quantitative analysis, crude mitochondria were isolated from the cells and were then resuspended in SEM buffer and analyzed for their YFP fluorescence using a Tecan infinite 200 microplate reader.

Photo-crosslinking. *In organello* photo cross-linking was performed by mixing isolated mitochondria at a final concentration of 1 mg ml^{-1} with the Bpa-containing linear or cyclic peptide in import buffer without BSA. The mixture was incubated for 10 min on ice before ultravoilet-irradiation for 30 min at 4 °C. For irradiation, a Blak-Ray B-100 AP ultravoilet lamp at a distance of 10 cm from the samples was used. After the ultravoilet-illumination, the mitochondria were re-isolated by centrifugation (20,000*g*, 10 min, 2 °C) and subjected to SDS–PAGE.

NMR analysis and structural assignment. Samples of the two peptides (1 mg peptide, ~903 µM) were prepared in peptide buffer (10 mM 3-(N-morpholino)-propanesulfonic acid, 80 mM KCl, 5 mM $MgCl_2$, pH 7.2 in 11% (v/v) dimethylsulfoxid (DMSO)) and 10% (v/v) D_2O was then added. The measurements were carried out on a Bruker Avance 800 MHz spectrometer equipped with a triple resonance cryogenic probe. For assignment of the HN and Hα resonances, ^1H, ^1H NOESY spectra with a WATERGATE water suppression scheme and a mixing time of 200 ms and two ^1H, ^1H TOCSY spectra with mixing times of 15 and 60 ms, respectively, were recorded at 5 °C. Spectra were processed and analyzed using Bruker TopSpin 2.1/3.2.

For studying the interaction of the β-hairpin peptide with dTom20 the cyclic peptide and uniformly [^{15}N]-labelled rat dTom20 ([^{15}N]-dTom20) were used. Preparation of [^{15}N]-dTom20 was performed as reported previously[39] with minor modifications. The gene for the cytosolic receptor domain of dTom20 from *Rattus norvegicus* (residues 51–145) lacking the stop codon was cloned into pET-22b (Merck Millipore) for expression of the fusion protein with a hexa-histidine tag at the C terminus. The *E. coli* strain BL21(DE3) transformed with this plasmid was cultured in M9 media (1 g l^{-1} of [^{15}N]-enriched NH_4Cl, 18 g l^{-1} of $Na_2HPO_4 \times 12H_2O$, 3 g l^{-1} of KH_2PO_4, 2 g l^{-1} D-glucose, 1 mM $MgSO_4 \times 7H_2O$, 0.1 mM $CaCl_2$, 10 mg l^{-1} thiamin) containing 50 µg ml^{-1} ampicillin at 37 °C until OD_{600} reached 0.5. Protein expression was induced by 0.5 mM isopropyl β-D-1-thiogalactopyranoside for 16 h at 16 °C. Then cells were collected by centrifugation and re-suspended in 20 mM Tris–HCl, pH 7.4, containing 300 mM NaCl followed by cell disruption by sonication. The cell lysate was subjected to centrifugation to remove cell debris and unbroken cells and the supernatant was loaded onto a Ni-NTA column (QIAGEN) for affinity purification. Eluted proteins were further purified by gel-filtration chromatography on a HiLoad 26/600 Superdex 200 pg column (GE Healthcare). Fractions containing [^{15}N]-dTom20 were pooled and dialyzed against 20 mM KPi, pH 6.4, containing 50 mM KCl and stored at 4 °C until use. NMR spectra were recorded on a Bruker AVANCE900 spectrometer equipped with a TCI cryogenic probe. For NMR titration experiments, aliquots of 10 mM β-hairpin peptide in DMSO were added to 210 µM [^{15}N]-dTom20 in 20 mM KPi, pH 6.4, 50 mM KCl, 5% (v/v) DMSO, D_2O/H_2O (5/95). To subtract the solvent effects of DMSO from chemical shift perturbation by the β-hairpin peptide, an NMR spectrum of [^{15}N]-dTom20 with 9% DMSO, the final DMSO concentration in the titration experiments, was also recorded with the assumption that the solvent effect is linear to the added solvent volume. The chemical shift changes of each backbone amide of dTom20 were calculated according to the equation $[(\Delta\delta(^1H_p - {}^1H_D)^2 + \Delta\delta((^{15}N_p - {}^{15}N_D)/5)^2)]^{1/2}$, where $\Delta\delta(^1H_p - {}^1H_D)$ and $\Delta\delta(^{15}N_p - {}^{15}N_D)$ are the net chemical shift differences for the peptide after subtraction of the effect of DMSO.

Data availability. The authors declare that all data supporting the findings of this study are available within the article and its Supplementary Information files or are available from the corresponding author upon request.

References

1. Bos, M. P., Robert, V. & Tommassen, J. Biogenesis of the gram-negative bacterial outer membrane. *Annu. Rev. Microbiol.* **61,** 191–214 (2007).
2. Voulhoux, R., Bos, M. P., Geurtsen, J., Mols, M. & Tommassen, J. Role of a highly conserved bacterial protein in outer membrane protein assembly. *Science* **299,** 262–265 (2003).
3. Wu, T. *et al.* Identification of a multicomponent complex required for outer membrane biogenesis in *Escherichia coli*. *Cell* **121,** 235–245 (2005).
4. Pfanner, N., Wiedemann, N., Meisinger, C. & Lithgow, T. Assembling the mitochondrial outer membrane. *Nat. Struct. Mol. Biol.* **11,** 1044–1048 (2004).
5. Paschen, S. A., Neupert, W. & Rapaport, D. Biogenesis of β-barrel membrane proteins of mitochondria. *Trends Biochem. Sci.* **30,** 575–582 (2005).
6. Kozjak, V. *et al.* An essential role of Sam50 in the protein sorting and assembly machinery of the mitochondrial outer membrane. *J. Biol. Chem.* **278,** 48520–48523 (2003).
7. Paschen, S. A. *et al.* Evolutionary conservation of biogenesis of β-barrel membrane proteins. *Nature* **426,** 862–866 (2003).
8. Gentle, I., Gabriel, K., Beech, P., Waller, R. & Lithgow, T. The Omp85 family of proteins is essential for outer membrane biogenesis in mitochondria and bacteria. *J. Cell Biol.* **164,** 19–24 (2004).
9. Wiedemann, N. *et al.* Machinery for protein sorting and assembly in the mitochondrial outer membrane. *Nature* **424,** 565–571 (2003).
10. Ishikawa, D., Yamamoto, H., Tamura, Y., Moritoh, K. & Endo, T. Two novel proteins in the mitochondrial outer membrane mediate β-barrel protein assembly. *J. Cell Biol.* **166,** 621–627 (2004).
11. Milenkovic, D. *et al.* Sam35 of the mitochondrial protein sorting and assembly machinery is a peripheral outer membrane protein essential for cell viability. *J. Biol. Chem.* **279,** 22781–22785 (2004).
12. Waizenegger, T. *et al.* Tob38, a novel essential component in the biogenesis of β-barrel proteins of mitochondria. *EMBO Rep.* **5,** 704–709 (2004).
13. Walther, D. M., Rapaport, D. & Tommassen, J. Biogenesis of β-barrel membrane proteins in bacteria and eukaryotes: evolutionary conservation and divergence. *Cell. Mol. Life Sci.* **66,** 2789–2804 (2009).

14. Kutik, S. *et al.* Dissecting membrane insertion of mitochondrial β-barrel proteins. *Cell* **132,** 1011–1024 (2008).
15. de Cock, H., Struyve, M., Kleerebezem, M., van der Krift, T. & Tommassen, J. Role of the carboxy-terminal phenylalanine in the biogenesis of outer membrane protein PhoE of *Escherichia coli* K-12. *J. Mol. Biol.* **269,** 473–478 (1997).
16. Walther, D. M., Papic, D., Bos, M. P., Tommassen, J. & Rapaport, D. Signals in bacterial β-barrel proteins are functional in eukaryotic cells for targeting to and assembly in mitochondria. *Proc. Natl Acad. Sci. USA* **106,** 2531–2536 (2009).
17. Kozjak-Pavlovic, V., Ott, C., Gotz, M. & Rudel, T. Neisserial omp85 protein is selectively recognized and assembled into functional complexes in the outer membrane of human mitochondria. *J. Biol. Chem.* **286,** 27019–27026 (2011).
18. Müller, J. E. *et al.* Mitochondria can recognize and assemble fragments of a β-barrel structure. *Mol. Biol. Cell* **22,** 1638–1647 (2011).
19. Ulrich, T. *et al.* Evolutionary conservation in biogenesis of β-barrel proteins allows mitochondria to assemble a functional bacterial trimeric autotransporter protein. *J. Biol. Chem.* **289,** 29457–29470 (2014).
20. Hoiczyk, E., Roggenkamp, A., Reichenbecher, M., Lupas, A. & Heesemann, J. Structure and sequence analysis of Yersinia YadA and Moraxella UspAs reveal a novel class of adhesins. *EMBO J.* **19,** 5989–5999 (2000).
21. Linke, D., Riess, T., Autenrieth, I. B., Lupas, A. & Kempf, V. A. Trimeric autotransporter adhesins: variable structure, common function. *Trends Microbiol.* **14,** 264–270 (2006).
22. Arnold, T., Poynor, M., Nussberger, S., Lupas, A. N. & Linke, D. Gene duplication of the eight-stranded β-barrel OmpX produces a functional pore: a scenario for the evolution of transmembrane β-barrels. *J. Mol. Biol.* **366,** 1174–1184 (2007).
23. Bayrhuber, M. *et al.* Structure of the human voltage-dependent anion channel. *Proc. Natl Acad. Sci. U S A* **105,** 15370–15375 (2008).
24. Hiller, S. *et al.* Solution structure of the integral human membrane protein VDAC-1 in detergent micelles. *Science* **321,** 1206–1210 (2008).
25. Wiedemann, N. *et al.* Biogenesis of the protein import channel Tom40 of the mitochondrial outer membrane: intermembrane space components are involved in an early stage of the assembly pathway. *J. Biol. Chem.* **279,** 18188–18194 (2004).
26. Hoppins, S. C. & Nargang, F. E. The Tim8-Tim13 complex of Neurospora crassa functions in the assembly of proteins into both mitochondrial membranes. *J. Biol. Chem.* **279,** 12396–12405 (2004).
27. Habib, S. J., Waizenegger, T., Lech, M., Neupert, W. & Rapaport, D. Assembly of the TOB complex of mitochondria. *J. Biol. Chem.* **280,** 6434–6440 (2005).
28. Vestweber, D. & Schatz, G. Point mutations destabilizing a precursor protein enhance its post-translational import into mitochondria. *EMBO J.* **7,** 1147–1151 (1988).
29. Sommer, M. S. *et al.* Chloroplast Omp85 proteins change orientation during evolution. *Proc. Natl Acad. Sci. USA* **108,** 13841–13846 (2011).
30. Ulrich, T., Gross, L. E., Sommer, M. S., Schleiff, E. & Rapaport, D. Chloroplast β-barrel proteins are assembled into the mitochondrial outer membrane in a process that depends on the TOM and TOB complexes. *J. Biol. Chem.* **287,** 27467–27479 (2012).
31. Machettira, A. B. *et al.* Protein-induced modulation of chloroplast membrane morphology. *Front. Plant Sci.* **2,** 118 (2011).
32. Blachly-Dyson, E., Song, J., Wolfgang, W. J., Colombini, M. & Forte, M. Multicopy suppressors of phenotypes resulting from the absence of yeast VDAC encode a VDAC-like protein. *Mol. Cell. Biol.* **17,** 5727–5738 (1997).
33. Rapaport, D. & Neupert, W. Biogenesis of Tom40, core component of the TOM complex of mitochondria. *J. Cell Biol.* **146,** 321–331 (1999).
34. Schleiff, E., Silvius, J. R. & Shore, G. C. Direct membrane insertion of voltage-dependent anion-selective channel protein catalyzed by mitochondrial Tom20. *J. Cell Biol.* **145,** 973–978 (1999).
35. Krimmer, T. *et al.* Biogenesis of the major mitochondrial outer membrane protein porin involves a complex import pathway via receptors and the general import pore. *J. Cell Biol.* **152,** 289–300 (2001).
36. Yamano, K. *et al.* Tom20 and Tom22 share the common signal recognition pathway in mitochondrial protein import. *J. Biol. Chem.* **283,** 3799–3807 (2008).
37. Hahne, K., Haucke, V., Ramage, L. & Schatz, G. Incomplete arrest in the outer membrane sorts NADH-cytochrome b5 reductase to two different submitochondrial compartments. *Cell* **79,** 829–839 (1994).
38. Meineke, B. *et al.* The outer membrane form of the mitochondrial protein Mcr1 follows a TOM-independent membrane insertion pathway. *FEBS Lett.* **582,** 855–860 (2008).
39. Abe, Y. *et al.* Structural basis of presequence recognition by the mitochondrial protein import receptor Tom20. *Cell* **100,** 551–560 (2000).
40. Court, D. A., Kleene, R., Neupert, W. & Lill, R. Role of the N- and C-termini of porin in import into the outer membrane of *Neurospora* mitochondria. *FEBS Lett.* **390,** 73–77 (1996).
41. Rapaport, D. *et al.* Structural requirements of Tom40 for assembly into preexisting TOM complexes of mitochondria. *Mol. Biol. Cell* **12,** 1189–1198 (2001).
42. Taylor, R. D., McHale, B. J. & Nargang, F. E. Characterization of *Neurospora crassa* Tom40-deficient mutants and effect of specific mutations on Tom40 assembly. *J. Biol. Chem.* **278,** 765–775 (2003).
43. Endo, T. & Yamano, K. Multiple pathways for mitochondrial protein traffic. *Biol. Chem.* **390,** 723–730 (2009).
44. Model, K. *et al.* Multistep assembly of the protein import channel of the mitochondrial outer membrane. *Nat. Struct. Biol* **8,** 361–370 (2001).
45. Millar, D. G. & Shore, G. C. Signal anchor sequence insertion into the outer mitochondrial membrane. *J. Biol. Chem.* **271,** 25823–25829 (1996).
46. Rimmer, K. A. *et al.* Recognition of mitochondrial targeting sequences by the import receptors Tom20 and Tom22. *J. Mol. Biol.* **405,** 804–818 (2011).
47. Shiota, T., Mabuchi, H., Tanaka-Yamano, S., Yamano, K. & Endo, T. *In vivo* protein-interaction mapping of a mitochondrial translocator protein Tom22 at work. *Proc. Natl Acad. Sci. USA* **108,** 15179–15183 (2011).
48. Skarp, K. P., Zhao, X., Weber, M. & Jantti, J. Use of bimolecular fluorescence complementation in yeast *Saccharomyces cerevisiae*. *Methods Mol. Biol.* **457,** 165–175 (2008).
49. von Arnim, A. G., Deng, X. W. & Stacey, M. G. Cloning vectors for the expression of green fluorescent protein fusion proteins in transgenic plants. *Gene* **221,** 35–43 (1998).
50. Daum, G., Böhni, P. C. & Schatz, G. Import of proteins into mitochondria: cytochrome b2 and cytochrome c peroxidase are located in the intermembrane space of yeast mitochondria. *J. Biol. Chem.* **257,** 13028–13033 (1982).
51. Zaidi, N. *et al.* A new approach for distinguishing cathepsin E and D activity in antigen-processing organelles. *FEBS J.* **274,** 3138–3149 (2007).
52. Gessmann, D. *et al.* Structural elements of the mitochondrial preprotein-conducting channel Tom40 dissolved by bioinformatics and mass spectrometry. *Biochim. Biophys. Acta* **1807,** 1647–1657 (2011).
53. Kurowski, M. A. & Bujnicki, J. M. GeneSilico protein structure prediction meta-server. *Nucleic Acids Res.* **31,** 3305–3307 (2003).
54. Hayat, S. & Elofsson, A. BOCTOPUS: improved topology prediction of transmembrane β-barrel proteins. *Bioinformatics* **28,** 516–522 (2012).
55. Bagos, P. G., Liakopoulos, T. D., Spyropoulos, I. C. & Hamodrakas, S. J. PRED-TMBB: a web server for predicting the topology of β-barrel outer membrane proteins. *Nucleic Acids Res.* **32,** W400–W404 (2004).
56. Flinner, N. *et al.* Mdm10 is an ancient eukaryotic porin co-occurring with the ERMES complex. *Biochim. Biophys. Acta* **1833,** 3314–3325 (2013).
57. Flinner, N., Schleiff, E. & Mirus, O. Identification of two voltage-dependent anion channel-like protein sequences conserved in Kinetoplastida. *Biol. Lett* **8,** 446–449 (2012).

Acknowledgements

We thank E. Kracker for technical support, D. Schmidt and S. Sauber for help in cloning, and Y. Miyanoiri and M. Kainosho for recording NMR spectra. This work was supported by the Deutsche Forschungsgemeinschaft (RA 1028/8-1 to D.R. and SCHL 585/8-1 to E.S.), and by JST, CREST (to T.E.) and JSPS KAKENHI 15H05705 (to T.E.).

Author contributions

T.J., A.K., L.G. and N.F. conducted the experiments; S.K., E.D-F. and J.W. performed the NMR analysis; H.K. synthesized and purified the peptides; T.J., T.E., E.S. and D.R. designed the experiments and wrote the paper.

Additional information

Supplementary Information accompanies this paper at http://www.nature.com/naturecommunications

Competing financial interests: The authors declare no competing financial interests.

Reprints and permission information is available online at http://npg.nature.com/reprintsandpermissions/

How to cite this article: Jores, T. *et al.* Characterization of the targeting signal in mitochondrial β-barrel proteins. *Nat. Commun.* 7:12036 doi: 10.1038/ncomms12036 (2016).

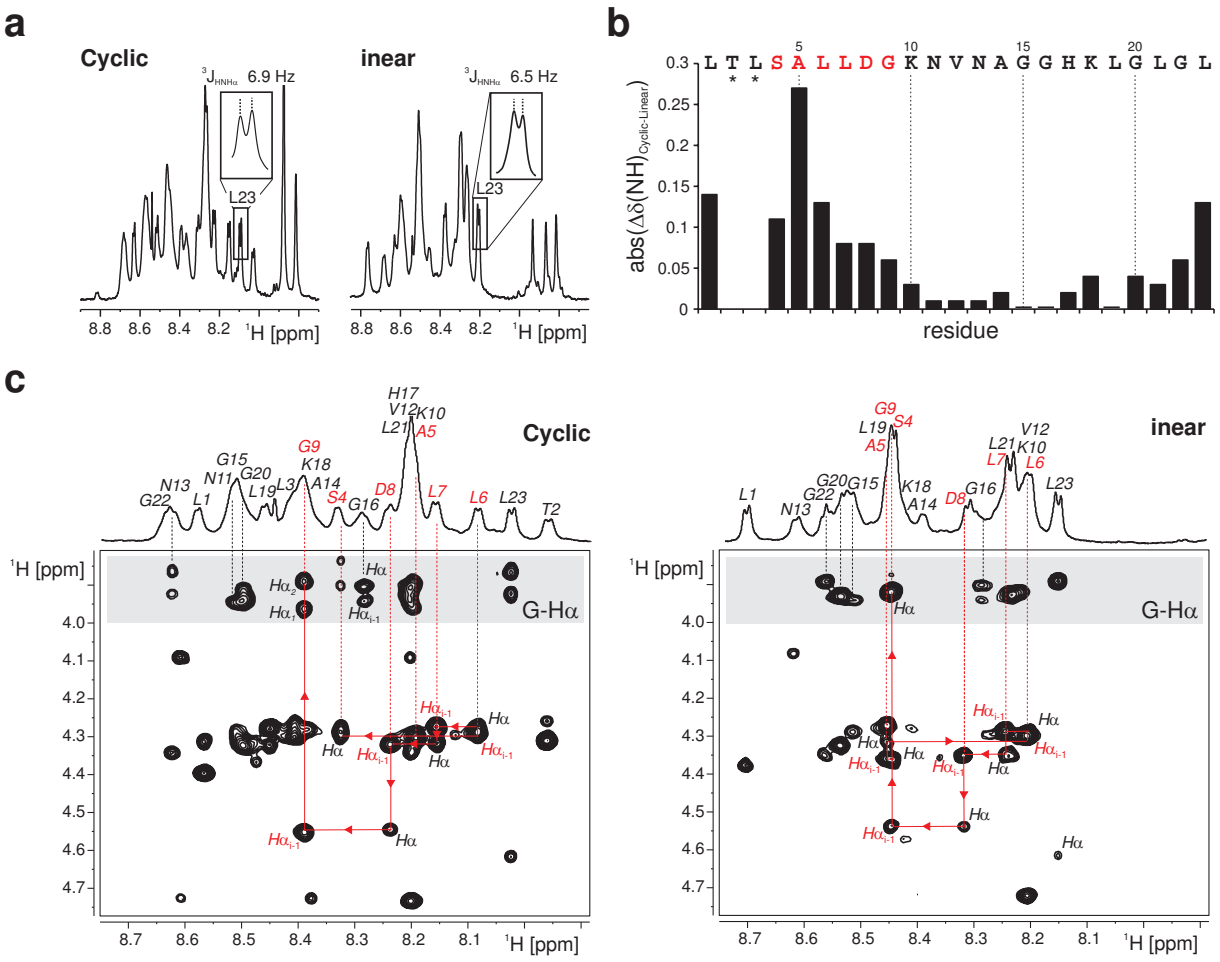

Supplementary Figure 1 | Structural analysis by NMR of the two peptides used for import competition. (**a**) Amide region of 1D ^{1}H spectra of the cyclic (left) and the linear (right) peptide at 10 °C. The inset shows the amide resonance of L23. The ^{3}J(HN,Hα) couplings splitting these resonances are indicated. (**b**) Amide proton chemical shift differences between the cyclic and the linear peptide at 5 °C. The sequence stretch, for which the sequential assignment is shown in (c), is highlighted in red. Residues, for which the difference could not be determined due to a lack in NH assignment, are labeled with an asterisk. (**c**) HN-Hα region of 2D ^{1}H,^{1}H NOESY spectra of the cyclic (left) and the linear (right) peptides at 5 °C. The assigned 1D ^{1}H spectrum of the amide region is shown on top. Intraresidual (HN-Hα$_i$, labeled in black) and sequential (HN-Hα$_{i-1}$, labeled in red) connections are indicated for the sequence stretch S4 to G9. The spectral region typical of glycine HN-Hα cross peaks residues is labeled in grey.

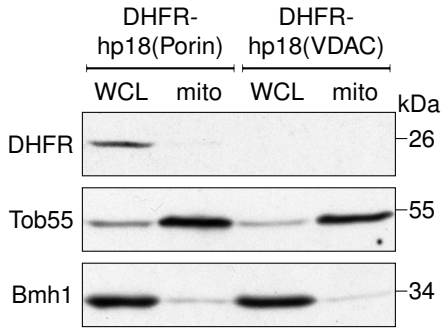

Supplementary Figure 2 | Fusion proteins with a β-hairpin fused C-terminally to DHFR are not targeted to mitochondria. Crude mitochondria were isolated from yeast cells expressing DHFR alone or the indicated fusion proteins. Samples from the whole cell lysate (WCL) and the crude mitochondria (mito) were analyzed by SDS-PAGE and immunodecoration with antibodies against the indicated proteins. Tob55, mitochondrial β-barrel protein; Bmh1, cytosolic protein.

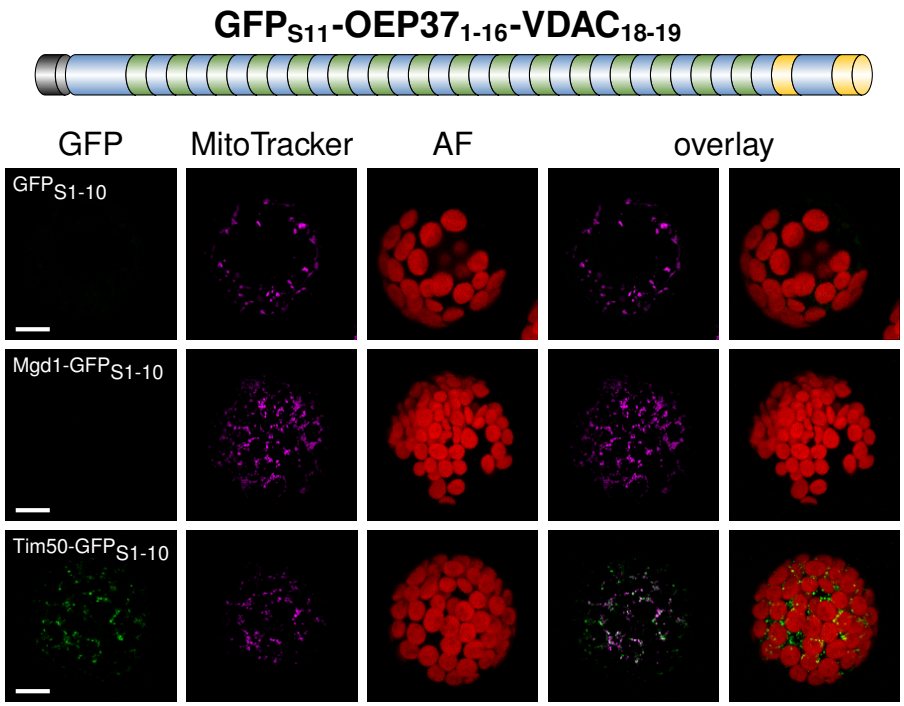

Supplementary Figure 3 | The last β-hairpin of atVDAC1 directs psOEP37 to mitochondria. GFP$_{S11}$-OEP37$_{1-16}$-VDAC$_{18-19}$ and the indicated reporter constructs were co-transformed into *A. thaliana* protoplasts. Signals and schemes are as in Fig. 3a. Scale bar: 10 µm.

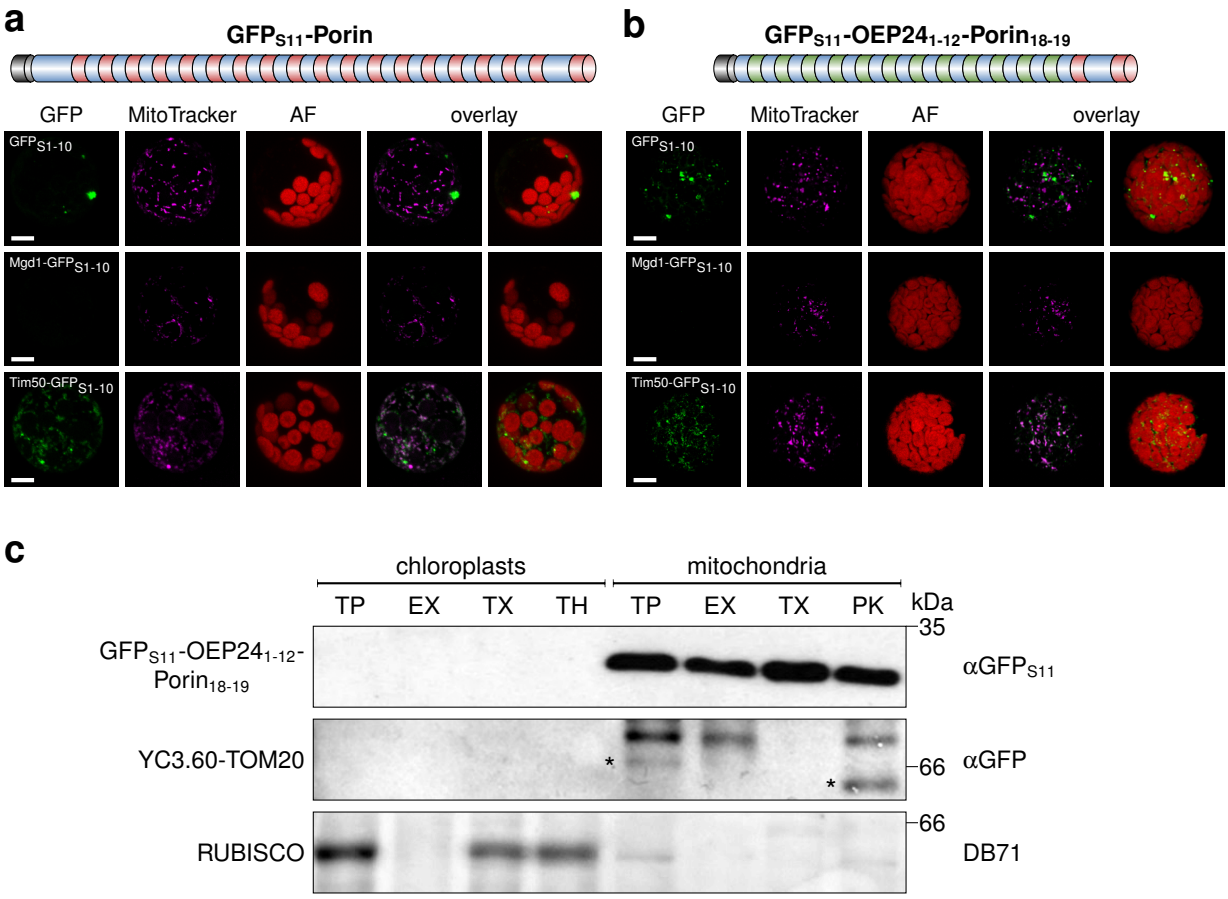

Supplementary Figure 4 | The last β-hairpin of scPorin targets psOEP24 to mitochondria. (**a** and **b**) GFP$_{S11}$-Porin (**a**) or GFP$_{S11}$-OEP24$_{1-12}$Porin$_{18-19}$ (**b**) and the indicated reporter constructs were co-transformed into *A. thaliana* protoplasts. Images were taken as described in the legend to Fig. 3a. Schemes of scPorin and the construct generated are shown. Red/green sections indicate transmembrane β-sheets of scPorin and psOEP24, respectively. The black section represents the GFP$_{S11}$-tag. Scale bar: 10 µm. (**c**) Organelles were carbonate extracted (EX), solubilized by addition of Triton X-100 (TX), or treated with either thermolysin (TH) or proteinase K (PK). Further treatment and analysis were as described in the legend to Figure 3b. Bands resulting from cross-reactivity of the GFP antibody are marked with an asterisk.

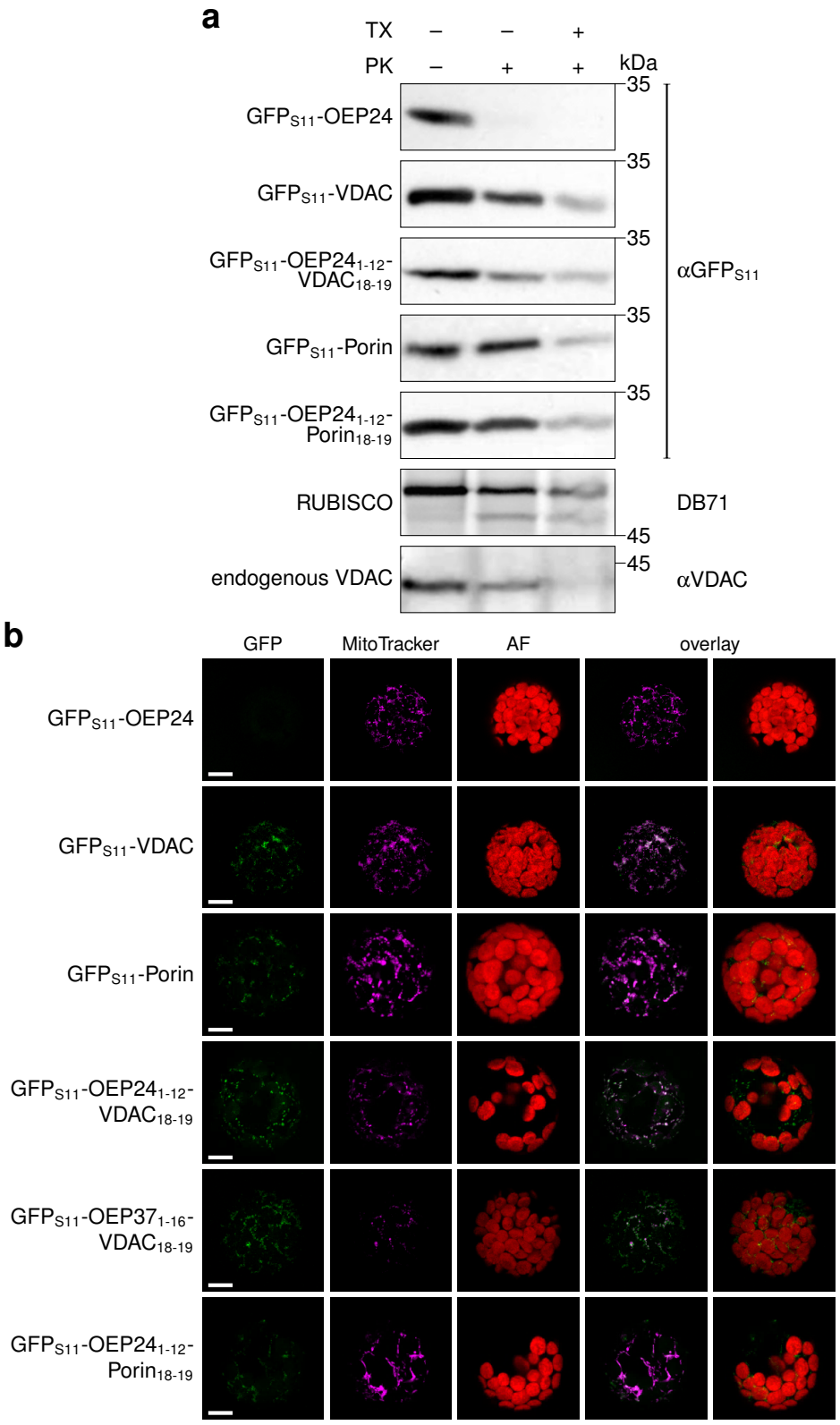

Supplementary Figure 5 | The last β-hairpin of atVDAC1 or scPorin targets chloroplast β-barrel proteins to the mitochondrial intermembrane space. (**a**) Plasmids coding for the indicated GFP_{S11}-tagged proteins were transformed individually into *A. thaliana* protoplasts. Protoplasts were lysed and incubated with proteinase K (PK, 5 µg/mL final concentration) and Triton X-100 (TX, 1 % final) where indicated. After incubation, the cell lysate was subjected to SDS-PAGE followed by Western blotting with antibodies against GFP_{S11}. DB71 staining was used to visualize RUBISCO and immunodecoration with antibodies against the endogenous mitochondrial protein atVDAC1 was used to confirm the experimental procedure. (**b**) The indicated proteins and the reporter construct Tim21(N)-GFP_{S1-10} were co-transformed into *A. thaliana* protoplasts. Images were taken as described in the legend to Fig. 3a. Scale bar: 10 µm.

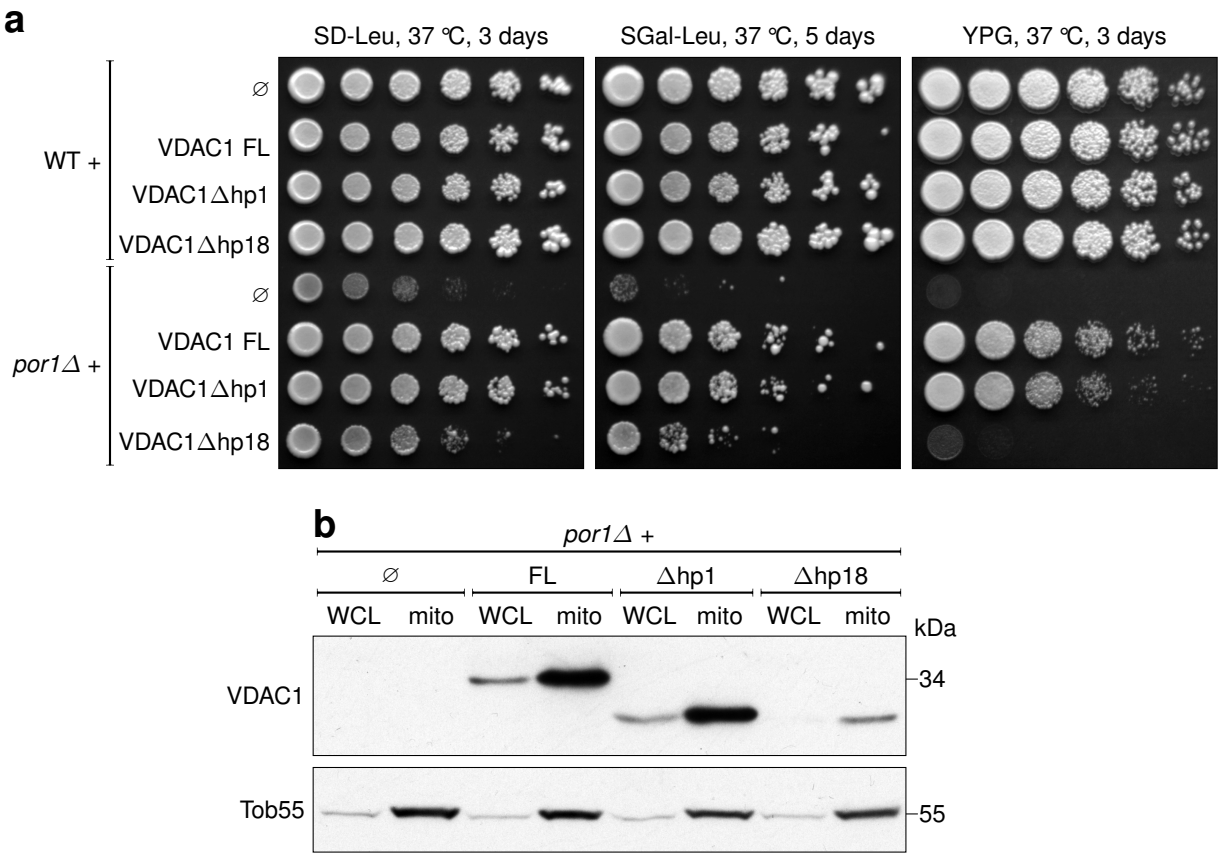

Supplementary Figure 6 | The last β-hairpin of atVDAC1 is important for mitochondrial targeting. (**a**) WT and *por1Δ* cells were transformed with an empty plasmid (∅) or with a plasmid encoding either full-length VDAC1 (VDAC1 FL) or a truncated VDAC1 variant where the first (VDAC1Δhp1) or last (VDAC1Δhp18) β-hairpin was deleted . The growth of the cells at elevated temperature (37 ℃) was analyzed by drop-dilution assay on the indicated media. (**b**) Crude mitochondria from the *por1Δ* cells described in (a) were isolated. The whole cell lysate (WCL) and the mitochondrial fraction (mito) were subjected to SDS-PAGE and immunoblotting with antibodies against VDAC1. Tob55 was used as a loading control.

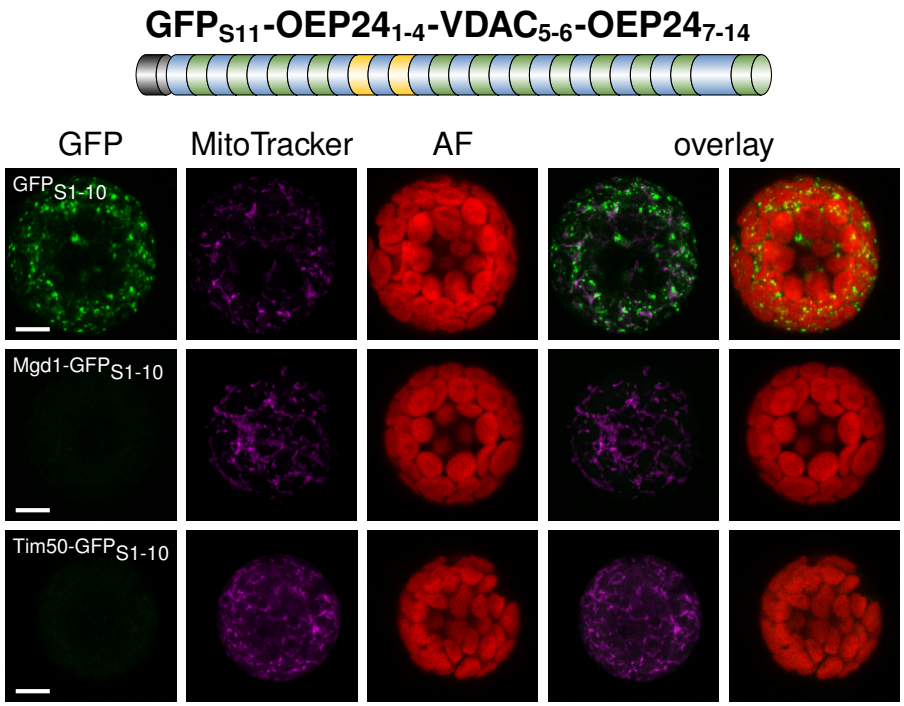

Supplementary Figure 7 | The fifth and sixth β-strands of atVDAC1 do not direct psOEP24 to mitochondria. The indicated fusion protein and reporter constructs were co-transformed into *A. thaliana* protoplasts. Signals and schemes are as in Fig. 3a. Scale bar: 10 µm.

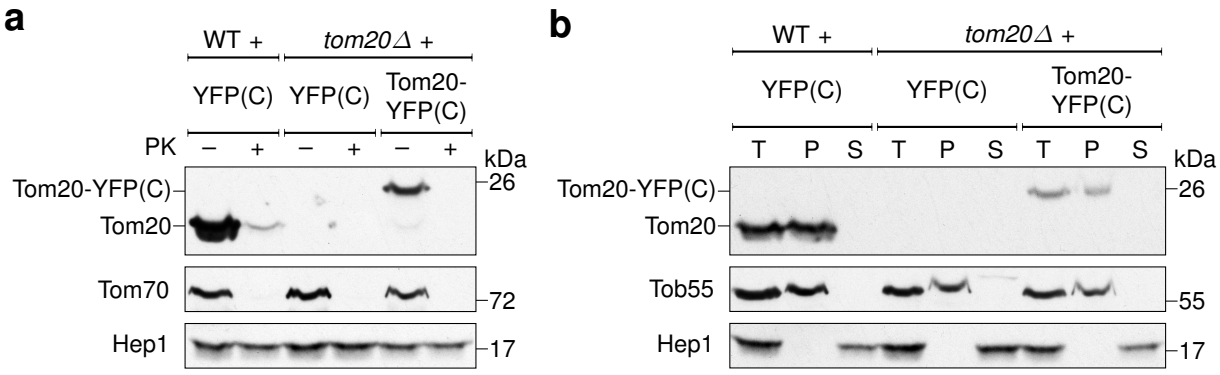

Supplementary Figure 8 | Tom20-YFP(C) is imported into the outer membrane of mitochondria in a native-like conformation. (**a**) Isolated mitochondria from either WT or *tom20Δ* strains expressing the C-terminal part of YFP (YFP(C)) or Tom20 fused N-terminally to YFP(C) were treated with 50 µg/mL proteinase K (PK) or left untreated. The samples were analyzed by SDS-PAGE and immunodecoration. Tom70, outer membrane protein exposed to the cytosol; Hep1, matrix protein. (**b**) Carbonate extraction of mitochondria isolated from the strains described in (a) was performed to separate membrane-embedded proteins in the pellet fraction (P) from soluble protein in the supernatant (S). T, total; Tob55, membrane-embedded β-barrel protein; Hep1, soluble matrix protein.

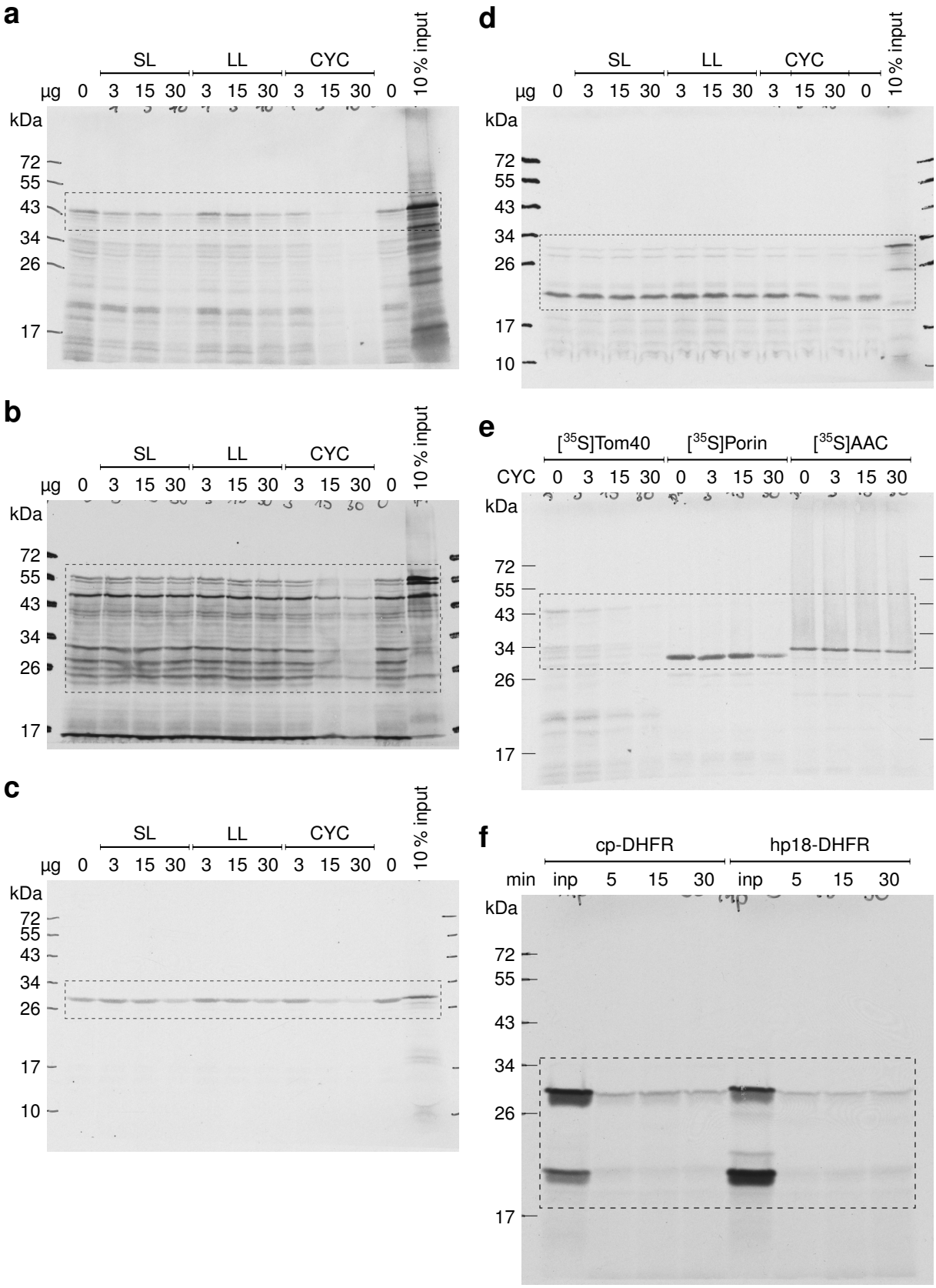
a
SL
LL
CYC
µg 0 3 15 30 3 15 30 3 15 30 0
10 % input
kDa
72
55
43
34
26
17
b
SL
LL
CYC
µg 0 3 15 30 3 15 30 3 15 30 0
10 % input
kDa
72
55
43
34
26
17
c
SL
LL
CYC
µg 0 3 15 30 3 15 30 3 15 30 0
10 % input
kDa
72
55
43
34
26
17
10
d
SL
LL
CYC
µg 0 3 15 30 3 15 30 3 15 30 0
10 % input
kDa
72
55
43
34
26
17
10
e
[35S]Tom40
[35S]Porin
[35S]AAC
CYC 0 3 15 30 0 3 15 30 0 3 15 30
kDa
72
55
43
34
26
17
f
cp-DHFR
hp18-DHFR
min inp 5 15 30 inp 5 15 30
kDa
72
55
43
34
26
17

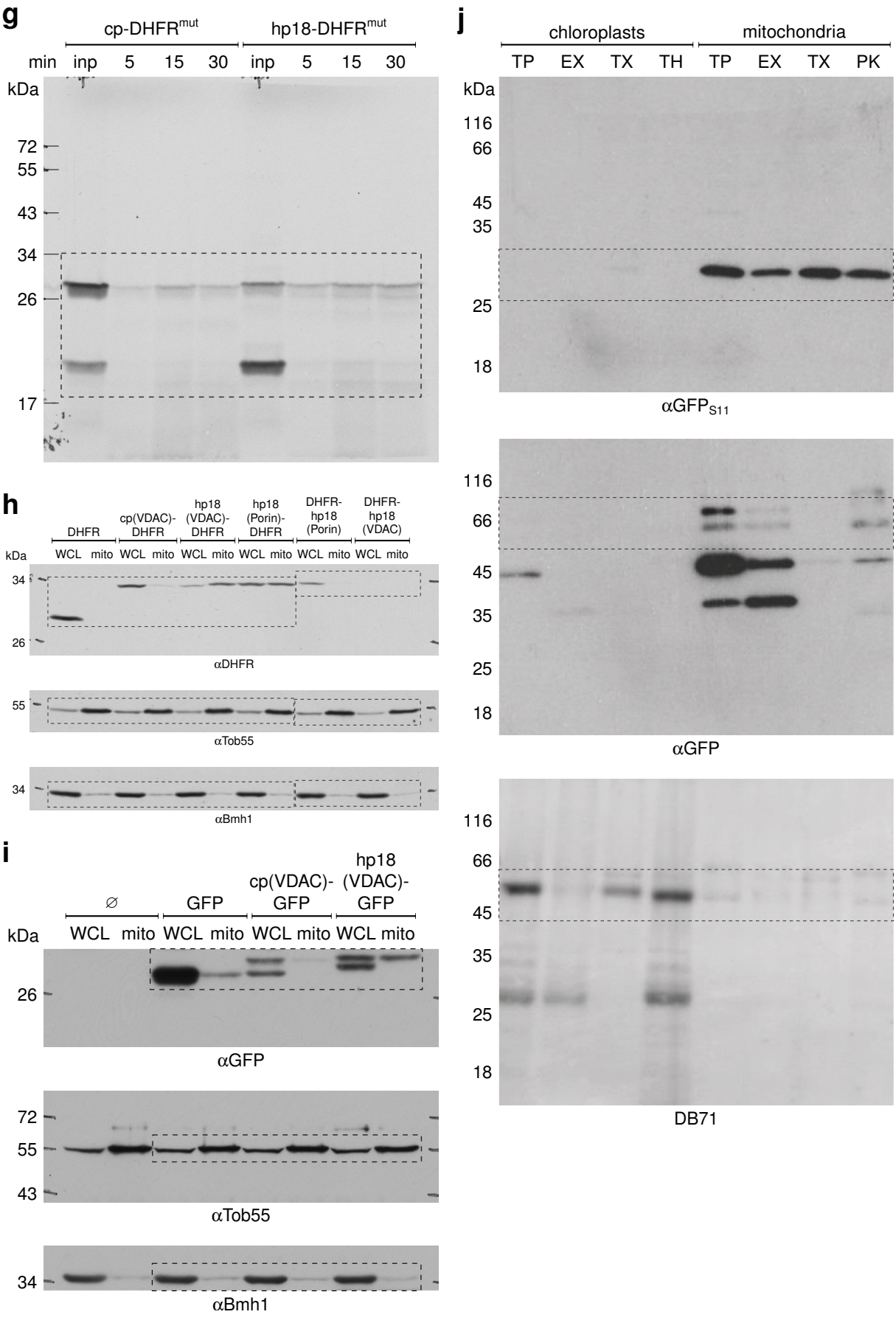
g
cp-DHFR^mut
hp18-DHFR^mut
min inp 5 15 30 inp 5 15 30
kDa
72
55
43
34
26
17
h
DHFR
cp(VDAC)-DHFR
hp18 (VDAC)-DHFR
hp18 (Porin)-DHFR
DHFR-hp18 (Porin)
DHFR-hp18 (VDAC)
kDa
WCL mito WCL mito WCL mito WCL mito WCL mito WCL mito
34
26
αDHFR
55
αTob55
34
αBmh1
i
∅
GFP
cp(VDAC)-GFP
hp18 (VDAC)-GFP
kDa
WCL mito WCL mito WCL mito WCL mito
26
αGFP
72
55
43
αTob55
34
αBmh1
j
chloroplasts
mitochondria
TP EX TX TH TP EX TX PK
kDa
116
66
45
35
25
18
αGFP_S11
αGFP
DB71

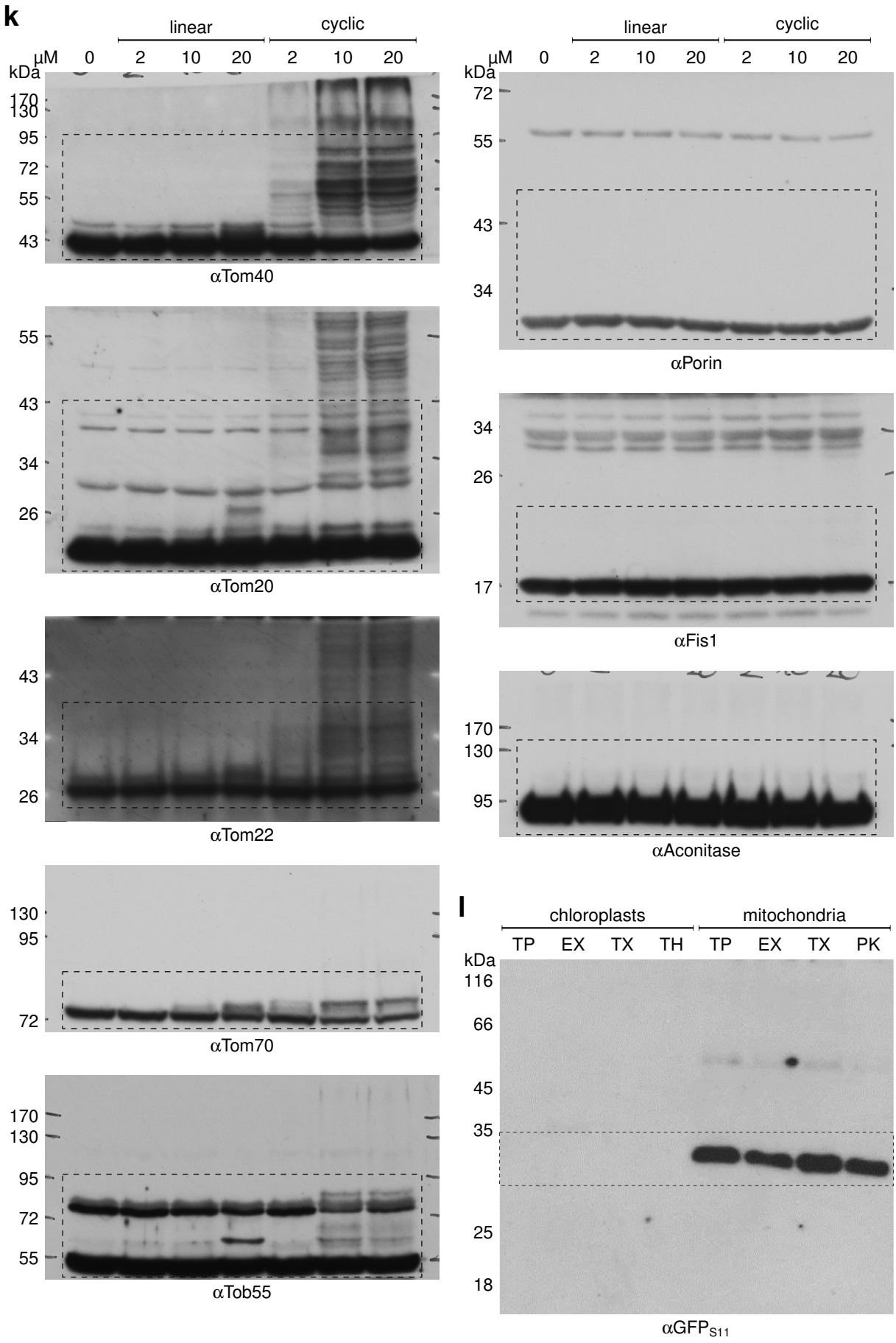
k
linear
cyclic
μM 0 2 10 20 2 10 20
kDa
170
130
95
72
55
43
αTom40
55
43
34
26
αTom20
43
34
26
αTom22
130
95
72
αTom70
170
130
95
72
55
αTob55
linear
cyclic
μM 0 2 10 20 2 10 20
kDa
72
55
43
34
αPorin
34
26
17
αFis1
170
130
95
αAconitase
l
chloroplasts
mitochondria
TP EX TX TH TP EX TX PK
kDa
116
66
45
35
25
18
αGFP$_{S11}$

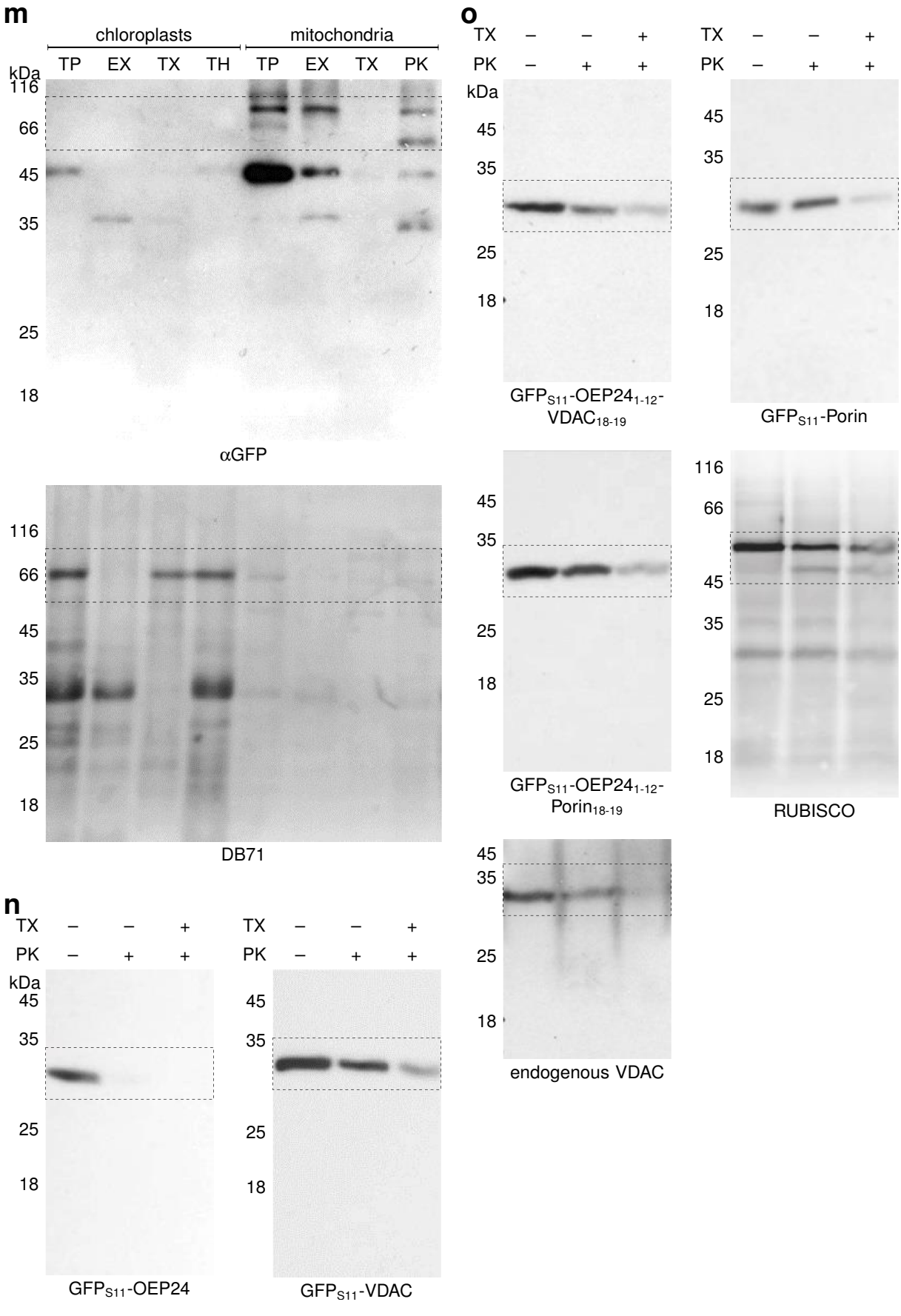
m
chloroplasts
mitochondria
TP EX TX TH TP EX TX PK
kDa
116
66
45
35
25
18
αGFP
DB71
n
TX – – +
PK – + +
GFPS11-OEP24
GFPS11-VDAC
o
GFPS11-OEP241-12-VDAC18-19
GFPS11-Porin
GFPS11-OEP241-12-Porin18-19
RUBISCO
endogenous VDAC

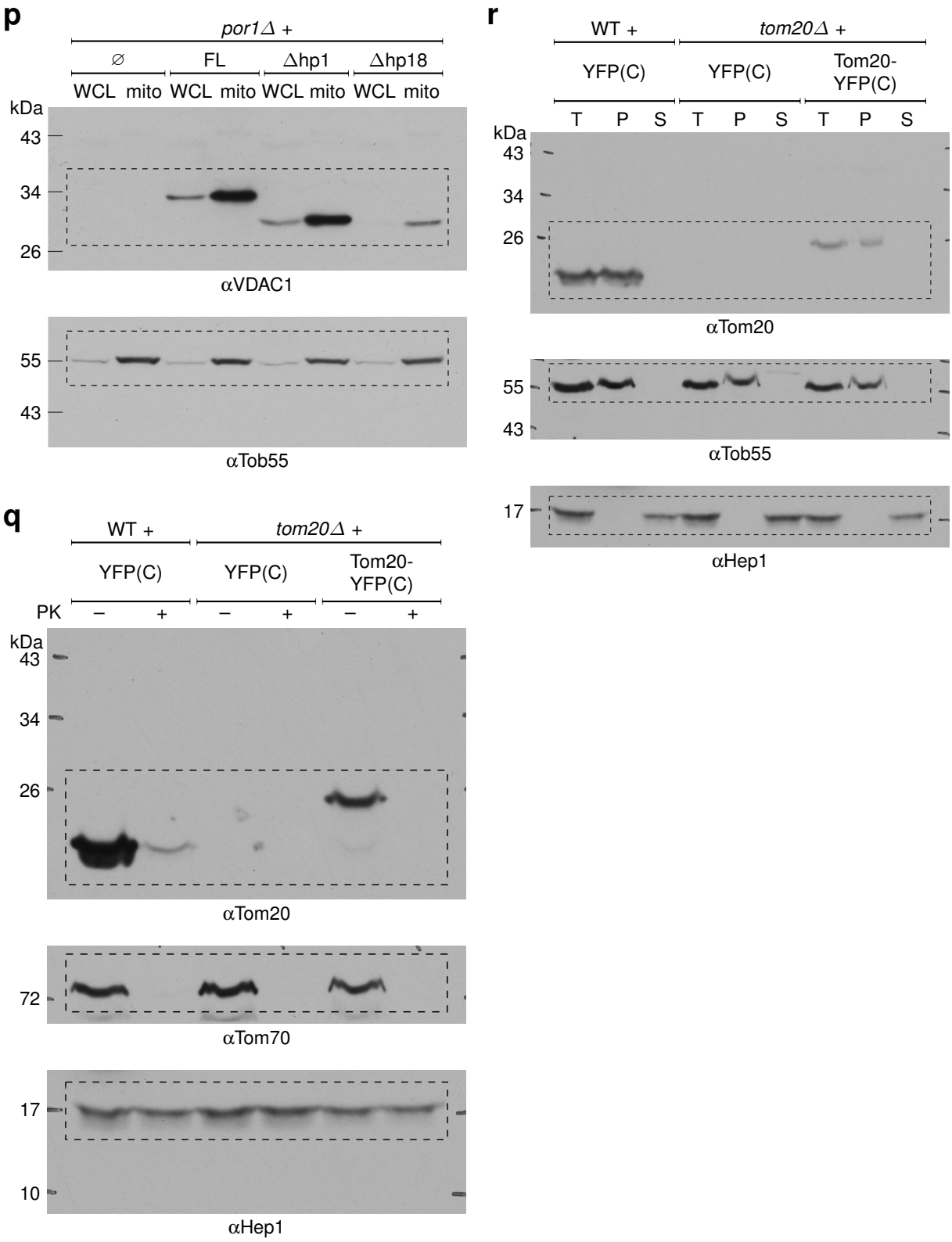

Supplementary Figure 9 | Full immunoblots and autoradiography films. (**a**-**r**) Original images of the blots shown in Figs. 1b (**a**), 1c (**b**), 1d (**c**), 1e (**d**), 1f (**e**), 2a (**f** and **g**), 2c (**h**), 2f (**i**), 3e (**j**), 7 (**k**) and in Supplementary Figs. 2 (**h**), 4c (**l** and **m**), 5a (**n** and **o**), 6b (**p**) 8a (**q**), and 8b (**r**). Cropped areas are marked by dashed lines.

Supplementary Table 1 | Primers used in this study.

Construct	Primer	Sequence (5' → 3')
GFP_{S11}-VDAC	atVDAC-1_FW	AATGGTACCATGGTGAAAGGTCCCGGTCTCTACACC
	atVDAC-1_RV	AATACTAGTAGGCTTGAGTGCGAGAGCCAATCC
GFP_{S11}-$OEP24_{1-10}$-$VDAC_{16-19}$	OEP+4VD_FW	CTACCTATGATGTTGCTCCCTTGACCTCTGTGAAGGC
	OEP+4VD_RV	CACAGAGGTCAAGGGAGCAACATCATAGGTAGGTTC
GFP_{S11}-$OEP24_{1-12}$-$VDAC_{18-19}$	OEP+2VD FW	GACAAGGAATTCCAAACCCAAGTCATTCTTCACAATC
	OEP+2VD_RV	GAAGAATGACTTGGGTTTGGAATTCCTTGTCCACTC
GFP_{S11}-$OEP24_{1-13}$-$VDAC_{**19}$	O-L1VD_RV	GTACACTAGTAGGCTTGAGTGCGAGAGCCAATCCAACTTTAGCACTCTTGTCAATTGACTTTGTGTTAACGGACGCCACAAC
GFP_{S11}-$OEP24_{1-13}$-$VDAC_{19}$	O-1VD_RV	CTAGTAGGCTTGAGTGCGAGAGCCAATCCAACTTTTTTGGGAATTTTC
GFP_{S11}-$OEP24_{1-4}$-$VDAC_{5-6}$-$OEP24_{7-14}$	O(1-4)-V(5-6)-O(7-14)_ FW	TCTACTTTTCTGATCACCGCTACCGTTGATGAGGCTGCACCCGGACTGAGGTCAATCTTCAGCTTCAAGGTTCCTGAGAAACCGTTGAATTTGGC
	O(1-4)-V(5-6)-O(7-14)_ RV	AGGAACCTTGAAGCTGAAGATTGACCTCAGTCCGGGTGCAGCCTCATCAACGGTAGCGGTGATCAGAAAAGTAGAGGGTTTCTCTACGGCGAGGACTAGGCC
GFP_{S11}-Porin	scPOR1Acc_FW	AATGGTACCATGTCTCCTCCAGTTTACAGCG
	scPOR1Bcu_RV	AATACTAGTAGCGTCGAAGGACAAAGACCAACC
GFP_{S11}-$OEP24_{1-12}$-$Porin_{18-19}$	O_2Por1_FW	CCTGGCGTCACTCTGGGTGTCGGTTCCTCTTTCGATGCTTTGAAGTTGTCTGAACCTGTTCACAAGCTAGGTTGGTCTTTGTCCTTCGACGCTACTAGTTAATCTAGAGTCCGCAAAAAT
	O_2Por1_RV	TAACTAGTAGCGTCGAAGGACAAAGACCAACCTAGCTTGTGAACAGGTTCAGACAACTTCAAAGCATCGAAAGAGGAACCGACACCCAGAGTGACGCCAGGTTGTTTGGAATTCCTTG
GFP_{S11}-$VDAC_{1-17}$-$OEP24_{13-14}$	VDAC+2O_FW	CAACACGAGTGGAAACAAACTGGTTGCTTCAAGGTTG
	VDAC+2O_RV	GAAGCAACCAGTTTGTTTCCACTCGTGTTGAATGAG
GFP_{S11}-$VDAC_{1-17}$-$OEP24_{13}VDAC1_{19}$	AK3-INT_FW	TCATTCTTCACAATCTCTGGAGAAGTCGACACAAAGTCAAAAATTCCCAAACTCAGTGTTGAGTCC
	AK3-INT_RV	GTCGACTTCTCCAGAGATTGTGAAGAATGACTTGGGTTTGGAATTCCTTGTCCACTCCAATCC
GFP_{S11}-$OEP37_{1-16}$-$VDAC_{18-19}$	OEP37_ 2VDAC1_FW	GGAGATGAAGGTGGGAAAGCATGGAAACCCAAGTCATTCTTCACAATCTCTGG
	OEP37_ 2VDAC1_RV	GATTGTGAAGAATGACTTGGGTTTCCATGCTTTCCCACCTTCATCTCCAACCCAAAGG
Tim21(N)-GFP_{S1-10}	Tim21-L1_KpnI_ FW	AATGGTACCATGGTGAAACCATCGGATTTCAAAGC

Construct	Primer	Sequence (5' → 3')
	Tim21-L1_ TPTMD_SpeI_ RV	ATTACTAGTTGTAAACCTTGAGCGGAGGTATAATCC
DHFR	TJ009	CCCGGTACCATGGTTCGACCATTGAACTGC
	TJ011	CCCGGATCCTTAGTCTTTCTTCTCGTAGAC
$DHFR^{mut}$	TJ081	CCCGGTACCATGGTTCGACCATTGAAC
	TJ011	CCCGGATCCTTAGTCTTTCTTCTCGTAGAC
cp(VDAC)	TJ022	CCCGAATTCATGGCTGTGCCACCCACG
	TJ023	CCCGGTACCACCAGCACCAGCACCCAAATCAAGCTTTATTAAGCCAAATC
hp18(VDAC)	TJ014	CCCGAATTCATGAAGCCAGGTATTAAACTGAC
	TJ015	CCCGGTACCACCAGCACCAGCACCTGCTTGAAATTCCAGTCCTAGACC
hp18(Porin)	TJ012	CCCGAATTCATGAAGCAATTGTTAAGACCTGG
	TJ013	CCCGGTACCACCAGCACCAGCACCAGCGTCGAAGGACAAAGACC
hp2(Porin)	TJ060	CCCGAATTCATGAATGGCATTAAGTTCTCATTGAAG
	TJ061	CCCGGTACCACCAGCACCAGCACCGGTTTGCTTGTCATTCAACTTTG
hp3(Porin)	TJ037	CCCGAATTCATGAAAGACGGTCCACTGTC
	TJ038	CCCGGTACCACCAGCACCAGCACCGTTTGTGTTAGACCAGCC
hp17(VDAC)	TJ058	CCCGAATTCATGAACTCCAGCCTGATAGGTTTAG
	TJ059	CCCGGTACCACCAGCACCAGCACCGTTCTTGCCATCCAGAAGAG
hp3(VDAC)	TJ039	CCCGAATTCATGGAGACCACCAAAGTGAC
	TJ040	CCCGGTACCACCAGCACCAGCACCATTGTCGGTATTCCATTTCTC
GFP	TJ032	CCCGGTACCATGAGTAAGGGTGAAGAACTTTTCAC
	TJ034	CCCGGATCCTTATTTGTATAGTTCATCCATGCC
VDAC1 FL	TJ092	CCCGGATCCAATGGCTGTGCCACCCACG
	TJ093	CCCGTCGACTTATGCTTGAAATTCCAGTCCTAGAC
VDAC1△hp1	TJ107	GGCTATGGATTTGGCACTGAGACCACCAAAGTGACG
	TJ108	CTTTGGTGGTCTCAGTGCCAAATCCATAGCCCTTGG
VDAC1△hp18	TJ092	CCCGGATCCAATGGCTGTGCCACCCACG
	TJ094	CCCGTCGACTTATAGAGTCTGAGTGTATCCTAAACC
hp18(F281A)-DHFR	TJ014	CCCGAATTCATGAAGCCAGGTATTAAACTGAC
	TJ066	CCCGGTACCACCAGCACCAGCACCTGCTTGTGCTTCCAGTCCTAGACC
hp18(F281Q)-DHFR	TJ014	CCCGAATTCATGAAGCCAGGTATTAAACTGAC

Construct	Primer	Sequence (5' → 3')
	TJ046	CCCGGTACCACCAGCACCAGCACCTGCTTGTTGTTC CAGTCCTAGACC
hp18(L259Q, F281Q)-DHFR	TJ077	GTATTAAACTGACACAATCAGCTCTTCTG
	TJ078	CAGAAGAGCTGATTGTGTCAGTTTAATAC
hp18(L259Q, L277Q, F281Q)-DHFR	TJ079	ACAAGCTTGGTCAAGGACTGGAACAA
	TJ080	TTGTTCCAGTCCTTGACCAAGCTTGT
hp17(Q249L)-DHFR	TJ095	GTTTAGGATACACTTTGACTCTAAAGCC
	TJ096	GGCTTTAGAGTCAAAGTGTATCCTAAAC
hp17(Y247F, Q249L)-DHFR	TJ097	GATAGGTTTAGGATTCACTTTGACTCTAAAGCC
	TJ098	GGCTTTAGAGTCAAAGTGAATCCTAAACCTATC
Tom20-YFP(C)	TJ052	CCCGGATCCATGTCCCAGTCGAACCCTATC
	TJ053	CCCAAGCTTGTCATCGATATCGTTAGCTTCAG
Mcr1(R4E, R7E)-YFP(C)	TJ067	CCCGAATTCATGTTTTCCGAATTATCCGAATCTCACT CAAAAGC
	TJ068	CCCAAGCTTAAATTTGAAAACTTGGTCCTTGGAG
YFP(N)	TJ054	CCCGGTACCATGGTGAGCAAGGGCGAG
	TJ055	CCCGGATCCTCACTCGATGTTGTGGCG

Supplementary Table 2 | Plasmids used in this study.

Construct	Accession Number(s)	Reference
GFP_{S11}-OEP24	CAA04468	[1]
GFP_{S11}-VDAC1	AT3G01280	current study
GFP_{S1-10}		[2]
Mgd1-GFP_{S1-10}	AT4G31780	[2]
Tim50-GFP_{S1-10}	AT1G55900	[3]
Tim21(N)-GFP_{S1-10}	AT2G40800	current study
YC3.60-Tom20	AT3G27070	[1]
GFP_{S11}-$OEP24_{1-10}$-$VDAC1_{16-19}$	CAA04468 / AT3G01280	current study
GFP_{S11}-$OEP24_{1-12}$-$VDAC1_{18-19}$	CAA04468 / AT3G01280	current study
GFP_{S11}-$OEP24_{1-13}$-$VDAC1_{**19}$	CAA04468 / AT3G01280	current study
GFP_{S11}-$OEP24_{1-13}$-$VDAC1_{19}$	CAA04468 / AT3G01280	current study
GFP_{S11}-$OEP24_{1-4}$-$VDAC1_{5-6}$-$OEP24_{7-14}$	CAA04468 / AT3G01280	current study
GFP_{S11}-Porin	EDN62755	current study
GFP_{S11}-$OEP24_{1-12}$-$Porin_{18-19}$	CAA04468 / EDN62755	current study
GFP_{S11}-$VDAC1_{1-17}$-$OEP24_{13-14}$	CAA04468 / AT3G01280	current study
GFP_{S11}-$VDAC1_{1-17}$-$OEP24_{13}$-$VDAC1_{19}$	CAA04468 / AT3G01280	current study
GFP_{S11}-$OEP37_{1-16}$-$VDAC1_{18-19}$	CAB50915 / AT3G01280	current study
pGEM4-hVDAC1	P21796	[4]
pGEM4-Tom40	P23644	[5]
pGEM4-Tob55	P53969	[5]
pGEM4-Porin	EDN62755	[6]
pGEM4-pSu9-DHFR	P00842 / P00375	[7]
pGEM4-pSu9-$DHFR^{mut}$	P00842	[8]
pGEM4-cp(VDAC)-$DHFR^{mut}$	P21796	current study
pGEM4-hp18(VDAC)-$DHFR^{mut}$	P21796	current study
pGEM4-AAC	P04710	[9]
pYX142-DHFR	P00375	current study
pYX142-cp(VDAC)-DHFR	P21796 / P00375	current study
pYX142-hp18(VDAC)-DHFR	P21796 / P00375	current study
pYX142-hp18(F281A)-DHFR	P21796 / P00375	current study
pYX142-hp18(F281Q)-DHFR	P21796 / P00375	current study
pYX142-hp18(L259Q, F281Q)-DHFR	P21796 / P00375	current study

Construct	Accession Number(s)	Reference
pYX142-hp18(L259Q, L277Q, F281Q)-DHFR	P21796 / P00375	current study
pYX142-hp18(Porin)-DHFR	EDN62755 / P00375	current study
pYX142-hp2(Porin)-DHFR	EDN62755 / P00375	current study
pYX142-hp3(Porin)-DHFR	EDN62755 / P00375	current study
pYX142-hp17(VDAC)-DHFR	P21796 / P00375	current study
pYX142-hp17(Q249L)-DHFR	P21796 / P00375	current study
pYX142-hp17(Y247F, Q249L)-DHFR	P21796 / P00375	current study
pYX142-hp3(VDAC)-DHFR	P21796 / P00375	current study
pYX142-mtGFP		[10]
pYX142-eGFP		current study
pYX142-cp(VDAC)-eGFP	P21796	current study
pYX142-hp18(VDAC)-eGFP	P21796	current study
pYX142-VDAC1	P21796	current study
pYX142-VDAC1△hp1	P21796	current study
pYX142-VDAC1△hp18	P21796	current study
pRS426-TPI-Tom20	P35180	[11]
pGEM4-Mcr1	P36060	[12]
C-YC426ADH		[13]
p426ADH-Tom20-YFP(C)	P35180	current study
p426ADH-Mcr1(R4E, R7E)-YFP(C)	P36060	current study
C-YN425ADH		[13]
pYX142-YFP(N)		current study
pYX142-cp(VDAC)-YFP(N)	P21796	current study
pYX142-hp18(VDAC)-YFP(N)	P21796	current study

Supplementary Table 3 | Antibodies used in this study.

Antibody directed against	Dilution	Number
S. cerevisiae (S.c.) Aconitase (purified full-length protein)	1:5000	sc-Aco
S.c. Bmh1 (QQPPAAAEGEAPK)	1:1000	sc-Bmh1
mouse DHFR	1:1000	610697 (BD Biosciences)
S.c. Fis1 (purified protein comprising AA 1-98 fused to MBP)	1:1000	309
GFP	1:5000	11814460001 (Roche)
GFP (β-strand #11, RDHMVLHEYVNAAGIT)	1:2000	(PSL GmbH)
N.c. Porin (SDIAKSANDLLNKDC, antiserum detects S.c. Porin)	1:3000	PorN5
S.c. Tob55 (purified his-tagged full-length protein)	1:2000	321
S.c. Tom20 (CKAESDAVAEANDIDD)	1:1000	sc-Tom20
S.c. Tom22 (CMVELTEIKDDVV)	1:1000	YTom22-N11
S.c. Tom40 (CADGNPLQALPQL)	1:4000	45300
S.c. Tom70 (purified protein comprising AA 33-616)	1:2000	312
A. thaliana VDAC1	1:5000	AS07 212 (Agrisera)
H. sapiens VDAC1	1 µg/mL	ab15895 (Abcam)

Supplementary References

1 Machettira, A. B. *et al.* The localization of Tic20 proteins in Arabidopsis thaliana is not restricted to the inner envelope membrane of chloroplasts. *Plant Mol. Biol.* **77**, 381-390 (2011).

2 Sommer, M. S. *et al.* Chloroplast Omp85 proteins change orientation during evolution. *Proc. Natl. Acad. Sci. U S A* **108**, 13841-13846 (2011).

3 Ulrich, T., Gross, L. E., Sommer, M. S., Schleiff, E. & Rapaport, D. Chloroplast β-barrel proteins are assembled into the mitochondrial outer membrane in a process that depends on the TOM and TOB complexes. *J. Biol. Chem.* **287**, 27467-27479 (2012).

4 Engl, G., Florian, S., Tranebjærg, L. & Rapaport, D. Alterations in expression levels of deafness dystonia protein 1 affect mitochondrial morphology. *Hum. Mol. Gen.* **21**, 287-299 (2012).

5 Paschen, S. A. *et al.* Evolutionary conservation of biogenesis of β-barrel membrane proteins. *Nature* **426**, 862-866 (2003).

6 Mayer, A., Lill, R. & Neupert, W. Translocation and insertion of precursor proteins into isolated outer membranes of mitochondria. *J. Cell Biol.* **121**, 1233-1243 (1993).

7 Pfanner, N., Muller, H. K., Harmey, M. A. & Neupert, W. Mitochondrial protein import: involvement of the mature part of a cleavable precursor protein in the binding to receptor sites. *EMBO J.* **6**, 3449-3454 (1987).

8 Vestweber, D. & Schatz, G. Point mutations destabilizing a precursor protein enhance its post-translational import into mitochondria. *EMBO J.* **7**, 1147-1151 (1988).

9 Pfanner, N. & Neupert, W. Distinct steps in the import of ADP/ATP carrier into mitochondria. *J. Biol. Chem.* **262**, 7528-7536 (1987).

10 Westermann, B. & Neupert, W. Mitochondria-targeted green fluorescent proteins: convenient tools for the study of organelle biogenesis in *Saccharomyces cerevisiae*. *Yeast* **16**, 1421-1427 (2000).

11 Waizenegger, T., Stan, T., Neupert, W. & Rapaport, D. Signal-anchor domains of proteins of the outer membrane of mitochondria: structural and functional characteristics. *J. Biol. Chem.* **278**, 42064-42071 (2003).

12 Meineke, B. *et al.* The outer membrane form of the mitochondrial protein Mcr1 follows a TOM-independent membrane insertion pathway. *FEBS Lett.* **582**, 855-860 (2008).

13 Skarp, K. P., Zhao, X., Weber, M. & Jantti, J. Use of bimolecular fluorescence complementation in yeast Saccharomyces cerevisiae. *Methods Mol. Biol.* **457**, 165-175 (2008).

The FEBS Journal

FEBS PRESS science publishing by scientists

The cytosolic cochaperone Sti1 is relevant for mitochondrial biogenesis and morphology

Hoda Hoseini[1], Saroj Pandey[1], Tobias Jores[1], Anja Schmitt[1], Mirita Franz-Wachtel[2], Boris Macek[2], Johannes Buchner[3], Kai Stefan Dimmer[1] and Doron Rapaport[1]

1 Interfaculty Institute of Biochemistry, University of Tübingen, Germany
2 Proteome Center Tübingen, Interfaculty Institute for Cell Biology, University of Tübingen, Germany
3 Department Chemie, Center for Integrated Protein Science, Technische Universität München, Garching, Germany

Keywords
chaperones; import receptors; mitochondria; protein import; TOM complex

Correspondence
D. Rapaport, Interfaculty Institute of Biochemistry, University of Tübingen, Hoppe-Seyler-Str. 4, 72076 Tübingen, Germany
Fax: +49 7071 294016
Tel: +49 7071 2974184
E-mail: doron.rapaport@uni-tuebingen.de

(Received 22 January 2016, revised 30 June 2016, accepted 12 July 2016)

doi:10.1111/febs.13813

Most mitochondrial proteins are synthesized in the cytosol prior to their import into the organelle. It is commonly accepted that cytosolic factors are required for delivering precursor proteins to the mitochondrial surface and for keeping newly synthesized proteins in an import-competent conformation. However, the identity of such factors and their defined contribution to the import process are mostly unknown. Using a presequence-containing model protein and a site-directed photo-crosslinking approach in yeast cells we identified the cytosolic chaperones Hsp70 (Ssa1) and Hsp90 (Hsp82) as well as their cochaperones, Sti1 and Ydj1, as putative cytosolic factors involved in mitochondrial protein import. Deletion of *STI1* caused both alterations in mitochondrial morphology and lower steady-state levels of a subset of mitochondrial proteins. In addition, double deletion of *STI1* with the mitochondrial import factors, *MIM1* or *TOM20*, showed a synthetic growth phenotype indicating a genetic interaction of *STI1* with these genes. Moreover, recombinant cytosolic domains of the import receptors Tom20 and Tom70 were able to bind *in vitro* Sti1 and other cytosolic factors. In summary, our observations point to a, direct or indirect, role of Sti1 for mitochondrial functionality.

Introduction

The vast majority of mitochondrial proteins are encoded by the nuclear genome and synthesized on cytosolic ribosomes. Therefore, importing precursor proteins into the organelle and sorting them to the correct submitochondrial compartment are essential processes for mitochondrial biogenesis. Most mitochondrial proteins harbor a cleavable targeting signal at their N terminus, the so-called presequence. In addition, many of the mitochondrial precursor proteins contain also hydrophobic segments. Thus, it is a major task for the cell to keep these hydrophobic precursor proteins in the cytosol in an import-competent soluble form. This requires prevention of aggregation on the one hand and similarly important hindering of the mitochondrial precursor protein from acquiring its final tightly folded state. The latter situation would interfere with the subsequent import of the precursor into mitochondria.

Several studies suggest that these tasks are performed by molecular chaperones and other cytosolic factors like Hsp90, Hsp70, Hsp40, nascent-polypeptide-associated complex, ribosome-associated complex, and mitochondrial import stimulation factor (MSF; for a review see [1,2]). For example, binding *in vitro*

Abbreviations
AAC, ADP–ATP carrier; AIP, arylhydrocarbon receptor-interacting protein; BPA, *p*-benzoyl-L-phenylalanine; CID, collision-induced dissociation; DHFR, dihydrofolate reductase; Hsp, heat-shock protein; MIM, mitochondrial import; MSF, mitochondrial import stimulation factor; SILAC, stable isotope labeling by amino acids in cell culture; TOM, translocase of the outer membrane.

of presequence peptides to yeast cytosolic Hsp70 (Ssa1) could be demonstrated [3], and the yeast homolog of Hsp40, Ydj1 was shown to play a role in protein import into mitochondria [4]. Furthermore, it was suggested that in mammalian cells the two chaperones Hsp70 and MSF are involved in two distinct pathways of protein import into mitochondria [5].

Newly synthesized mitochondrial proteins are recognized on the surface of the organelles by the import receptors Tom20 and Tom70 [6–8]. Both Tom20 and Tom70 are anchored to the outer membrane via a single transmembrane domain at their N termini exposing a large C-terminal domain to the cytosol [9]. This topology makes these two proteins natural candidates to interact with cytosolic factors. Indeed, a direct cooperation between the cytosolic chaperones Hsp70 and Hsp90 and Tom70 has been demonstrated to be required for the import pathway of precursors of metabolite carrier proteins [10,11]. Similarly, Tom20 in mammalian cells was reported to interact with arylhydrocarbon receptor-interacting protein (AIP). The extreme C-terminal acidic segment of Tom20 was required for interaction with the tetratricopeptide repeats (TPR) of AIP [12].

Although these cytosolic chaperones are clearly involved in the import of precursor proteins into mitochondria, their precise contribution to the molecular mechanism of the import process is still poorly understood. Similarly unclear is whether the aforementioned factors are the only chaperones involved or whether additional elements, yet to be discovered, also play an important role.

To address these open questions we used various *in vivo*, *in organello*, and *in vitro* assays and were able to shed new light on the interaction of the cytosolic cochaperone Sti1 with both mitochondrial precursor proteins and the organelle import machinery.

Results

Identification of presequence-interacting cytosolic factors by *in vivo* cross-linking

In this study, we aimed to identify cytosolic factors that assist the targeting of presequence-containing mitochondrial precursor proteins to the organelle. To this end, we used *in vivo* site-directed photo-crosslinking employing the widely used model precursor protein pCyb2-DHFR-His_9. This fusion protein consists of the N-terminal mitochondrial targeting sequence (a.a. 1–87) of cytochrome b2 fused to the well-studied model protein dihydrofolate reductase (DHFR) followed by a C-terminal His-tag. *In vivo* site-directed photo-crosslinking requires the efficient integration of the photoreactive, unnatural amino acid *p*-benzoyl-L-phenylalanine (BPA) at a specific site within the protein of interest. To this end, a mutant version of the protein containing an internal amber stop codon (TAG) at a specific position is coexpressed with an amber suppressor tRNA, which recognizes the amber stop codon, and an aminoacyl-tRNA synthetase that charges the suppressor tRNA with BPA [13,14].

In initial photo-crosslinking experiments various constructs of pCyb2-DHFR-His_9 harboring the amber stop codon at different positions within the mitochondrial targeting sequence (i.e., residues 4, 8, 10, 13, or 16) were tested. Assuming that the presequence is forming an amphiphilic α-helix, these residues are distributed in both the hydrophobic and the polar faces of the helix (Fig. 1A). From all these constructs, the replacement of codon 16 (Ala_{16}), which is surrounded by positively charged residues, by TAG codon (pCyb2^{amber16}- DHFR-His_9) gave rise to the highest number of cross-linking adducts (Fig. 1B,C). Thus, this construct was used in all further experiments.

Yeast cells expressing this photo-reactive protein were illuminated by UV light and subsequently the photo-adducts were enriched from the cell lysate by affinity purification of the His-tagged proteins via Ni-nitrilotriacetic acid beads. Samples containing photo-adduct proteins were subjected to SDS/PAGE and immunodecoration with antibodies against the His-tag or one of the known cytosolic chaperones. Specific photo-adduct bands, appearing only after UV irradiation, were detected for the molecular chaperones Hsp82 (Hsp90) and Ssa1 (one of the cytosolic Hsp70s) as well as for their cochaperones Ydj1 and Sti1 (Fig. 2). Of note, despite the unspecific binding of these chaperones to the Ni-nitrilotriacetic acid beads, the cross-linking adducts were visible only upon UV irradiation and in the presence of BPA (Figs 1 and 2). More than one specific band was detected for Sti1 probably due to different cross-linking configurations that are migrating at different apparent molecular weights in SDS/PAGE. In contrast, no specific photo-adducts were detected for other cytosolic factors like Sis1, Hsp26, Aha1, or Sba1 (data not shown).

The specific interaction of the precursor protein with the aforementioned cytosolic factors could be also confirmed by stable isotope labeling by amino acids in cell culture (SILAC) experiments. Two experiments were performed; in the first one control cells were grown with a medium containing heavy lysine, whereas those harboring the tagged-precursor were fed with a medium harboring normal lysine. In the second

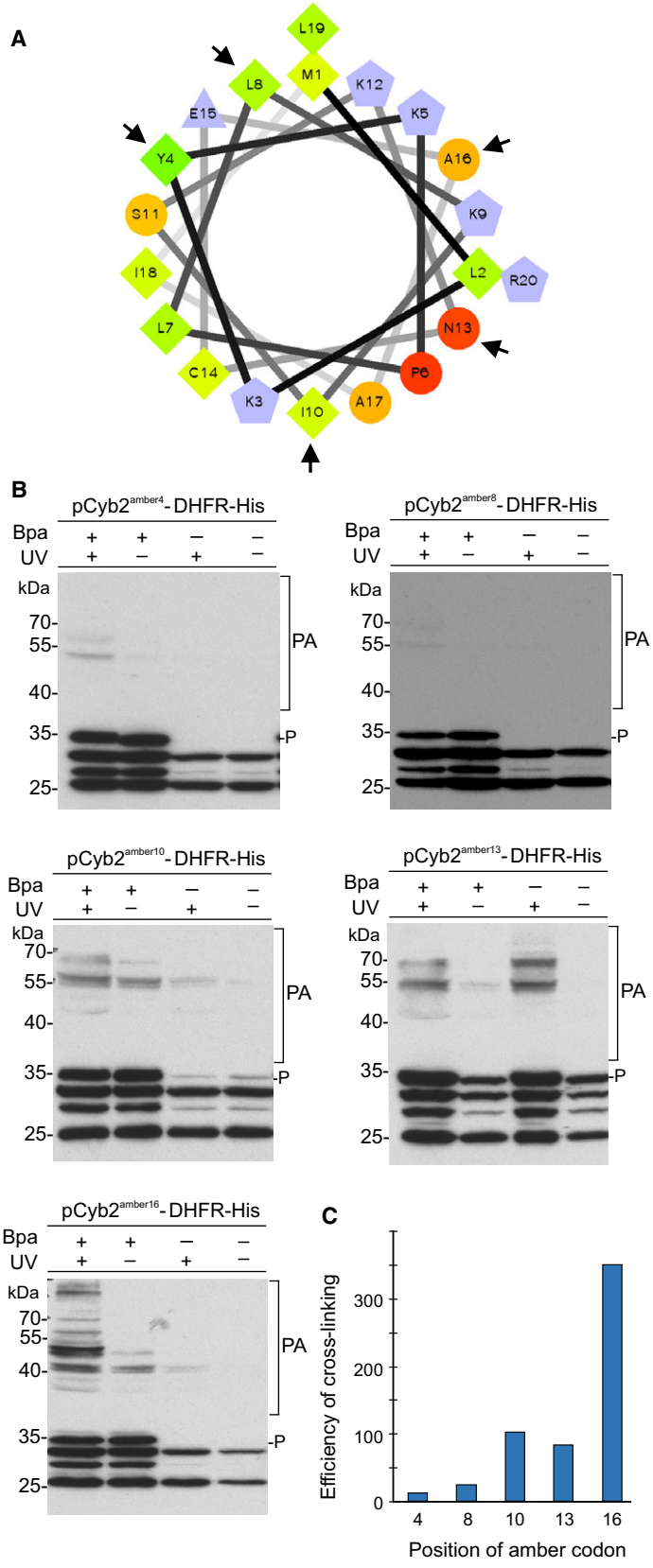

Fig. 1. BPA at position 16 of Cyb2-(1–87)-DHFR provides the best cross-linking results. (A) Helical wheel projection of residues 1–20 of cytochrome b2. Hydrophilic residues are presented as circles, hydrophobic residues as diamonds, potentially negatively charged as triangles, and potentially positively charged as pentagons. Hydrophobicity is color coded: the most hydrophobic residue is green, and the amount of green is decreasing proportionally to the hydrophobicity, with zero hydrophobicity coded as yellow. Hydrophilic residues are coded red with pure red being the most hydrophilic (uncharged) residue, and the amount of red decreasing proportionally to the hydrophilicity. The potentially charged residues are light blue. Residues that were replaced by BPA are indicated by an arrow. (B) Photo-crosslinking experiments were performed with the indicated constructs. In some samples BPA was omitted from the medium and the indicated aliquots were illuminated with UV light. Samples were analysed by SDS/PAGE and immunodecoration with antibodies against DHFR. P, precursor protein; PA, photo-adducts. (C) The bands corresponding to photo-adducts in three independent experiments like those in (B) as well as those corresponding to the full-length precursor protein were quantified. The ratio of the total intensity of the PA bands in comparison to the intensity of the precursor band is presented.

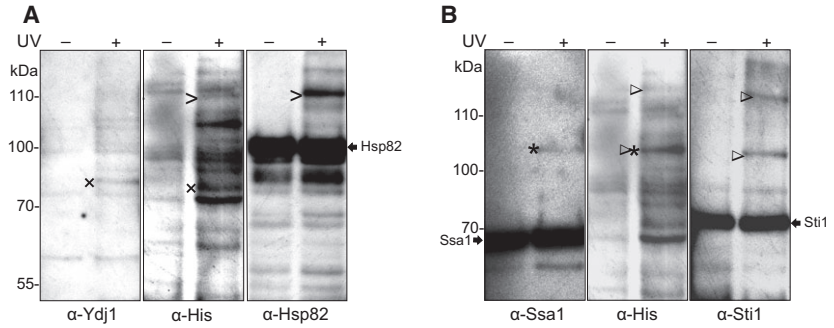

Fig. 2. Sti1, Ssa1, Hsp82, and Ydj1 are potential interaction partners of pCyb2-DHFR-His_9. (A) Photo-crosslinking experiments were performed and photo-adducts were affinity-purified from cells lysates using Ni-nitrilotriacetic acid beads. The bound material was analyzed by SDS/PAGE and immunodecoration with the indicated antibodies. The middle panel (His-tag antibody) shows all photo-adducts. Ydj1and Hsp82-containing photo-adducts are indicated with an 'x' or an arrowhead, respectively. (B) Experiments were performed and analyzed as described in (A). Ssa1- and Sti1-containing photo-adducts are indicated with an asterisk or a triangle, respectively.

experiment, the control cells were grown in the presence of the normal lysine and those containing the tagged precursor protein were grown with heavy lysine. In these experiments the photo-crosslinking was followed by SDS/PAGE and mass spectrometry analysis of selected bands. Analysis of bands corresponding to molecular size range of 85–150 kDa indicated that Sti1 and Ssa1/2 gave in these experiments the highest score for specific interaction partners (Fig. 3).

These results are in line with previous observations where Ssa1 and Ydj1 were found to be involved in the import of mitochondrial preproteins [4,15]. In contrast, the potential involvement of Sti1 and Hsp82 in the import of such client proteins has not been reported so far. Since the involvement of Hsp70, Hsp90, and Ydj1 in mitochondrial protein import was already shown, we focused on the newly discovered role of Sti1. This protein is an Hsp90 cochaperone and a homolog to mammalian Hop. It also acts as an adapter between Hsp70 and Hsp90 and mediates their assembly to form a functional complex, which assists the substrate transfer from Hsp70 to the Hsp90 chaperone machinery [16,17].

Deletion of *STI1* affects the steady-state levels of a subset of mitochondrial proteins

To better understand the role of Sti1 in mitochondrial protein biogenesis, we next tested whether the deletion of *STI1* has an effect on the levels and/or the stability of presequence-containing mitochondrial precursor proteins. To that end, the life-span of pCyb2-DHFR-His_9 and other mitochondrial proteins was monitored at an elevated temperature (34 °C) in wild-type (WT) and *sti1*Δ strains. The translation inhibitor cycloheximide was added to cultures during the logarithmic growth phase and samples were taken after various time periods. The cells were harvested, lysed, and the whole cell lysates were subjected to SDS/PAGE and immunodecoration with antibodies against DHFR and other cellular proteins. The results indicate that although the life-span of mitochondrial preproteins like pCyb2-DHFR-His_9 or Hep1 (see below) is not affected in cells lacking Sti1, the steady-state levels of these proteins are dramatically reduced in the deletion strain (Fig. 4). In contrast, the levels of the mitochondrial outer membrane protein, Tom40, was only slightly reduced in *sti1*Δ cells and those of the cytosolic protein hexokinase were unaffected (Fig. 4).

To further investigate the effect of the *STI1* deletion on the biogenesis of mitochondrial proteins, whole cell lysates of both WT and *sti1Δ* cells were prepared and the steady-state levels of several mitochondrial proteins were analyzed by SDS/PAGE and immunoblotting. The levels of the examined presequence-containing proteins (Jac1 and mtHsp70), mitochondrial outer membrane β-barrel proteins (Porin and Tom40) and the cytosolic protein, Bmh1, were not significantly altered upon the deletion of *STI1* (Fig. 5A). However, the outer membrane protein Fis1 and the matrix protein, Hep1, showed a significant decrease in their steady-state levels in *sti1Δ* cells at 37 °C (Fig. 5A–C). Taken together, it seems that Sti1 is required, especially at elevated temperatures, for the optimal biogenesis of some mitochondrial proteins.

To substantiate the contribution of Sti1 for mitochondrial import, we performed an *in vitro* import assay, where the recombinantly expressed model substrate protein, pSu9-DHFR-His_6 was incubated with mitochondria isolated from *sti1Δ* cells. The import reaction was performed in the presence of the cytosolic fraction of either WT or *sti1Δ* cells. Both the precursor and mature forms of the protein were detected in lower

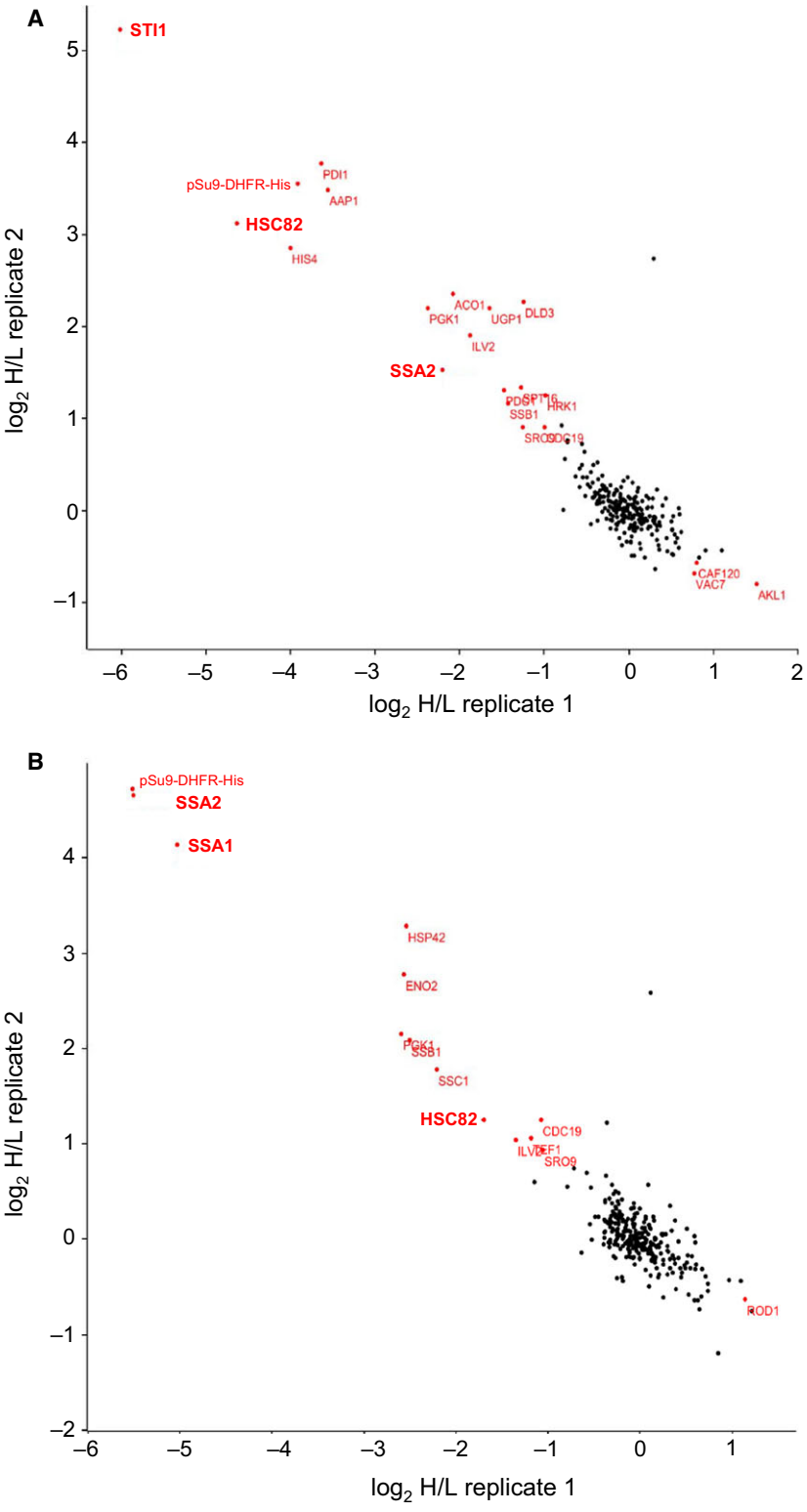

Fig. 3. Mass spectrometry analysis identifies selected cytosolic chaperones as interaction partners of pCyb2-DHFR-His_9. Scatter plot illustrating high reproducibility between replicate pull-downs. (A) Pearson correlation of normalized $\log_2$ ratios when comparing SDS/PAGE region 95–150 kDa (slice 3); $R = -0.91$. (B) Pearson correlation of normalized $\log_2$ ratios when comparing SDS/PAGE region 85–95 kDa (slice 4); $R = -0.906$. Red labeled dots show proteins that were significantly regulated (P-value < 0.01) in both replicates. H, heavy; L, light. Negative correlation reflects inversion of SILAC labels in replicate experiments.

amounts in mitochondria incubated with cytosol from *sti1Δ* cells. Thus, the results of this experiment indicate that cytosol lacking Sti1 supports mitochondrial import to a reduced extent in comparison to cytosol from WT cells (Fig. 6). We conclude that Sti1 is required for optimal import of some mitochondrial proteins.

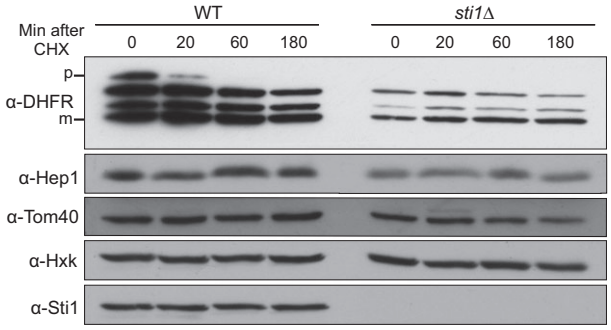

Fig. 4. Role of Sti1 in the homeostasis of mitochondrial precursor proteins. WT and *sti1Δ* cells expressing pCyb2-DHFR-His_9 were grown at 34 °C in liquid medium. Cycloheximide was added to the cultures ($t = 0$), and cells were further incubated for the indicated time periods. Cells were lysed and the whole cell lysates were analyzed by SDS/PAGE and immunodecoration with antibodies against the indicated proteins. The precursor and mature forms of pCyb2-DHFR-His_9 are indicated with p and m, respectively.

Absence of Sti1 affects mitochondrial morphology

The aforementioned results indicate an involvement of Sti1 in mitochondrial biogenesis. Since the absence of some mitochondrial import factors affects, probably indirectly, also mitochondrial morphology [18–21], we asked whether the absence of Sti1 will also result in a morphology phenotype. To that goal, WT and *sti1Δ* cells were transformed with a plasmid encoding matrix-targeted GFP (mt-GFP) and their mitochondrial morphology upon growth at 37 °C was analyzed by fluorescence microscopy. Mitochondria of WT yeast form branched or tubular networks distributed around the cell, but upon deletion of *STI1* they were mostly fragmented and aggregated (Fig. 7A). Statistical analysis of the mitochondrial morphology showed that most *sti1Δ* cells harbor mitochondria with an abnormal morphology (Fig. 7B). Since the stained structures in the deletion strain can, at least in theory, represent aggregated protein molecules rather than fragmented organelles, we analyzed mitochondrial morphology with two additional markers. First, we employed the membrane-potential sensitive dye, rhodamine B hexyl ester, and observed again fragmented structures in the mutated cells (Fig. 7C,D). Second, we used immunofluorescence microscopy with monoclonal antibodies against the mitochondrial inner membrane protein ADP–ATP carrier (AAC). In agreement with the previous observations, the anti-AAC antibodies stained fragmented mitochondria in cells lacking Sti1 (Fig. 7E). Collectively, similar to the absence of other mitochondrial import factors, the deletion of *STI1* results in an alteration of the organelle morphology.

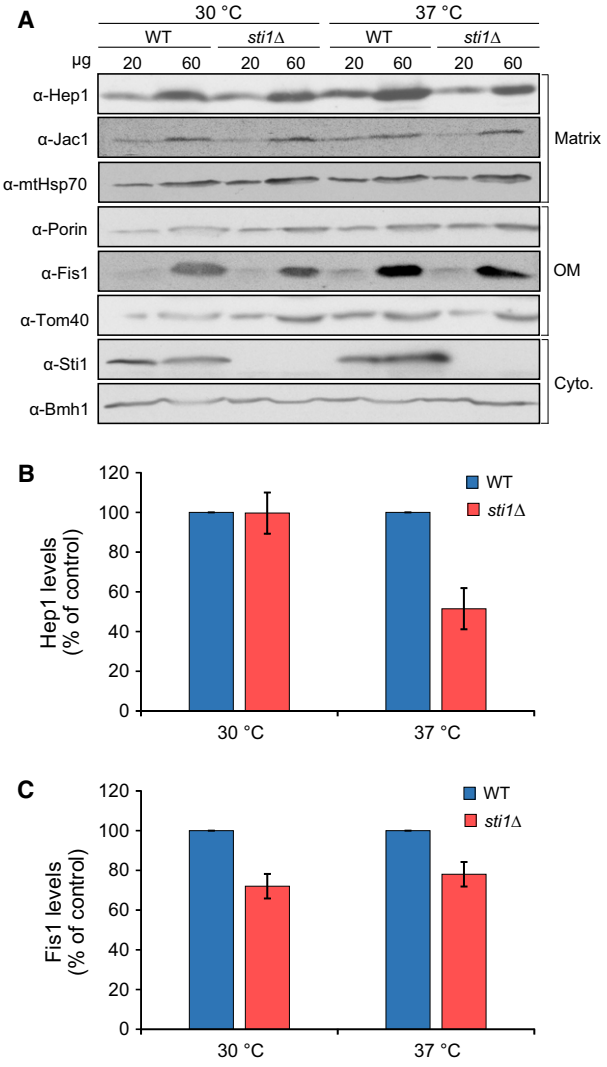

Fig. 5. Steady-state levels of Hep1 are reduced in *sti1Δ* cells. (A) WT and *sti1Δ* cells were cultivated in YPD medium at 30 °C or 37 °C, then harvested and lysed. The specified amounts of whole cell lysates were subjected to SDS/PAGE and immunoblotting with antibodies against the indicated proteins. The cytosolic protein Bmh1 was used as loading control. (B, C) Quantitative analysis of Hep1 (B) or Fis1 (C) steady-state levels. The intensities of bands from three independent experiments were quantified and the protein levels in WT cells were set to 100%. Error bars represent standard deviation. OM, proteins of the mitochondrial outer membrane; Cyto., cytosolic proteins.

Sti1 is required for optimal growth at elevated temperature and genetically interacts with *MIM1* and *TOM20*

To better understand the importance of Sti1 for cellular processes, the requirement of this cochaperone for optimal growth of yeast cells was investigated. WT and *sti1*Δ cells were grown in liquid synthetic

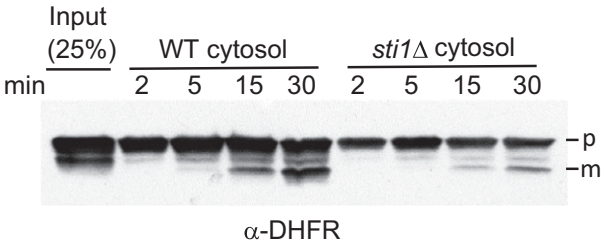

Fig. 6. Cytosol lacking Sti1 has reduced import capacity. Recombinant pSu9-DHFR-His_6 was incubated with mitochondria isolated from *sti1Δ* cells in the presence of cytosol fraction isolated from either WT or *sti1Δ* cells. At the end of the import reaction mitochondria were reisolated. The organelles were analyzed by SDS/PAGE and immunodecoration with antibodies against DHFR. The precursor and mature forms of pSu9-DHFR-His_6 are indicated with p and m, respectively. Results of a representative experiment of three independent experiments are shown.

glucose-containing medium at 30 °C or 37 °C and their growth was monitored. As shown in Fig. 8A,B, the deletion strain showed the same growth behavior as the WT strain at 30 °C, but grew much slower at elevated temperature (37 °C). Similar results were also obtained with rich glucose-containing medium (data not shown). To substantiate these findings, the growth of both strains was evaluated also on solid medium by a drop-dilution assay and, similarly to the liquid medium, growth retardation at 37 °C was observed (Fig. 8C,D). These observations underscore the physiological importance of Sti1 for cellular functions at elevated temperature.

Next, we asked whether the involvement of Sti1 in mitochondrial biogenesis is reflected by a genetic interaction with the import factors *TOM20* or *MIM1*. Indeed, the growth at 37 °C of the double-deletion strains was hampered more than could be expected by the additive effect of the single deletions, suggesting a synthetic phenotype of *sti1Δ* with either *mim1Δ* or *tom20Δ* at elevated temperatures (Fig. 8C,D). Such a genetic interaction can reveal a functional relationship between Sti1 and each of these two proteins and thus supports an involvement of Sti1 in mitochondrial protein import.

Alterations in the steady-state levels of mitochondrial proteins and cytosolic factors in *sti1Δtom20Δ* cells

The synthetic growth defect of the double-deletion *sti1Δtom20Δ* cells led us to assess the steady-state levels of cytosolic chaperones and mitochondrial proteins in these cells. For comparison, the protein levels in the single-deletion strains were also analyzed. Cells were grown on rich glycerol-containing (YPG) medium and after harvesting and lysis, mitochondrial and cytosolic fractions of all strains were subjected to SDS/PAGE and immunodecoration with antibodies against cytosolic factors and mitochondrial proteins (Fig. 9). Interestingly, the steady-state levels of some cytosolic factors like Ssa1, Sis1, and Hsp26 were elevated especially in the double-deletion strain (Fig. 9). In contrast, other chaperones like Sba1, Ydj1, and Hsp82 were hardly altered in this strain. These results might indicate that Hsp26, Sis1, and Ssa1 play an important role, probably as part of a cellular compensatory mechanism, in the absence of both Tom20 and Sti1. In an alternative, but not mutually exclusive, scenario the elevated steady-state levels of these cytosolic factors can be explained by their participation in a stress response that occurs in the absence of both Tom20 and Sti1. Such stress conditions in the *sti1Δtom20Δ* double-deletion cells are in line with the severe growth phenotype of this strain.

In contrast to the elevated levels of some chaperones in the double-deletion strain, the steady-state levels of most of the examined mitochondrial proteins did not change in response to the deletion of *STI1* and *TOM20*. Only the levels of Porin were substantially decreased in mitochondria from the double-deletion strain (Fig. 9). Porin is a high-abundance protein in the mitochondrial outer membrane that is known to be recognized during its import by Tom20 [22,23]. It appears that in the absence of Tom20, Sti1 becomes more important for the import of Porin, probably because it contributes to the alternative import pathway via Tom70.

Deletion of *MIM* components affects association of Sti1, Ssa1, and Hsp82 with mitochondria

Considering that cytosolic chaperones are associated with mitochondrial precursor proteins, small portions of these factors can be expected to physically interact with the organelle. Indeed, western blotting of isolated mitochondria with antibodies against these proteins resulted in their detection in the mitochondrial fraction (Fig. 10A). We next aimed to demonstrate that such an association with mitochondria is related to the functionality of the TOM complex. Hence, we compared the amounts of these chaperones on mitochondria isolated from control cells to those on organelles lacking Mim1 or Mim2. Both proteins are known to be required for the proper assembly and function of the TOM complex [20,24–26]. The results suggest that the absence of Mim1 or Mim2 causes marginal decline in the amounts of Sti1 and a significant reduction in

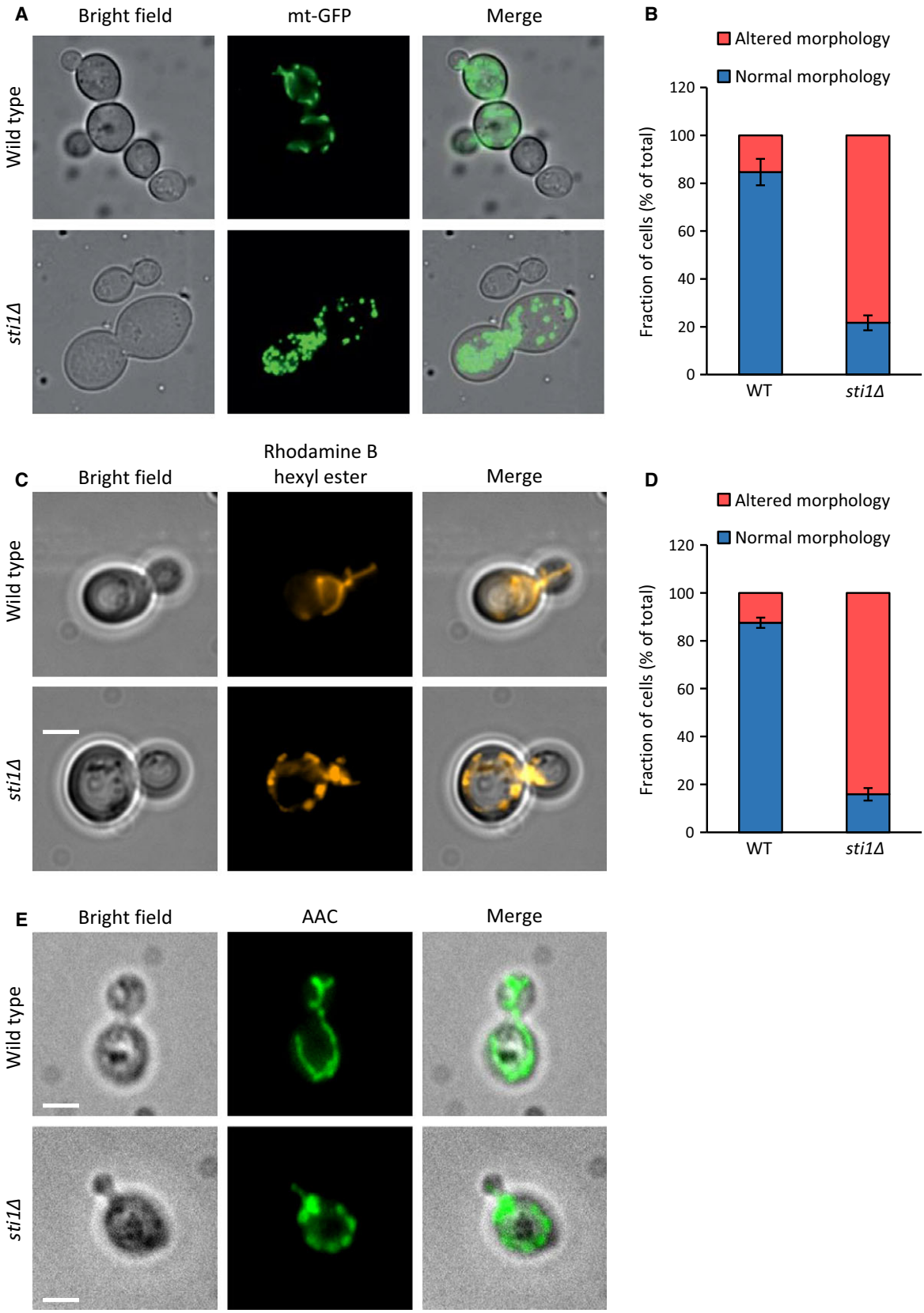
A
Bright field
mt-GFP
Merge
Wild type
sti1Δ
B
Altered morphology
Normal morphology
Fraction of cells (% of total)
120
100
80
60
40
20
0
WT
sti1Δ
C
Bright field
Rhodamine B hexyl ester
Merge
Wild type
sti1Δ
D
Altered morphology
Normal morphology
Fraction of cells (% of total)
120
100
80
60
40
20
0
WT
sti1Δ
E
Bright field
AAC
Merge
Wild type
sti1Δ

Fig. 7. Deletion of *STI1* affects mitochondrial morphology. (A) Mitochondrial morphology was analyzed by fluorescence microscopy in WT and *sti1Δ* cells expressing mt-GFP grown at 37 °C. (B) The statistical analysis of the depicted strains shows the average percentage with standard deviation (SD) bars of three independent experiments with at least $n = 100$ cells per experiment. (C) Mitochondrial morphology was analyzed at 37 °C by fluorescence microscopy in WT and *sti1Δ* cells upon the addition of the fluorescent dye rhodamine B hexyl ester. (D) Statistical analysis of three independent experiments with $n > 100$ cells in each experiment was performed and presented as in (B). (E) Immunofluorescence microscopy with antibodies against AAC of WT and *sti1Δ* cells grown at 37 °C.

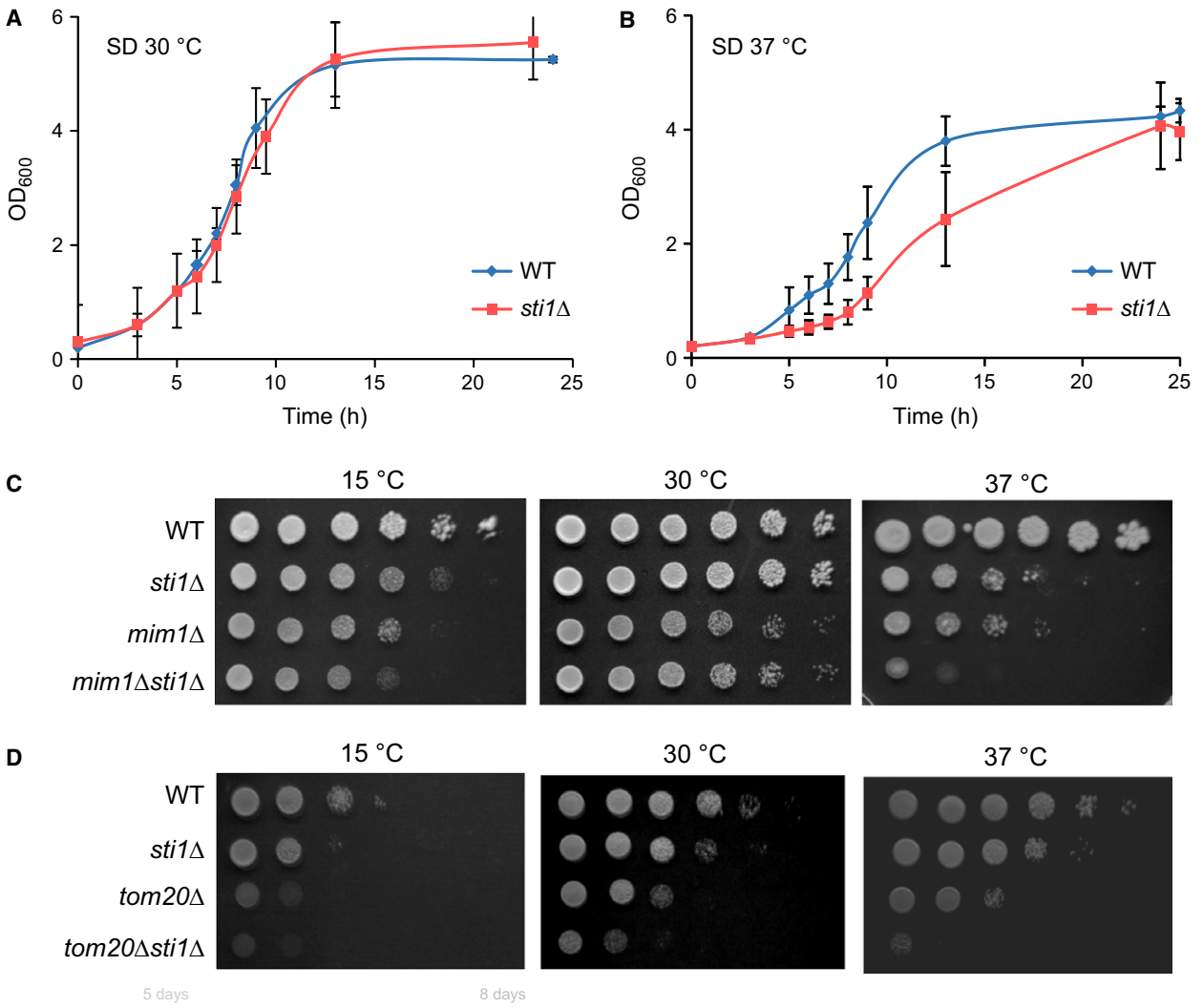

Fig. 8. *STI1* genetically interacts with *MIM1* and *TOM20* and its deletion affects cell growth. (A, B) Deletion of *STI1* affects cell growth at elevated temperatures. WT and *sti1Δ* cells were grown in SD medium at 30 °C (A) or 37 °C (B) and the growth of three independent cultures was monitored by measuring the OD_{600} over time. Error bars represent SD. (C) Drop dilution assay of WT, *sti1Δ*, *mim1Δ*, and *mim1Δsti1Δ* cells at the indicated temperatures on YPD medium. (D) Drop dilution assay of WT, *sti1Δ*, *tom20Δ*, and *sti1Δtom20Δ* strains at the indicated temperatures on YPG medium.

those of Ssa1 on the mitochondrial surface in comparison to WT cells. As expected, the levels of Tom40 are reduced in organelles from the deletion strain, whereas those of the phosphate carrier of the inner membrane, Pic2 are not affected (Fig. 10). The lower levels of associated Ssa1 can be explained by previous observations that this chaperone is associated with mitochondria via Tom70. Cells depleted for the MIM complex show alterations in the assembly of the TOM complex and have lower levels of Tom70 [10]. Taken together,

these findings support the assumption that the proper function of the TOM and/or MIM complex is required for the association of Ssa1 and Sti1 with mitochondria.

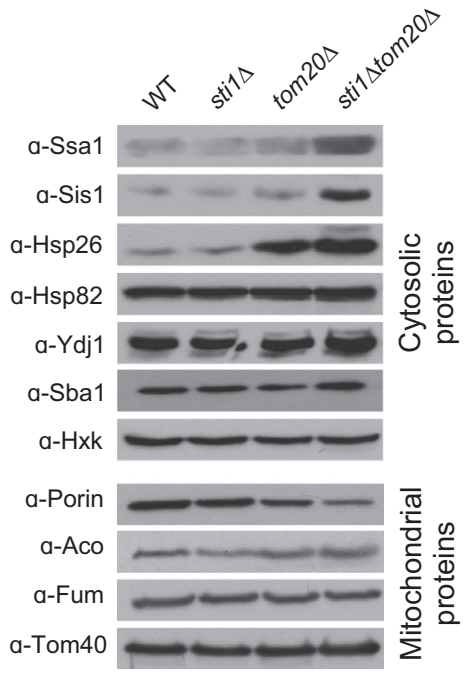

Fig. 9. The steady-state levels of some cytosolic factors are elevated in *sti1Δtom20Δ* double-deletion cells. Cells from the indicated strains were grown on YPG medium, harvested and lysed to separate cytosolic and mitochondrial fractions. The obtained fractions were subjected to SDS/PAGE followed by immunodecoration with the indicated antibodies. Hexokinase (Hxk) was used as a loading control for the cytosolic fractions.

Interaction of cytosolic factors with the import receptors Tom20 and Tom70

To further characterize the involvement of cytosolic chaperones in mitochondrial protein import, their binding *in vitro* to the import receptors Tom20 and Tom70 was monitored. To this end, N-terminally, GST-tagged recombinant versions of the cytosolic domains of Tom70 (Tom70-GST) or Tom20 (Tom20-GST) were expressed in *E. coli* cells and purified. In addition, GST alone was expressed as a control protein. Next, the purified proteins were bound to glutathione affinity beads and the protein-coated matrix was incubated with the cytosolic fraction of yeast cells. Bound material was subjected to SDS/PAGE and immunodecoration with antibodies against different cytosolic factors (Fig. 11).

The results indicate that Sti1, Ssa1, and Hsp82 bind specifically to both receptors with a clear preference for Tom70. These findings confirm a previous report on the interaction of Ssa1 with Tom70 [10]. On the other hand, Sis1 and Ydj1 preferably bind to Tom20, whereas Sba1 did not bind to any of the receptors. These assays clearly demonstrate a direct physical interaction between the mitochondrial import receptors and the cytosolic (co-)chaperones.

Discussion

In this study we identified a new role for the cytosolic cochaperone, Sti1, as a mediator of protein import to mitochondria. Sti1 is a cochaperone of Hsp70 (yeast Ssa1) and Hsp90 (yeast Hsp82), and indeed its two partners were previously identified as chaperones

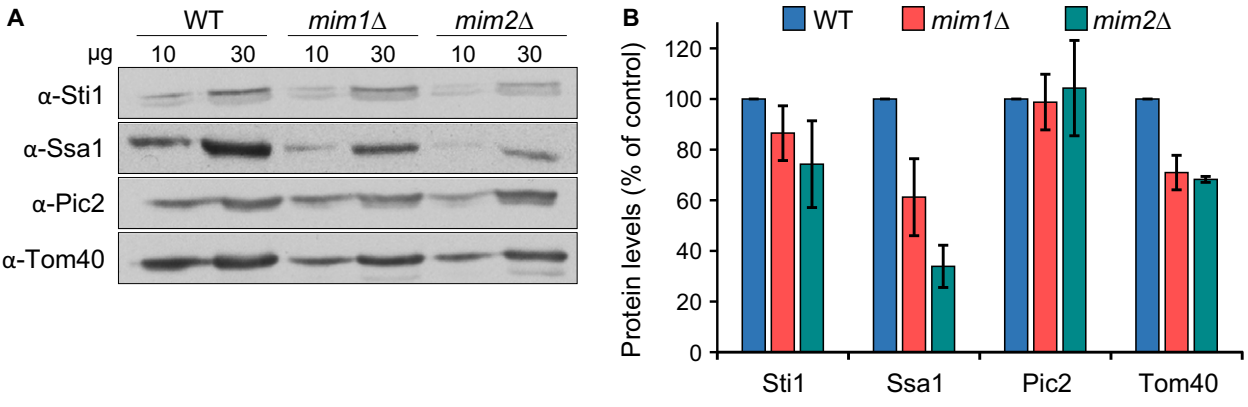

Fig. 10. Deletion of MIM complex components affects association of cytosolic factors with mitochondria. (A) WT, *mim1Δ*, and *mim2Δ* cells were grown on YPG medium. Mitochondria were isolated and analyzed by SDS/PAGE and immunodecoration with the indicated antibodies. Pic2 was used as a loading control, whereas Tom40 biogenesis is known to be affected by deletion of MIM subunits. (B) The bands of three independent experiments as described in (A) were quantified. For each protein the level in WT cells was set as 100%. Error bars represent SD.

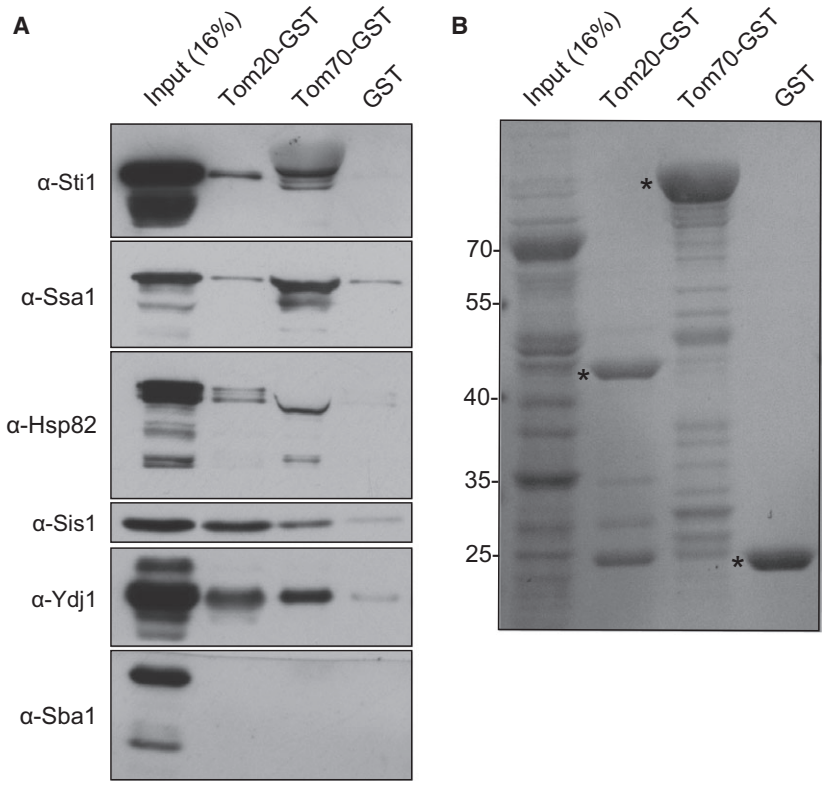

Fig. 11. The cytosolic domains of Tom20 and Tom70 directly bind cytosolic factors. (A) The indicated recombinant GST-tagged proteins were first bound to GSH-sepharose beads and subsequently incubated with cytosol isolated from yeast WT cells. After washing, the bound material was eluted from the beads and analyzed by SDS/PAGE and immunodecoration with the indicated antibodies. (B) To verify equal amounts of the recombinant proteins, the same membrane as in (A) was stained with Ponceau S to detect the GST-tagged proteins (indicated with asterisks).

involved in mitochondrial protein import [1,3,10]. Hence, our current results might suggest that Sti1 is involved in protein import as a subunit of a complex with Hsp70 and/or Hsp90 although an independent function of Sti1 cannot be excluded. At least in mammalian cells the complex scenario is more likely since Hop, the mammalian homolog of Sti1, was found to be part of a complex comprising at least five different proteins (Hsp90, Hsp70, Hop, Cdc37, and Tom34) and this complex was shown to associate with mitochondrial preproteins [27]. Currently, it is unclear whether our observation that Sti1 preferably binds to Tom70 rather than to Tom20 is caused by differences in the affinity of Sti1 to these receptors or is a result of its association with Hsp70 and/or Hsp90 that in turn are known to bind to Tom70 [10].

However, regardless of the actual mode of interaction it seems that Sti1 is involved in the ternary association of client proteins, chaperones, and Tom70. In this respect, our current findings join a growing number of reports suggesting an involvement of Tom70 not only in the import of multispan membrane proteins with internal targeting signals [10,28] but rather also in the biogenesis of presequence-containing precursor proteins [29–31]. Interestingly, it appears that the involvement of Tom70 is required if the mature domains of the preproteins are prone to aggregation [29,30]. Such precursor proteins that tend to aggregate are also the natural clients of cytosolic chaperones. Along this line, the requirement for Sti1 function is more apparent at elevated temperatures, most likely due to the higher risk of aggregation under these conditions.

The strong effect of *STI1* deletion on the morphology of mitochondria is striking considering the moderate influence of this mutation on the biogenesis of mitochondrial proteins. This difference raises the interesting possibility that the Hsp70-Sti1-Hsp90 system affects directly, in a yet unknown mechanism, the morphology of the organelle.

The general ability of chaperones to protect newly synthesized proteins against misfolding and/or aggregation could also indirectly support the process of protein import into mitochondria. Hence, we aimed to show that the contribution of Sti1 to protein import into mitochondria diverges from its general role in protein biogenesis. Indeed, the genetic and physical interactions of Sti1 with the mitochondrial import machinery suggest that this cochaperone is part of a guiding complex that allows the precursor protein to reach the organelle surface in an import-competent conformation. Taken together, our study adds Sti1 to the family of cytosolic factors that impact, directly or indirectly, on the biogenesis of mitochondrial proteins.

Materials and methods

Yeast strains and growth conditions

Standard genetic techniques were applied for the growth and manipulation of *Saccharomyces cerevisiae* cells. Yeast strains were grown in standard rich medium YP (2% [w/v] bacto peptone, 1% [w/v] yeast extract), synthetic medium (0.67% [w/v] bacto-yeast nitrogen base without amino acids with either glucose (2% [w/v]) or glycerol (3% [w/v]), SD, or SG, respectively), or lactate medium (0.3% [w/v] yeast extract, 0.5 $g \cdot L^{-1}$ glucose, 0.5 $g \cdot L^{-1}$ NaCl, 1 $g \cdot L^{-1}$ KH_2PO_4, 1 $g \cdot L^{-1}$ NH_4Cl, 0.6 $g \cdot L^{-1}$ $MgCl_2$, 0.5 $g \cdot L^{-1}$ $CaCl_2$, 2% [v/v] lactic acid, pH 5.5). For drop dilution assays, cells were cultured to an OD_{600} of 1.0 and diluted in fivefold increments. Then, 5 μL of each cell suspension was spotted on the corresponding solid medium.

Yeast strains used in this study are summarized in Table 1 together with the corresponding references. The strains used were isogenic to W303a/α or YPH499/500/501. Transformation of yeast was carried out according to the lithium-acetate method. The *mim1Δsti1Δ* and *tom20Δsti1Δ* double-deletion strains were obtained by mating of the single-deletion strains followed by tetrad dissection.

Biochemical methods

Mitochondria of yeast cells were isolated by differential centrifugation as described previously [33]. For isolation of the crude mitochondrial fraction, cells from liquid culture at the logarithmic growth phase were harvested by centrifugation (3000 ***g***, 5 min, RT) and washed once with water. The cell pellets were resuspended in SEM buffer (250 mM sucrose, 1 mM EDTA, 10 mM MOPS, pH 7.4). After adding 600-mg glass beads to the suspension, cells were lysed by vigorous vortexing (five times) for 30 s each with pauses on ice in between. After centrifugation (1000 ***g***, 5 min, 4 °C), the supernatant, which contains the whole cell lysate, was transferred to a new tube and the protein concentration was determined. Crude mitochondria were harvested from the whole cell lysate by centrifugation (13 200 ***g***, 10 min, 4 °C). The pellet contains the crude mitochondria, whereas the supernatant contains the cytosolic and ER fractions. The mitochondrial fraction was dissolved directly in sample buffer, whereas proteins of the supernatant were precipitated first with trichloroacetic acid (TCA) before addition of sample buffer. All samples were subjected to SDS/PAGE and immunoblotting using the ECL system.

Table 1. Yeast strains used in this study.

Strain	Genotype	Reference
sti1Δ	W303α, *sti1::HIS3MX6*	This study
tom20Δ	W303α, *tom20::Kan*MX4	[32]
tom20Δsti1Δ	W303α, *sti1::HIS3MX6, tom20::KanMX4*	This study
mim1Δ	W303α, *mim1::Kan*MX4	[20]
mim1Δ	YPH499, *mim1::HIS3MX6*	This study
mim1Δsti1Δ	YPH499, *mim1::HIS3MX6, sti1::KanMX4*	This study

To study the stability of yeast proteins, cells were grown in liquid culture to an OD_{600} of 0.8–1.0. Next, cycloheximide (100 $\mu g \cdot mL^{-1}$) was added to the culture (time = 0) and then aliquots of 100 mL were removed after different time periods. The cells were harvested by centrifugation (3000 ***g***, 5 min, RT) and the whole cell lysate was analyzed by SDS/PAGE and immunoblotting.

For the *in vitro* import assay, pSu9-DHFR-His6 was expressed in *E. coli* cells and purified by affinity chromatography. The purified protein was incubated at 25 °C for various time periods with mitochondria isolated from *sti1Δ* cells in the presence of cytosolyc fraction from either WT or *sti1Δ* cells. At the end of the import reaction samples were shifted to 4 °C. Mitochondria were then reisolated and analyzed by SDS/PAGE and immunodecoration with antibodies against DHFR.

Fluorescence microscopy

For visualization of mitochondria, yeast cells were transformed with a vector encoding GFP fused to mitochondrial presequence [34], or they were incubated for 10 min with 1 $\mu g \cdot mL^{-1}$ rhodamine B hexyl ester. Microscopy images were obtained with an Axioskop20 fluorescence microscope equipped with an Axiocam MRm camera using the 38 Endow GFP and 43 Cy3 filter sets and the AXIOVISION software (Zeiss, Jena, Germany).

In vivo site-directed photo cross-linking

Site-specific cross-linking was used according to a previously published protocol with some modifications [14]. Yeast cells were transformed with two plasmids to introduce the photo-reactive cross-linking residue, BPA (Bachem, Bubendorf, Switzerland) into the protein of interest. One plasmid contains the coding sequence for the protein of interest, which harbors an amber stop codon (TAG) in the desired position, and the other plasmid contains the coding sequence of both an amber suppressor tRNA and its cognate aminoacyl-tRNA synthetase that specifically charge the suppressor tRNA with BPA [13]. Precultures of yeast cells containing both plasmids were grown overnight at 30 °C on selective medium (SD-trp-leu-phe supplemented with BPA) and diluted in 200 mL of the same media to an OD_{600} = 0.3. BPA was dissolved in 1 M NaOH and freshly added to the culture to a final concentration of 0.2–0.6 mM. As a control, cells were also grown on a medium without BPA. The cells were incubated at 30 °C with slight shaking to reach to an OD_{600} = 1.0–1.2 and afterward harvested by centrifugation (3000 ***g***, 5 min, RT).

For photo-crosslinking reactions, the cell pellets were resuspended in water and divided into two samples of 800 μL each (OD_{600} = 75 units of cells per sample) and transferred to a 12-well plate. The suspensions were placed on ice and one sample was exposed to UV light (Blak-Ray® Ultraviolet Lamp, B-100 AP; UVP, Upland, CA, USA, λ = 365 nm) for 1 h at 4 °C (+UV). The other half of the cells sample served as a control and was stored at 4 °C without exposure to light (−UV). Next, both irradiated cells (+UV) and nonirradiated cells (−UV) were transferred to 2-mL microcentrifuge tubes, washed once with water and resuspended in 200 μL SEM buffer supplemented with 2 mM PMSF. The cells were disrupted and after determination of the protein concentration in the whole cell lysates the samples were subjected first to a pull-down assay or equal amounts of samples (+/− BPA, +/− UV) were applied directly to SDS/PAGE analysis.

Pull-down assays

Cells were resuspended in 500 μL lysis buffer (20 mM sodium phosphate buffer, 300 mM NaCl, 2 mM PMSF, EDTA-free Complete protease inhibitors (Roche, Basel, Switzerland), 10 mM imidazole, pH 7.5.) and then disrupted with glass beads. The cell lysate was cleared from glass beads and unopened cells by centrifugation (1000 ***g***, 5 min, 4 °C) and membranes were solubilized with 1% Triton X-100 for 30 min at 4 °C. To clarify the lysate from undissolved material, the mixture was centrifuged (30 000 ***g***, 30 min, 4 °C). In parallel, Ni-nitrilotriacetic acid agarose beads (50 μL of 1 : 1 slurry) were washed once with water and preequilibrated with lysis buffer for 1 h at 4 °C. The cleared cell lysate was applied to the equilibrated beads and the mixture was incubated for 1 h at 4 °C on an overhead shaker. Afterwards the beads were harvested by centrifugation (400 ***g***, 2 min, 4 °C) and washed twice with wash buffer (20 mM sodium phosphate buffer, 300 mM NaCl, 50 mM imidazole, pH 7.5.) for 5 min at 4 °C. Finally, the beads were sedimented again and proteins were eluted in 50 μL sample buffer. All samples were applied to SDS/PAGE analysis.

SILAC experiments

The eluates of pull-down experiments as described above were separated on a one-dimensional SDS/PAGE and the lanes were cut into 13 slices each and in-gel digested by endoproteinase LysC as described previously [35]. Peptide fractions were collected and desalted separately using C18 StageTips. LC-MS/MS analyses were performed on an EasyLC nano-HPLC (Proxeon Biosystems, Waltham, MA, USA) coupled to an LTQ Orbitrap XL (Thermo Scientific, Waltham, MA, USA). Binding and chromatographic separation of the peptides was performed on a 15-cm fused silica emitter with an inner diameter of 75 μm (Proxeon Biosystems), in-house packed with reversed-phase ReproSil-Pur C18-AQ 3 μm resin (Dr. Maisch GmbH, Ammerbuch-Entringen, Germany). The peptide mixtures were injected in HPLC solvent A (0.5% acetic acid) at a flow rate of 500 nL·min^{-1} and subsequently eluted with an 127-min segmented gradient of 5–33–50–90% of HPLC solvent B (80% acetonitrile in 0.5% acetic acid) at a flow rate of 200 nL·min^{-1}.

The mass spectrometer was operated in the data-dependent mode to automatically switch between MS and MS/MS acquisition. Precursor ions were acquired in the mass range of 300–2000 m/z in the Orbitrap mass analyzer at a resolution of 60 000. Accumulation target value of 10^6 charges was set and the lock mass option was used for internal calibration [36]. The 10 most intense ions were sequentially isolated and fragmented in the linear ion trap using collision-induced dissociation (CID) at the ion accumulation target value of 5000 and default CID settings. The ions already selected for MS/MS were dynamically excluded for 90 s. The resulting peptide fragment ions were recorded in the linear ion trap.

The MS data were processed using default parameters of the MAXQUANT software (v1.5.2.8, Max-Planck-Institute of Biochemistry, Martinsried, Germany). Extracted peak lists were submitted to database search using the Andromeda search engine [37] to query a target-decoy database of *S. cerevisiae* proteome, the sequence of the construct pSu9-DHFR-His6 and 285 commonly observed contaminants. In database search, full LysC digestion specificity was required and up to two missed cleavages were allowed. A false discovery rate of 1% was applied at the peptide and protein level. For protein group quantitation, a minimum of two quantified peptides were required.

Binding experiments with recombinant proteins

Constructs representing N-terminally GST-tagged cytosolic domains of Tom20 or Tom70 were expressed in *E. coli* cells and purified with GSH-sepharose™ 4B beads (GE Healthcare, Freiburg, Germany). Next, the GST-tagged proteins and GST alone (as control), were incubated for 2 h at 4 °C with 100 μL of GSH-sepharose™ 4B beads, which were previously washed five times with GST basic buffer (20 mM HEPES-NaOH, pH 7.25, 100 mM NaCl, 1.5 mM $MgCl_2$), in a final volume of 400 μL on an overhead shaker. Afterward the proteins-coated GSH-sepharose™ beads were treated with 3% BSA in cytosol lysis buffer (CLB, 0.6 M Sorbitol, 10 mM Tris-HCl, and pH 7.4) to block unspecific binding sites. Finally the cleared cytosol was incubated overnight at 4 °C on an overhead shaker with the protein-coated GSH-sepharose™ beads. After the incubation, the mixture was centrifuged (13 000 ***g***, 1 min, 4 °C) and the supernatant was discarded. The beads were washed three times with CLB supplemented with 100 mM NaCl and then

bound proteins were eluted in 200 μL of sample buffer and analyzed by SDS/PAGE.

Acknowledgements

We thank E. Kracker for technical assistance and Dr D. Mokranjac for plasmids and recombinant proteins. This work was supported by the Deutsche Forschungsgemeinschaft (RA 1028/2-2 and RA 1028/4-2 to D.R.).

Author contributions

HH, SP, TJ, AS, and KSD conducted experiments and analyzed the data; HH, JB, and DR designed the experiments; MF and BM performed the mass spectrometry analysis; and HH and DR wrote the article.

References

1 Beddoe T & Lithgow T (2002) Delivery of nascent polypeptides to the mitochondrial surface. *Biochim Biophys Acta* **1592**, 35–39.
2 Hoogenraad NJ, Ward LA & Ryan MT (2002) Import and assembly of proteins into mitochondria of mammalian cells. *Biochim Biophys Acta* **1592**, 97–105.
3 Endo T, Mitsui S, Nakai M & Roise D (1996) Binding of mitochondrial presequences to yeast cytosolic heat shock protein 70 depends on the amphiphilicity of the presequence. *J Biol Chem* **271**, 4161–4167.
4 Caplan AJ, Cyr DM & Douglas MG (1992) YDJ1p facilitates polypeptide translocation across different intracellular membranes by a conserved mechanism. *Cell* **71**, 1143–1155.
5 Komiya T, Sakaguchi M & Mihara K (1996) Cytoplasmic chaperones determine the targeting pathway of precursor proteins to mitochondria. *EMBO J* **15**, 399–407.
6 Neupert W & Herrmann JM (2007) Translocation of proteins into mitochondria. *Annu Rev Biochem* **76**, 723–749.
7 Bolender N, Sickmann A, Wagner R, Meisinger C & Pfanner N (2008) Multiple pathways for sorting mitochondrial precursor proteins. *EMBO Rep* **9**, 42–49.
8 Endo T & Yamano K (2009) Multiple pathways for mitochondrial protein traffic. *Biol Chem* **390**, 723–730.
9 Dukanovic J & Rapaport D (2011) Multiple pathways in the integration of proteins into the mitochondrial outer membrane. *Biochim Biophys Acta* **1808**, 971–980.
10 Young JC, Hoogenraad NJ & Hartl F-U (2003) Molecular chaperones Hsp90 and Hsp70 deliver preproteins to the mitochondrial import receptor Tom70. *Cell* **112**, 41–50.
11 Wiedemann N, Pfanner N & Ryan MT (2001) The three modules of ADP/ATP carrier cooperate in receptor recruitment and translocation into mitochondria. *EMBO J* **20**, 951–960.
12 Yano M, Terada K & Mori M (2003) AIP is a mitochondrial import mediator that binds to both import receptor Tom20 and preproteins. *J Cell Biol* **163**, 45–56.
13 Chin JW, Cropp TA, Anderson JC, Mukherji M, Zhang Z & Schultz PG (2003) An expanded eukaryotic genetic code. *Science* **301**, 964–967.
14 Tamura Y, Harada Y, Shiota T, Yamano K, Watanabe K, Yokota M, Yamamoto H, Sesaki H & Endo T (2009) Tim23-Tim50 pair coordinates functions of translocators and motor proteins in mitochondrial protein import. *J Cell Biol* **184**, 129–141.
15 Deshaies RJ, Koch BD, Werner-Washburne M, Craig EA & Schekman R (1988) A subfamily of stress proteins facilitates translocation of secretory and mitochondrial precursor polypeptides. *Nature* **332**, 800–805.
16 Scheufler C, Brinker A, Bourenkov G, Pegoraro S, Moroder L, Bartunik H, Hartl F-U & Moarefi I (2000) Structure of TPR domain-peptide complexes: critical elements in the assembly of the Hsp70-Hsp90 multichaperone machine. *Cell* **101**, 199–210.
17 Wegele H, Haslbeck M, Reinstein J & Buchner J (2003) Sti1 is a novel activator of the Ssa proteins. *J Biol Chem* **278**, 25970–25976.
18 Kawai A, Nishikawa S, Hirata A & Endo T (2001) Loss of the mitochondrial Hsp70 functions causes aggregation of mitochondria in yeast cells. *J Cell Sci* **114**, 3565–3574.
19 Meisinger C, Rissler M, Chacinska A, Szklarz LK, Milenkovic D, Kozjak V, Schonfisch B, Lohaus C, Meyer HE, Yaffe MP *et al.* (2004) The mitochondrial morphology protein Mdm10 functions in assembly of the preprotein translocase of the outer membrane. *Dev Cell* **7**, 61–71.
20 Dimmer KS, Papic D, Schumann B, Sperl D, Krumpe K, Walther DM & Rapaport D (2012) A crucial role for Mim2 in the biogenesis of mitochondrial outer membrane proteins. *J Cell Sci* **125**, 3464–3473.
21 Engl G, Florian S, Tranebjaerg L & Rapaport D (2012) Alterations in expression levels of deafness dystonia protein 1 affect mitochondrial morphology. *Hum Mol Genet* **21**, 287–299.
22 Krimmer T, Rapaport D, Ryan MT, Meisinger C, Kassenbrock CK, Blachly-Dyson E, Forte M, Douglas MG, Neupert W, Nargang FE *et al.* (2001) Biogenesis of the major mitochondrial outer membrane protein porin involves a complex import pathway via receptors and the general import pore. *J Cell Biol* **152**, 289–300.
23 Schleiff E, Silvius JR & Shore GC (1999) Direct membrane insertion of voltage-dependent anion-selective channel protein catalyzed by mitochondrial Tom20. *J Cell Biol* **145**, 973–978.

24 Ishikawa D, Yamamoto H, Tamura Y, Moritoh K & Endo T (2004) Two novel proteins in the mitochondrial outer membrane mediate β-barrel protein assembly. *J Cell Biol* **166**, 621–627.
25 Waizenegger T, Schmitt S, Zivkovic J, Neupert W & Rapaport D (2005) Mim1, a protein required for the assembly of the TOM complex of mitochondria. *EMBO Rep* **6**, 57–62.
26 Hulett JM, Lueder F, Chan NC, Perry AJ, Wolynec P, Likic VA, Gooley PR & Lithgow T (2008) The transmembrane segment of Tom20 is recognized by Mim1 for docking to the mitochondrial TOM complex. *J Mol Biol* **376**, 694–704.
27 Faou P & Hoogenraad NJ (2012) Tom34: a cytosolic cochaperone of the Hsp90/Hsp70 protein complex involved in mitochondrial protein import. *Biochim Biophys Acta* **1823**, 348–357.
28 Brix J, Rudiger S, Bukau B, Schneider-Mergener J & Pfanner N (1999) Distribution of binding sequences for the mitochondrial import receptors Tom20, Tom22, and Tom70 in a presequence-carrying preprotein and a non-cleavable preprotein. *J Biol Chem* **274**, 16522–16530.
29 Hines V & Schatz G (1993) Precursor binding to yeast mitochondria. A general role for the outer membrane protein Mas70p. *J Biol Chem* **268**, 449–454.
30 Yamamoto H, Fukui K, Takahashi H, Kitamura S, Shiota T, Terao K, Uchida M, Esaki M, Nishikawa S, Yoshihisa T *et al.* (2009) Roles of Tom70 in import of presequence-containing mitochondrial proteins. *J Biol Chem* **284**, 31635–31646.
31 Melin J, Kilisch M, Neumann P, Lytovchenko O, Gomkale R, Schendzielorz A, Schmidt B, Liepold T, Ficner R, Jahn O *et al.* (2015) A presequence-binding groove in Tom70 supports import of Mdl1 into mitochondria. *Biochim Biophys Acta* **1853**, 1850–1859.
32 Müller JE, Papic D, Ulrich T, Grin I, Schutz M, Oberhettinger P, Tommassen J, Linke D, Dimmer KS, Autenrieth IB *et al.* (2011) Mitochondria can recognize and assemble fragments of a β-barrel structure. *Mol Biol Cell* **22**, 1638–1647.
33 Daum G, Böhni PC & Schatz G (1982) Import of proteins into mitochondria: cytochrome b2 and cytochrome c peroxidase are located in the intermembrane space of yeast mitochondria. *J Biol Chem* **257**, 13028–13033.
34 Westermann B & Neupert W (2000) Mitochondria-targeted green fluorescent proteins: convenient tools for the study of organelle biogenesis in *Saccharomyces cerevisiae*. *Yeast* **16**, 1421–1427.
35 Borchert N, Dieterich C, Krug K, Schuetz W, Jung S, Nordheim A, Sommer RJ & Macek B (2010) Proteogenomics of *Pristionchus pacificus* reveals distinct proteome structure of nematode models. *Genome Res* **20**, 837–846.
36 Olsen JV, de Godoy LM, Li G, Macek B, Mortensen P, Pesch R, Makarov A, Lange O, Horning S & Mann M (2005) Parts per million mass accuracy on an Orbitrap mass spectrometer via lock mass injection into a C-trap. *Mol Cell Proteomics* **4**, 2010–2021.
37 Cox J, Neuhauser N, Michalski A, Scheltema RA, Olsen JV & Mann M (2011) Andromeda: a peptide search engine integrated into the MaxQuant environment. *J Proteome Res* **10**, 1794–1805.

FEBS Letters

FEBS PRESS science publishing by scientists

REVIEW ARTICLE

Early stages in the biogenesis of eukaryotic β-barrel proteins

Tobias Jores and Doron Rapaport

Interfaculty Institute of Biochemistry, University of Tuebingen, Germany

Correspondence
D. Rapaport, Interfaculty Institute of Biochemistry, University of Tübingen, Hoppe-Seyler-Str. 4, 72076 Tübingen, Germany
Fax: +49 7071 294016
Tel: +49 7071 2974184
E-mail: doron.rapaport@uni-tuebingen.de

(Received 17 May 2017, revised 8 June 2017, accepted 16 June 2017, available online 2 July 2017)

doi:10.1002/1873-3468.12726

Edited by Wilhelm Just

The endosymbiotic organelles mitochondria and chloroplasts harbour, similarly to their prokaryotic progenitors, β-barrel proteins in their outer membrane. These proteins are encoded on nuclear DNA, translated on cytosolic ribosomes and imported into their target organelles by a dedicated machinery. Recent studies have provided insights into the import into the organelles and the membrane insertion of these proteins. Although the cytosolic stages of their biogenesis are less well defined, it is speculated that upon their synthesis, chaperones prevent β-barrel proteins from aggregation and keep them in an import-competent conformation. In this Review, we summarize the current knowledge about the biogenesis of β-barrel proteins, focusing on the early stages from the translation on cytosolic ribosomes to the recognition on the surface of the organelle.

Keywords: chloroplasts; mitochondria; β-barrel proteins

Mitochondria and chloroplasts are eukaryotic organelles that originated from the endosymbiotic uptake of an α-proteobacterium and a cyanobacterium, respectively [1]. During their evolution, most of the organellar proteins were transferred to the host cell's nucleus and the organelles underwent many changes to adapt to the new environment. Yet, both organelles retained several features of their prokaryotic progenitors, one of these being the occurrence of β-barrel proteins in the outer membrane. Of note, chloroplasts represent only one type of plant plastids; however, the other plastid types also contain β-barrel proteins. Since not much is known about the biogenesis pathways in the other plastids, we refer here to chloroplasts. Importantly, the outer membranes of mitochondria, chloroplasts and Gram-negative bacteria are the only membranes that contain β-barrel proteins. Such proteins span the membrane with a cylindrical β-sheet formed by 8–26 antiparallel β-strands, thereby forming a hydrophilic membrane pore.

Whereas a vast number of different β-barrel proteins reside in the outer membranes of Gram-negative bacteria, only few of them exist in eukaryotes. Mitochondria from yeast and human cells contain five β-barrel proteins and nine β-barrel proteins were identified in *Arabidopsis thaliana* chloroplasts. Most β-barrel proteins, such as the mitochondrial voltage-dependent anion channel (VDAC; called Porin in yeast), and the chloroplast outer envelope protein 21 (OEP21), OEP24 and OEP37 function as transporters for ions, small molecules, peptides and nucleic acids. Another group of β-barrel proteins, including Tom40, Tob55/Sam50 and Toc75, play an essential role in the import of proteins into mitochondria and plastids. Furthermore, eukaryotic β-barrel proteins are also involved in a variety of cellular processes, including signalling, organelle interactions and apoptosis [2,3]. The targeting of β-barrel proteins to and their assembly into the outer membrane of chloroplasts and mitochondria is essential for the biogenesis, morphology and maintenance

Abbreviations
BAM, β-barrel assembly machinery; Mdm10, mitochondrial distribution and morphology 10; PTMs, posttranslational modifications; TIM, translocase of the inner membrane; TOC, translocase of the chloroplast outer membrane; TOM, translocase of the outer membrane; VDAC, voltage-dependent anion channel.

of these organelles and thus for the viability of the cells containing them.

During the evolution of mitochondria and chloroplasts, most organellar genes, including all those encoding β-barrel proteins, were transferred to the nuclear genome. Therefore, genes encoding eukaryotic β-barrel proteins are transcribed in the nucleus and translated on cytosolic ribosomes. To assure that the newly synthesized proteins reach their correct destination, namely the outer membrane of either mitochondria or chloroplasts, the eukaryotic cells had to develop robust targeting and import machineries. In the past years, the import machinery of mitochondrial β-barrel proteins has been extensively studied (Fig. 1A, reviewed in Refs [4] and [5]). Shortly, β-barrel proteins are transported across the mitochondrial outer membrane by the translocase of the outer membrane (TOM) complex. The central subunit of the TOM complex, Tom40, is by itself a β-barrel protein and forms the general entry pore for most mitochondrial proteins. In addition to Tom40, the TOM complex comprises the receptor proteins Tom70, Tom20 and Tom220 (see below) and the small TOM subunits Tom5, Tom6 and Tom7. In the intermembrane space, the *in transit* β-barrel proteins interact with the small translocase of the inner membrane (TIM) chaperone complexes (Tim9/10 and Tim8/13) that prevent the β-barrel proteins from aggregation. Finally, the topogenesis of outer membrane β-barrel proteins (TOB) complex (also known as sorting and assembly machinery) mediates the membrane insertion of β-barrel proteins. Tob55/Sam50, the core component of the TOB complex, is a β-barrel protein and homologous to BamA, the central subunit of the β-barrel assembly machinery (BAM) complex in bacteria. The yeast TOB complex contains two additional proteins, Tob38/Sam35 and Mas37/Sam37. For the efficient transfer of β-barrel proteins, the TOM and TOB complexes associate to form a supercomplex. The formation of this supercomplex is facilitated by the interaction of Tom22 with Mas37/Sam37 [6,7]. To ensure correct intraorganellar sorting, mitochondrial β-barrel proteins contain a consensus sequence in their C-terminal β-strand. This sequence was termed β-signal and is recognized by Tob38/Sam35 [8]. Of note, this β-signal is not strictly necessary for the biogenesis of β-barrel

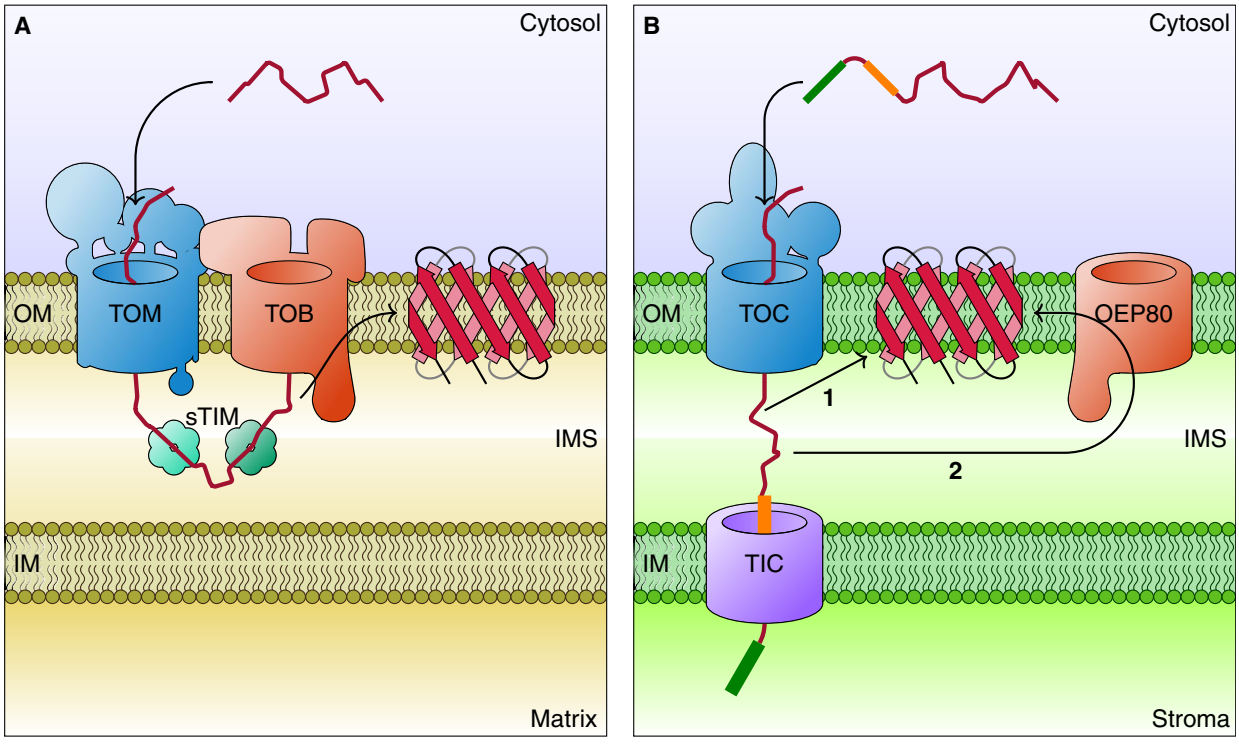

Fig. 1. Biogenesis pathways of β-barrel proteins. (A) The import and assembly of mitochondrial β-barrel proteins is facilitated by the TOM and TOB complexes together with the small TIM chaperones (sTIM). (B) The β-barrel protein Toc75 is imported into chloroplasts with the help of the TOC and TIC complexes and inserted into the outer membrane either by the TOC complex (1) or by OEP80 (2). IM, inner membrane; OM, outer membrane; IMS, intermembrane space.

proteins in mitochondria, as bacterial β-barrel proteins that are devoid of such a β-signal could be assembled in the outer membrane of mitochondria (see below).

While many aspects of the biogenesis of mitochondrial β-barrel proteins could recently be revealed, much less is known about the biogenesis process of their chloroplast counterparts [5]. The translocase of the chloroplast outer membrane (TOC) complex is required for the import of the β-barrel protein Toc75 that also functions as the core subunit of this complex. Another chloroplast β-barrel protein, OEP80, was proposed to mediate the membrane insertion of chloroplast β-barrel proteins, as it is an essential protein that is related to BamA and Tob55 [9,10] (Fig. 1B). This idea was supported by the reduced Toc75 levels observed in chloroplasts from OEP80-knockdown cells [11]. However, direct experimental evidence for this hypothesis is still missing.

At least in the mitochondrial system, we have reached a decent understanding of the intra-organellar events in the biogenesis of β-barrel proteins, whereas the early, cytosolic stages of this biogenesis pathway are less well defined. In this review, we will focus on these stages and summarize the current knowledge about the biogenesis of mitochondrial and chloroplast β-barrel proteins from their translation on cytosolic ribosomes until their recognition on the organelle's surface. We will discuss the nature of the targeting sequences of these proteins and the role that potential interaction partners play in their way through the cytosol. Finally, we will evaluate possible modes for the regulation of the import of β-barrel proteins.

Import mode: is it co- or posttranslational?

β-Barrel proteins are imported from the cytosol into their target organelle. In general, this import can occur cotranslationally, i.e. while the protein is still being translated, or posttranslationally after the protein translation was completed.

In the late 1970s, it was demonstrated that presequence-containing precursor proteins that were synthesized in a cell-free system could be imported into isolated mitochondria [12] or chloroplasts [13,14]. These early experiments show that both organelles are capable of importing at least some proteins in a posttranslational manner. Posttranslational mitochondrial import of matrix-destined preproteins was also observed in experiments with intact yeast cells [15]. Later studies reported on a posttranslational *in vitro* import of several β-barrel proteins including chloroplast Toc75, OEP80, OEP37, OEP24 and OEP21 [16–18], as well as mitochondrial Porin, Tom40 and Tob55 [19–21].

However, another set of studies demonstrated that mitochondrial import can also occur in an apparently cotranslational mode. These findings were sparked by the detection of cytosolic polysomes on the mitochondrial surface where they localized to contact sites between the outer and inner membrane, i.e. the region where protein import occurs [22]. Experiments performed with both *in vitro* and *in vivo* systems confirmed the existence of a cotranslational import mode for a limited number of mitochondrial precursor proteins [23–27]. In accordance with a cotranslational import mode, mRNAs encoding many mitochondrial proteins were found to be localized to mitochondria [28,29]. While a few mitochondrial proteins that are imported cotranslationally were identified, such an import mode was shown so far only for one chloroplast protein [30].

The aforementioned examples of cotranslational import into mitochondria and chloroplasts raised the question whether this import form is also true for β-barrel proteins. In one of the initial studies of cotranslational import *in vitro*, the β-barrel protein Porin was proposed to require coupled translation and translocation [23]. Of note, while a posttranslational *in vitro* import of Porin was observed by several studies (e.g. [19]), the system used in Ref. [23] was not capable of importing Porin posttranslationally. Hence, it seems that under most of the employed experimental conditions, posttranslational import of β-barrel proteins is possible.

Analysing the localization of mRNAs encoding β-barrel proteins can give another hint at their import mode. In yeast, the mRNAs of Tom40, Tob55 and the two isoforms of Porin showed little or no mitochondrial localization, while the mRNA of another β-barrel protein, mitochondrial distribution and morphology 10 (Mdm10) seemed to be partially enriched in the vicinity of mitochondria [29]. In plant cells, mRNA encoding the β-barrel protein VDAC3 was shown to be associated with mitochondria [31]. However, while a cotranslational import leads to an mRNA localization to the site of import, the reverse is not necessarily true. In fact, targeting of VDAC3 mRNA to mitochondria is not required for an efficient import of the protein [31].

In summary, although it cannot be excluded that the import of mitochondrial and chloroplast β-barrel proteins is already initiated while they are still bound to a ribosome, the observations that many of them can be imported posttranslationally and that the corresponding mRNAs show little or no colocalization with the organelles suggest that the posttranslational import

mode is the predominant one for these proteins. A strictly cotranslational import, where an association with ribosomes is required for the nascent chains to be targeted to and imported into their corresponding organelle, can be excluded for β-barrel proteins, as they can be imported *in vitro* in the absence of ribosomes.

Targeting signals of β-barrel proteins

Most precursor proteins of mitochondria and chloroplasts contain an N-terminal, cleavable presequence that targets the protein to the correct intracellular location. Apart from Toc75 and OEP80 (see below), mitochondrial and chloroplast β-barrel proteins do not contain a cleavable targeting signal. This absence of an obvious targeting sequence raised the question how the targeting information of β-barrel proteins is encoded.

The targeting information was conserved during evolution

Since the prokaryotic ancestors of mitochondria and chloroplasts contain β-barrel proteins in their outer membrane, it is possible that the features that allowed correct targeting of these prokaryotic proteins were conserved during evolution and are now able to direct also eukaryotic β-barrels to their proper destination. To analyse this possibility, several studies were performed in which the capacity of β-barrel proteins to assemble into foreign membranes was assessed. In these studies, bacterial β-barrel proteins were shown to assemble into the outer membrane of mitochondria in both yeast and human cells [32–34]. Interestingly, the reverse is also true. Upon expression in bacteria, the eukaryotic β-barrel protein VDAC was targeted to and assembled into the outer membrane [35]. These results show that the targeting information of β-barrel proteins was conserved from bacteria to mitochondria and is functional in both systems.

To test whether this conservation of the targeting information also extends to chloroplast β-barrel proteins, two proteins of this group, OEP37 and OEP24, were tested for their ability to be imported into yeast mitochondria. Insertion into the mitochondrial outer membrane was observed for these proteins both *in vivo* and *in vitro* [17]. Interestingly, in an *in vitro* import assay containing both chloroplasts and mitochondria, OEP37 and OEP24 were imported into both organelles, whereas the import of the mitochondrial β-barrel protein VDAC into chloroplasts was rather inefficient [17]. Taken together, chloroplast β-barrel proteins contain sufficient targeting information for import and assembly into the mitochondrial outer membrane, whereas they seem to contain additional information that is lacking in mitochondrial β-barrel proteins but is required for an efficient import into chloroplasts. This implies that in plant cells a mechanism should exist that actively directs chloroplasts β-barrel proteins into their corresponding organelle while preventing their mistargeting to mitochondria.

The targeting signal of mitochondrial β-barrel proteins

To characterize further the targeting information of mitochondrial β-barrel proteins, several research groups tried to identify a conserved linear amino acid sequence that could serve as a targeting signal. Such a linear signal could not be detected by bioinformatic analyses or a study using hybrid β-barrel proteins [33]. It was thus proposed that the targeting information is encoded by a structural feature of mitochondrial β-barrel proteins. This hypothesis was also supported by the finding that the *in vitro* import of Tom40 was decreased when the precursor was unfolded by urea treatment prior to the import reaction [20]. The observation that bacterial and chloroplast β-barrel proteins can be targeted to and inserted into the mitochondrial outer membrane (see above) further substantiated this idea, as the tested nonmitochondrial proteins have low sequence homology to their mitochondrial counterparts but fold into similar structures.

Experiments using the bacterial trimeric autotransporter protein Yersinia adhesion A (YadA) could show that even a partial β-barrel structure is sufficient for mitochondrial targeting. When inserted into the outer membrane of bacteria, YadA forms a trimeric β-barrel with 12 β-strands to which each monomer contributes four β-strands [36]. Upon expression in yeast cells, YadA was targeted to and inserted into the mitochondrial outer membrane [37,38]. The four β-strands of YadA must, therefore, contain all the information necessary for targeting the protein to the mitochondrial outer membrane. This observation prompted the question whether even a β-hairpin could be sufficient for mitochondrial targeting. This structural motif comprises two β-strands with a short connecting loop and was described as the minimal building block of all β-barrel proteins [39].

In a recent study, we used several *in vitro* and *in vivo* approaches to test whether a β-hairpin motif can serve as a targeting signal of mitochondrial β-barrel proteins. We could show that a peptide derived from the last β-hairpin of human VDAC1 can competitively inhibit the

in vitro import of β-barrel proteins into isolated mitochondria. Furthermore, we demonstrated that hybrid proteins composed of this β-hairpin peptide fused to a soluble passenger domain (like dihydrofolate reductase or green fluorescent protein) was targeted within intact yeast cells to mitochondria [40].

However, not any β-hairpin motif can serve as such a targeting signal. We observed a clear correlation between the mitochondrial targeting capacity and the hydrophobicity of the β-hairpins. Of note, not the overall hydrophobicity of the β-hairpin is relevant, but only the hydrophobicity of the residues that are exposed on the hydrophobic face formed by the two β-strands [40]. Collectively, we could identify the targeting signal of mitochondrial β-barrel proteins as a β-hairpin motif with a very hydrophobic face (Fig. 2A).

Targeting signals of chloroplast β-barrel proteins

While none of the mitochondrial β-barrel proteins contains a cleavable targeting sequence, the situation is more complex for the chloroplast ones. Of all the chloroplast β-barrel proteins, the biogenesis of Toc75 has been studied the most. Interestingly, Toc75 contains a cleavable, bipartite targeting signal. This targeting peptide is composed of two parts: an N-terminal transit peptide with a stroma targeting potential and downstream to it a sorting signal that contains a polyglycine stretch, which prevents the translocation of Toc75 across the inner membrane [41,42]. The transit peptide and the following sorting peptide are cleaved by the stromal processing peptidase and the plastidic type I signal peptidase 1 (Plsp1), respectively [41,43] (Fig. 2B).

Another chloroplast β-barrel protein, OEP80, was shown to be processed during import [16]. However, OEP80 does not contain a polyglycine stretch and, therefore, might use a different import pathway than Toc75. Furthermore, the chloroplast β-barrel proteins OEP37 and OEP24 were predicted to contain transit peptides; however, they are imported into chloroplast without a change in their size [17]. Yet another group of chloroplast β-barrel proteins, including OEP21 and Toc75-IV, has no predicted transit peptides. Taken together, the various β-barrel proteins of chloroplasts seem to contain distinct types of targeting signals and might reach the chloroplast outer membrane by different pathways (Fig. 2B).

Interestingly, exchanging the last β-hairpin of OEP24 or OEP37 with the last β-hairpin of human VDAC1 or yeast Porin leads to a mislocalization of these proteins to mitochondria [40]. This indicates that deleting the C-terminal β-hairpin of OEP24 or OEP37 disrupts their chloroplast targeting signal and/or that a mitochondrial targeting signal, in the form of a β-hairpin with a strongly hydrophobic face, takes precedence over a chloroplast targeting signal. A bioinformatic inspection of the sequences of C-terminal β-hairpins from mitochondrial or chloroplasts β-barrel proteins could not identify a clear difference in the hydrophobicity pattern of the two groups (A. Kessel, personal communication). Thus, it seems that the overall hydrophobicity rather than a specific pattern creates the difference between these two sets of β-hairpins.

Cytosolic factors interacting with β-barrel proteins

Since the import of β-barrel proteins can proceed in a posttranslational manner, the cell is faced with a major challenge, namely keeping the newly synthesized proteins in an import-competent state. This is especially

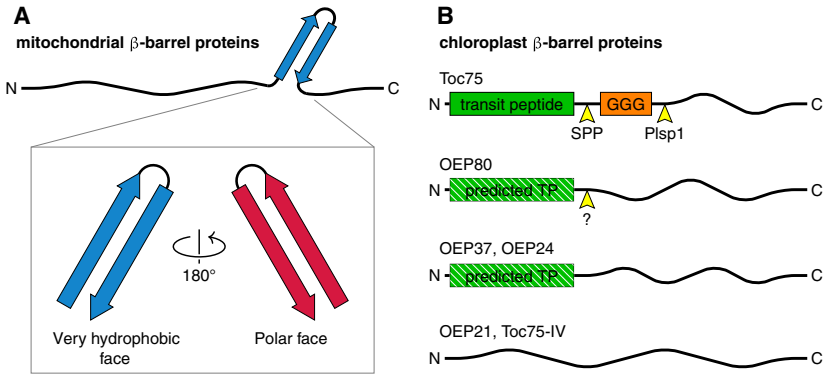

Fig. 2. Targeting signals of β-barrel proteins. (A) Mitochondrial β-barrel proteins contain a β-hairpin motif with one very hydrophobic face that serves as a targeting signal. (B) Chloroplast proteins harbour different types of targeting information including transit peptides (TP) and a polyglycine stretch (GGG). Peptidase cutting sites for processed proteins are indicated.

demanding, as β-barrel proteins are prone to aggregation due to their hydrophobic nature and their propensity to form β-sheets [44]. It is, thus, easily conceivable that the cell must contain cytosolic proteins that prevent the aggregation of β-barrel proteins. While interactions of newly synthesized β-barrel proteins with cytosolic factors have not been reported to date, there are some hints that point into this direction.

One of the early indications for such an involvement is the observation that a pool of ATP outside of mitochondria is required for an optimal *in vitro* import of the mitochondrial β-barrel proteins Porin and Tom40 [20,45,46]. It was proposed that this ATP is utilized by cytosolic factors that keep the β-barrel proteins in an import-competent state; however, experimental evidence for this hypothesis is lacking. Of note, extra-mitochondrial ATP is also required for the import of several non-β-barrel mitochondrial precursor proteins [47]. The extra-mitochondrial ATP-consumption can, at least in part, be explained by the interaction of the precursor proteins with cytosolic, ATP-dependent chaperones of the heat shock protein 70 (Hsp70) and Hsp90 families that keep the precursors in an import-competent conformation [48–50]. Hsp70 and Hsp90 chaperones are also involved in the import of chloroplast precursor proteins [51,52]. Yet, whether they also interact with chloroplast β-barrel proteins is still unclear.

Apart from a role in preventing β-barrel proteins from aggregating, cytosolic factors could also play a more active role in the targeting of their substrate proteins. However, to date, such targeting factors for β-barrel proteins were not detected. In contrast, for non-β-barrel proteins of mitochondria and chloroplasts, several cytosolic proteins were suggested to function as targeting factors [53–57]. Yet, whether any of these proteins can also bind to newly synthesized β-barrel proteins remains to be seen.

The presence of β-barrel protein-specific cytosolic targeting factors is especially likely for plant cells, since they must distinguish between β-barrel proteins destined for either mitochondria or chloroplasts. While in intact plant cells mislocalization of chloroplast β-barrel proteins to mitochondria was not observed, it can occur in *in vitro* import reactions containing both organelles. Here, the chloroplast β-barrel proteins OEP37 and OEP24 were imported into chloroplasts and mitochondria with a similar efficiency [17]. These findings suggest that the plant cytosol probably contains factors that prevent the mistargeting of chloroplast β-barrel proteins *in vivo*. Nonetheless, so far, the nature of these factors has not been elucidated.

Taken together, while a role of cytosolic factors in the biogenesis of mitochondrial and chloroplast β-barrel proteins seems likely, so far, such components were not identified and this issue should be addressed in future studies.

Recognition at the organelle's surface

After withstanding the cytosolic environment, presumably with the help of cytosolic factors, the newly synthesized β-barrel proteins will reach the surface of their target organelle. Here, they interact with specific receptor proteins to initiate the organellar import.

Mitochondrial import receptors

As part of their biogenesis pathway, mitochondrial β-barrel proteins must cross the outer membrane, as the TOB complex-mediated membrane insertion occurs from the intermembrane space face of the membrane [4,5]. Translocation across the outer membrane is facilitated by the TOM complex that contains three receptor subunits: Tom70, Tom20 and Tom22. Tom20 and Tom22 are mainly involved in the recognition of presequence-containing mitochondrial proteins [58–60], whereas Tom70 mostly recognizes mitochondrial proteins with an internal targeting signal [61,62] and interacts with the chaperones of the Hsp70 and Hsp90 families [50] (Fig. 3A).

Despite these apparently different recognition patterns, it is becoming clear that the substrate specificities of Tom20 and Tom70 partially overlap and that the proteins can complement the absence of one another in yeast cells [63,64]. The atomic structure of Tom20 revealed a hydrophobic groove on the surface of the receptor as the place where it binds presequence peptides [65]. Recently, Tom70 was shown to also contain a presequence-binding groove [66]. Of note, plant mitochondria do not contain Tom70, but they harbour another outer membrane protein, OM64, that can bind mitochondrial preproteins and cytosolic chaperones [67,68].

Several studies concluded that Tom20 is important for the biogenesis of mitochondrial β-barrel proteins as mitochondria lacking this receptor had a reduced import efficiency for the β-barrel proteins Tom40 and Porin [60,69]. Furthermore, crosslinking experiments with *in vitro* translated Tom40 and Porin revealed that both proteins form crosslinking adducts with Tom20 [20,69]. As part of our efforts to characterize the targeting signal of mitochondrial β-barrel proteins, we could show that a β-hairpin peptide is sufficient for the recognition by Tom20. Moreover, NMR analysis of this interaction indicated that the β-hairpin binds to Tom20 in the hydrophobic presequence-binding groove

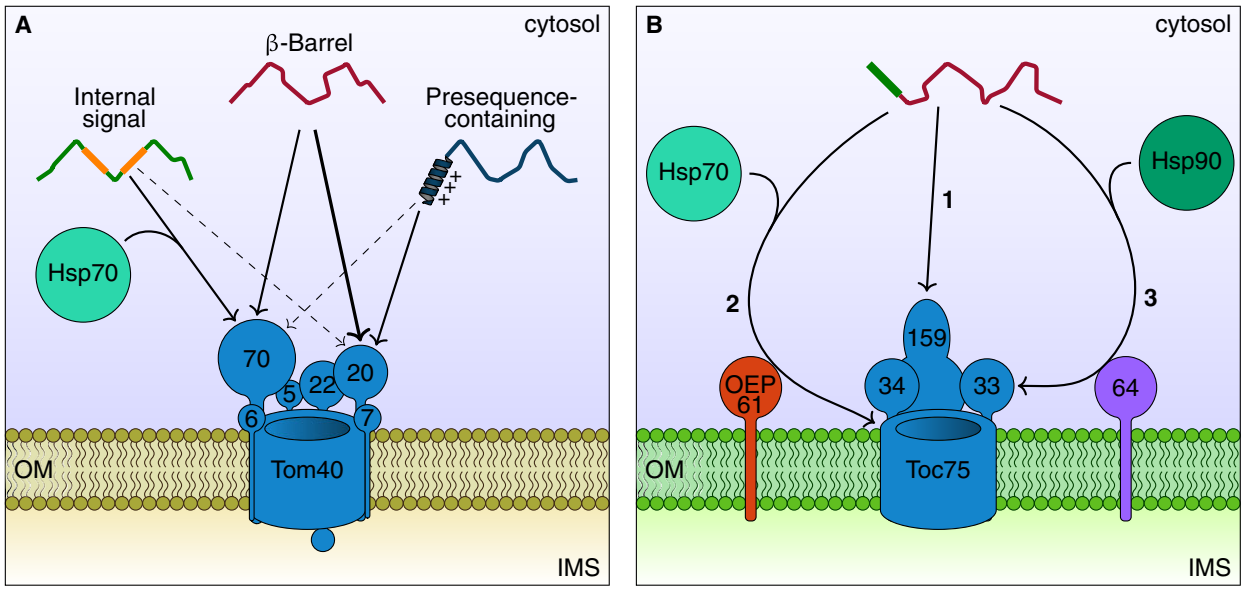

Fig. 3. Import receptors of mitochondria and chloroplasts. (A) The two receptors of the TOM complex, Tom20 and Tom70, have different, but partially overlapping, substrate specificities. (B) Precursor proteins destined for chloroplasts can directly interact with the receptors of the TOC complex (1). When they are in contact with Hsp70 or Hsp90, they can be recognized by OEP61 (2) or Toc64 (3), respectively.

[40]. This finding is in line with the observation that a presequence peptide can competitively inhibit the import of the β-barrel protein Porin [70].

Nevertheless, Tom20 is probably not the only receptor for mitochondrial β-barrel proteins; *in vitro* import experiments showed a strong decrease in the mitochondrial import of Tom40 when the mitochondria were pretreated with antibodies against Tom70 [71]. This finding is supported by the observation of crosslinking adducts between Tom70 and a β-hairpin peptide corresponding to a β-barrel protein-targeting signal [40]. Along this line, binding studies with *in vitro* synthesized plant receptors and precursor proteins demonstrated that Tom40 can be bound by both Tom20 and OM64 [67]. The involvement of Tom70 and OM64 in the biogenesis of mitochondrial β-barrel proteins supports the notion that cytosolic chaperones interact with newly synthesized β-barrel proteins, as both receptors were reported to bind Hsp70 and Hsp90 chaperones.

Import receptors of chloroplasts

In contrast to the situation in mitochondria, where all β-barrels cross the outer membrane to be inserted into this membrane from its intermembrane space face, a similar pathway was shown, so far, only for the chloroplast β-barrel protein Toc75. Outer membrane translocation of, at least a part of, Toc75 is mediated by the general import pore of chloroplasts, the TOC complex [72]. The TOC complex is composed of the pore-forming subunit Toc75 and two GTPases, Toc34 and Toc159, that function as transit peptide receptors [73–75]. Several studies showed that the *in vitro* import of Toc75 is inhibited by the addition of transit peptides, thereby indicating that it interacts with the receptors Toc34 and/or Toc159 [72]. In addition to these receptors, two further chloroplast outer membrane proteins, Toc64 and OEP61, were reported to be involved in the import of chloroplast proteins. Toc64 and OEP61 bind not only to the precursor proteins but also to Hsp90 or Hsp70, respectively [52,76,77] (Fig. 3B). Toc64 in cooperation with Toc33, a Toc34 homologue, was reported to be important for the biogenesis of the chloroplast β-barrel protein Toc75 [76].

While Toc75 requires the TOC complex and its receptors, some chloroplast β-barrel proteins were proposed to be imported independently of this complex. The chloroplast β-barrel OEP21 was shown to be efficiently imported into the outer membrane, even when the chloroplasts were pretreated with the protease thermolysin [18]. Since thermolysin degrades the chloroplast import receptors, OEP21 seems to be imported without the help of these proteins. This observation can be explained by a receptor-independent interaction with the pore component Toc75. An alternative hypothesis suggests that OEP21, and maybe other chloroplast β-barrel proteins, can directly insert into

the chloroplast outer membrane [78]. Experimental support for any of the above two alternatives is, however, still missing.

Regulation of β-barrel protein import

Mitochondria and chloroplasts are both dynamic organelles that can adapt to the cell's needs. This adaptiveness requires changes in the protein composition of the organelles. Since most mitochondrial and chloroplast proteins are encoded in the nucleus and imported into the organelles, a tight regulation of this import is important to ensure the proper protein configuration in response to external stimuli. Transcriptional and translational up- or downregulation of precursor proteins destined for mitochondria or chloroplasts can affect the protein composition of these organelles. However, a more direct regulation of the protein import has been reported for both mitochondria and chloroplasts. The main import machineries as well as precursor proteins can acquire diverse posttranslational modifications (PTMs) which lead to changes in the organellar import capacity. Phosphorylation was reported for several subunits of the TOM complex of mitochondria [79], as well as for the TOC complex of chloroplasts [73,80]. Furthermore, it was proposed that the TOC complex is additionally regulated by changes in the redox status of the cell and by the ubiquitin-proteasome system [81,82].

While regulation on the level of the TOM or TOC complexes will influence the import of many precursor proteins at the same time, PTMs of individual precursor proteins can lead to an altered import of only these modified proteins. In yeast cells, it was established that the precursor of the mitochondrial β-barrel protein Tom40 can be phosphorylated by protein kinase A and that this phosphorylation inhibits the import of the precursor protein [83]. In contrast, a direct phosphorylation of newly synthesized chloroplast β-barrel proteins has not been reported to date. However, phosphorylation of chloroplast transit peptides has been reported to inhibit the import of the precursor proteins [84]. Since the chloroplast β-barrel protein Toc75 contains a transit peptide, it could also be subject to this type of phosphorylation.

Conclusions and Perspectives

Our knowledge about the biogenesis pathway of mitochondrial β-barrel proteins has dramatically increased in the past years. However, this is mainly true for the intramitochondrial stages of this pathway. Information about cytosolic processes that are required for β-barrel protein biogenesis is scarce. Identification of cytosolic factors that interact with newly synthesized β-barrel proteins could help to understand how the cell keeps these proteins in an import-competent conformation. Furthermore, deciphering the involvement of these factors might answer the question whether the targeting information of β-barrel proteins is already decoded in the cytosol or only later by the import receptors on the mitochondrial surface.

In contrast to the biogenesis of mitochondrial β-barrel proteins, little is known about the biogenesis of their chloroplast counterparts. Elucidating the nature of the targeting information of these proteins will help to understand not only how they are recognized by the chloroplast import receptors but also how the plant cell is able to distinguish between mitochondrial and chloroplast β-barrel proteins. Furthermore, the components of the import machinery necessary for the import and assembly of chloroplast β-barrel need to be defined. The identification of these factors will also help in understanding how the biogenesis of chloroplast proteins is regulated.

Acknowledgements

We thank E. Schleiff for helpful discussions. Our work is supported by the Deutsche Forschungsgemeinschaft (RA 1028/8-1 to DR).

Author contributions

TJ and DR wrote the manuscript.

References

1 Gray MW (1999) Evolution of organellar genomes. *Curr Opin Genet Dev* **9**, 678–687.
2 Kornmann B, Currie E, Collins SR, Schuldiner M, Nunnari J, Weissman JS and Walter P (2009) An ER-mitochondria tethering complex revealed by a synthetic biology screen. *Science* **325**, 477–481.
3 Shimizu S, Narita M and Tsujimoto Y (1999) Bcl-2 family proteins regulate the release of apoptogenic cytochrome c by the mitochondrial channel VDAC. *Nature* **399**, 483–487.
4 Höhr AIC, Straub SP, Warscheid B, Becker T and Wiedemann N (2015) Assembly of β-barrel proteins in the mitochondrial outer membrane. *Biochim Biophys Acta* **1853**, 74–88.
5 Ulrich T and Rapaport D (2015) Biogenesis of beta-barrel proteins in evolutionary context. *Int J Med Microbiol* **305**, 259–264.
6 Qiu J, Wenz LS, Zerbes RM, Oeljeklaus S, Bohnert M, Stroud DA, Wirth C, Ellenrieder L, Thornton N, Kutik

S *et al*. (2013) Coupling of mitochondrial import and export translocases by receptor-mediated supercomplex formation. *Cell* **154**, 596–608.
7 Wenz LS, Ellenrieder L, Qiu J, Bohnert M, Zufall N, van der Laan M, Pfanner N, Wiedemann N and Becker T (2015) Sam37 is crucial for formation of the mitochondrial TOM-SAM supercomplex, thereby promoting β-barrel biogenesis. *J Cell Biol* **210**, 1047–1054.
8 Kutik S, Stojanovski D, Becker L, Becker T, Meinecke M, Krüger V, Prinz C, Meisinger C, Guiard B, Wagner R *et al*. (2008) Dissecting membrane insertion of mitochondrial beta-barrel proteins. *Cell* **132**, 1011–1024.
9 Patel R, Hsu SC, Bédard J, Inoue K and Jarvis P (2008) The Omp85-related chloroplast outer envelope protein OEP80 is essential for viability in Arabidopsis. *Plant Physiol* **148**, 235–245.
10 Soll J and Schleiff E (2004) Protein import into chloroplasts. *Nat Rev Mol Cell Biol* **5**, 198–208.
11 Huang W, Ling Q, Bédard J, Lilley K and Jarvis P (2011) In vivo analyses of the roles of essential Omp85-related proteins in the chloroplast outer envelope membrane. *Plant Physiol* **157**, 147–159.
12 Maccecchini ML, Rudin Y, Blobel G and Schatz G (1979) Import of proteins into mitochondria: precursor forms of the extramitochondrially made F1-ATPase subunits in yeast. *Proc Natl Acad Sci USA* **76**, 343–347.
13 Highfield PE and Ellis RJ (1978) Synthesis and transport of the small subunit of chloroplast ribulose bisphosphate carboxylase. *Nature* **271**, 420–424.
14 Chua NH and Schmidt GW (1978) Post-translational transport into intact chloroplasts of a precursor to the small subunit of ribulose-1,5-bisphosphate carboxylase. *Proc Natl Acad Sci USA* **75**, 6110–6114.
15 Reid GA and Schatz G (1982) Import of proteins into mitochondria. Yeast cells grown in the presence of carbonyl cyanide m-chlorophenylhydrazone accumulate massive amounts of some mitochondrial precursor polypeptides. *J Biol Chem* **257**, 13056–13061.
16 Day PM, Potter D and Inoue K (2014) Evolution and targeting of Omp85 homologs in the chloroplast outer envelope membrane. *Front Plant Sci* **5**, 535.
17 Ulrich T, Gross LE, Sommer MS, Schleiff E and Rapaport D (2012) Chloroplast β-barrel proteins are assembled into the mitochondrial outer membrane in a process that depends on the TOM and TOB complexes. *J Biol Chem* **287**, 27467–27479.
18 Bölter B, Soll J, Hill K, Hemmler R and Wagner R (1999) A rectifying ATP-regulated solute channel in the chloroplastic outer envelope from pea. *EMBO J* **18**, 5505–5516.
19 Freitag H, Janes M and Neupert W (1982) Biosynthesis of mitochondrial porin and insertion into the outer mitochondrial membrane of Neurospora crassa. *Eur J Biochem* **126**, 197–202.
20 Rapaport D and Neupert W (1999) Biogenesis of Tom40, core component of the TOM complex of mitochondria. *J Cell Biol* **146**, 321–331.
21 Habib SJ, Waizenegger T, Lech M, Neupert W and Rapaport D (2005) Assembly of the TOB complex of mitochondria. *J Biol Chem* **280**, 6434–6440.
22 Kellems RE, Allison VF and Butow RA (1975) Cytoplasmic type 80S ribosomes associated with yeast mitochondria. IV. Attachment of ribosomes to the outer membrane of isolated mitochondria. *J Cell Biol* **65**, 1–14.
23 Fujiki M and Verner K (1991) Coupling of protein synthesis and mitochondrial import in a homologous yeast in vitro system. *J Biol Chem* **266**, 6841–6847.
24 Fujiki M and Verner K (1993) Coupling of cytosolic protein synthesis and mitochondrial protein import in yeast. Evidence for cotranslational import in vivo. *J Biol Chem* **268**, 1914–1920.
25 Knox C, Sass E, Neupert W and Pines O (1998) Import into mitochondria, folding and retrograde movement of fumarase in yeast. *J Biol Chem* **273**, 25587–25593.
26 Yogev O, Karniely S and Pines O (2007) Translation-coupled translocation of yeast fumarase into mitochondria in vivo. *J Biol Chem* **282**, 29222–29229.
27 Mukhopadhyay A, Ni L and Weiner H (2004) A co-translational model to explain the in vivo import of proteins into HeLa cell mitochondria. *Biochem J* **382**, 385–392.
28 Marc P, Margeot A, Devaux F, Blugeon C, Corral-Debrinski M and Jacq C (2002) Genome-wide analysis of mRNAs targeted to yeast mitochondria. *EMBO Rep* **3**, 159–164.
29 Saint-Georges Y, Garcia M, Delaveau T, Jourdren L, Le Crom S, Lemoine S, Tanty V, Devaux F and Jacq C (2008) Yeast mitochondrial biogenesis: a role for the PUF RNA-binding protein Puf3p in mRNA localization. *PLoS One* **3**, e2293.
30 Uniacke J and Zerges W (2009) Chloroplast protein targeting involves localized translation in *Chlamydomonas*. *Proc Natl Acad Sci USA* **106**, 1439–1444.
31 Michaud M, Ubrig E, Filleur S, Erhardt M, Ephritikhine G, Maréchal-Drouard L and Duchêne AM (2014) Differential targeting of VDAC3 mRNA isoforms influences mitochondria morphology. *Proc Natl Acad Sci USA* **111**, 8991–8996.
32 Walther DM, Papić D, Bos MP, Tommassen J and Rapaport D (2009) Signals in bacterial beta-barrel proteins are functional in eukaryotic cells for targeting to and assembly in mitochondria. *Proc Natl Acad Sci USA* **106**, 2531–2536.
33 Müller A, Rassow J, Grimm J, Machuy N, Meyer TF and Rudel T (2002) VDAC and the bacterial porin PorB of *Neisseria gonorrhoeae* share mitochondrial import pathways. *EMBO J* **21**, 1916–1929.
34 Kozjak-Pavlovic V, Ott C, Götz M and Rudel T (2011) Neisserial Omp85 protein is selectively recognized and

assembled into functional complexes in the outer membrane of human mitochondria. *J Biol Chem* **286**, 27019–27026.
35 Walther DM, Bos MP, Rapaport D and Tommassen J (2010) The mitochondrial porin, VDAC, has retained the ability to be assembled in the bacterial outer membrane. *Mol Biol Evol* **27**, 887–895.
36 Shahid SA, Bardiaux B, Franks WT, Krabben L, Habeck M, van Rossum BJ and Linke D (2012) Membrane-protein structure determination by solid-state NMR spectroscopy of microcrystals. *Nat Methods* **9**, 1212–1217.
37 Müller JEN, Papic D, Ulrich T, Grin I, Schütz M, Oberhettinger P, Tommassen J, Linke D, Dimmer KS, Autenrieth IB *et al*. (2011) Mitochondria can recognize and assemble fragments of a beta-barrel structure. *Mol Biol Cell* **22**, 1638–1647.
38 Ulrich T, Oberhettinger P, Schütz M, Holzer K, Ramms AS, Linke D, Autenrieth IB and Rapaport D (2014) Evolutionary conservation in biogenesis of β-barrel proteins allows mitochondria to assemble a functional bacterial trimeric autotransporter protein. *J Biol Chem* **289**, 29457–29470.
39 Arnold T, Poynor M, Nussberger S, Lupas AN and Linke D (2007) Gene duplication of the eight-stranded beta-barrel OmpX produces a functional pore: a scenario for the evolution of transmembrane beta-barrels. *J Mol Biol* **366**, 1174–1184.
40 Jores T, Klinger A, Groß LE, Kawano S, Flinner N, Duchardt-Ferner E, Wöhnert J, Kalbacher H, Endo T, Schleiff E *et al*. (2016) Characterization of the targeting signal in mitochondrial β-barrel proteins. *Nat Commun* **7**, 12036.
41 Tranel PJ and Keegstra K (1996) A novel, bipartite transit peptide targets OEP75 to the outer membrane of the chloroplastic envelope. *Plant Cell* **8**, 2093–2104.
42 Endow JK, Rocha AG, Baldwin AJ, Roston RL, Yamaguchi T, Kamikubo H and Inoue K (2016) Polyglycine acts as a rejection signal for protein transport at the chloroplast envelope. *PLoS One* **11**, e0167802.
43 Inoue K, Baldwin AJ, Shipman RL, Matsui K, Theg SM and Ohme-Takagi M (2005) Complete maturation of the plastid protein translocation channel requires a type I signal peptidase. *J Cell Biol* **171**, 425–430.
44 Hecht MH (1994) De novo design of beta-sheet proteins. *Proc Natl Acad Sci USA* **91**, 8729–8730.
45 Pfanner N, Pfaller R, Kleene R, Ito M, Tropschug M and Neupert W (1988) Role of ATP in mitochondrial protein import. Conformational alteration of a precursor protein can substitute for ATP requirement. *J Biol Chem* **263**, 4049–4051.
46 Hwang ST and Schatz G (1989) Translocation of proteins across the mitochondrial inner membrane, but not into the outer membrane, requires nucleoside triphosphates in the matrix. *Proc Natl Acad Sci USA* **86**, 8432–8436.
47 Wachter C, Schatz G and Glick BS (1994) Protein import into mitochondria: the requirement for external ATP is precursor-specific whereas intramitochondrial ATP is universally needed for translocation into the matrix. *Mol Biol Cell* **5**, 465–474.
48 Murakami H, Pain D and Blobel G (1988) 70-kD heat shock-related protein is one of at least two distinct cytosolic factors stimulating protein import into mitochondria. *J Cell Biol* **107**, 2051–2057.
49 Terada K, Ohtsuka K, Imamoto N, Yoneda Y and Mori M (1995) Role of heat shock cognate 70 protein in import of ornithine transcarbamylase precursor into mammalian mitochondria. *Mol Cell Biol* **15**, 3708–3713.
50 Young JC, Hoogenraad NJ and Hartl FU (2003) Molecular chaperones Hsp90 and Hsp70 deliver preproteins to the mitochondrial import receptor Tom70. *Cell* **112**, 41–50.
51 Rial DV, Arakaki AK and Ceccarelli EA (2000) Interaction of the targeting sequence of chloroplast precursors with Hsp70 molecular chaperones. *Eur J Biochem* **267**, 6239–6248.
52 Qbadou S, Becker T, Mirus O, Tews I, Soll J and Schleiff E (2006) The molecular chaperone Hsp90 delivers precursor proteins to the chloroplast import receptor Toc64. *EMBO J* **25**, 1836–1847.
53 Murakami K and Mori M (1990) Purified presequence binding factor (PBF) forms an import-competent complex with a purified mitochondrial precursor protein. *EMBO J* **9**, 3201–3208.
54 Hachiya N, Alam R, Sakasegawa Y, Sakaguchi M, Mihara K and Omura T (1993) A mitochondrial import factor purified from rat liver cytosol is an ATP-dependent conformational modulator for precursor proteins. *EMBO J* **12**, 1579–1586.
55 Faou P and Hoogenraad NJ (2012) Tom34: a cytosolic cochaperone of the Hsp90/Hsp70 protein complex involved in mitochondrial protein import. *Biochim Biophys Acta* **1823**, 348–357.
56 May T and Soll J (2000) 14-3-3 proteins form a guidance complex with chloroplast precursor proteins in plants. *Plant Cell* **12**, 53–64.
57 Bae W, Lee YJ, Kim DH, Lee J, Kim S, Sohn EJ and Hwang I (2008) AKR2A-mediated import of chloroplast outer membrane proteins is essential for chloroplast biogenesis. *Nat Cell Biol* **10**, 220–227.
58 Söllner T, Griffiths G, Pfaller R, Pfanner N and Neupert W (1989) MOM19, an import receptor for mitochondrial precursor proteins. *Cell* **59**, 1061–1070.
59 Moczko M, Gärtner F and Pfanner N (1993) The protein import receptor MOM19 of yeast mitochondria. *FEBS Lett* **326**, 251–254.
60 Yamano K, Yatsukawa YI, Esaki M, Hobbs AEA, Jensen RE and Endo T (2008) Tom20 and Tom22 share

the common signal recognition pathway in mitochondrial protein import. *J Biol Chem* **283**, 3799–3807.
61 Söllner T, Pfaller R, Griffiths G, Pfanner N and Neupert W (1990) A mitochondrial import receptor for the ADP/ATP carrier. *Cell* **62**, 107–115.
62 Hines V, Brandt A, Griffiths G, Horstmann H, Brütsch H and Schatz G (1990) Protein import into yeast mitochondria is accelerated by the outer membrane protein MAS70. *EMBO J* **9**, 3191–3200.
63 Steger HF, Söllner T, Kiebler M, Dietmeier KA, Pfaller R, Trülzsch KS, Tropschug M, Neupert W and Pfanner N (1990) Import of ADP/ATP carrier into mitochondria: two receptors act in parallel. *J Cell Biol* **111**, 2353–2363.
64 Ramage L, Junne T, Hahne K, Lithgow T and Schatz G (1993) Functional cooperation of mitochondrial protein import receptors in yeast. *EMBO J* **12**, 4115–4123.
65 Abe Y, Shodai T, Muto T, Mihara K, Torii H, Nishikawa S, Endo T and Kohda D (2000) Structural basis of presequence recognition by the mitochondrial protein import receptor Tom20. *Cell* **100**, 551–560.
66 Melin J, Kilisch M, Neumann P, Lytovchenko O, Gomkale R, Schendzielorz A, Schmidt B, Liepold T, Ficner R, Jahn O *et al*. (2015) A presequence-binding groove in Tom70 supports import of Mdl1 into mitochondria. *Biochim Biophys Acta* **1853**, 1850–1859.
67 Lister R, Carrie C, Duncan O, Ho LHM, Howell KA, Murcha MW and Whelan J (2007) Functional definition of outer membrane proteins involved in preprotein import into mitochondria. *Plant Cell* **19**, 3739–3759.
68 Schweiger R, Soll J, Jung K, Heermann R and Schwenkert S (2013) Quantification of interaction strengths between chaperones and tetratricopeptide repeat domain-containing membrane proteins. *J Biol Chem* **288**, 30614–30625.
69 Krimmer T, Rapaport D, Ryan MT, Meisinger C, Kassenbrock CK, Blachly-Dyson E, Forte M, Douglas MG, Neupert W, Nargang FE *et al*. (2001) Biogenesis of porin of the outer mitochondrial membrane involves an import pathway via receptors and the general import pore of the TOM complex. *J Cell Biol* **152**, 289–300.
70 Millar DG and Shore GC (1996) Signal anchor sequence insertion into the outer mitochondrial membrane. Comparison with porin and the matrix protein targeting pathway. *J Biol Chem* **271**, 25823–25829.
71 Keil P, Weinzierl A, Kiebler M, Dietmeier K, Söllner T and Pfanner N (1993) Biogenesis of the mitochondrial receptor complex. Two receptors are required for binding of MOM38 to the outer membrane surface. *J Biol Chem* **268**, 19177–19180.
72 Tranel PJ, Froehlich J, Goyal A and Keegstra K (1995) A component of the chloroplastic protein import apparatus is targeted to the outer envelope membrane via a novel pathway. *EMBO J* **14**, 2436–2446.
73 Sveshnikova N, Soll J and Schleiff E (2000) Toc34 is a preprotein receptor regulated by GTP and phosphorylation. *Proc Natl Acad Sci USA* **97**, 4973–4978.
74 Smith MD, Rounds CM, Wang F, Chen K, Afitlhile M and Schnell DJ (2004) atToc159 is a selective transit peptide receptor for the import of nucleus-encoded chloroplast proteins. *J Cell Biol* **165**, 323–334.
75 Becker T, Jelic M, Vojta A, Radunz A, Soll J and Schleiff E (2004) Preprotein recognition by the Toc complex. *EMBO J* **23**, 520–530.
76 Sommer M, Rudolf M, Tillmann B, Tripp J, Sommer MS and Schleiff E (2013) Toc33 and Toc64-III cooperate in precursor protein import into the chloroplasts of *Arabidopsis thaliana*. *Plant Cell Environ* **36**, 970–983.
77 von Loeffelholz O, Kriechbaumer V, Ewan RA, Jonczyk R, Lehmann S, Young JC and Abell BM (2011) OEP61 is a chaperone receptor at the plastid outer envelope. *Biochem J* **438**, 143–153.
78 Schleiff E and Klösgen RB (2001) Without a little help from 'my' friends: direct insertion of proteins into chloroplast membranes? *Biochim Biophys Acta* **1541**, 22–33.
79 Schmidt O, Harbauer AB, Rao S, Eyrich B, Zahedi RP, Stojanovski D, Schönfisch B, Guiard B, Sickmann A, Pfanner N *et al*. (2011) Regulation of mitochondrial protein import by cytosolic kinases. *Cell* **144**, 227–239.
80 Fulgosi H and Soll J (2002) The chloroplast protein import receptors Toc34 and Toc159 are phosphorylated by distinct protein kinases. *J Biol Chem* **277**, 8934–8940.
81 Stengel A, Benz JP, Buchanan BB, Soll J and Bölter B (2009) Preprotein import into chloroplasts via the Toc and Tic complexes is regulated by redox signals in *Pisum sativum*. *Mol Plant* **2**, 1181–1197.
82 Ling Q, Huang W, Baldwin A and Jarvis P (2012) Chloroplast biogenesis is regulated by direct action of the ubiquitin-proteasome system. *Science* **338**, 655–659.
83 Rao S, Schmidt O, Harbauer AB, Schönfisch B, Guiard B, Pfanner N and Meisinger C (2012) Biogenesis of the preprotein translocase of the outer mitochondrial membrane: protein kinase A phosphorylates the precursor of Tom40 and impairs its import. *Mol Biol Cell* **23**, 1618–1627.
84 Waegemann K and Soll J (1996) Phosphorylation of the transit sequence of chloroplast precursor proteins. *J Biol Chem* **271**, 6545–6554.

b) Manuscripts in revision

5. **Jores**, **T.**, J. Lawatscheck, V. Beke, M. Franz-Wachtel, K. Yunoki, B. Macek, T. Endo, H. Kalbacher, J. Buchner, and D. Rapaport (2017). Cytosolic Hsp70 and Hsp40 chaperones enable the biogenesis of mitochondrial β-barrel proteins. *in revision*.

Cytosolic Hsp70 and Hsp40 chaperones enable the biogenesis of mitochondrial β-barrel proteins

Tobias Jores[1], Jannis Lawatscheck[2], Viktor Beke[1], Mirita Franz-Wachtel[3], Kaori Yunoki[4], Boris Macek[3], Toshiya Endo[4], Hubert Kalbacher[1], Johannes Buchner[2], and Doron Rapaport[1]*

[1] Interfaculty Institute of Biochemistry, University of Tübingen, 72076 Tübingen, Germany

[2] Center for Integrated Protein Science, Department Chemie, Technische Universität München, 85748 Garching, Germany

[3] Proteome Center Tübingen, Interfaculty Institute for Cell Biology, University of Tübingen, 72076 Tübingen, Germany

[4] Faculty of Life Sciences, Kyoto Sangyo University, Kyoto 603-8555, Japan

* To whom correspondence should be addressed:
Interfaculty Institute of Biochemistry, University of Tübingen, Hoppe-Seyler-Str. 4, 72076 Tübingen, Germany.
Tel: +49-7071-2974184; Fax: +49-7071-294016; E-mail: doron.rapaport@uni-tuebingen.de.

Running title: Cytosolic chaperones and β-barrel proteins

Summary:

Mitochondrial β-barrel proteins are imported from the cytosol into the organelle. Jores et al. provide new insights into the early events of this process by describing an array of cytosolic Hsp70s chaperones and Hsp40s co-chaperones that associate with newly synthesized β-barrel proteins and assure their optimal biogenesis.

Abstract

Mitochondrial β-barrel proteins are encoded in the nucleus, translated by cytosolic ribosomes and then imported into the organelle. Recently, a detailed understanding of the intra-mitochondrial import pathway of β-barrel proteins was obtained. In contrast, it is still completely unclear how newly synthesized β-barrel proteins reach the mitochondrial surface in an import-competent conformation. In this study, we show that cytosolic Hsp70 chaperones and their Hsp40 co-chaperones Ydj1 and Sis1 interact with newly synthesized β-barrel proteins. These interactions are highly relevant for proper biogenesis as inhibiting the activity of the cytosolic Hsp70, preventing its docking to the mitochondrial receptor Tom70, or depleting both Ydj1 and Sis1 resulted in a significant reduction in the import of such substrates into mitochondria. Further experiments demonstrate that the interactions between β-barrel proteins and Hsp70 chaperones and their importance are conserved also in mammalian cells. Collectively, this study outlines a novel mechanism in the early events of the biogenesis of mitochondrial outer membrane β-barrel proteins.

Introduction

In eukaryotes, membrane-embedded β-barrel proteins can be found in the outer membrane (OM) of chloroplasts and mitochondria where they perform many crucial functions including the transport of ions, small molecules and nucleic acids. Additionally, some β-barrel proteins have essential roles in the organellar import of cytosolically synthesized proteins and in exchange of lipids with other compartments.

Mitochondrial β-barrel proteins are translated on cytosolic ribosomes and then imported into their target organelles (Höhr et al., 2015; Ulrich and Rapaport, 2015). Upon reaching the mitochondrial surface, they are translocated across the OM into the intermembrane space (IMS) with the help of the translocase of the mitochondrial outer membrane (TOM) complex (Pfanner et al., 2004; Rapaport and Neupert, 1999). The β-barrel precursor proteins interact with the import receptor Tom20 that can recognize them via their targeting signal, which is composed of a highly hydrophobic β-hairpin motif (Jores et al., 2016; Krimmer et al., 2001; Rapaport and Neupert, 1999; Schleiff et al., 1999; Söllner et al., 1989; Yamano et al., 2008). Next, they are translocated across the OM via a pore formed by Tom40, the core subunit of the TOM complex, At the IMS, the small translocase of the inner membrane (TIM) chaperone complexes Tim8/13 and Tim9/10 prevent the aggregation of the β-barrel precursor proteins (Habib et al., 2005; Hoppins and Nargang, 2004; Wiedemann et al., 2004). Finally, OM insertion of the β-barrel proteins is facilitated by the topogenesis of outer membrane β-barrel proteins (TOB) complex (also known as sorting and assembly machinery, SAM) (Chan and Lithgow, 2008; Paschen et al., 2003; Wiedemann et al., 2003).

While the mitochondrial steps of the β-barrel biogenesis are rather well defined, much less is known about the early events of the biogenesis that take place in the cytosol. Importantly, during their transit through the cytosol, the newly synthesized β-barrel proteins must be kept in an import-competent conformation. This is a difficult task as β-barrel proteins are prone to aggregation due to their high overall hydrophobicity and their tendency to form β-sheets (Hecht, 1994).

The cell possesses a multitude of different molecular chaperones and co-chaperones that should prevent misfolding and aggregation of their client proteins (Kim et al., 2013). The ATP-dependent chaperones of the heat shock protein 70 (Hsp70) family help in the folding of newly-synthesized proteins but can also unfold and disaggregate misfolded proteins (Clerico et al., 2015; Mayer, 2013; Morano, 2007; Nillegoda and Bukau, 2015). While Hsp70 chaperones can interact with a vast range of proteins, their activity and substrate specificity are often fine-tuned by co-chaperones of the Hsp40 family, also known as J proteins (Clerico et al., 2015; Kampinga

and Craig, 2010; Walsh et al., 2004). Proteins of the Hsp90 family form a second group of ATP-dependent multipurpose chaperones that are often involved in the maturation of signaling molecules (Schopf et al., 2017; Terasawa et al., 2005; Young et al., 2001).

Chaperones of the Hsp90 and Hsp70 families as well as some of their co-chaperones have been implicated in the import of mitochondrial presequence-containing proteins (Caplan et al., 1992; Deshaies et al., 1988; Endo et al., 1996; Hoseini et al., 2016; Xie et al., 2017), and of carrier proteins in the mitochondrial inner membrane (Bhangoo et al., 2007; Young et al., 2003). Furthermore, the OM protein Mim1, was shown to interact specifically with the Hsp40 protein Djp1 (Papić et al., 2013). In many cases, however, the data was only obtained in *in vitro* experiments and the physiological relevance of the chaperone-precursor interaction is unclear. Additionally, the role of the individual chaperones in the biogenesis of the mitochondrial proteins is often not well defined. Similarly unclear is whether the chaperones are solely preventing the aggregation of the newly synthesized proteins or whether they are also involved in the mitochondrial targeting of their substrates. Finally, it is still unknown whether the involvement of molecular chaperones in the biogenesis of mitochondrial precursor proteins is specific to only some mitochondrial proteins or whether this is a general principle. For example, so far, β-barrel proteins were not reported to interact with any cytosolic chaperone or co-chaperone.

To address these open questions and to better understand the early events in the biogenesis of mitochondrial β-barrel proteins, we characterized their interactions with cytosolic factors and analyzed the importance of these interactions for the biogenesis pathway of these proteins. We found that, in yeast, several chaperones of the Hsp90, Hsp70 and Hsp40 families interact with β-barrel proteins and that these β-barrel protein/chaperone interactions are required for an efficient mitochondrial import *in vitro* and *in vivo*. Furthermore, our experiments indicated that the involvement of Hsp70 chaperones in the biogenesis of mitochondrial β-barrel proteins is also conserved in mammals. Collectively, the current study sheds new light on the early events in the biogenesis of mitochondrial β-barrel proteins.

Results

Cytosolic chaperones interact *in vitro* with newly synthesized β-barrel proteins

To remain import-competent, newly synthesized mitochondrial β-barrel proteins should avoid aggregation in the cytosol, a task that might require the function of chaperones. To study the role of cytosolic chaperones in the biogenesis of mitochondrial β-barrel proteins, we first wanted to identify the chaperones that interact with such proteins. To that goal, we performed pull-down experiments with an HA-tagged version of the β-barrel protein Porin translated *in vitro* in yeast extract. We reasoned that, since the yeast extract does not contain mitochondria, the newly synthesized proteins cannot be integrated into a membrane, implying that they should be kept in solution by proteins present in the extract. After pulling-down Porin-HA with anti-HA beads, we identified co-purified proteins by mass spectrometry. Among the co-eluted proteins, we identified molecular chaperones of the Hsp90 and Hsp70 families as well as Hsp40 family co-chaperones (Table 1).

To verify these results and to test whether the chaperones also interact with other β-barrel proteins, we translated HA-tagged variants of either the β-barrel proteins Porin (P), Tom40 (40), or Tob55 (55) as well as the control protein, DHFR (D) in yeast extracts and analyzed the co-purified proteins by immunodecoration with antibodies against several chaperones and co-chaperones (Fig. 1A). To assure that potential interactions are not mediated by the N-terminal POTRA domain of Tob55, we used a truncated version of Tob55 that is composed only of its β-barrel domain (Pfitzner et al., 2016). We found that all three β-barrel proteins co-eluted with the Hsp70 chaperones Ssa1/Ssa2 and the Hsp90 chaperones Hsc82/Hsp82. Of note, the paralogues proteins Ssa1/Ssa2 and Hsc82/Hsp82 are very similar to each other and our antibodies cannot discriminate between the two isoforms. Additionally, the eluates contained the Hsp40 co-chaperones Ydj1, Sis1, and Djp1, two co-chaperones interacting with Hsp90 proteins, namely Sti1 and Aha1, and two chaperones that function as disaggregases, Hsp104 and Hsp42. The co-chaperones Sba1 and Hch1, as well as the cytosolic protein Bmh1 were not co-eluted with any of the translated proteins. Control reactions without any translated protein or with newly synthesized DHFR lead to a negligible co-purification, if at all, of the above-mentioned chaperones (Fig. 1A). These findings indicate specific interactions of newly synthesized β-barrel proteins with a subset of cytosolic chaperones.

The interactions of chaperone with β-barrel proteins are dynamic

Having established an assay to monitor specific association of cytosolic factors with β-barrel proteins, we next wanted to test whether the observed interactions can dynamically adapt to

changing conditions. Since Hsp70 and Hsp90 chaperones are ATPases, we were interested to see how their interactions respond to changes in the energy level of the yeast extract. To this end, we translated Porin in yeast extract that was left untreated, was depleted of ATP by the addition of apyrase, or was supplemented with excess ATP. Then we performed a pull-down of the newly translated β-barrel protein and analyzed its interaction partners (Fig. 1B). We observed that the levels of co-eluted Ssa1 were reduced in the sample from the ATP-depleted extract but increased when the extract was supplemented with additional ATP. Conversely, the levels of Hsp82 were not changed by the ATP depletion and were reduced when the amount of ATP was increased. Interestingly, we found that increasing the amount of ATP had a strong impact on the levels of the co-eluted Hsp40 co-chaperones. Adding an excess of ATP to the extracts, reduced the amount of co-purified Ydj1 and Djp1 but lead to a substantial increase of co-eluted Sis1 (Fig. 1B). These findings indicate that the association of (co-)chaperones with β-barrel proteins is dynamic and can be modulated.

Next, we analyzed whether the observed interactions are invariable over extended periods. When we increased the *in vitro* translation reactions from 30 to 120 min, we observed that the levels of most chaperones were reduced over time. Interestingly, the levels of the disaggregase proteins Hsp104 and Hsp42 were slightly increased in the samples from longer incubation times (Fig. 1C). These findings suggest that the Hsp70 and Hsp90 chaperone systems are early interaction partners that can keep the newly synthesized β-barrel proteins in solution for only a limited time. Longer incubation times, therefore, lead to an increased aggregation of the substrate protein and consequently also to an increased association with disaggregase factors.

Finally, we tested if the chaperones depend on each other for binding to newly synthesized β-barrel proteins. To this end, we translated Porin in yeast extracts prepared from cells that were lacking the co-chaperones Sti1, Ydj1, or Sis1 (Fig. S1). The absence of Sti1 lead to a strongly decreased association of Hsp82. This is in line with the reported function of Sti1 as mediator of the transfer of substrate proteins from Hsp70 to Hsp90 chaperones (Scheufler et al., 2000; Wegele et al., 2003). Additionally, the amount of co-purified Ydj1 is increased while the level of Djp1 is reduced in the eluates obtained from the *sti1Δ* extract (Fig. S1A). When an extract from *ydj1Δ* cells was used, the levels of co-eluted Sis1 and Djp1 were reduced, while the disaggregase proteins Hsp104, Hsp42 and Hsp26 were present in the eluate in higher amounts (Fig. S1B). These observations substantiate the importance of Ydj1 in preventing aggregation of newly synthesized β-barrel proteins.

To prepare a yeast extract without Sis1, we constructed a yeast strain that contains the *SIS1* gene under the control of a tetracycline-repressible promoter. Cells were depleted of Sis1 by adding the tetracycline analogue doxycycline (Dox) to the growth medium and the obtained yeast extract was compared to one from the same cells grown without Dox. As expected, Sis1 could not be detected in the Dox-treated cells (Fig. S1C). Using these extracts, we observed a slightly increased association of Ssa1, Hsp82, Sti1 and Hsp104 with the newly synthesized Porin, whereas the levels of co-purified Ydj1 and Djp1 were reduced (Fig. S1C). Collectively, these results show that the chaperone system that prevents the aggregation of newly synthesized β-barrel proteins can dynamically adapt to the energy status and the chaperone composition of the cell. It seems that the association with chaperones is not critically dependent on any single co-chaperone as the lack of Sti1, Ydj1 or Sis1 can be compensated by the remaining chaperones and co-chaperones.

A β-hairpin motif is sufficient for the interaction with chaperones

Since we could demonstrate that full-length β-barrel proteins can interact with several chaperones and co-chaperones, we asked if a β-hairpin motif, as the smallest building block of all β-barrel proteins, is sufficient for this interaction. To address this question, we used a linear and cyclic β-hairpin peptide derived from the human β-barrel protein VDAC1. In a previous study, we showed that the cyclic β-hairpin peptide is recognized by the cell as a mitochondrial targeting signal of β-barrel proteins and interacts with various components of the TOM complex (Jores et al., 2016). The peptides used in this study harbor the photo-reactive amino acid *p*-benzoyl-L-phenylalanine (Bpa) and can form covalent bonds to nearby proteins upon irradiation with ultraviolet (UV) light. When we mixed the Bpa-containing peptides with a yeast extract and illuminated the sample with UV light, we observed a dose-dependent formation of photo-adducts (PA) of the cyclic, but not the linear, β-hairpin peptide with Ssa1, Ydj1, Djp1 and Hsp104 (Fig. 1D). For some chaperones we observed the formation of several PAs that are migrating at an apparent molecular mass higher than expected for an adduct of the chaperones with a single peptide molecule. Such multiple bands were observed in previous crosslinking experiments (Jores et al., 2016; Plath et al., 1998; Wu et al., 2017), and might result from multiple peptides binding to the same chaperone molecule and/or from different SDS-PAGE mobility of the various PAs. The observed adducts are specific, as the co-chaperone Hch1, which was not pulled-down by β-barrel proteins, did not form any photo-adduct with the β-hairpin peptide. We conclude that the β-hairpin motif is sufficient for a direct interaction with cytosolic chaperones and co-chaperones.

To further characterize the interaction between the β-hairpin peptide and the Hsp70 chaperone Ssa1, we analyzed their binding kinetics and affinity by fluorescence anisotropy. The fluorescence anisotropy of a rhodamine-labeled variant of the cyclic β-hairpin peptide increased upon addition of recombinant Ssa1 indicating the formation of a peptide-Ssa1 complex (Fig. 2A, black circles). This interaction is specific as the addition of the control protein BSA did not lead to such an increase (Fig. 2A, gray circles). When the Ssa1/rhodamine-labeled peptide complex was subjected to an excess of unlabeled cyclic β-hairpin peptide, the labeled peptide dissociated from Ssa1 demonstrating that the chaperone can also interact with the unlabeled peptide (Fig. 2B). Next, we used titration experiments with increasing concentrations of Ssa1 to determine the affinity between the chaperone and the cyclic β-hairpin peptide (Fig. 2C). A dissociation constant (K_d) of 3.5 µM was derived from a hyperbolic regression curve fitted to the data. This affinity is in line with previous studies that reported affinities in the low micromolar range for the interaction of Hsp70 chaperones with substrate peptides (Endo et al., 1996; Pierpaoli et al., 1997; Ricci and Williams, 2008; Schmid et al., 1994; Schneider et al., 2016).

Next, we performed similar experiments with a recombinant co-chaperone Ydj1, and observed an association of Ydj1 with both the rhodamine-labeled (Fig. 2D) and the unlabeled cyclic β-hairpin peptide (Fig. 2E). Titration experiment revealed the K_d of the Ydj1/peptide interaction to be 46.8 µM (Fig. 2F). Similar two-digit micromolar affinities have been previously determined for interactions of Hsp40 co-chaperones with their substrate peptides (Li and Sha, 2004; Pierpaoli et al., 1997). Taken together, a cyclic β-hairpin peptide can be bound directly, with micromolar affinities, by both the Hsp70 chaperone Ssa1 and its Hsp40 co-chaperone Ydj1.

Hsp70 chaperones are required for the biogenesis of β-barrel proteins

Having established that chaperones can bind to newly synthesized β-barrel proteins, we wanted to test if these interactions are required for an efficient mitochondrial import of these proteins. To this end, we performed *in vitro* import experiments with β-barrel proteins and the requirement for chaperones was assessed by testing if the C-terminal domain of human Hsp90 (C90) can inhibit the β-barrel protein import. Previous studies showed that C90 inhibits the import of mitochondrial inner membrane carrier proteins by obliging the chaperone binding site on the mitochondrial import receptor Tom70 (Bhangoo et al., 2007; Young et al., 2003).

Importantly, the *in vitro* import of radiolabeled Porin, as measured by its resistance to alkaline extraction, was reduced by approximately 50% in the presence of C90 (Fig. 3A).

Comparable results were obtained when we used Tom40 from *Neurospora crassa* (NcTom40) as an imported protein (Fig. 3B). The proper membrane integration of NcTom40 was monitored by the formation of a proteinase K-protected fragment of 26 kDa (F26) (Rapaport and Neupert, 1999). In a third import assay, we tested the effect of C90 on the assembly of *Saccharomyces cerevisiae* Tom40 (ScTom40) into the TOM complex, as monitored by BN-PAGE. On its assembly pathway into the mature TOM complex, Tom40 forms two stable intermediates that are detected by BN-PAGE, a first assembly intermediate (Int I) with the TOB complex, and a second intermediate (Int II) composed of Tom40, Tom22, and the small TOM subunits (Model et al., 2001; Rapaport and Neupert, 1999; Wiedemann et al., 2003). We observed that the addition of C90 to the import reaction caused a clear reduction in the formation of the two assembly intermediates and of the mature TOM complex (Fig. 3C). The impaired formation of Int I indicates that the import of Tom40 is inhibited in an early step before its association with the TOB complex.

To exclude the possibility that the observed import inhibition is caused by a general import deficiency of the C90-treated mitochondria, we performed import experiments using the matrix-destined precursor protein pSu9-DHFR. Supporting a specific effect on β-barrel proteins, the presence of C90 in the import reaction did not affect the import of pSu9-DHFR (Fig. S2A). Collectively, these results demonstrate that binding of chaperones to Tom70 is required for an efficient import of mitochondrial β-barrel proteins.

As C90 blocks the binding of both Hsp70 and Hsp90 family chaperones to Tom70, the aforementioned experiments cannot distinguish whether the requirement is for the former or the latter group of chaperones. To directly analyze the putative involvement of Hsp70 chaperones, we performed *in vitro* import experiments in the presence of the Hsp70 inhibitor cBag that is composed of the C-terminal Bag domain of human Bag-1M (Bhangoo et al., 2007; Young et al., 2003). The mitochondrial import of Porin and NcTom40 as well as the assembly of ScTom40 were reduced by 30–70% when these proteins were synthesized in cBag-treated yeast extract (Fig. 3D-F). As a control, the import of the matrix-destined protein pSu9-DHFR was not affected under these conditions (Fig. S2B). Taken together, these experiments show that Hsp70 chaperones are required for proper import of mitochondrial β-barrel proteins.

Cytosolic chaperones interact *in vivo* with a β-hairpin peptide

We next asked whether the interactions that we observed in the yeast extract can be detected also *in vivo*. To this end, we used a hybrid protein composed of the β-hairpin peptide mentioned before fused to the passenger domain DHFR-HA. We demonstrated previously that this fusion

protein is targeted to mitochondria (Jores et al., 2016). As we expected only transient binding of the β-hairpin peptide and chaperones, we employed a photo-crosslinking approach to take a snapshot of the interactions of the β-hairpin peptide. For this aim, we used an amber suppression system to insert *in vivo* the unnatural amino acid Bpa into the β-hairpin moiety (Chen et al., 2007).

When cells expressing the Bpa-containing version of the β-hairpin fusion protein were irradiated with UV light, we observed the formation of several PAs (Fig. 4, upper panel). The specificity of the formation of these PAs is demonstrated by the observations that no PAs were obtained when the cells were either not exposed to UV light or upon usage of proteins lacking the Bpa residue (Fig. 4, -UV and/or -BPA). To analyze if the β-hairpin is crosslinked to chaperones, we first performed a pull-down with anti-HA beads to enrich the fusion protein and its PAs. Then, we probed the samples with antibodies against some of the chaperones that we found to bind *in vitro* to β-barrel proteins. In this way, we detected specific PAs for Ssa1, Hsp82, Ydj1 and Sis1 (Fig. 4, lower panels). In all cases, no PAs were observed in the absence of UV irradiation or using constructs without Bpa residue. These results demonstrate that cytosolic (co)chaperones directly interact *in vivo* with β-barrel proteins.

Hsp40 co-chaperones are required for the biogenesis of β-barrel proteins

Since we observed that the Hsp40 co-chaperones Ydj1 and Sis1 can bind to β-barrel proteins both *in vitro* and *in vivo*, we wanted to gain insight whether this interaction is of functional relevance in the context of the β-barrel protein biogenesis. Ydj1 was previously implicated with the import of the mitochondrial presequence-containing inner membrane protein $F_1\beta$ and the same study also showed that overexpression of Sis1 can partially complement the growth phenotype of yeast cells harboring a temperature-sensitive allele of *YDJ1* (Caplan et al., 1992). However, so far, Sis1 was not reported to be involved in the import of mitochondrial proteins. Sis1 is an essential protein and yeast cells with a deletion of *YDJ1* have a severe growth defect and tend to accumulate suppressors. Therefore, we created strains that express *SIS1*, *YDJ1*, or both genes under the control of a tetracycline-repressible promoter. To further speed up the depletion of the corresponding proteins, they were fused at their N-termini with Ubiquitin followed by a leucine residue. After translation, the Ubiquitin part is cleaved off leaving Ydj1 or Sis1 with an N-terminal leucine residue that reduces the half-life of the proteins (Gnanasundram and Koš, 2015).

We employed a protocol where cells harboring endogenous Porin-HA were grown for four hours in the presence or absence of Dox, followed by one hour incubation in medium

without methionine. Then, the medium was supplemented with ^{35}S-methionine and the cells were harvested immediately or 5, 15, or 30 min afterwards. The cells were lysed, a crude mitochondrial fraction was obtained, solubilized, and subjected to a pull-down of the HA-tagged Porin. Of note, two populations of Porin-HA molecules can be detected in such experiments: freshly synthesized radiolabeled ones by autoradiography and preexisting ones together with the newly synthesized molecules by immunodecoration with anti-HA antibodies. Initially, as a control, we performed these experiments with wild type (WT) cells that does not contain tetracycline-repressible promoters. As expected, the levels of radiolabeled Porin-HA from Dox-treated or untreated cells were indistinguishable (Fig. 5A), verifying that the addition of Dox does not affect the biogenesis of Porin-HA.

Next, we tested if a depletion of Ydj1 hampers the biogenesis of Porin-HA and observed only a marginal reduction in the level of the radiolabeled β-barrel protein (Fig. 5B). Comparable results were obtained when Sis1 was depleted (Fig. 5C). Since it was reported that Sis1 can partially complement for the absence of Ydj1, we also analyzed the effect of a double depletion of both proteins on the biogenesis of Porin-HA. Interestingly, the levels of radiolabeled Porin-HA in the mitochondrial fraction was reduced by approximately 50% when cells were ablated for both, Ydj1 and Sis1 (Fig. 5D). In addition, we could also observe a reduction in the overall amounts of Porin-HA as detected by the immunodecoration with the anti-HA antibody (Fig. 5D). Collectively, these results show that Ydj1 and Sis1 are involved in the biogenesis of mitochondrial β-barrel proteins. As they have somewhat redundant functions in this process, they can complement the absence of each other.

Mammalian Hsp70 is involved in the biogenesis of β-barrel proteins

To test whether the involvement of cytosolic Hsp70s in the biogenesis of β-barrel proteins is also conserved in higher eukaryotes, we performed pull-down experiments with β-barrel proteins translated in rabbit reticulocyte lysate. We found that the mammalian Hsp70 chaperone, Hsc70 co-elutes with yeast Porin (P) and its human homologue VDAC1 (V). Only negligible levels were obtained when no protein was synthesized or when the control protein DHFR (D) was used as a substrate protein (Fig. 6A). As a negative control, the cytosolic protein GAPDH did not co-elute with any of the tested proteins.

Next, we analyzed whether mammalian Hsc70 is required for the biogenesis of Porin. To this end, we performed mitochondrial import experiments using isolated mitochondria and Porin-containing rabbit reticulocyte lysate that was treated with the Hsp70 inhibitor cBag. A severe reduction of approx. 60% in the import of Porin after cBag-treatment was observed (Fig.

6B). Taken together, these results indicate that also in mammals, Hsp70 chaperones are required for the biogenesis of mitochondrial β-barrel proteins.

Discussion

Currently, little is known about the mechanisms that assure the safe passage of mitochondrial precursor proteins through the cytosol. To keep these newly synthesized proteins in an import-competent conformation, a tight folding as well as an aggregation of the precursors must be prevented. In this study, we identified several molecular chaperones in the cytosol of yeast and mammalian cells that can bind to newly synthesized β-barrel proteins. We further demonstrate that this binding has a physiological significance as inhibiting the cytosolic Hsp70 chaperones of the Ssa subfamily or down-regulating the Hsp40 co-chaperones Ydj1 and Sis1 hampered the biogenesis of β-barrel proteins. Although pull-down experiments followed by mass spectrometry analysis identified yeast Hsp90 as an interaction partner of β-barrel proteins, subsequent assays with inhibitors of this chaperone failed to detect any effect on the biogenesis of these substrate proteins. Hence, it seems that the binding to Hsp90 is not absolutely required under the tested conditions. This situation is rather similar to the binding preferences in yeast cells of carrier proteins of the mitochondrial inner membrane. These latter proteins required for their proper import in yeast cells cytosolic Hsp70 but not Hsp90 (Young et al., 2003). As Hsp70 and Hsp90 chaperones require ATP for their proper function, their involvement in the biogenesis of β-barrel proteins shed light on previous unexplained observations namely, that the biogenesis of these proteins requires ATP (Asai et al., 2004; Hwang and Schatz, 1989; Pfanner et al., 1988; Rapaport and Neupert, 1999).

Members of the Hsp70 and Hsp90 families serve as multi-purpose chaperones and were implicated with the mitochondrial import of inner membrane proteins (Deshaies et al., 1988; Young et al., 2003). Hsp70 and Hsp90 chaperones have a very broad substrate range and specificity is often generated by interaction with co-chaperones (Kampinga and Craig, 2010; Röhl et al., 2013; Walsh et al., 2004). In line with this, we found that newly synthesized β-barrel proteins are bound by several co-chaperones that can also interact with Hsp70 and/or Hsp90 chaperones. Notable, the lower affinity of the association of the β-hairpin motif with the co-chaperone Ydj1 as compared with the affinity to Hsp70 is in line with the assumption that the substrate might be recognized first by the co-chaperone and then transferred to the better binder, the Hsp70 chaperone.

When we analyzed the role that these co-chaperones play *in vivo* in the biogenesis of mitochondrial β-barrel proteins, we found that they have overlapping functions, as none of them is absolutely required for the binding of β-barrel proteins to other chaperones and co-chaperones. This multifaceted involvement of co-chaperones matches emerging concepts about the function of these proteins as fine tuner of the ability of Hsp70s to participate in diverse cellular processes (Craig and Marszalek, 2017; Cyr and Ramos, 2015). Furthermore, we could demonstrate that cells depleted of Ydj1 or Sis1 alone imported β-barrel proteins with only slightly reduced efficiency as compared to non-depleted cells. However, when the cells were depleted of both proteins simultaneously, the biogenesis of mitochondrial β-barrel proteins was reduced by about 50%. While Ydj1 and its mammalian orthologue DNAJA1 were reported to be involved in the import of mitochondrial inner membrane proteins (Bhangoo et al., 2007; Caplan et al., 1992), an involvement of Sis1 in the mitochondrial protein import was not described so far. Our observation that a certain level of import is still maintained in the double deletion strain might suggest that additional, yet unknown, co-chaperones can replace the absence of Ydj1 and Sis1. Alternatively, the remaining import levels might reflect the basal chaperoning function of Hsp70 without contribution of co-chaperones. Our findings regarding the binding of β-barrel proteins to multiple (co-)chaperones are in line with a systematic study that found that a given yeast protein can interact with up to 25 different chaperones during its lifetime in the cell (Gong et al., 2009).

Of note, we found that a β-hairpin, which can serve as a targeting signal for mitochondrial β-barrel proteins is sufficient for the binding to cytosolic chaperones. This raises the possibility that the initial binding of newly synthesized β-barrel proteins to chaperones can occur already co-translationally, namely while the rest of the molecule is still being synthesized. In this way, premature aggregation of the hydrophobic segments of the protein will be prevented already upon their exit from the ribosome.

In this study, we could show that, apart from keeping the β-barrel proteins in an import-competent conformation, the Hsp70 chaperones are also directly involved in the mitochondrial import of their substrates, probably by targeting them to the receptor Tom70. Interestingly, so far, Tom20 was assumed to be the major import receptor for mitochondrial β-barrel proteins (Jores et al., 2016; Krimmer et al., 2001; Rapaport and Neupert, 1999; Schleiff et al., 1999; Söllner et al., 1989; Yamano et al., 2008). The results obtained in this study, however, demonstrate, that Tom70 is also involved in the biogenesis of β-barrel proteins. This involvement can be via direct recognition of the β-barrel precursor protein and/or serving as an anchor for the cytosolic chaperones. Our findings are also in line with previous reports

suggesting that Tom70 is playing a role in the import of β-barrel precursor proteins (Habib et al., 2005; Jores et al., 2016; Keil et al., 1993).

Our current findings together with previous knowledge allow us to suggest a detailed working model for the early stages of the biogenesis of mitochondrial β-barrel proteins (Fig. 7). Upon their synthesis on cytosolic chaperones, or shortly afterwards, these proteins associate with various co-chaperones that mediate their association with Hsp70s. This interaction keeps the newly synthesized proteins in an import-competent conformation. The chaperone/substrate complex then docks on the import receptor Tom70 while appropriate β-hairpin elements, which serve as targeting signal, can be recognized by the import receptor Tom20. Both alternatives of initial binding to either Tom20 or Tom70 can be envisaged. The combined action of both receptors increases the fidelity of the recognition, provides a double-check mechanism, and supports productive continuation of the import process by transfer of the substrate to the import pore of the TOM complex. The results obtained with the mammalian lysate and the human substrate VDAC1 suggest that these principles are conserved also in higher eukaryotes. Collectively, our findings outline a novel mechanism in the early events of the biogenesis of mitochondrial β-barrel proteins.

Materials and Methods

Yeast strains and growth methods

Standard genetic techniques were used for growth and manipulation of yeast strains. All strains used in this study are listed in Table S1. For strains with genes under the control of a tetracycline-repressible promoter, the strain YMK120 was used (Gnanasundram and Koš, 2015). The tetracycline operator was inserted into the genome by homologous recombination using an insertion cassette amplified from the plasmids pMK632 (Gnanasundram and Koš, 2015), pMK632Kan or pMK632His. Strains with two genes under the control of the tetracycline operator were obtained by mating of strains with a single tet-regulated gene followed by tetrad dissection. Strains with genomically HA-tagged Porin were created by homologous recombination using an insertion cassette amplified from the plasmid pFA6a-3HA-NatNT2.

Recombinant DNA techniques

The plasmid pGEM4 (Promega) was amplified by PCR using primers TJ207 and TJ208 to create pGEM4polyA with a poly-A stretch after the multiple cloning site.

The plasmid pRS316-Atg32-3HAn was used as template for the PCR-amplification of a triple HA-tag. The amplification product was inserted into either pGEM4polyA or pRS426-TPI using BamHI and SalI restriction sites. The DHFR, *POR1*, *TOM40*, *TOB55*, NcTOM40 and VDAC1 genes were amplified by PCR from pGEM4 plasmids harboring these genes and were then inserted into pGEM4polyA or pGEM4polyA-3HA using suitable restriction sites. The plasmids pGEM4-pSu9-DHFR and pGEM4-VDAC1 were used as templates for the amplification of the pSu9 and hp18(VDAC) gene fragments. The amplification products were cloned into pGEM4polyA-DHFR-3HA using EcoRI and KpnI restriction sites.

The Thr258Bpa mutation within hp18(VDAC) was introduced via site-directed mutagenesis using the QuikChange Site-Directed Mutagenesis Kit (Stratagene) according to the manufacturer's instructions. The hp18(VDAC)-DHFR-3HA constructs were sub-cloned into pRS426-TPI using EcoRI and SalI restriction sites. The C-terminal triple HA-tag and CYC1 terminator from pRS426-TPI-3HA were amplified by PCR and inserted into the plasmid pFA6A-NatNT2 using HindIII and BamHI restriction sites. For the exchange of the NatMX cassette in pMK632, the plasmid was PCR-amplified using primers TJ203 and TJ204. The HIS3MX and KanMX cassettes were amplified by PCR using the plasmids pFA6a-HIS3MX6 and pFA6a-KanMX4 as templates and TJ201 and TJ202 as primers. The PCR products were combined using a previously described method (Jacobus and Gross, 2015). All primers and plasmids used in this study are listed in Tables S2 and S3, respectively.

Immunoblotting

A list of primary antibodies used in this study is included in Table S4. The secondary antibodies were Horseradish peroxidase-coupled goat-anti-rabbit (Bio-Rad, cat. # 1721019) or goat-anti-rat (abcam, cat. # ab6845) that were diluted 1:10 000 or 1:2000, respectively.

Protein purification

Recombinant cBag and C90 were expressed in BL21 cells from the plasmid pPROEX HTa cBag or pPROEX HTa C90 (kind gift of Dr. F.U. Hartl) (Young et al., 2003). Expression was induced with 1 mM IPTG for 4 h at 37 °C. The cells were harvested, resuspended in French Press buffer (40 mM HEPES, 100 mM KCl, 20 mM imidazole, 2 mM PMSF, 1 x EDTA-free cOmplete protease inhibitor [Roche], pH 7.5) and lysed with an EmulsiFlex-C5 French Press. The cell lysate was subjected to a clarifying spin (15000 x g, 15 min, 4 °C) and the recombinant proteins were purified using a 1 mL HisTrap HP column (GE Healthcare) on an ÄKTA Start chromatography system (GE Healthcare). The bound proteins were washed with 20 mL wash

buffer (40 mM HEPES, 100 mM KCl, 50 mM imidazole, pH 7.5) and eluted with elution buffer (40 mM HEPES, 100 mM KCl, 300 mM imidazole, pH 7.5).

Ssa1 was expressed and purified as described earlier (Schmid et al., 2012). For recombinant Ydj1, BL21-Codon Plus (DE3)-RIL cells were used containing a pET28 vector carrying the full length Ydj1 gene and an N-terminal His_6-SUMO-tag. Expression was induced with 1 mM IPTG for 4 h at 30 °C. Cells were harvested and resuspended in Ni-NTA buffer A (40 mM NaH_2PO_4, 500 mM NaCl, 20 mM imidazole, 2 mM β-mercaptoethanol, pH 8.0) supplemented with EDTA-free protease inhibitor [SERVA] and DNase1. Cells were lysed using a Cell Disruption System (Constant Systems) at 1.8 kbar. After lysate clarification (20000 x g, 1 h, 4 °C), the supernatant was loaded on a 5 mL HisTrap HP column (GE Healthcare), washed with 10 column volumes (CV) Ni-NTA buffer A and 10 CV 5 % Ni-NTA buffer B (40 mM NaH_2PO_4, 500 mM NaCl, 500 mM imidazole, 2 mM β-mercaptoethanol, pH 8.0). The bound proteins were eluted with 100% Ni-NTA buffer B (40 mM NaH_2PO_4, 500 mM NaCl, 500 mM imidazole, 2 mM β-mercaptoethanol, pH 8.0). Fractions were diluted 1:10 with Ni-NTA buffer A/H_2O (1:1), supplemented with His_6-tagged SUMO-protease and incubated overnight at 4 °C. The protein solution was then loaded on a 5 mL HisTrap HP column. The flow-through was concentrated and loaded on a Superdex 16/60 200 pg SEC column (GE Healthcare). Proteins were eluted with SEC buffer (40 mM HEPES, 150 mM KCl, 5 mM $MgCl_2$, 1 mM DTT). Purity was checked by SDS-PAGE and the identity of the protein was confirmed by mass specrometry.

In vitro translation and import of radiolabeled proteins

Yeast extracts for *in vitro* translation were prepared as described (Wu and Sachs, 2014). Proteins were synthesized in yeast extract or rabbit reticulocyte lysate (Promega) after *in vitro* transcription by SP6 polymerase from pGEM4 vectors. Radiolabeled proteins were synthesized in the presence of ^{35}S-methionine (Hartmann Analytik). If not indicated otherwise, the translation times were 30 min for the yeast extract and 60 min for the rabbit reticulocyte lysate. After translation, the reactions were centrifuged (100000xg, 45 min, 2 °C) to remove ribosomes. The supernatant was diluted with import buffer (250 mM sucrose, 0.25 mg/ml BSA, 80 mM KCl, 5 mM $MgCl_2$, 10 mM MOPS, 2 mM NADH, 2 mM ATP, pH 7.2) and incubated for 10 min at 25 °C. Where indicated, the supernatant was supplemented with 20 µM cBag or, as a control, with an equivalent amount of BSA. To remove aggregated proteins, the supernatant was centrifuged (16000xg, 10 min). Isolated mitochondria were diluted in import buffer and, where indicated, supplemented with 20 µM of either C90 or, as a control, BSA. The import

reactions composed of the precursor proteins mixed with isolated mitochondria were performed by incubation at 25 °C for the indicated times. The import reactions were stopped by diluting the samples with SEM-K^{80} buffer (250 mM sucrose, 80 mM KCl, 10 mM MOPS, 1 mM EDTA, pH 7.2) and mitochondria were reisolated (13200xg, 2 min, 2 °C).

The import of Porin and Porin-3HA was analyzed by carbonate extraction. The mitochondria were resuspended in 0.1 M Na_2CO_3, incubated on ice for 30 min and reisolated by centrifugation (100000xg, 30 min, 2 °C). The pellets were resuspended in 2 x Lämmli buffer, incubated for 10 min at 95 °C and subjected to SDS-PAGE. The import of pSu9-DHFR-3HA and NcTom40 was analyzed by proteinase K (PK) treatment (50 µg/mL PK for 30 min on ice) and resistance of the mature form (pSu9-DHFR-3HA) or the formation of typical proteolytic fragments (NcTom40). After inhibition of PK with 5 mM PMSF, the samples were boiled at 95 °C for 10 min before their analysis by SDS-PAGE.

The assembly of Tom40 was analyzed by BN-PAGE. The mitochondria were solubilized with digitonin buffer (1% digitonin, 20 mM Tris, 0.1 mM EDTA, 50 mM NaCl, 10% glycerol, pH 7.4) for 30 min at 4 °C on an overhead shaker (12 rpm). After a clarifying spin (30000xg, 15 min, 2°C), 10x sample buffer (5% [wt/vol] Coomassie brilliant blue G-250, 100 mM Bis-Tris, 500 mM 6-aminocaproic acid, pH 7.0) was added and the mixture was analyzed by electrophoresis in a blue native gel containing an 8-13% gradient of acrylamide (Schägger et al., 1994). In all cases, gel separation was followed by Western blotting and autoradiography. For dissipation of membrane potential, isolated mitochondria were mixed with 20 µM CCCP and incubated for 5 min at 4 °C prior to the import reaction.

Pull-down of *in vitro* translated proteins

Reactions containing proteins translated in either yeast extract or rabbit reticulocyte lysate were loaded onto magnetic anti-HA beads (ThermoFisher) that were previously equilibrated with KHM buffer (110 mM potassium acetate, 20 mM HEPES, 2 mM $MgCl_2$, pH 7.4). Binding to the beads was performed for 2 h at 4 °C on an overhead shaker (12 rpm). The beads were then washed 4 times with KHM buffer. In the third washing step, the beads were transferred to a new reaction tube. Bound proteins were eluted by addition of 2x Lämmli buffer containing 0.05% H_2O_2 and 5 min incubation at 95 °C. The beads were collected and the supernatant was transferred to a new tube, supplemented with 5% β-mercaptoethanol and incubated for another 5 min at 95 °C before analysis by SDS-PAGE followed by Western blotting or mass spectrometry.

Mass spectrometry

Eluted proteins were purified on an SDS-PAGE and Coomassie-stained gel pieces were digested in gel with trypsin as described previously (Borchert et al., 2010). After desalting using C18 Stage tips, extracted peptides were separated on an EasyLC nano-HPLC (Thermo Scientific) coupled to an LTQ Orbitrap Elite (Thermo Scientific) as described elsewhere (Franz-Wachtel et al., 2012) with slight modifications: The peptide mixtures were separated using a 127 minute segmented gradient from to 5–33-50-90% of HPLC solvent B (80% acetonitrile in 0.1% formic acid) in HPLC solvent A (0.1% formic acid) at a flow rate of 200 nl/min. The 15 most intense precursor ions were sequentially fragmented in each scan cycle using collision-induced dissociation (CID). The target values for MS/MS fragmentation were 5000 charges and 106 charges for the MS scan. Acquired MS spectra were processed with MaxQuant software with integrated Andromeda search engine (Cox et al., 2011). Database search was performed against a target-decoy *Saccharomyces cerevisiae* database obtained from Uniprot, the sequences of the constructs DHFR-3HA and Porin-3HA, and 285 commonly observed contaminants. Initial maximum allowed mass tolerance was set to 4.5 ppm (for the survey scan) and 0.5 Da for CID fragment ions. A false discovery rate of 1% was applied at the peptide and protein level.

Metabolic labelling

Yeast cells grown in 25 mL SD medium at 30 °C to early logarithmic phase ($OD_{600} \approx 0.3$) were supplemented with 2 µg/mL doxycycline and grown for another 4 h. The cells were harvested, washed with water and resuspended in SD medium lacking methionine (SD-Met). After 1 h shaking at 30 °C, the cells were harvested and resuspended in 2.5 mL SD-Met. Following 10 min at 30 °C, the cultures were supplemented with 10 µmol ^{35}S-methionine and incubated further at 30 °C with shaking. Samples (540 µL) were collected after various time periods and mixed with sodium azide and methionine (final concentration 10 mM and 0.003%, respectively). The samples were centrifuged (5000xg, 1 min, 2 °C) and the cell pellets were washed with a 10 mM sodium azide solution.

For isolation of crude mitochondria, the cells were resuspended in 350 µL lysis buffer (10 mM Tris, 1 mM EDTA, 2 mM PMSF, pH 8.0) mixed with 300 mg glass beads (0.25-0.5 mm Ø) and lysed by 5 cycles of vortexing for 1 min, with 1 min break on ice in between. The glass beads and cellular debris were removed by centrifugation (1000xg, 3 min, 2 °C) and crude mitochondria were isolated from the supernatant by centrifugation (8000xg, 10 min, 2 °C). The mitochondrial pellet was solubilized in 300 µL solubilization buffer (50 mM Tris, 5 mM EDTA,

150 mM NaCl, 0.5% Triton X-100, pH 8.0) for 30 min at 4 °C on an overhead shaker (12 rpm). After a clarifying spin (30000xg, 15 min, 2 °C), the supernatant was loaded onto magnetic anti-HA beads (ThermoFisher) and further treatment was as described above for the pull-down of in vitro synthesized proteins.

UV induced crosslinking

Synthesis of the Bpa-containing linear and cyclic β-hairpin peptides was described before (Jores et al., 2016). *In vitro* photo-crosslinking was performed by mixing yeast extract with Bpa-containing β-hairpin peptides in import buffer without BSA. The mixture was incubated for 10 min on ice before ultraviolet (UV)-irradiation for 30 min at 4 °C using a Blak-Ray B-100 AP UV lamp at a distance of 10 cm from the samples. After the UV-illumination, the samples were mixed with 4x Lämmli buffer, incubated at 95 °C for 5 min and subjected to analysis by SDS-PAGE followed by Western blotting.

In vivo photo-crosslinking was performed according to a previously published protocol (Shiota et al., 2013). Yeast cells were transformed with a plasmid coding for hp18(VDAC)-DHFR-3HA with or without the Thr258Bpa mutation and with the plasmid pBpa2-PGK1+3SUP4-tRNA$_{CUA}$ that harbors a suppressor tRNA and an aminoacyl-tRNA synthetase that can charge it with Bpa. The cells were grown at 30 °C in 500 mL SD-Ura-Trp medium supplemented with 0.6 mM Bpa (Bachem) to logarithmic phase ($OD_{600} \approx 1$) and harvested by centrifugation (3000xg, 5 min, RT). For photo-crosslinking, the cells were resuspended in 6 mL water, divided into four samples of 1.5 mL each and two samples were transferred to a four-section glass petri dish. The petri dish was wrapped with aluminum foil on the bottom and sides and was placed on ice. A UV lamp as above, was placed immediately on top of the petri dish and the cells were subjected to UV-irradiation for 15 min at 4 °C. The remaining two samples were kept in the dark. Irradiated and non-irradiated cells were harvested by centrifugation (3000xg, 5 min, 2 °C) and resuspended in 1.2 mL lysis buffer (10 mM Tris, 150 mM NaCl, 2 mM PMSF, 1 x EDTA-free cOmplete protease inhibitor [Roche], 5 mM EDTA, pH 7.5). The cell suspension was distributed into two 1.5 mL test-tubes and crude mitochondria were isolated as described above. Membranes were solubilized with 1% Triton X-100 for 30 min at 4 °C on an overhead shaker (12 rpm). After a clarifying spin (30000xg, 30 min, 2 °C), the supernatant was loaded onto magnetic anti-HA beads (ThermoFisher) and further treatment was as described above for the pull-down of in vitro synthesized proteins.

Fluorescence anisotropy measurements

Cyclic β-hairpin peptides were synthesized as described (Jores et al., 2016), coupled to 5(6)-Carboxytetramethylrhodamine and used for the determination of binding kinetics and affinity of peptide/chaperone complexes by fluorescence anisotropy. Measurements were performed at 30 °C in a Jasco FP-8500 Fluorospectrometer equipped with polarizers. Excitation and emission wavelengths were set to 554 nm and 579 nm, respectively. Samples containing 2 µM rhodamine-labeled peptide were equilibrated for approximately 15 min before 10 µM Ssa1, 30 µM Ydj1, or 30 µM BSA were added. After reaching steady-state, a 100-fold molar excess of the unlabeled cyclic β-hairpin peptide was added to the cuvette and dissociation was recorded. For affinity measurements, 2 µM rhodamine-labeled peptide were supplemented with the indicated concentrations of Ssa1 or Ydj1 and the difference in anisotropy of bound and free peptide were plotted against the (co-)chaperone concentration.

Acknowledgements

We thank E. Kracker and G. Hack for technical support and Dr. F.U. Hartl for constructs. This work was supported by the Deutsche Forschungsgemeinschaft (RA 1028/8-1 and RA 1028/10-1 to D.R and SFB766 TPs Z1 and B11 to B.M. and D.R.).

Author contributions

T.J., J.L., V.B., and K.Y. conducted experiments; M.F-W. and B.M. performed the mass spectrometry analysis; H.K. synthesized and purified peptides; J.B. and T.E. designed experiments and analyzed data, T.J. and D.R. designed the experiments, analyzed data and wrote the manuscript.

Competing interests

The authors declare no competing financial interests.

References

Asai, T., T. Takahashi, M. Esaki, S. Nishikawa, K. Ohtsuka, M. Nakai, and T. Endo. 2004. Reinvestigation of the requirement of cytosolic ATP for mitochondrial protein import. *J. Biol. Chem.* 279:19464-19470.

Bhangoo, M.K., S. Tzankov, A.C.Y. Fan, K. Dejgaard, D.Y. Thomas, and J.C. Young. 2007. Multiple 40-kDa heat-shock protein chaperones function in Tom70-dependent mitochondrial import. *Mol. Biol. Cell*. 18:3414-3428.

Borchert, N., C. Dieterich, K. Krug, W. Schütz, S. Jung, A. Nordheim, R.J. Sommer, and B. Macek. 2010. Proteogenomics of Pristionchus pacificus reveals distinct proteome structure of nematode models. *Genome Res.* 20:837-846.

Caplan, A.J., D.M. Cyr, and M.G. Douglas. 1992. YDJ1p facilitates polypeptide translocation across different intracellular membranes by a conserved mechanism. *Cell*. 71:1143-1155.

Chan, N.C., and T. Lithgow. 2008. The peripheral membrane subunits of the SAM complex function codependently in mitochondrial outer membrane biogenesis. *Mol. Biol. Cell*. 19:126-136.

Chen, S., P.G. Schultz, and A. Brock. 2007. An improved system for the generation and analysis of mutant proteins containing unnatural amino acids in Saccharomyces cerevisiae. *J. Mol. Biol.* 371:112-122.

Clerico, E.M., J.M. Tilitsky, W. Meng, and L.M. Gierasch. 2015. How Hsp70 molecular machines interact with their substrates to mediate diverse physiological functions. *J. Mol. Biol.* 427:1575-1588.

Cox, J., N. Neuhauser, A. Michalski, R.A. Scheltema, J.V. Olsen, and M. Mann. 2011. Andromeda: a peptide search engine integrated into the MaxQuant environment. *J. Proteome. Res.* 10:1794-1805.

Craig, E.A., and J. Marszalek. 2017. How Do J-Proteins Get Hsp70 to Do So Many Different Things? *Trends Biochem. Sci.* 42:355-368.

Cyr, D.M., and C.H. Ramos. 2015. Specification of Hsp70 function by Type I and Type II Hsp40. *Subcell. Biochem.* 78:91-102.

Deshaies, R.J., B.D. Koch, M. Werner-Washburne, E.A. Craig, and R. Schekman. 1988. A subfamily of stress proteins facilitates translocation of secretory and mitochondrial precursor polypeptides. *Nature*. 332:800-805.

Endo, T., S. Mitsui, M. Nakai, and D. Roise. 1996. Binding of mitochondrial presequences to yeast cytosolic heat shock protein 70 depends on the amphiphilicity of the presequence. *J. Biol. Chem.* 271:4161-4167.

Franz-Wachtel, M., S.A. Eisler, K. Krug, S. Wahl, A. Carpy, A. Nordheim, K. Pfizenmaier, A. Hausser, and B. Macek. 2012. Global detection of protein kinase D-dependent phosphorylation events in nocodazole-treated human cells. *Mol. Cell. Proteomics*. 11:160-170.

Gnanasundram, S.V., and M. Koš. 2015. Fast protein-depletion system utilizing tetracycline repressible promoter and N-end rule in yeast. *Mol. Biol. Cell*. 26:762-768.

Gong, Y., Y. Kakihara, N. Krogan, J. Greenblatt, A. Emili, Z. Zhang, and W.A. Houry. 2009. An atlas of chaperone-protein interactions in Saccharomyces cerevisiae: implications to protein folding pathways in the cell. *Mol. Syst. Biol.* 5:275.

Habib, S.J., T. Waizenegger, M. Lech, W. Neupert, and D. Rapaport. 2005. Assembly of the TOB complex of mitochondria. *J. Biol. Chem.* 280:6434-6440.

Hecht, M.H. 1994. De novo design of beta-sheet proteins. *Proc. Natl. Acad. Sci. USA*. 91:8729-8730.

Höhr, A.I.C., S.P. Straub, B. Warscheid, T. Becker, and N. Wiedemann. 2015. Assembly of β-barrel proteins in the mitochondrial outer membrane. *Biochim. Biophys. Acta*. 1853:74-88.

Hoppins, S.C., and F.E. Nargang. 2004. The Tim8-Tim13 complex of Neurospora crassa functions in the assembly of proteins into both mitochondrial membranes. *J. Biol. Chem.* 279:12396-12405.

Hoseini, H., S. Pandey, T. Jores, A. Schmitt, M. Franz-Wachtel, B. Macek, J. Buchner, K.S. Dimmer, and D. Rapaport. 2016. The cytosolic cochaperone Sti1 is relevant for mitochondrial biogenesis and morphology. *FEBS J.* 283:3338-3352.

Hwang, S.T., and G. Schatz. 1989. Translocation of proteins across the mitochondrial inner membrane, but not into the outer membrane, requires nucleoside triphosphates in the matrix. *Proc. Natl. Acad. Sci. USA*. 86:8432-8436.

Jacobus, A.P., and J. Gross. 2015. Optimal cloning of PCR fragments by homologous recombination in Escherichia coli. *PLoS One*. 10:e0119221.

Jores, T., A. Klinger, L.E. Groß, S. Kawano, N. Flinner, E. Duchardt-Ferner, J. Wöhnert, H. Kalbacher, T. Endo, E. Schleiff, and D. Rapaport. 2016. Characterization of the targeting signal in mitochondrial β-barrel proteins. *Nat. Commun.* 7:12036.

Kampinga, H.H., and E.A. Craig. 2010. The HSP70 chaperone machinery: J proteins as drivers of functional specificity. *Nat. Rev. Mol. Cell Biol.* 11:579-592.

Keil, P., A. Weinzierl, M. Kiebler, K. Dietmeier, T. Söllner, and N. Pfanner. 1993. Biogenesis of the mitochondrial receptor complex. Two receptors are required for binding of MOM38 to the outer membrane surface. *J. Biol. Chem.* 268:19177-19180.

Kim, Y.E., M.S. Hipp, A. Bracher, M. Hayer-Hartl, and F.U. Hartl. 2013. Molecular chaperone functions in protein folding and proteostasis. *Annu. Rev. Biochem.* 82:323-355.

Krimmer, T., D. Rapaport, M.T. Ryan, C. Meisinger, C.K. Kassenbrock, E. Blachly-Dyson, M. Forte, M.G. Douglas, W. Neupert, F.E. Nargang, and N. Pfanner. 2001. Biogenesis of porin of the outer mitochondrial membrane involves an import pathway via receptors and the general import pore of the TOM complex. *J. Cell Biol.* 152:289-300.

Li, J., and B. Sha. 2004. Peptide substrate identification for yeast Hsp40 Ydj1 by screening the phage display library. *Biol. Proced. Online*. 6:204-208.

Mayer, M.P. 2013. Hsp70 chaperone dynamics and molecular mechanism. *Trends Biochem. Sci.* 38:507-514.

Model, K., C. Meisinger, T. Prinz, N. Wiedemann, K.N. Truscott, N. Pfanner, and M.T. Ryan. 2001. Multistep assembly of the protein import channel of the mitochondrial outer membrane. *Nat. Struct. Biol.* 8:361-370.

Morano, K.A. 2007. New tricks for an old dog: the evolving world of Hsp70. *Ann. N. Y. Acad. Sci.* 1113:1-14.

Nillegoda, N.B., and B. Bukau. 2015. Metazoan Hsp70-based protein disaggregases: emergence and mechanisms. *Front. Mol. Biosci.* 2:57.

Papić, D., Y. Elbaz-Alon, S.N. Koerdt, K. Leopold, D. Worm, M. Jung, M. Schuldiner, and D. Rapaport. 2013. The role of Djp1 in import of the mitochondrial protein Mim1 demonstrates specificity between a cochaperone and its substrate protein. *Mol. Cell. Biol.* 33:4083-4094.

Paschen, S.A., T. Waizenegger, T. Stan, M. Preuss, M. Cyrklaff, K. Hell, D. Rapaport, and W. Neupert. 2003. Evolutionary conservation of biogenesis of β-barrel membrane proteins. *Nature*. 426:862-866.

Pfanner, N., R. Pfaller, R. Kleene, M. Ito, M. Tropschug, and W. Neupert. 1988. Role of ATP in mitochondrial protein import. Conformational alteration of a precursor protein can substitute for ATP requirement. *J. Biol. Chem.* 263:4049-4051.

Pfanner, N., N. Wiedemann, C. Meisinger, and T. Lithgow. 2004. Assembling the mitochondrial outer membrane. *Nat. Struct. Mol. Biol.* 11:1044-1048.

Pfitzner, A.-K., N. Steblau, T. Ulrich, P. Oberhettinger, I.B. Autenrieth, M. Schütz, and D. Rapaport. 2016. Mitochondrial-bacterial hybrids of BamA/Tob55 suggest variable requirements for the membrane integration of β-barrel proteins. *Sci. Rep.* 6:39053.

Pierpaoli, E.V., E. Sandmeier, A. Baici, H.J. Schönfeld, S. Gisler, and P. Christen. 1997. The power stroke of the DnaK/DnaJ/GrpE molecular chaperone system. *J. Mol. Biol.* 269:757-768.

Plath, K., W. Mothes, B.M. Wilkinson, C.J. Stirling, and T.A. Rapoport. 1998. Signal sequence recognition in posttranslational protein transport across the yeast ER membrane. *Cell*. 94:795-807.

Rapaport, D., and W. Neupert. 1999. Biogenesis of Tom40, core component of the TOM complex of mitochondria. *J. Cell Biol.* 146:321-331.

Ricci, L., and K.P. Williams. 2008. Development of fluorescence polarization assays for the molecular chaperone Hsp70 family members: Hsp72 and DnaK. *Curr. Chem. Genomics*. 2:90-95.

Röhl, A., J. Rohrberg, and J. Buchner. 2013. The chaperone Hsp90: changing partners for demanding clients. *Trends Biochem. Sci.* 38:253-262.

Schägger, H., W.A. Cramer, and G. von Jagow. 1994. Analysis of molecular masses and oligomeric states of protein complexes by blue native electrophoresis and isolation of membrane protein complexes by two-dimensional native electrophoresis. *Anal. Biochem.* 217:220-230.

Scheufler, C., A. Brinker, G. Bourenkov, S. Pegoraro, L. Moroder, H. Bartunik, F.U. Hartl, and I. Moarefi. 2000. Structure of TPR domain-peptide complexes: critical elements in the assembly of the Hsp70-Hsp90 multichaperone machine. *Cell*. 101:199-210.

Schleiff, E., J.R. Silvius, and G.C. Shore. 1999. Direct membrane insertion of voltage-dependent anion-selective channel protein catalyzed by mitochondrial Tom20. *J. Cell Biol.* 145:973-978.

Schmid, A.B., S. Lagleder, M.A. Gräwert, A. Röhl, F. Hagn, S.K. Wandinger, M.B. Cox, O. Demmer, K. Richter, M. Groll, H. Kessler, and J. Buchner. 2012. The architecture of functional modules in the Hsp90 co-chaperone Sti1/Hop. *EMBO J.* 31:1506-1517.

Schmid, D., A. Baici, H. Gehring, and P. Christen. 1994. Kinetics of molecular chaperone action. *Science*. 263:971-973.

Schneider, M., M. Rosam, M. Glaser, A. Patronov, H. Shah, K.C. Back, M.A. Daake, J. Buchner, and I. Antes. 2016. BiPPred: Combined sequence- and structure-based prediction of peptide binding to the Hsp70 chaperone BiP. *Proteins*. 84:1390-1407.

Schopf, F.H., M.M. Biebl, and J. Buchner. 2017. The HSP90 chaperone machinery. *Nat. Rev. Mol. Cell Biol.* 18:345-360.

Shiota, T., S.-i. Nishikawa, and T. Endo. 2013. Analyses of protein-protein interactions by in vivo photocrosslinking in budding yeast. *Methods Mol. Biol.* 1033:207-217.

Söllner, T., G. Griffiths, R. Pfaller, N. Pfanner, and W. Neupert. 1989. MOM19, an import receptor for mitochondrial precursor proteins. *Cell*. 59:1061-1070.

Terasawa, K., M. Minami, and Y. Minami. 2005. Constantly updated knowledge of Hsp90. *J. Biochem.* 137:443-447.

Ulrich, T., and D. Rapaport. 2015. Biogenesis of β-barrel proteins in evolutionary context. *Int. J. Med. Microbiol.* 305:259-264.

Walsh, P., D. Bursać, Y.C. Law, D. Cyr, and T. Lithgow. 2004. The J-protein family: modulating protein assembly, disassembly and translocation. *EMBO Rep*. 5:567-571.

Wegele, H., M. Haslbeck, J. Reinstein, and J. Buchner. 2003. Sti1 is a novel activator of the Ssa proteins. *J. Biol. Chem.* 278:25970-25976.

Wiedemann, N., V. Kozjak, A. Chacinska, B. Schönfisch, S. Rospert, M.T. Ryan, N. Pfanner, and C. Meisinger. 2003. Machinery for protein sorting and assembly in the mitochondrial outer membrane. *Nature*. 424:565-571.

Wiedemann, N., K.N. Truscott, S. Pfannschmidt, B. Guiard, C. Meisinger, and N. Pfanner. 2004. Biogenesis of the protein import channel Tom40 of the mitochondrial outer membrane: intermembrane space components are involved in an early stage of the assembly pathway. *J. Biol. Chem.* 279:18188-18194.

Wu, C., and M.S. Sachs. 2014. Preparation of a Saccharomyces cerevisiae cell-free extract for in vitro translation. *Methods Enzymol.* 539:17-28.

Wu, X., L. Li, and H. Jiang. 2017. Mitochondrial inner-membrane protease Yme1 degrades outer-membrane proteins Tom22 and Om45. *J. Cell Biol.*

Xie, J.L., I. Bohovych, E.O.Y. Wong, J.-P. Lambert, A.-C. Gingras, O. Khalimonchuk, L.E. Cowen, and M.D. Leach. 2017. Ydj1 governs fungal morphogenesis and stress response, and facilitates mitochondrial protein import via Mas1 and Mas2. *Microb. Cell*. 4:342-361.

Yamano, K., Y.-I. Yatsukawa, M. Esaki, A.E.A. Hobbs, R.E. Jensen, and T. Endo. 2008. Tom20 and Tom22 share the common signal recognition pathway in mitochondrial protein import. *J. Biol. Chem.* 283:3799-3807.

Young, J.C., N.J. Hoogenraad, and F.U. Hartl. 2003. Molecular chaperones Hsp90 and Hsp70 deliver preproteins to the mitochondrial import receptor Tom70. *Cell*. 112:41-50.

Young, J.C., I. Moarefi, and F.U. Hartl. 2001. Hsp90: a specialized but essential protein-folding tool. *J. Cell Biol.* 154:267-273.

Figure legends

Figure 1. Cytosolic chaperones interact with newly synthesized β-barrel proteins. (A) *In vitro* translation reactions using yeast extracts without mRNA (Ø) or programmed with mRNA encoding DHFR-HA (D), Porin-HA (P), Tom40-HA (40), or Tob55Δ120-HA (55) were subjected to a pull-down assay with anti-HA beads. Samples from the input and the eluates were analyzed by SDS-PAGE and immunodecoration with the indicated antibodies. (B) Translation reactions were performed as in (A). At their end, the samples were supplemented with 5 mM $CaCl_2$ and either water (–), 1.5 U apyrase (apy) or 5 mM ATP (ATP). After further 15 min incubation at 25 °C, the reactions were subjected to a pull-down with anti-HA beads and analyzed as in (A). (C) Yeast extracts programmed with mRNA encoding for Porin-HA were incubated for *in vitro* translation at 26 °C for the indicated times. Afterwards, the reactions were subjected to an anti-HA pull-down and analyzed as in (A). (D) Yeast extracts were incubated with a Bpa-containing linear or cyclic β-hairpin peptide at the indicated concentrations. Some samples were illuminated with UV light (+UV) to induce crosslinking, whereas others were left in darkness (-UV). Then, the samples were analyzed by SDS-PAGE and immunodecoration with the indicated antibodies. Specific photo-adducts (PA) are indicated.

Figure 2. Cyclic β-hairpin peptide binds directly to Ssa1 or Ydj1. (A-F) The fluorescence anisotropy of a rhodamine-labeled cyclic β-hairpin peptide was measured in the presence of Ssa1 (A-C, black circles), BSA (A, gray circles), or Ydj1 (D-F). After association of the rhodamine-labeled peptide with the indicated proteins (A, D), the samples were supplemented with a 100-fold excess of the unlabeled cyclic β-hairpin peptide and dissociation was recorded (B, E). For affinity determinations, the rhodamine-labeled peptide was mixed with the indicated concentrations of either Ssa1 (C) or Ydj1 (F) and the difference in anisotropy (Δ anisotropy) of the bound and free peptide was plotted against the (co)chaperone concentration. The data was fitted using a hyperbolic regression curve (gray).

Figure 3. Cytosolic chaperones are required for the *in vitro* import of β-barrel proteins. (A-F) Top panels: Radiolabeled precursor proteins of Porin-HA (A, D), *N. crassa* Tom40 (NcTom40; B, E) or yeast Tom40 (C, F) were subjected to *in vitro* import reactions using isolated mitochondria. Prior to the import reaction, the mitochondria were mixed with either 20 µM C90 or BSA (A-C). Alternatively, the precursor protein-containing translation reactions were supplemented with 20 µM of either cBag or BSA (D-F). After import for the indicated

times, the mitochondria were subjected to carbonate extraction (A, D) or were treated with proteinase K (B, E). The samples were subjected to SDS-PAGE (A, B, D, E) or BN-PAGE (C, F) and autoradiography. Lower panels: The intensities of the bands corresponding to Porin-HA, the protease-protected fragment F26 of NcTom40, or assembly intermediate I of Tom40 from three independent experiments were quantified and the mean intensity from the 20 min (A, B, D, E) or 15 min (C, F) import in the presence of BSA was set to 100%. Error bars represent standard deviation. FL, full-length. F26, protease-protected fragment of 26 kDa. The migration of the assembled TOM complex and assembly intermediates (Int) I and II of Tom40 are indicated.

Figure 4. Cytosolic chaperones interact *in vivo* with a β-hairpin peptide. Yeast cells expressing either control hp18(VDAC)-DHFR-HA (-Bpa) or a variant with Bpa inserted in the β-hairpin (+Bpa) were subjected to *in vivo* photo-crosslinking (+UV) or kept in the dark (-UV). Next, the cells were lysed and subjected to a pull-down with anti-HA beads. Samples from the input and the eluates were analyzed by SDS-PAGE and immunodecoration with the indicated antibodies. Specific photo-adducts (PA) are indicated.

Figure 5. The Hsp40 co-chaperones Ydj1 and Sis1 are required for the *in vivo* biogenesis of Porin. Yeast cells harboring endogenously HA-tagged Porin from a wildtype strain (A) or from strains with a tetracycline-repressible promoter controlling the expression of *YDJ1* (B), *SIS1* (C) or both (D) were grown for 4 h in the absence (-Dox) or presence (+Dox) of doxycycline (Dox) followed by 1 h of methionine starvation. Synthesis of radiolabeled proteins was initiated by addition of ^{35}S-Met to the medium and cells were harvested after the indicated time periods. Then, a crude mitochondrial fraction was obtained, solubilized, and subjected to a pull-down with anti-HA beads. Input samples from the whole cell lysate (inp) and the eluates were analyzed by SDS-PAGE, autoradiography (autorad.) and immunodecoration with the indicated antibodies. Cox2 was used as a loading control. Lower panels: The intensities of the bands corresponding to Porin-HA from three independent experiments were quantified and the mean intensity from the 30 min samples without Dox was set to 100%. Error bars represent standard deviation.

Figure 6. Mammalian Hsc70 is involved in the biogenesis of β-barrel proteins. (A) *In vitro* translation reactions using rabbit reticulocyte lysate without mRNA (Ø) or programmed with mRNA encoding DHFR-HA (D), Porin-HA (P), or VDAC1-HA (V) were subjected to a pull-

down with anti-HA beads. Samples from the input and the eluates were analyzed by SDS-PAGE and immunodecoration with the indicated antibodies. (B) Top panel: Rabbit reticulocyte lysate was used to synthesize radiolabeled Porin. After translation, the lysate was supplemented with either cBag or BSA and subjected to *in vitro* import reactions using isolated mitochondria. After import for the indicated times, the mitochondria were subjected to carbonate extraction and the samples were analyzed by SDS-PAGE and autoradiography. Lower panels: The intensities of the bands corresponding to Porin from three independent experiments were quantified and the mean intensity from the 20 min import with BSA was set to 100%. Error bars represent standard deviation.

Figure 7. Working model for the early events in the biogenesis of mitochondrial β-barrel proteins. Mitochondrial β-barrel proteins are encoded by nuclear genes (1). Upon their synthesis on cytosolic ribosomes (2), these proteins associate with Hsp70 and Hsp40 chaperones that keep the newly synthesized proteins in an import-competent conformation. On the mitochondrial surface, the chaperone/substrate complex can dock to the import receptor Tom70 while the β-barrel targeting signal in the form of a β-hairipin motif is recognized by the import receptor Tom20 (3). For further assembly into the mitochondrial OM, the newly synthesized protein is translocated across the OM through the import pore of the TOM complex (4).

Table 1. **Proteins that co-purified with *in vitro* translated Porin.** Only the 20 proteins with the highest iBAQ* value are shown. Proteins with a chaperone-like function are highlighted.

Protein name	**Gene name**	**iBAQ**
Ubiquitin	RPS31;RPL40B;RPL40A;UBI4	255830000
Porin	POR1	234220000
Heat shock protein SSA2	SSA2	138040000
Elongation factor 1-alpha	TEF1	135660000
Mitochondrial protein import protein MAS5	YDJ1	105990000
Heat shock protein 60, mitochondrial	HSP60	92565000
Glyceraldehyde-3-phosphate dehydrogenase 3	TDH3	78971000
Tryptophan-tRNA ligase, cytoplasmic	WRS1	64375000
Pyruvate kinase 1	CDC19	59277000
Heat shock protein SSB1	SSB1	57047000
ATP-dependent RNA helicase eIF4A	TIF1	44960000
Tubulin beta chain	TUB2	39876000
Plasma membrane ATPase 1/2	PMA1;PMA2	35671000
Long-chain-fatty-acid-CoA ligase 4	FAA4	32266000
40S ribosomal protein S3	RPS3	31676000
H/ACA ribonucleoprotein complex subunit 2	NHP2	30161000
ATP-dependent molecular chaperone HSC82	HSC82	27457000
60S ribosomal protein L27-A/B	RPL27B;RPL27A	23564000
Acetolactate synthase catalytic subunit, mitochondrial	ILV2	21029000
60S ribosomal protein L17-B	RPL17B	20275000

* iBAQ, intensity-based absolute quantification.

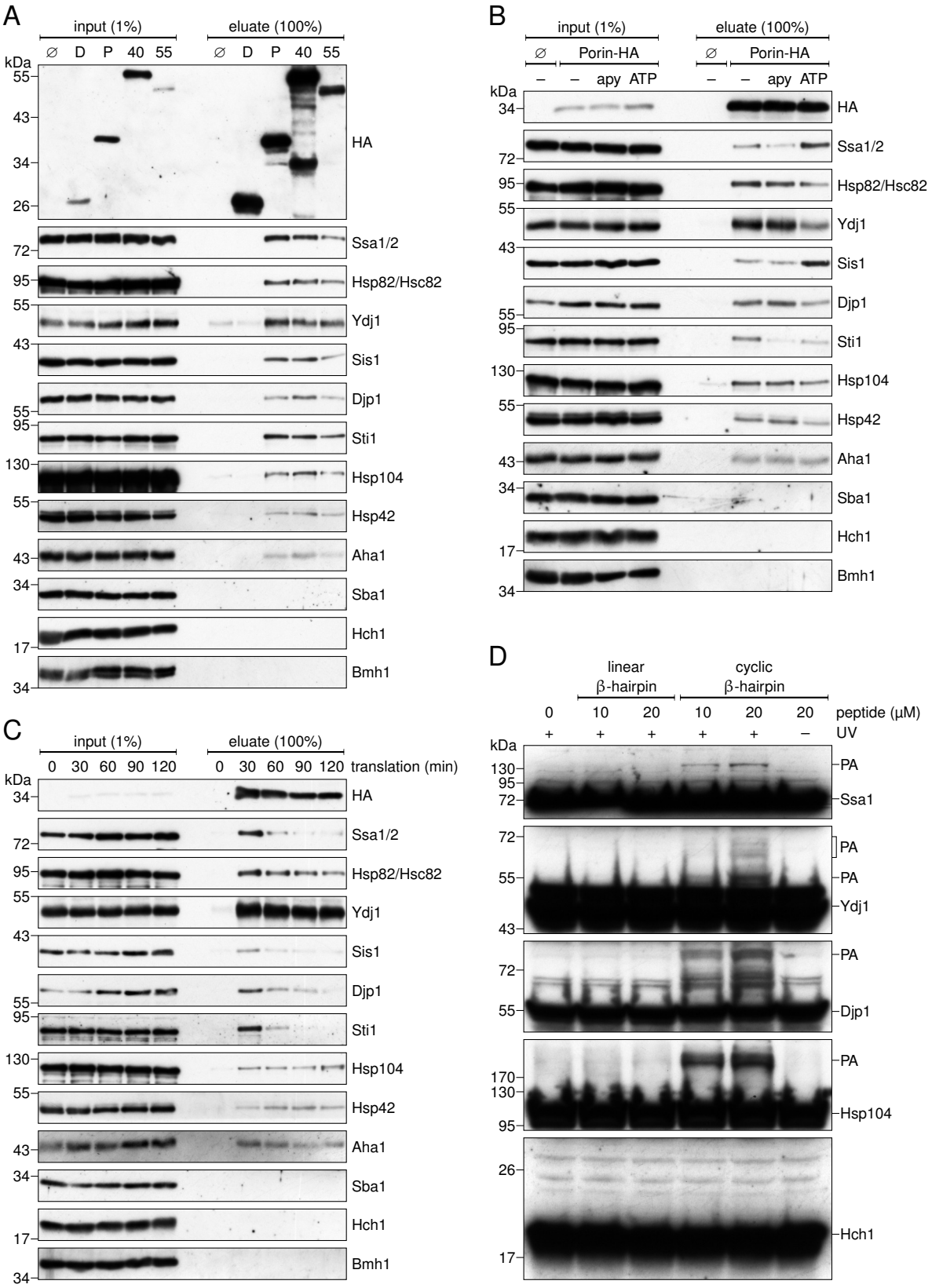

Jores *et al.*, Fig. 1

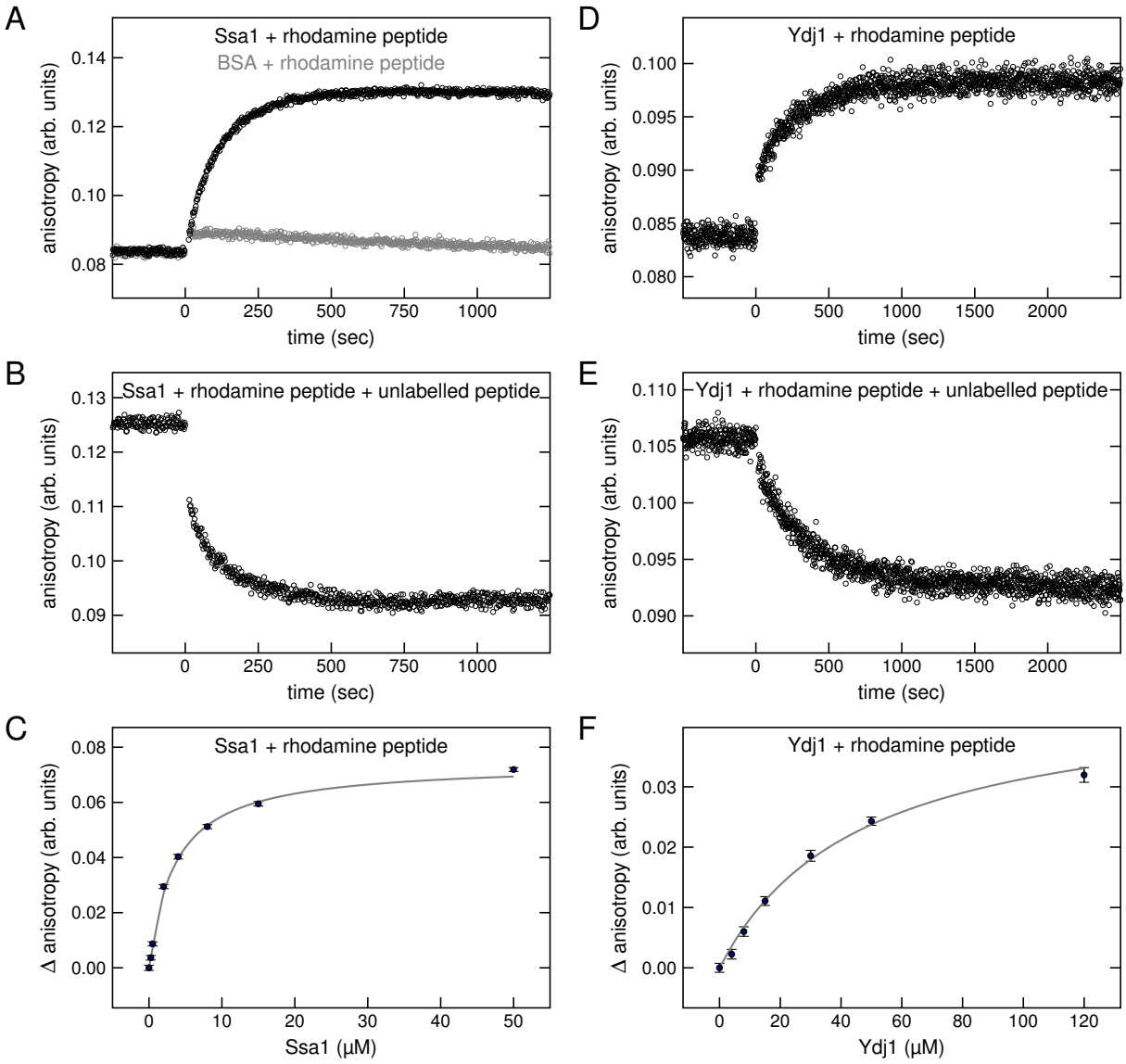
A
Ssa1 + rhodamine peptide
BSA + rhodamine peptide
anisotropy (arb. units)
time (sec)
B
Ssa1 + rhodamine peptide + unlabelled peptide
anisotropy (arb. units)
time (sec)
C
Ssa1 + rhodamine peptide
Δ anisotropy (arb. units)
Ssa1 (μM)
D
Ydj1 + rhodamine peptide
anisotropy (arb. units)
time (sec)
E
Ydj1 + rhodamine peptide + unlabelled peptide
anisotropy (arb. units)
time (sec)
F
Ydj1 + rhodamine peptide
Δ anisotropy (arb. units)
Ydj1 (μM)

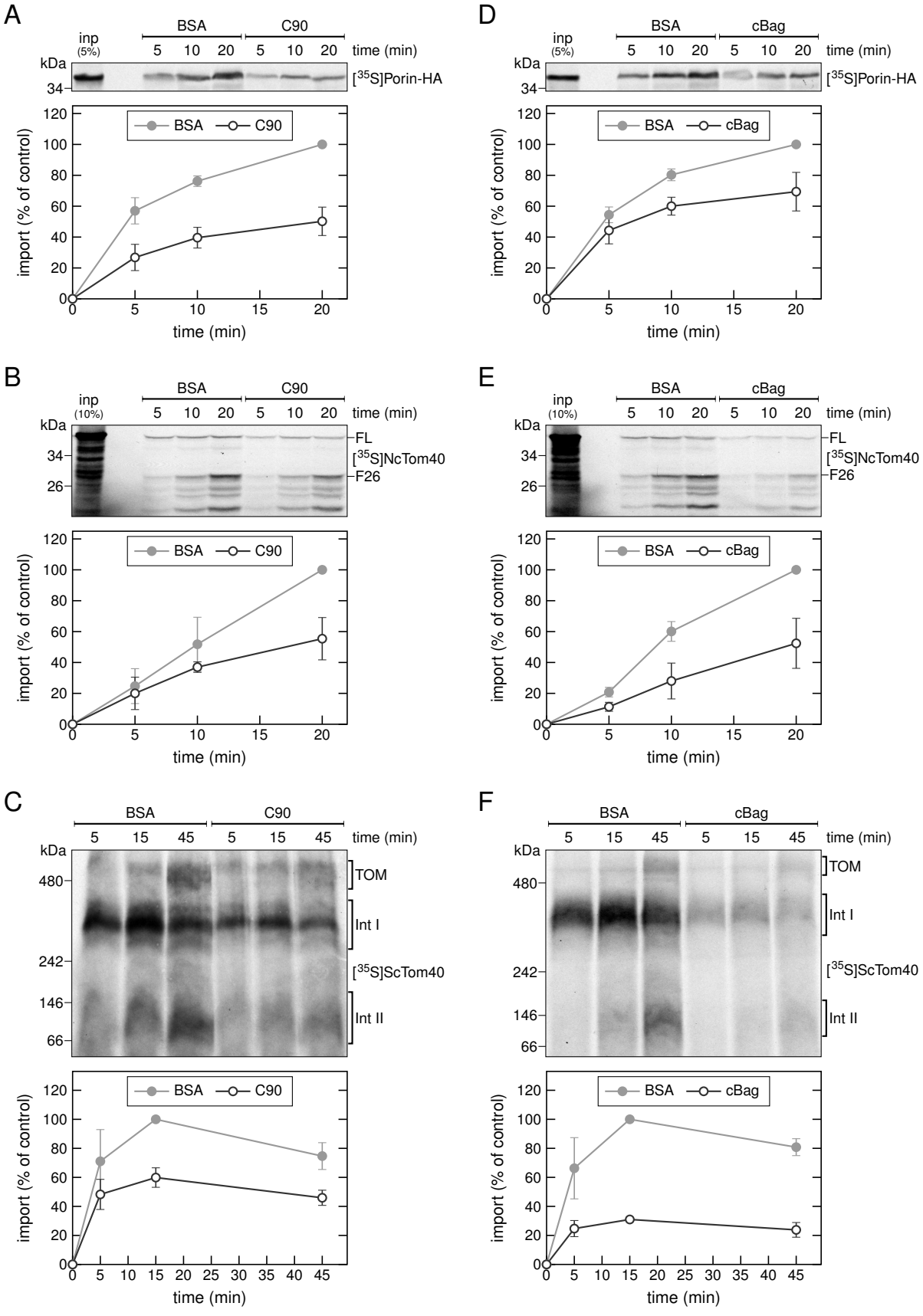

Jores *et al.*, Fig. 3

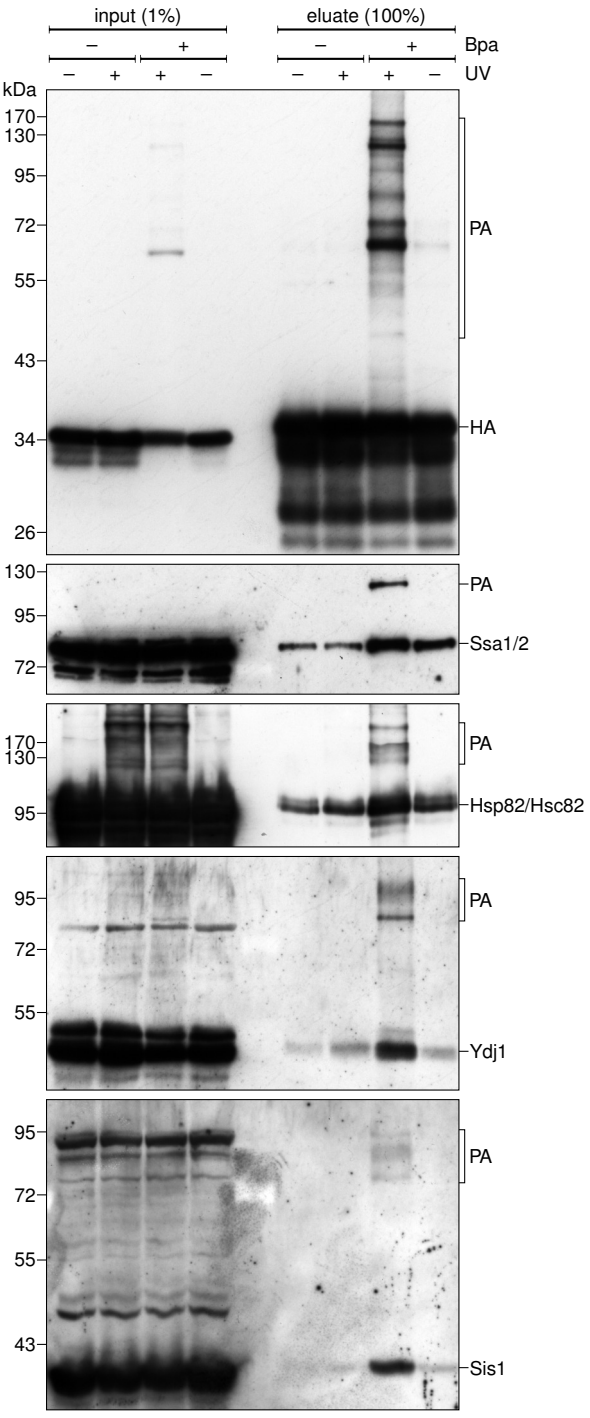

Jores *et al.*, Fig. 4

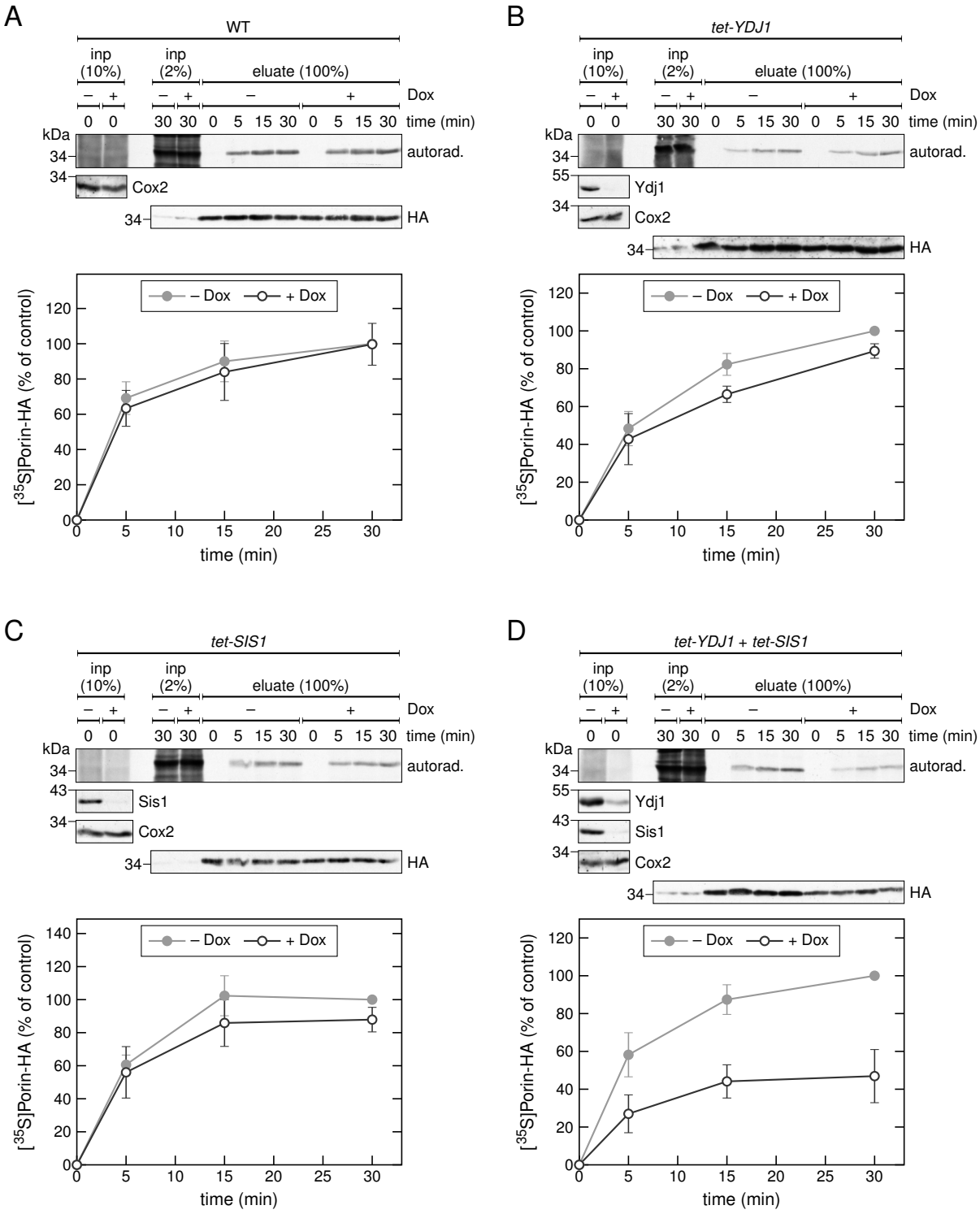

Jores *et al.*, Fig. 5

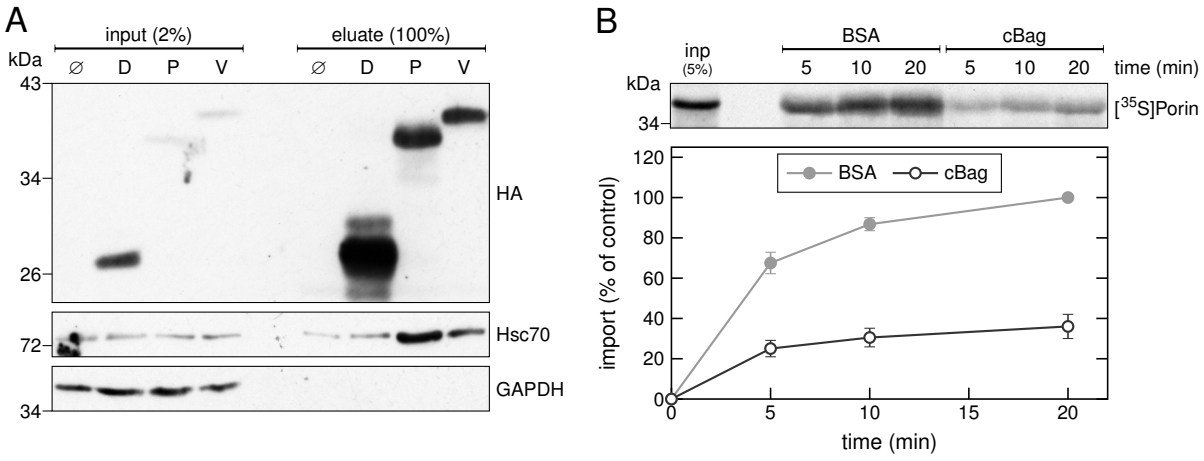
A
input (2%)
eluate (100%)
kDa
∅ D P V
∅ D P V
43
34
26
HA
72
Hsc70
34
GAPDH
B
inp
(5%)
BSA
cBag
5 10 20 5 10 20
time (min)
kDa
34
[35S]Porin
120
100
80
60
40
20
0
import (% of control)
BSA
cBag
0 5 10 15 20
time (min)

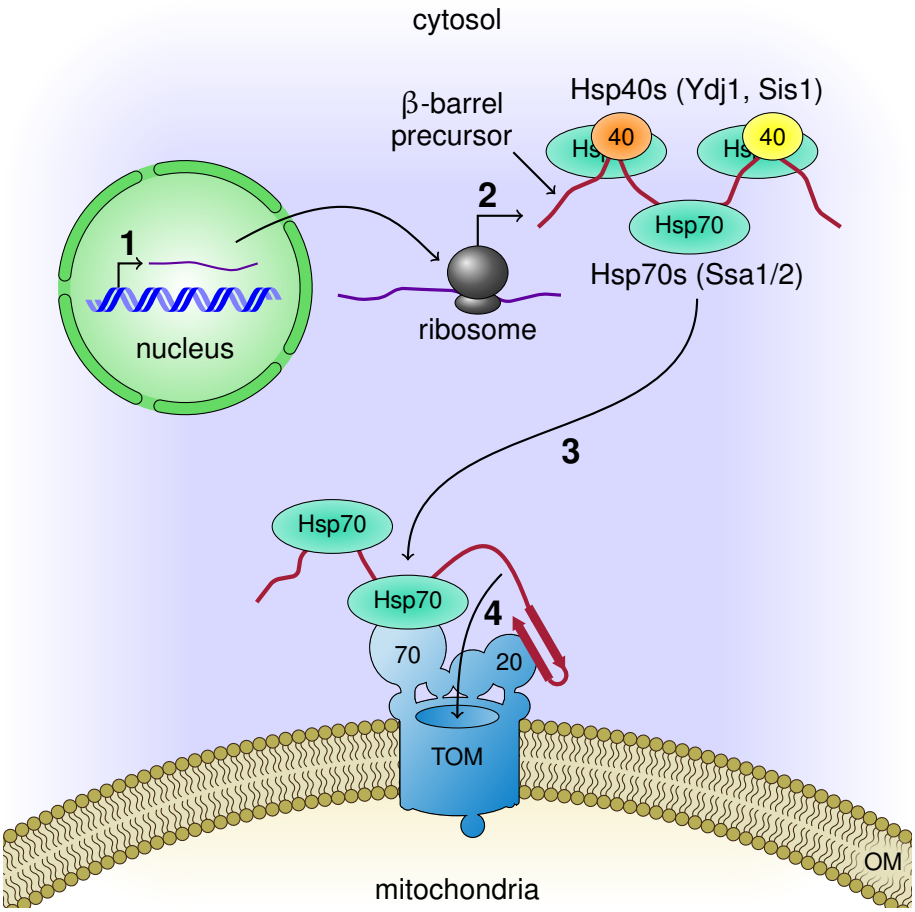

Jores *et al.*, Fig. 7

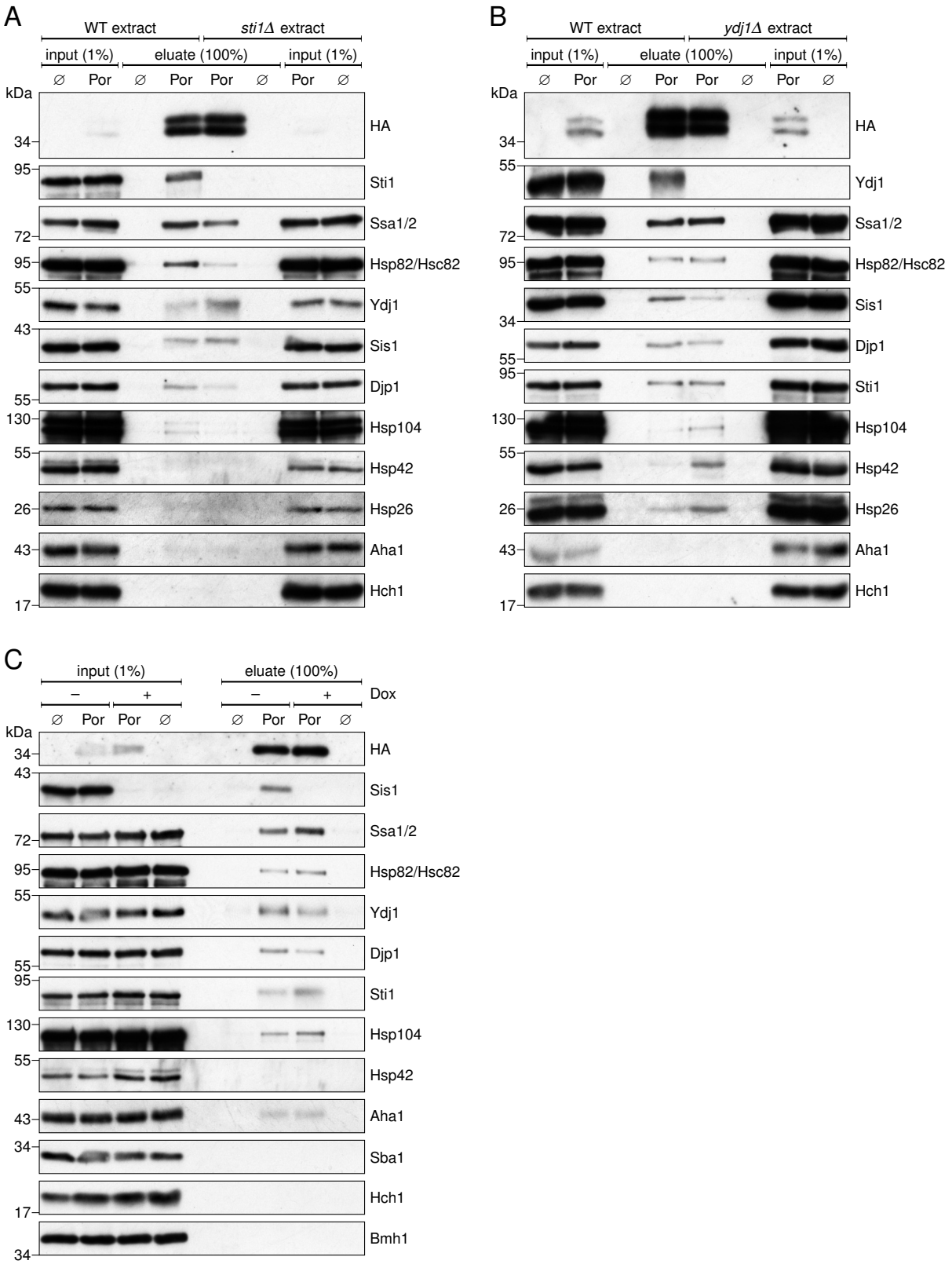

Figure S1. **The absence of a certain co-chaperone affects the binding of β-barrel proteins to other (co-)chaperones. (A and B)** *In vitro* translation reactions using yeast extracts prepared from WT, *sti1Δ* (A), or *ydj1Δ* (B) cells without mRNA (Ø) or programmed with mRNA encoding Porin-HA (Por) were subjected to a pull-down with anti-HA beads. Samples from the input and the eluate were analyzed by SDS-PAGE and immunodecoration with the indicated antibodies. **(C)** Yeast extracts were prepared from cells that were left untreated (–Dox) or depleted for Sis1 by addition of doxycyline to the growth medium for 8 h (+Dox). The extracts were then used for *in vitro* translation followed by a pull-down assay as in (A).

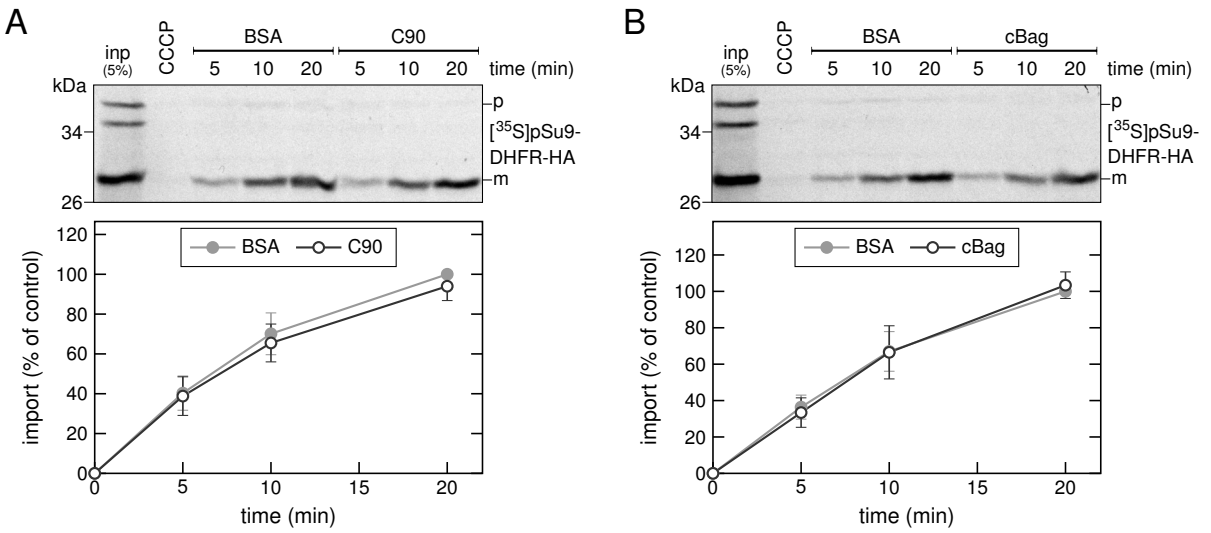

Figure S2. **The import of pSu9-DHFR-HA is not affected by chaperone inhibitors. (A and B)** Top panels: Radiolabeled precursor molecules of pSu9-DHFR-HA were subjected to *in vitro* import reactions using isolated mitochondria. Prior to the import reaction, the mitochondria were mixed with either 20 µM C90 or an equivalent amount of BSA (A), or the precursor protein-containing translation reactions were supplemented with either 20 µM cBag or an equivalent amount of BSA (B). After import for the indicated times, the mitochondria were treated with proteinase K. The samples were subjected to SDS-PAGE and autoradiography. In a control reaction, the mitochodria were treated with the uncoupler CCCP prior to the import reaction. Lower panels: The intensities of the bands corresponding to the protease-protected, mature form (m) of pSu9-DHFR-HA from three independent experiments were quantified and the mean intensity from the 20 min import with BSA was set to 100%. Error bars represent standard deviation. p, precursor form of pSu9-DHFR-HA.

Table S1. **Yeast strains used in this study.**

strain	genotype	reference
sti1Δ	W303α, *sti1Δ::HIS3MX6*	Hoseini et al. (2016)
ydj1Δ	BY4741, *ydj1Δ::KanMX4*	EUROSCARF
tetO$_7$-Sis1	YMK120a, *sis1::tetO$_7$-SIS1(NatMX)*	this study
Porin-3HA tetO$_7$-Ubi-L-Ydj1	YMK120α, *por1::POR1-3HA NatNT2, ydj1::tetO$_7$-Ubiquitin-Leu-YDJ1 HIS3MX*	this study
Porin-3HA tetO$_7$-Ubi-L-Sis1	YMK120α, *por1::POR1-3HA NatNT2, sis1::tetO$_7$-Ubiquitin-Leu-SIS1 HIS3MX*	this study
Porin-3HA tetO$_7$-Ubi-L-Ydj1/Sis1	YMK120α, *por1::POR1-3HA NatNT2, ydj1::tetO$_7$-Ubiquitin-Leu-YDJ1 HIS3MX, sis1::tetO$_7$-Ubiquitin-Leu-SIS1 KanMX*	this study

Table S2. **Primers used in this study.**

construct	primer	sequence
Porin-3HA	TJ207	AGTTGTCTGAACCTGTTCACAAGCTAGGTTGGTCTTTGTCCTTCGACGCT-CTGAAGCTTTACCCATACGATGTTCCTG
	TJ208	CGAGCACATATATGGTATATAGTGAACATATATATATTAGATATATACGT-GAGCTCGATTACAACAGGTGTTGTCC
tetO$_7$-Sis1	TJ196	GGATAAGTTGTTTGCATTTTAAGATTTTTTTTTTAATACATTCACATCAA-CAGTATAGCGACCAGCATTCACATACG
	TJ198	GCACTTGGAGATACTCCAAGTAAATCATAAAGTTTTGTCTCCTTGACCAT-AAGCTTATCGATACCGTCGATCCCC
tetO$_7$-Ubi-L-Ydj1	TJ192	CATATCTTTTGATAGAACATAATTAAAAATTATCCAAACTGAATTCTACA-CAGTATAGCGACCAGCATTCACATACG
	TJ193	GTGGCAGTTACTGGAACACCTAGAATATCGTAAAACTTAGTTTCTTTAAC-CAAACCACCTCTCAATCTCAAGACCAAG
tetO$_7$-Ubi-L-Sis1	TJ196	GGATAAGTTGTTTGCATTTTAAGATTTTTTTTTTAATACATTCACATCAA-CAGTATAGCGACCAGCATTCACATACG
	TJ197	TTAGCACTTGGAGATACTCCAAGTAAATCATAAAGTTTTGTCTCCTTGAC-CAAACCACCTCTCAATCTCAAGACCAAG
tetO$_7$-Ssa1	TJ233	TCTATTTGTAAGATAAGCACATCAAAAGAAAAGTAATCAAGTATTACAAG-CAGTATAGCGACCAGCATTCACATAC
	TJ260	GCAACACACGAGTATGTTGTACCTAAATCAATACCGACAGCTTTTGACAT-AAGCTTATCGATACCGTCGATCCCC
tetO$_7$-Ssa2	TJ237	TCTCTTATTTAAGTTACTTCTATTCTTCAATTGATTAATTCCAACAGATC-CAGTATAGCGACCAGCATTCACATAC
	TJ261	GCAACACAGGAGTAGGTAGTACCTAAATCAATACCGACAGCTTTAGACAT-AAGCTTATCGATACCGTCGATCCCC
tetO$_7$-Hsp82	TJ253	CGCTGTATTAGAGTTCAAGAAATCATACCTGATAGAAAATAGAGTCCTAT-CAGTATAGCGACCAGCATTCACATAC
	TJ263	CTCATCAACTGAGTAATTTCAGCTTGAAATTCAAAAGTTTCACTAGCCAT-AAGCTTATCGATACCGTCGATCCCC
tetO$_7$-Hsc82	TJ249	TTTTGTGATATATTCTTTCTCTTGTTTTCTTTTTCTTGAAACGCTACAGA-CAGTATAGCGACCAGCATTCACATAC
	TJ262	CTCATCAACTGAGTGATTTCAGCTTGAAATTCAAAAGTTTCACCAGCCAT-AAGCTTATCGATACCGTCGATCCCC
ssa3Δ	TJ240	AATGTTTGTCACTAAACGGATAGAATAGGTACTAAACGCTACAAAGAAAA-CGTCGACCTCGAGGCCAGAAG
	TJ241	TAAAAGGTTAAACATAAAAAGTAGCTAAATAGAACACTATAGAAGAATAA-TTCATCTCCGGTTCTGCTGCTAG
ssa4Δ	TJ245	ATAAAAAGTAAATAACAAAAACAAGAAAAAAAATAAACAAAACAATAATC-CAGCTGAAGCTTCGTACGCTGC
	TJ246	GGAAAACTAAGAAATTCGATGCTGCTACTTCATCGCATCTTTGTATTTAT-GCATAGGCCACTAGTGGATCTGGAC
pGEM4polyA	TJ154	AAAAAAAAAAAAAAAAAAAAAAAAAAAAAA-GCGGCCGC-CCGGTCTCCCTATAGTGAGTCGTATTAATTTC
	TJ155	TTTTTTTTTTTTTTTTTTTTTTTTTTTTTT-AAGCTTGCATGCCTGCAGGTCGACTC
3HA	TJ024	CCC-GGATCC-A-TACCCATACGATGTTCC
	TJ025	CCC-GTCGAC-TTA-ACCAGCGTAATCTGG
DHFR-3HA	TJ009	CCC-GGTACC-ATGGTTCGACCATTGAACTGC
	TJ010	CCC-GGATCC-CC-GTCTTTCTTCTCGTAGAC
yk DHFR-3HA	TJ144	CACAC-GGTACC-AAAAAAATGTCT-GTTCGACCATTGAACTGCATC
	TJ010	CCC-GGATCC-CC-GTCTTTCTTCTCGTAGAC
yk Porin-3HA	TJ149	CACAC-GGTACC-AAAAAA-ATGTCTCCTCCAGTTTACAGC

	TJ150	CACAC-GGATCC-CC-AGCGTCGAAGGACAAAGAC
yk Tom40-3HA	TJ180	CACAC-GAGCTC-AAAAAA-ATGTCTGCACCAACTCCATTAGC
	TJ181	CACAC-GGATCC-CC-CAATTGAGGAAGAGCTTGCAATG
yk Tob55(bbd)-3HA	TJ184	CACAC-GAGCTC-AAAAAAATGTCT-AAAACGTTTACAGCGAAGACAG
	TJ183	CACAC-GGATCC-CC-TAAAAATGCCAGACCAAGACCAAAC
yk NcTom40	TJ187	CACAC-GAGCTC-AAAAAA-ATGGCTTCGTTTTCCACCG
	TJ188	CACAC-GGATCC-TTA-AAAGGGGATGTTGAGGGAC
yk Tom40	TJ180	CACAC-GAGCTC-AAAAAA-ATGTCTGCACCAACTCCATTAGC
	TJ186	CACAC-GGATCC-TTA-CAATTGAGGAAGAGCTTGCAATG
yk pSu9-DHFR-3HA	TJ157	CACAC-GAATTC-AAAAAAATGTCT-GCCTCCACTCGTGTCCTC
	TJ158	CACAC-GGTACC-ACCAGCACCAGCACC-GGAAGAGTAGGCGCGC
hp18(VDAC, Bpa258)	TJ090	GGTATTAAACTG-TAG-CTGTCAGCTCTTC
	TJ091	GAAGAGCTGACAG-CTA-CAGTTTAATACC
hp18(VDAC)-DHFR-3HA	TJ014	CCC-GAATTC-ATG-AAGCCAGGTATTAAACTGAC
	TJ010	CCC-GGATCC-CC-GTCTTTCTTCTCGTAGAC
mk DHFR-3HA	TJ141	CACAC-GGTACC-GCCACC-ATGGTTCGACCATTGAACTGC
	TJ010	CCC-GGATCC-CC-GTCTTTCTTCTCGTAGAC
mk Porin-3HA	TJ148	CACAC-GGTACC-GCCACCATGGCT-TCTCCTCCAGTTTACAGCG
	TJ150	CACAC-GGATCC-CC-AGCGTCGAAGGACAAAGAC
mk VDAC1-3HA	TJ151	CACAC-GGTACC-GCCACC-ATGGCTGTGCCACCCACG
	TJ153	CACAC-GGATCC-CC-TGCTTGAAATTCCAGTCCTAGAC
3HA NatNT2	TJ205	CACAC-AAGCTT-TACCCATACGATGTTCCTGACTATG
	TJ206	CACAC-GGATCC-CTTCGAGCGTCCCAAAACCTTC
pMK632	TJ203	GGAGGGTATTCTGGGCCTCCATGTC
	TJ204	GTATGTGAATGCTGGTCGCTATACTG
KanMX/HIS3MX	TJ201	GACATGGAGGCCCAGAATACCCTCC
	TJ202	CAGTATAGCGACCAGCATTCACATAC

Table S3. **Plasmids used in this study.**

If not indicated otherwise, gene sequences are from *S. cerevisiae*

plasmid	insert	reference
pGEM4polyA	poly-A stretch (72 x A)	this study
pRS316-Atg32-3HAn	Atg32 with internal 3 x HA-tag	Okamoto et al. (2009)
pGEM4polyA-3HA	C-terminal 3 x HA-tag	this study
pRS426-TPI-3HA	C-terminal 3 x HA-tag	this study
pGEM4-pSu9-DHFR	presequence of *N. crassa* ATP synthase subunit 9 (aa M1-S69)-*M. musculus* DHFR	Pfanner et al. (1987)
pGEM4-Tom40	Tom40	Paschen et al. (2003)
pGEM4-Tob55	Tob55	Paschen et al. (2003)
pGEM4-NcTom40	*N. crassa* Tom40	Rapaport and Neupert (1999)
pGEM4-VDAC1	*H. sapiens* VDAC1	Engl et al. (2012)
pGEM4polyA-DHFR-3HA	*M. musculus* DHFR-3 x HA-tag	this study
pGEM4polyA-yk-DHFR-3HA	yeast kozak sequence (AAAAAAATGTCT) *M. musculus* DHFR-3 x HA-tag	this study
pGEM4polyA-yk-Porin-3HA	yeast kozak sequence (AAAAAAATGTCT) Porin-3 x HA-tag	this study
pGEM4polyA-yk-Tom40-3HA	yeast kozak sequence (AAAAAAATGTCT) Tom40-3 x HA-tag	this study
pGEM4polyA-yk-Tob55(Δ1-120)-3HA	yeast kozak sequence (AAAAAAATGTCT) Tob55 β-barrel domain (aa K121-end)-3 x HA-tag	this study
pGEM4polyA-yk-NcTom40	yeast kozak sequence (AAAAAAATGGCT) *N. crassa* Tom40	this study
pGEM4polyA-yk-Tom40	yeast kozak sequence (AAAAAAATGTCT) Tom40	this study
pGEM4polyA-yk-pSu9-DHFR-3HA	yeast kozak sequence (AAAAAAATGTCT) presequence of *N. crassa* ATP synthase subunit 9 (aa M1-S69)-*M. musculus* DHFR-3 x HA-tag	this study
pBpa2-PGK1+3SUP4-tRNA$_{CUA}$	tRNA aaRS + tRNA$_{CUA}$	Chen et al. (2007)
pRS426-TPI-hp18(VDAC)-DHFR-3HA	hairpin 18 of *H. sapiens* VDAC1 (aa K252-A283)-*M. musculus* DHFR-3 x HA-tag	this study
pRS426-TPI-hp18(VDAC, Bpa258)-DHFR-3HA	hairpin 18 of *H. sapiens* VDAC1 (aa K252-A283; Thr258Bpa)-*M. musculus* DHFR-3 x HA-tag	this study
pGEM4polyA-mk-DHFR-3HA	mammalian kozak sequence (GCCACCATGG) *M. musculus* DHFR-3 x HA-tag	this study
pGEM4polyA-mk-Porin-3HA	mammalian kozak sequence (GCCACCATGG) Porin-3 x HA-tag	this study
pGEM4polyA-mk-VDAC1-3HA	mammalian kozak sequence (GCCACCATGG) *H. sapiens* VDAC1-3 x HA-tag	this study
pGEM4-Porin	Porin	Mayer et al. (1993)
pFA6a-NatNT2	NatNT2 cassette	Janke et al. (2004)
pFA6a-KanMX4	KanMX4 cassette	Wach et al. (1994)

pFA6a-HIS3MX6	HIS3MX6 cassette	Wach et al. (1997)
pFA6a-3HA-NatNT2	3 x HA-tag CYC1 terminator NatNT2 cassette	this study
pMK632	NatMX cassette $tetO_7$-CYC1 promoter-Ubiquitin-Leucin-HA-tag	Gnanasundram and Koš (2015)
pMK632Kan	KanMX cassette $tetO_7$-CYC1 promoter-Ubiquitin-Leucin-HA-tag	this study
pMK632His	HIS3MX cassette $tetO_7$-CYC1 promoter-Ubiquitin-Leucin-HA-tag	this study

Table S4. **Antibodies used in this study.**

If not indicated otherwise, target proteins are from *S. cerevisiae.*

antibody directed against	dilution	Identifier
Aha1	1:2000	N/A
Bmh1	1:1000	N/A
Cox2	1:1000	N/A
Djp1	1:2000	N/A
***H. sapiens* GAPDH**	1:1000	CSA-335 (Stressgen)
HA	1:1000	11867423001 (Roche)
Hch1	1:4000	N/A
***H. sapiens* Hsc70**	1:1000	ADI-SPA-815 (Enzo)
Hsp104	1:25 000	N/A
Hsp26	1:4000	N/A
Hsp42	1:4000	N/A
Hsp82/Hspc82	1:20 000	N/A
Sba1	1:2500	N/A
Sis1	1:20 000	N/A
Ssa1/2	1:20 000	N/A
Sti1	1:10 000	N/A
Ydj1	1:10 000	N/A

References

Chen, S., P.G. Schultz, and A. Brock. 2007. An improved system for the generation and analysis of mutant proteins containing unnatural amino acids in Saccharomyces cerevisiae. *J. Mol. Biol.* 371:112-122.

Engl, G., S. Florian, L. Tranebjærg, and D. Rapaport. 2012. Alterations in expression levels of deafness dystonia protein 1 affect mitochondrial morphology. *Hum. Mol. Genet.* 21:287-299.

Gnanasundram, S.V., and M. Koš. 2015. Fast protein-depletion system utilizing tetracycline repressible promoter and N-end rule in yeast. *Mol. Biol. Cell*. 26:762-768.

Hoseini, H., S. Pandey, T. Jores, A. Schmitt, M. Franz-Wachtel, B. Macek, J. Buchner, K.S. Dimmer, and D. Rapaport. 2016. The cytosolic cochaperone Sti1 is relevant for mitochondrial biogenesis and morphology. *FEBS J.* 283:3338-3352.

Janke, C., M.M. Magiera, N. Rathfelder, C. Taxis, S. Reber, H. Maekawa, A. Moreno-Borchart, G. Doenges, E. Schwob, E. Schiebel, and M. Knop. 2004. A versatile toolbox for PCR-based tagging of yeast genes: new fluorescent proteins, more markers and promoter substitution cassettes. *Yeast*. 21:947-962.

Mayer, A., R. Lill, and W. Neupert. 1993. Translocation and insertion of precursor proteins into isolated outer membranes of mitochondria. *J. Cell Biol.* 121:1233-1243.

Okamoto, K., N. Kondo-Okamoto, and Y. Ohsumi. 2009. Mitochondria-anchored receptor Atg32 mediates degradation of mitochondria via selective autophagy. *Dev. Cell*. 17:87-97.

Paschen, S.A., T. Waizenegger, T. Stan, M. Preuss, M. Cyrklaff, K. Hell, D. Rapaport, and W. Neupert. 2003. Evolutionary conservation of biogenesis of β-barrel membrane proteins. *Nature*. 426:862-866.

Pfanner, N., H.K. Müller, M.A. Harmey, and W. Neupert. 1987. Mitochondrial protein import: involvement of the mature part of a cleavable precursor protein in the binding to receptor sites. *EMBO J.* 6:3449-3454.

Rapaport, D., and W. Neupert. 1999. Biogenesis of Tom40, core component of the TOM complex of mitochondria. *J. Cell Biol.* 146:321-331.

Wach, A., A. Brachat, C. Alberti-Segui, C. Rebischung, and P. Philippsen. 1997. Heterologous HIS3 marker and GFP reporter modules for PCR-targeting in Saccharomyces cerevisiae. *Yeast*. 13:1065-1075.

Wach, A., A. Brachat, R. Pöhlmann, and P. Philippsen. 1994. New heterologous modules for classical or PCR-based gene disruptions in Saccharomyces cerevisiae. *Yeast*. 10:1793-1808.